This article has been accepted for publication in a future issue of this journal, but has not been fully edited. Content may change prior to final publication. Citation information: DOI 10.1109/ACCESS.2021.3101845, IEEE Access

RF Impairments in Wireless Transceivers: Phase Noise, CFO, and IQ Imbalance – A Survey

AMIRHOSSEIN MOHAMMADIAN[1], (Student Member, IEEE), CHINTHA TELLAMBURA[1](Fellow, IEEE)
[1] Department of Electrical and Computer Engineering, University of Alberta, Edmonton, AB, T6G 1H9, Canada
Corresponding author: Amirhossein Mohammadian (e-mail: am11@ualberta.ca).

ABSTRACT
Wireless transceivers for mass-market applications must be cost effective. We may achieve this goal by deploying non-ideal low-cost radio frequency (RF) analog components. However, their imperfections may result in RF impairments, including phase noise (PN), carrier frequency offset (CFO), and in-phase (I) and quadrature-phase (Q) imbalance. These impairments introduce in-band and out-of-band interference terms and degrade the performance of wireless systems. In this survey, we present RF-impairment signal models and discuss their impacts. Moreover, we review RF-impairment estimation and compensation in single-carrier (SC) and multicarrier systems, especially orthogonal frequency division multiplexing (OFDM). Furthermore, we discuss the effects of the RF impairments in already-established wireless technologies, e.g., multiple-input multiple-output (MIMO), massive MIMO, full-duplex, and millimeter-wave communications and review existing estimation and compensation algorithms. Finally, future research directions investigate the RF impairments in emerging technologies, including cell-free massive MIMO communications, non-orthogonal multicarrier systems, non-orthogonal multiple access (NOMA), ambient backscatter communications, and intelligent reflecting surface (IRS)-assisted communications. Furthermore, we discuss artificial intelligence (AI) approaches for developing estimation and compensation algorithms for RF impairments.

INDEX TERMS RF impairments, PN, CFO, IQ imbalance

I. INTRODUCTION
DRAMATIC mobile data traffic growth requires deploying high-data-rate services in fifth-generation (5G) and beyond wireless communication systems. Fig. 1 illustrates mobile data traffic forecast for 2022 by Cisco [1]. Moreover, 5G networks must support several applications such as enhanced mobile broadband (eMBB), massive machine-type communications (mMTC), ultra-reliable, low-latency communications (URLLC), vehicle-to-everything (eV2X) communications [2], [3]. To meet these massive connectivity demands, 5G sets critical targets, including the 1000 times increase in the data rate, below 100 ms latency, 50% network cost reduction, and 95% availability in bad coverage locations [4]–[6]. To this end, wireless technologies have emerged to enhance the system throughput and improve spectral efficiency. These include (multiple input multiple output) MIMO and massive MIMO systems [7], relaying cooperative communications [8], cognitive radio networks [9], full-duplex wireless [10], and millimeter-wave systems [11]–[13]. Transceivers for these systems require a baseband section, multiple radio frequency front-ends, multiple antennas, and more. Design criteria are to maximize the diversity and multiplexing gain, guarantee the quality service of users, minimize the out-of-band emission, achieve a predefined maximum rate, minimize the outage probabilities, and optimize the data detection performance.

However, the ongoing development of highly flexible radio transceivers for mass-market applications requires cost efficiency. This factor depends on power consumption and chip areas, e.g., the cost-efficiency of 5G networks should be 10-100X smaller than 4G networks [14]. Another issue is operational feasibility. For example, sensors in Internet-of-Things (IoT) networks [15] require an uninterrupted power supply for a long lifetime. Frequent charging of sensor batteries may not be feasible. These requirements imply that the power consumption of their transceivers should be low. These networks may cover a wide area with high accuracy, requiring many sensors; thus, their circuits should be low cost and small. Another example is cell densification in future mobile networks for supporting more users, which requires

This article has been accepted for publication in a future issue of this journal, but has not been fully edited. Content may change prior to final publication. Citation information: DOI 10.1109/ACCESS.2021.3101845, IEEE Access

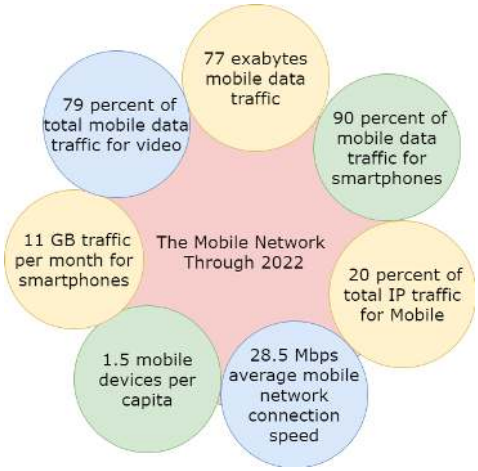

FIGURE 1: Mobile data traffic forecast for 2022 [1].

low complexity and inexpensive transceivers. These may use non-ideal low-cost radio frequency (RF) components to address these requirements with a long operational lifetime. However, more imperfections can happen with such components because of manufacturing errors, aging, and other reasons, thus introducing RF impairments.

Thus, RF impairments in transceivers impact multiple specifications, e.g., adjacent channel leakage power ratio (ACLR), error vector magnitude (EVM), sensitivity power levels, and in-band and out-of-band blocking, and others. For example, Table. 1 lists the requirements of a wide-area base station in different standards and systems, namely, global system for mobile communications (GSM)/enhanced data rate for GSM evolution (EDGE), universal mobile telecommunications system-frequency-division duplexing (UMTS-FDD), evolved universal terrestrial radio access (E-UTRA), narrowband-IoT (NB-IoT), and new radio (NR) for 5G systems [16]–[18]. To meet the requirements of these and other standards, it is necessary to mitigate the impact of RF impairments.

In terms of generating RF impairments, one of the most critical analog components is the oscillator, which generates a reference signal for frequency and timing synchronization. However, non-ideal imperfections and time-domain instabilities of the oscillator are the sources of significant impairments, including phase noise (PN), carrier frequency offset (CFO), and in-phase (I) and quadrature-phase (Q) imbalance - Fig. 2. These impairments cause in-band and out-of-band distortions. In-band distortions fall inside the operating bandwidth and destroy the system's performance, e.g., they destroy the orthogonality of subcarriers in orthogonal frequency division multiplexing (OFDM) systems and introduce inter-carrier interference (ICI). In contrast, out-of-band distortions fall outside the operating bandwidth. For instance, spectrum spreading results in interference to adjacent channels. Due to these distortions, the system performance significantly degrades. This degradation can manifest in several ways: (1) a decrease in the signal-to-noise ratio (SNR) and increase the bit error rate (BER), (2) an increase of the EVM because of phase and amplitude distortions in the signal constellation, (3) a decrease in achievable rates and increase in outages, and (4) a reduction in the quality of channel estimations. Thus, the impacts of RF impairments on wireless transceivers are substantial.

A. PN

PN occurs when the oscillator cannot generate pure sinusoidal waves with the Dirac spectrum. This spectral widening happens because of rapid, short-term, random fluctuations in the carrier wave phase generated by oscillators in up-conversion or down-conversion processes of the baseband signal and radio frequency chain. Fig. 2a illustrates an ideal oscillator with the Dirac spectrum versus the real oscillator with PN. Engineers typically specify PN in the frequency domain over one Hz bandwidth at an offset of Δf from the carrier. The PN power over this bandwidth is normalized relative to the carrier power – dBc/Hz. For example, in GSM applications, the oscillator's PN should fall below -115 dBc/Hz at 600 kHz offset [19].

PN causes dramatic changes in the frequency spectrum and timing properties of the oscillator output. Specifically, PN widens the power spectral density (PSD) to either side of a signal (Fig. 2a), which may cause adjacent channel interference (ACI). For example, the spectrum seen at the receiver is the convolution of the passband received signal spectrum and the local oscillator spectrum. However, the latter spreads because of PN, leading to spectral spreading. In Fig. 3, the resulting spreading can inject the interference signals into the signal bandwidth, which degrades the system's performance. Moreover, PN is a fundamental challenge for multicarrier signals such as OFDM because it destroys the orthogonality among the subcarriers. This results in inter-channel interference, phase errors on all subcarriers, and ICI among subcarriers.

Furthermore, a critical effect of PN is the induced time variation of the channel. That is, the effective channel seen by the receiver becomes time-varying, and the transmit signal constellation rotates from symbol to symbol. PN also destroys the coherency between the channel estimate and the actual channel gain during the data frame duration. In sum, all these effects will degrade wireless system performance, i.e., reducing the effective SNR, limiting the BER, and reducing data rates. For all these reasons, characterizing PN in practical applications is essential. PN estimation and compensation are vital for accurate data detection.

B. CFO

The CFO occurs when the down-converting local oscillator in the receiver does not perfectly synchronize with the received signal's carrier. Two effects cause this frequency mismatch, namely local oscillator errors and Doppler shifts. First, local oscillator errors occur because of the local oscillators' different physical properties and errors, such that they can never oscillate at an identical frequency. Wireless standards

This article has been accepted for publication in a future issue of this journal, but has not been fully edited. Content may change prior to final publication. Citation information: DOI 10.1109/ACCESS.2021.3101845, IEEE Access

TABLE 1: Wide area base station specifications [16]–[18]

	Standards and Systems				
Requirements	GSM/EDGE (2G)	UMTS-FDD (3G)	E-UTRA (LTE-4G)	NB-IoT (5G)	NR-FR1[a] (5G)
Channel raster[b]	200 kHz	200 kHz	100 kHz	100 kHz	100 kHz
Channel spacing	200 kHz	5 MHz	$(BW_1+BW_2)/2$[c]	$(BW_1+BW_2)/2$	$(BW_1+BW_2)/2$
Tx-output power dynamics (dB) [Channel bandwidth]	$\geq P_m - 2N$[d]	≥18	≥16.9 [10 MHz] ≥18.7 [15 MHz] ≥20 [20 MHz]	≥6	≥10.4 [10 MHz] ≥12.5 [15 MHz] ≥13.8 [20 MHz]
Tx-EVM (%) [Modulation type]	≥9 [8-PSK]	≥17.5 [QPSK] ≥12.5 [16-QAM]	≥17.5 [QPSK] ≥12.5 [16-QAM] ≥8 [64-QAM]	≥ 17.5 [QPSK]	≥17.5 [QPSK] ≥12.5 [16-QAM] ≥8 [64-QAM]
Tx-Time alignment	-	0.25-0.5 T_c(chip duration)	<65 ns	<65 ns	<65 ns
Tx- spurious emissions[e] (dBm) [Measurement bandwidth]	-36 [10 kHz] -30 [1 MHz]	-36 [10 kHz] -30 [1 MHz]	-36 [10 kHz] -30 [1 MHz]	-36 [10 kHz] -30 [1 MHz]	-36 [10 kHz] -30 [1 MHz]
Tx-ACLR[f]	-	-15 dBm/MHz	-15 dBm/MHz	-15 dBm/MHz	-13 dBm/MHz
Rx-sensitivity power level, P_{refsens}[g](dBm) [channel bandwidth or data rate]	-104	-121 [12.2 kbps]	-106.8 [1.4 MHz] -103 [3 MHz] -101.5 [5;10;15 MHz]	-101.7 [200 kHz] (sub-carrier spacing 15 kHz)	-101.5 [5;10;15 MHz] (sub-carrier spacing 15 kHz)
Rx-dynamic range[h] [Interferer power]	-	12.2 kbps [-73 dBm]	-70.2 dBm [-76.4;-77.7;-79.5 dBm]	-99.7 dBm [-96 dBm]	-70.7 dBm [-77.5;-79.3;-82.5 dBm] (sub-carrier spacing 15 kHz)
Rx-in-band blocking[i] [Interferer power]	P_{refsens}+3 dB [-49 dBm]	P_{refsens}+6 dB [-49 dBm]	P_{refsens}+6 dB [-49 dBm]	P_{refsens}+6 dB [-49 dBm]	P_{refsens}+6 dB [-49 dBm]
Rx-out-of-band blocking[j] (CW carrier) [Interferer power]	P_{refsens}+3 dB [-15 dBm]	P_{refsens}+6 dB [-15 dBm]	P_{refsens}+6 dB [-15 dBm]	P_{refsens}+6 dB [-15 dBm]	P_{refsens}+6 dB [-15 dBm]

[a] FR1 indicates the frequency range of 410 MHz – 7125 MHz
[b] The centre frequency has to be an integer multiple of this value
[c] BW_1 and BW_2 indicate the channel bandwidths of the two respective carriers.
[d] P_m is the maximum power that depends on the modulation type and N is the radio frequency power step.
[e] Maximum interferer level at an offset from the carrier
[f] ACLR is the ratio of the filtered mean power centred on the assigned channel frequency to the filtered mean power centred on an adjacent channel frequency
[g] the minimum mean power received at the antenna connector at which a throughput requirement shall be met for a specified reference measurement channel
[h] A measure of the capability of the receiver to receive a wanted signal in the presence of an interfering signal inside the received channel bandwidth
[i] A measure of the receiver ability to receive a wanted signal in the presence of an unwanted interferer inside of the operating band
[j] A measure of the receiver ability to receive a wanted signal in the presence of an unwanted interferer out of the operating band

specify the oscillator precision tolerance, e.g., the IEEE 802.11a OFDM-based wireless local area network (WLAN) requires an error less than ±20 parts per million (PPM), which results that the CFO should be in the range from -40 PPM to +40 PPM [20]. For example, if the transmit and the receive oscillators run at a frequency that is 20 PPM above and 20 PPM below the identical carrier frequency, receptively, the received baseband signal will have a CFO of 40 PPM. For a carrier frequency of 5.2 GHz, the CFO is thus up to ±208 kHz. Second, the relative motion between the transmitter and the receiver shifts the carrier frequency seen by the receiver, which is the Doppler shift. For example, when a car moves at v =350 km/h, and wireless carrier operates at f_c =2.4 GHz frequency point, the maximum Doppler frequency offset will be over $f_d = \frac{v f_c}{c} = 800$ Hz, where c is speed of light. For several practical cases, Table. 2 shows the normalized CFO and Doppler frequency for three different commercial systems.

CFO causes a rotation and an attenuation of transmit symbols and thus introduces intersymbol interference (ISI) and ICI in single-carrier (SC) and multicarrier systems. Since the CFO shifts the signal in the frequency domain, it breaks the mutual orthogonality between OFDM subcarriers, and each subcarrier interferes with the remaining subcarrier signals. Thus, OFDM systems are especially susceptible to the CFO. If the receiver does not estimate correctly and compensate the CFO before data detection, the BER of OFDM systems will increase. Moreover, [22] shows that in the presence of CFO, increasing the number of training symbols cannot improve the mean squared error (MSE) performance of channel estimation, and CFO destroys the functionality of the channel estimator. Therefore, it is essential to characterize the impacts of CFO on practical systems, estimate CFO, and compensate for it.

C. IQ IMBALANCE

The IQ modulator and demodulator are part of the RF front-end of wireless transceivers to transform the complex baseband signals to passband centered at the carrier frequency and vice versa. There are two widely used receiver

This article has been accepted for publication in a future issue of this journal, but has not been fully edited. Content may change prior to final publication. Citation information: DOI 10.1109/ACCESS.2021.3101845, IEEE Access

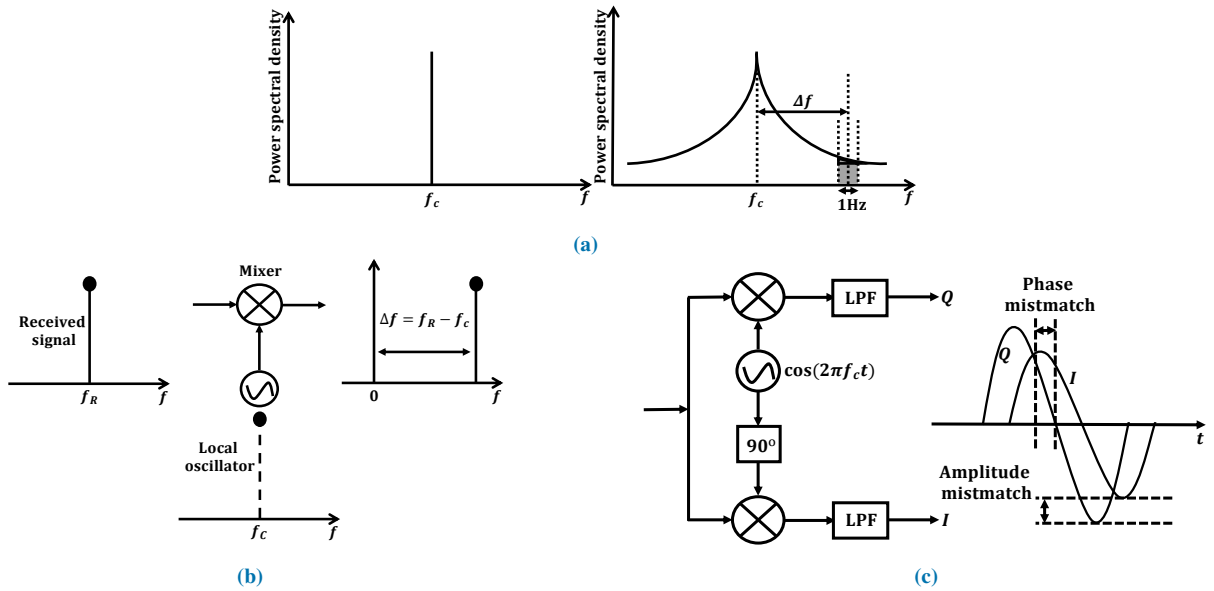

FIGURE 2: RF impairments: PN, CFO and IQ imbalance. (a) Spectral spreading due to PN, (b) CFO between the received signal and the local oscillator and (c) IQ demodulator with amplitude and phase mismatches.

TABLE 2: Doppler frequency and normalized CFO [21]

System	Carrier frequency (f_c)	Subcarrier spacing (Δf)	Velocity (ν)	Maximum Doppler frequency (f_d)	Normalized CFO (ϵ)
DMB	375 MHz	1 kHz	120 km/h	41.67 Hz	0.042
3GPP	2 GHz	15 kHz	120 km/h	222.22 Hz	0.0148
Mobile WIMAX	2.3 GHz	9.765 kHz	120 km/h	255.55 Hz	0.0263

structures: superheterodyne and direct-conversion (or zero-intermediate frequency (IF)) – Fig. 4. The superheterodyne receiver performs two stages to down-convert an RF received signal to a baseband signal. The first stage transforms the received signal into a low-frequency IF signal using a low-noise amplifier, a mixer, and band-pass filters. The resulting IF signal is converted to baseband signal through the IQ demodulator with an in-phase local oscillator, quadrature-phase local oscillator, two mixers, and low-pass filters.

In contrast, the direct-conversion receiver translates the RF signal directly to the baseband signal in one stage through the IQ demodulator. Compared to the superheterodyne structure, the direct-conversion scheme is more attractive for RF designs. For example, IEEE 802.11a OFDM-based systems

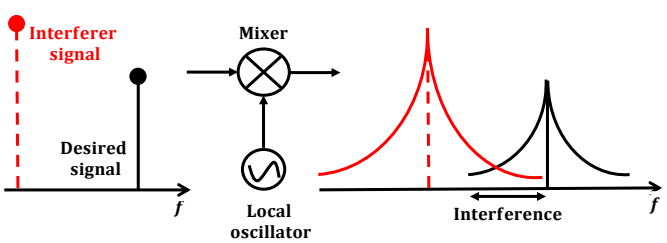

FIGURE 3: PN injecting interference signals into the signal bandwidth.

deploy direct-conversion receivers because they eliminate the IF stage, avoid the image-rejection filter, and have fewer off-chip components (e.g., costly IF filters). These factors enable easier integration with lower cost, area, and power consumption. However, direct conversion suffers from mismatches between the I and Q branches.

Ideal IQ modulators and demodulators provide two orthogonal channels for the complex signal's real and imaginary parts. However, mismatches between I and Q branches destroy this orthogonality and lead to IQ imbalance, which degrades the signal quality. We can attribute the mismatches to fabrication process variations, including doping concentration, oxide thickness, mobility, and geometrical sizes over the chip [23]. One can divide the mismatches causing the IQ imbalance into two groups regarding their influences: 1) frequency-flat IQ imbalance causing imperfect 90 phase difference and unequal amplitudes of the I and Q local oscillators, which is constant over the signal bandwidth, 2) frequency-selective IQ imbalance causing the component mismatching in I and Q branches, e.g., imperfect matched low-pass filters, which has different frequency responses over the signal bandwidth. Note that the frequency-selective IQ is severe in wideband systems.

These IQ imbalances result in harmful mirror interference and degrade the system's performance, e.g., BER, Signal-

to-interference plus-noise ratio (SINR), capacity, and EVM. For example, in SC systems, IQ imbalance in transmitter and receiver causes ISI on neighboring signals. In multicarrier systems, like OFDM, IQ imbalance generates ICI terms on mirror subcarriers (the mirror subcarrier of the k-th OFDM subcarrier is -k). Moreover, IQ imbalance degrades the performance of channel estimation techniques by introducing mirror interference terms. Thus, one must compensate IQ imbalance to meet the requirements of standards, e.g., the specifications of 3-rd Generation Partnership Project (3GPP) LTE/LTE-Advanced radio systems limit the minimum attenuation for the in-band image component in the transmitter to 25 dB or 28 dB [24]. Accordingly, we can calibrate IQ imbalance in the analog domain [25]–[27], e.g., [25] reduces IQ mismatches by increasing the physical size of the devices. However, these techniques have drawbacks, such as increasing the compensation power and a long calibration process and can not meet the required specifications for systems alone. Hence, IQ imbalance estimation and compensation algorithms in the digital domain based on signal processing techniques can benefit.

D. CONTRIBUTION AND ORGANIZATION

We comprehensively survey the three primary RF impairments – PN, CFO, and IQ imbalance in wireless transceivers. So what is the need for this survey? There are several reasons. First, Table. 3 shows that no previous survey paper comprehensively treats all these three together. Second, existing surveys have also been published a while ago and thus do not cover emerging wireless technologies and the impact of RF impairments on them. Hence, an up-to-date survey is critically needed. Third, this paper is the first survey paper that provides a comprehensive overview of all RF impairments to the best of our knowledge. It discusses modeling and impacts of the RF impairments and explores

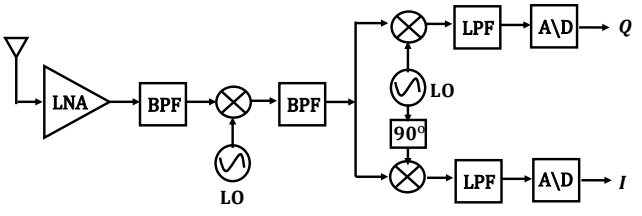

(a) Superheterodyne

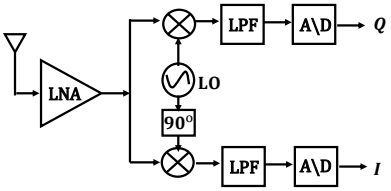

(b) Direct-conversion

FIGURE 4: (a) Superheterodyne and (b) direct-conversion receivers with the IQ demodulator.

TABLE 3: Previous survey articles

Publication	RF impairment(s)
[28] (2014)	This paper studies PN in different oscillator topologies but focuses on circuit theory.
[29] (2015)	This paper discusses PN mitigation techniques for OFDM only but without exploring estimation schemes.
[30] (2015)	This paper discusses CFO estimation for OFDM but without exploring compensation schemes.
[31] (2016)	This paper reviews CFO in OFDM and MIMO OFDM systems over period 2010–2014. However, more efficient, recent techniques are not reviewed. Moreover, it does not cover CFO issues in emerging technologies, e.g., backscatter communications and roconfigurable intelligent surfaces, and others.
[32] (2016)	This paper reviews the effects of IQ imbalance on OFDM and MIMO OFDM but no compensation schemes.
[33] (2005)	This paper studies the impacts of PN and IQ imbalance on OFDM and discusses estimation and compensation schemes. However, it is now more than 15 years old.

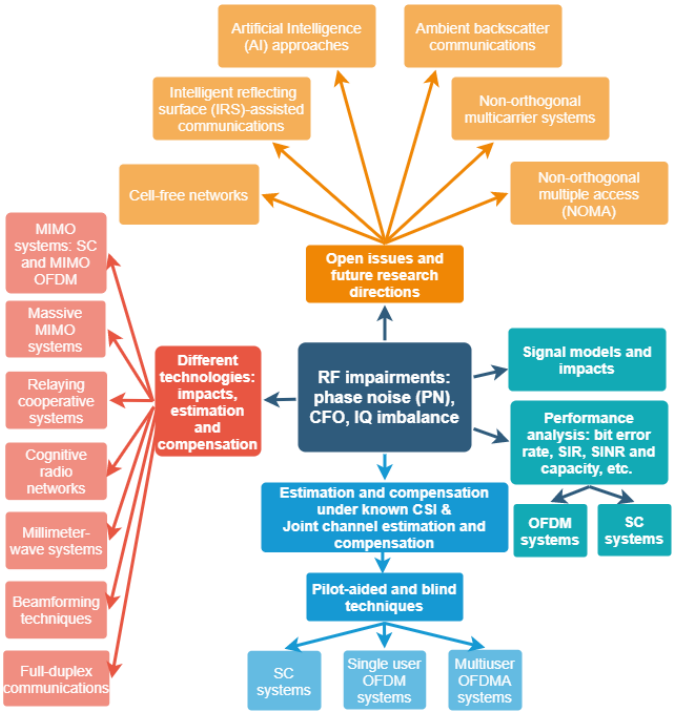

FIGURE 5: Summary of main contributions.

their estimation and compensation techniques for emerging wireless technologies. Specifically, the main contributions of this survey can be summarized as follows:

- We describe baseband equivalent models for the impairments, which characterize their influence on the baseband signal. Next, we discuss their impacts on the performance of the SC and OFDM systems. We mainly focus on OFDM because (a) current 4G systems widely use OFDM, and (b) being a multicarrier waveform,

OFDM is especially vulnerable to RF impairments.

- Following that, we review the estimation and compensation of the impairments in SC, single-user OFDM, and multiuser orthogonal frequency-division multiple access (OFDMA) systems. Moreover, we explore the joint estimation and compensation of channels and the RF impairments. We could classify the existing estimators as pilot-aided and blind techniques (semi-blind estimators are a special case of pilot-aided estimators). The former relies on periodically transmitted training symbols or a combination of pilot and data symbols at the expense of bandwidth efficiency. Moreover, they typically require several iterations for convergence, increasing the computational complexity. In the latter ones, the principal idea is to exploit signals' structural and statistical properties without using prior knowledge at the receiver. These techniques improve spectral efficiency since they do not transmit many pilots, but they often require averaging over numerous data symbols for satisfactory performance. Furthermore, they may suffer from ill convergence problems, high complexity, and relatively poor performance in comparison with the pilot-aided ones [34].
- Next, we review RF impairment effects on the emerging and/or future technologies, such as MIMO (SC, MIMO OFDM, and multiuser MIMO OFDMA), massive MIMO, cognitive radio networks, millimeter-wave systems, relaying cooperative communication, beamforming techniques, and full-duplex communications. Furthermore, we survey the relevant estimation and compensation techniques.
- Finally, we mention open issues, challenges, and future research directions. The necessity of evaluating the impairments in the state-of-the-art technologies for 5G networks such as cell-free massive MIMO communications, non-orthogonal multiple access (NOMA), ambient backscatter communications, and intelligent reflecting surface (IRS)-assisted communications is discussed. In addition, we review the works on non-orthogonal multicarrier systems such as filter bank multicarrier (FBMC) [35], [36], which are potential alternatives for OFDM systems. Moreover, the advantages of using artificial intelligence (AI) algorithms, including deep learning and reinforcement learning, are highlighted in the estimation and compensation of the impairments.

Fig. 5 outlines the summary of this survey's main contributions. The survey is organized as follows. We discuss PN, CFO, and IQ imbalance in Section II, Section III, and Section IV, respectively. Each section presents the impairment, signal models, and impacts. We review the studies that evaluate the systems' performance with RF impairments. We also discuss the estimation and compensation of the impairment. Finally, we review the impacts of the impairment in the emerging technologies. Section V addresses open issues, challenges, and future research directions. Section VI concludes the survey. Table 4 lists the abbreviations.

TABLE 4: List of abbreviations

Acronym	Definition
ACI	Adjacent channel interference
ACLR	Adjacent channel leakage power ratio
AF	Aamplify-and-forward
AI	Artificial intelligence
AP	Access point
AWGN	Additive white Gaussian noise
BEP	Bit error probability
BER	Bit error rate
BPSK	Binary phase-shift-keyed
CCI	Co-channel interference
CDF	Cumulative distribution function
CDMA	Code-division multiple access
CFO	Carrier frequency offset
CMOS	Complementary metal–oxide–semiconductor
CPFSK	Continuous-phase frequency-shift keying
CRLB	Cramér-Rao lower bound
CSI	Channel state information
DF	Decode-and-forward
DFT	Discrete Fourier transform
DS-CDMA	Direct-sequence code division multiple access
EM	Expectation-maximization
EVM	Error vector magnitude
FBMC	Filter bank multicarrier
FFT	Fast Fourier transform
FSK	Frequency-shift-keyed
GFDM	Generalized frequency division multiplexing
GSM	Global system for Mobile Communications
ICI	Intercarrier interference
IoT	Internet-of-Things
IQ imbalance	In-phase (I) and quadrature phase (Q) imbalance
IRS	Intelligent reflecting surface
ISI	Intersymbol interference
LMMSE	Linear minimum mean square error
LMS	Least-mean-squares
LS	Least-squares
LTE	Long Term Evolution
MAP	Maximum a posteriori
MF	Matched-filter
MIMO	Multiple-input multiple-output
MISO	Multiple-input single-output
ML	Maximum likelihood
MMSE	Minimum mean squared error
MRC	Maximum-ratio combining
MRT	Maximum-ratio transmission
MSE	Mean squared error
MSK	Minimum shift keying
MUI	Multiuser interference
NOMA	Non-orthogonal multiple access
OFDM	Orthogonal frequency division multiplexing
OFDMA	Orthogonal frequency division multiple access
OQAM	Offset quadrature amplitude modulation
PDF	Probability density function
PLL	Phase locked loop
PN	Phase noise
PPM	Parts per million
PSD	Power spectral density
QAM	Quadrature amplitude modulation
SAGE	Space-alternating generalized expectation-maximization
SC	Single-carrier
SC-FDE	Single-carrier frequency-domain equalization
SER	Symbol error rate
SFO	Sampling frequency offset
SI	Self-interference
SIC	Successive interference cancellation
SIMO	Single-input multiple-output
SINR	Signal-to-interference plus-noise ratio
SISO	Single-input single-output
SNR	Signal-to-noise ratio
TDMA	Time division multiple access
UE	User equipment
VCO	Voltage control oscillator
ZF	Zero-forcing

This article has been accepted for publication in a future issue of this journal, but has not been fully edited. Content may change prior to final publication. Citation information: DOI 10.1109/ACCESS.2021.3101845, IEEE Access

II. PN

In this section, we first describe the PN signal models and then discuss their harmful effects. Second, we review the current works on the performance of SC and OFDM systems with the PN impairment. Third, we comprehensively survey the studies related to PN's estimation and compensation in SC, single-user OFDM, and multiuser OFDMA systems. Moreover, we review joint channel and PN estimation and compensation, discuss PN's impacts in emerging technologies, and present a review of existing works.

A. SIGNAL MODEL AND IMPACTS

The output signal of a noisy, complex oscillator can be modeled as

$$C_{osc} = e^{j(2\pi f_c t + \phi(t))}, \tag{1}$$

where f_c is carrier frequency and $\phi(t)$ is the PN. The PN is generally described in the frequency domain through its PSD in dBc/Hz. In practice, two types of oscillators are used, 1) free-running oscillator [37], [38], and 2) phase-locked loop (PLL) synthesizer [39]. Free-running oscillators operate without a PLL. In these oscillators, the generated phase is modeled as the accumulation of random frequency divisions. However, in PLL synthesizers, a close-loop tracks the phase variations of the carrier signal. In [40], [41], theory and numerical techniques for characterizing the PN in practical oscillators are proposed. In these works, white-noise sources (e.g., shot and thermal noise) are considered for oscillators. However, other types of noise sources that have colored spectral density (e.g., $1/f$ and burst noise) are not considered, which significantly affect practical oscillators' PN performance. Thus, [42], [43], characterize stochastic PN in oscillators due to colored noise sources. Furthermore, this work extends the results to both white and colored noise sources. The following characteristics of $\phi(t)$ are addressed for the two types of oscillators.

1) Free-running oscillators

Since these have no synchronization input, such as a reference clock, they are called free-running. Since they run without a reference, their PN depends on the startup conditions [28]. The free-running oscillator model is simple and is widely used for simulations and mathematical analyses. PN generated by a free-running oscillator is typically assumed a Wiener process with white noise sources (following Brownian motion). Accordingly, the PN can be modeled as [44]

$$\phi(t) = \sqrt{\nu} W(t), \tag{2}$$

where ν is a constant, which describes spectral spreading in a noisy oscillator with white noise sources [42] and $W(t)$ indicates the standard Brownian motion or Wiener process. The Wiener process is a real-valued continuous-time stochastic process where the difference $W(t_2) - W(t_1)$ is normally distributed with mean zero and variance $|t_2 - t_1|$; that is, $W(t_2) - W(t_1) \sim \mathcal{N}(0, |t_2 - t_1|)$. Therefore, single parameter ν completely describes the PN process. The variance of (2) can be written as [37], [44]

$$\sigma_\phi^2(t) = \nu t, \tag{3}$$

which is linearly increasing with time. In order to characterize this PN model, the decay rate of the PSD is commonly deployed. The single-sided PSD of the free-running oscillator signal C_{osc} in (1) around the carrier frequency has a Lorenzian spectrum [37], which is given by

$$L(f) = \log_{10}\left(\frac{\nu}{(2\pi f)^2 + (\frac{\nu}{2})^2}\right). \tag{4}$$

With (4), we see that the 3 dB bandwidth of the PSD is given by $\beta = \frac{\nu}{4\pi}$. This parameter is commonly used for free-running oscillator characterizations with white noise sources.

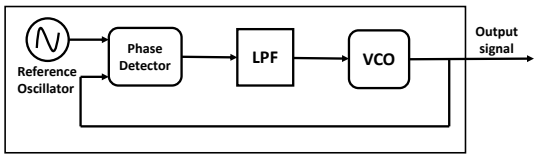

FIGURE 6: PLL block diagram.

2) PLL synthesizer

Communication systems widely deploy the PLL as a frequency synthesizer. The basic block diagram of PLL (Fig. 6) comprises multiple interconnected components in a negative feedback configuration. The phase detector compares the voltage control oscillator (VCO) phase and that of the reference oscillator. The filtered phase difference controls the VCO's frequency. The reference oscillator and VCO can be modeled as free-running oscillators. In [45], the author proposes a stochastic differential equation for the PLLs with white noise sources and a Brownian motion phase deviation in the reference signal. In a locked state, the phase of PLL can be written as a summation of the phase of the reference signal as a Brownian motion process and one component of a multidimensional Ornstein-Uhlenbeck process. However, the effects of flicker noise (colored noise) are not considered, e.g., low-quality complementary metal-oxide-semiconductor (CMOS) PLLs suffer from significant levels of flicker noise [46], [47]. The effect of flicker noise on the PN performance is visible above the PLL bandwidth [48]. A linear time-invariant phase domain PLL model is considered in [49] that assumes white and flicker noises for free-running VCO and white noise for free-running reference oscillator. According to [42], the single-sided PSD of a baseband equivalent free-running VCO, specified in dBc/Hz, in the presence of white and flicker noises is derived as

$$L(f) = 10\log_{10}\left(\frac{f_c^2(c_w + c_f S_f(f))}{\pi^2 f_c^4 (c_w + c_f S_f(f))^2 + f^2}\right), \tag{5}$$

where the frequency independent c_w and c_f coefficients are the constants describing white and flicker noise perturbations, respectively. Furthermore, $S_f(f)$ is the PSD of flicker noise which is described as a stationary process in the form

This article has been accepted for publication in a future issue of this journal, but has not been fully edited. Content may change prior to final publication. Citation information: DOI 10.1109/ACCESS.2021.3101845, IEEE Access

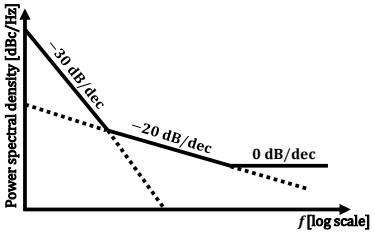

(a) Free-running oscillator

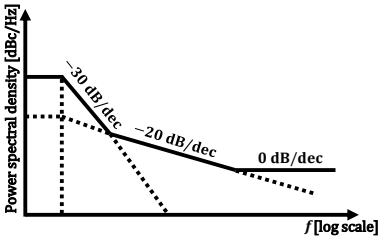

(b) PLL synthesizer

FIGURE 7: PN PSD of free-running oscillator and PLL synthesizer.

of

$$S_f(f) = \frac{1}{|f|} - \frac{4}{2\pi f}\tan^{-1}\left(\frac{\gamma_c}{2\pi f}\right), \tag{6}$$

where γ_c indicates deviation frequency from the flicker PSD $1/f$ slope. Note that γ_c, c_w and c_f coefficients can be obtained from two single point single-sided PSD measurements of VCO [42], [49]. In addition, we can derive the single-sided PSD of a baseband equivalent free-running reference oscillator with (5) without flicker noise, $S_f(f) = 0$. Moreover, the authors in [49] combine the PSD of VCO and reference oscillator and derive the output PSD of a 3-rd order charge-pump PLL synthesizer.

Note that the Lorentzian spectrum for the free-running oscillator in (4) is based on a white noise source without considering the flicker noise sources. However, (5) is the general single-sided PSD of a free-running oscillator in the presence of both white and flicker noise sources. For example, without considering flicker noise $S_f(f) = 0$ and by substituting the constant $\nu = 4c_w(\pi f_c)^2$ in (5), we can derive the Lorentzian spectrum (4).

To recap, PN of the free-running oscillator can be modeled as a superposition of three independent processes [51]

$$\phi(t) = \phi_2(t) + \phi_1(t) + \phi_0(t), \tag{7}$$

where $\phi_2(t)$ indicates PN model with -30 dB/decade slope caused by flicker noise, $\phi_1(t)$ shows PN model with -20 dB/decade slope caused by white noise, and $\phi_0(t)$ models the flat noise floor originated by thermal noise. The PSD of independent processes in (7) can be represented as power-law spectra [52]: $S_{\phi_2} = K_2/f^3$, $S_{\phi_1} = K_1/f^2$, and $S_{\phi_0} = K_0$, where PN levels K_2, K_1 and K_0 can be find through measurements. Fig. 7 illustrates the PN PSD of the free-running oscillator and PLL synthesizer. We assume

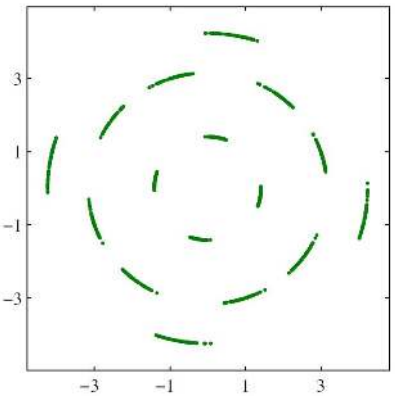

FIGURE 8: SC 16-QAM signal with PN. Horizontal and vertical axis indicates I and Q components, respectively [50].

that the PN of the reference oscillator is negligible compared to the PN of free-running VCO, which is proved in [53]. Because of the negative feedback loop, the PLL synthesizer behaves like a high-pass filter compared to the free-running oscillator. Below a certain frequency, it approaches a constant value.

PN can be generated in local oscillators of both transmitter and receiver. It introduces the phase rotation, ISI, and ICI terms that degrade the system's performance, e.g., BER, achievable rate, and EVM. For example, Fig. 8 illustrates the phase error impact of PN on the constellation of an SC system with 16-quadrature amplitude modulation (QAM) [50]. Moreover, PN speeds the spectrum, which results in out-of-band emission and interchannel interference. Fig. 9 shows the spectrum spreading for an OFDM system. To gain insight into the impact of PN, we assume an OFDM system over Additive white Gaussian noise (AWGN) channel with perfect frequency and timing synchronization. The received N-OFDM signal in the k-th subcarrier can be expressed as

$$r[k] = J[0]x[k] + \sum_{l=0,\, l\neq k}^{N-1} J_{k-l}x[l] + w[k], \tag{8}$$

where $x[k]$ is the data symbol transmitted on the k-th subcarrier and $w[k]$ indicates the AWGN. Furthermore, $J[k]$ is the k-th frequency-domain coefficient of $\{e^{j\phi[p]}\}$, $p = 0, 1, .., N-1$, given by

$$J[k] = \frac{1}{N}\sum_{p=0}^{N-1} e^{j\phi[p] - j2\pi pk/N}, \tag{9}$$

where $\phi[p]$ sampled random variables that represent the PN at sample instant p. According to (8), PN causes two types of distortions: 1) common phase error, which is the same constant phase rotation for all subcarriers, denoted by $J[0]$, and 2) ICI, which refers to the interference of neighboring subcarriers on each other, represented by the second term in the right-hand side of (8).

Moreover, in Fig. 10, we plot the BER of an OFDM system with 128 subcarriers versus SNR for different values of PN

This article has been accepted for publication in a future issue of this journal, but has not been fully edited. Content may change prior to final publication. Citation information: DOI 10.1109/ACCESS.2021.3101845, IEEE Access

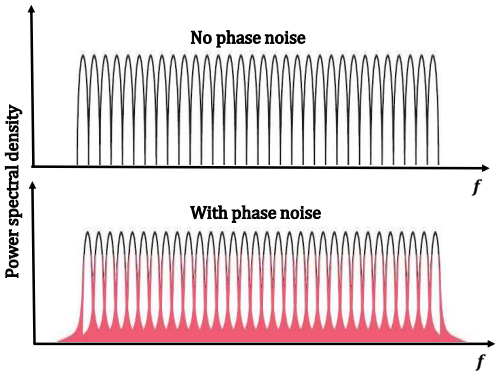

FIGURE 9: Spectrum spreading for a OFDM due to PN.

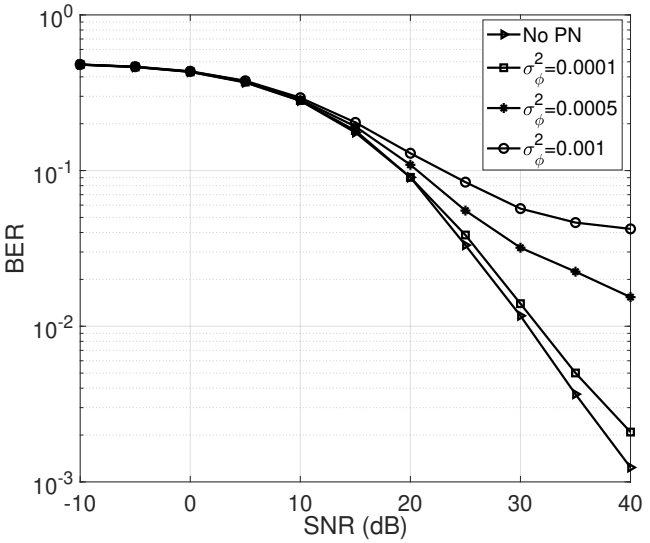

FIGURE 10: BER versus SNR for an OFDM system with different values of PN variance.

variance σ^2_ϕ. Furthermore, ITU outdoor multipath channel model A is considered with power delay profile of 0 dB, -1 dB, -9 dB, -10 dB, -15 dB and -20 dB for delays of 0, 3, 7, 11, 17 and 25 samples. We see that the increasing variance of PN boosts the power of interference terms, and the BER degrades.

B. PERFORMANCE ANALYSIS

Herein, we first review performance analyses of SC systems and multi-carrier (e.g., OFDM) systems under PN. The authors in [54], [55] consider an SC system with a PLL receiver in the presence of continuous wave interference over the AWGN channel. They derive the probability density function (PDF) of phase error regarding the ratio of interference to the desired signal power and the loop SNR. They show that with an interfering signal, the loop phase error variance will increase. On the other hand, the effects of PN spectral characteristics on decoding performance, especially BER, in coherent digital systems, binary phase-shift-keyed (BPSK), noncoherent digital systems, and M-array frequency-shift-keyed (FSK), are studied in [56] and [57], respectively. These works illustrate that PN system performance degradation will be more significant in high band carriers. As well, the bit error probability (BEP) of M-QAM with PN under AWGN and flat-fading channels is studied in [58]. This work considers a PLL oscillator and derives the bit error floor (BEF). It shows that in the high input SNR regime, the impact of PN on error probability becomes dominant.

On the other hand, PN impacts on multicarrier code-division multiple access (CDMA) are investigated in [59]–[61]. Multicarrier CDMA combines multicarrier (e.g., OFDM) and CDMA, which simultaneously supports multiple users over the same frequency band. It spreads data stream over different subcarriers by deploying spreading code in frequency-domain. References [59], [60] consider the cellular downlink and a free-running oscillator (2) and derives the error probability. PN's effect becomes more pronounced as the number of tones increases. Additionally, [61] investigates PN's effect with a PLL oscillator and shows the SNR performance degradation. The PN effects on multicarrier CDMA are also studied in [62], [63]. Coherent detection with BPSK modulation and a practical PLL oscillator is considered. Upper bound or approximation of the PN variance in a subcarrier and the ICI are derived. Moreover, PN significantly degrades the performance of the system, especially BER.

OFDM as a multicarrier waveform exhibits a significant sensitivity to the PN of oscillators. The BER of an OFDM system with PN is evaluated in [64], [65], and exact error probability formulas are derived. A free-running oscillator is considered, which models PN as a Wiener process. PN significantly degrades the BER performance, and the degradation increases with the increasing number of subcarriers. Furthermore, PN degrades SNR more in OFDM than in SC systems. The error terms induced by the PN on the OFDM systems are common phase rotation and the ICI or loss of orthogonality [66]. Moreover, the study in [67] investigated the error terms' statistical behavior and computed each error term's variance for a free-running oscillator.

In [68], BER and capacity of an OFDM system affected by transmitter non-linearities, PN, channel estimation error, and frequency-selective channels are numerically studied. However, the capacity is not derived in closed-form and requires a numerical evaluation. Thus, authors in [69] study PN's effects on capacity and SINR of OFDM systems. They derive a closed-form statistical expression for the distribution of the ICI. Note that both [68] and [69] consider the free-running oscillator, and their results are limited to the Wiener PN.

The investigation [70] analyzes the OFDM system's rate in the presence of practical PLL oscillators. Moreover, ICI power distribution is derived as a sum of correlated gamma random variables. Furthermore, the optimal subcarrier number for maximizing the rate for a given cyclic prefix length, SNR, and bandwidth is calculated. Besides, authors in [71] analytically study mutual information between the trans-

mitter and the receiver, at one arbitrary OFDM subcarrier, in the presence of PN, IQ imbalance, and the block-fading Rayleigh channel. Mutual information quantifies the reduction in uncertainty about one random variable when the value of another one is observed and vice versa. This work expresses the average mutual information as a series representation under uncorrelated and fully correlated mirror subcarriers. The mutual information saturates because of the impairments, even if the SNR approaches infinity. Moreover, the work in [72] derives the exact signal-to-interference ratio (SIR) of the OFDM system under the combined effects of PN, CFO, and time-selective channels where the coherence time of the channel is lower than the symbol period. The SIR decreases as the impairments increases.

Finally, in [73], impacts of PN on vector OFDM (V-OFDM) for single transmit antenna systems are investigated. OFDM and SC frequency-domain equalization (SC-FDE) are two special V-OFDM cases that adjust the number of vector blocks and the length of blocks. Note that LTE systems deploy OFDM/OFDMA (Orthogonal Frequency Division Multiple Access) in downlink for achieving high data rates, and SC-FDE/SC-FDMA (SC frequency division multiple access) is deployed in the uplink for reducing the cost. V-OFDM suffers from a typical vector block phase error and inter vector block carrier interference. Moreover, the authors derive a closed-form expression for the SINR of V-OFDM and show that the SINR eventually reaches a floor for significant PN variances. They illustrate that V-OFDM with PN outperforms OFDM without PN at a certain PN level.

C. ESTIMATION AND COMPENSATION

Harmful impacts of the PN on the wireless performance strongly motivate the estimation and compensation algorithms for mitigating PN effects. We can classify the existing estimators as pilot-aided or blind techniques. Pilot-aided PN estimators use well-designed training symbols or pilot and data symbols at the expense of bandwidth efficiency. Indeed, in this approach, prior knowledge in the receiver is deployed to estimate the PN. In contrast, in the blind methods, prior knowledge is not available in the receiver. These techniques improve spectral efficiency since many pilots' transmission is not required, while for satisfactory performance, they often require numerous symbols. PN estimators use a cost function of the general form of $f(\widetilde{\phi}, P, r)$ and the PN is estimated by $\hat{\phi} = \arg\min_{\widetilde{\phi}} f(\widetilde{\phi}, P, r)$, where $\widetilde{\phi}$, P and r indicate trail value of PN, training (pilot) sequence and received signal, respectively. Moreover, each type of estimator determines the cost function in different ways. It can be defined based on unbiased estimators, e.g., least-squares (LS), or biased estimators, e.g., minimum mean squared error (MMSE). In former ones, no prior knowledge about the statistics of unknown parameters, e.g., channel and phase noise, is required. In contrast, in the latter, second-order statistics and noise variance are required. Furthermore, it can be defined based on the PN trial value and the received signal, which relies on structural and statistical properties of signals and exhaustive search.

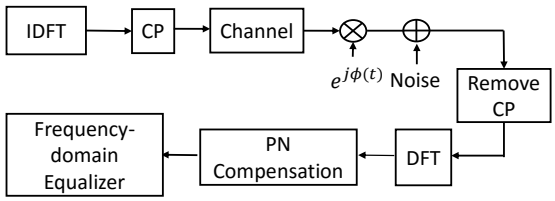

FIGURE 11: An OFDM system with PN compensation and frequency-domain equalizer .

Herein, we review PN estimation and compensation techniques for SC, single-user OFDM, and mutiuser OFDMA systems. Moreover, we highlight the joint estimation and compensation of channel and PN.

1) SC systems

PN estimation and cancellation problems in SC systems have been investigated to avoid the deleterious effects of PN. In [74], authors investigate pilot-aided carrier recovery in the presence of PN for SC systems over AWGN channels. They assume PN, which is generated by a free-running oscillator, affects the incoming carrier. Moreover, an optimal Wiener filter for PN estimation is proposed based on a sequence of equally spaced pilot symbols. The optimal filter is derived by minimizing the MSE between the carrier phase and the recovered phase. Furthermore, reference [75] proposes a PN estimation and compensation scheme for low-density parity-check coded M-QAM transmission systems over AWGN channels. Similar to [74], equally-spaced known pilot symbols are deployed. In this scheme, phase errors at the pilot positions are estimated, and then a Wiener filter interpolates them over the other positions.

Besides, the work in [76] addresses a pilot-aided PN estimation algorithm for free-running oscillators with colored noise sources. An SC system and AWGN channels are considered, and pilot symbols are used. This work proposes a maximum a posteriori (MAP)-based PN estimator. A modified soft-input extended Kalman smoother with a low-order autoregressive approximation of the colored PN is presented that performs close to the former estimator to reduce the complexity. On the other hand, authors in [77] propose a blind iterative algorithm for joint decoding and PN estimation and compensation in SC-FDMA systems by exploiting the low-pass nature of the PN process without prior knowledge about the exact PN model. Both the transmitter and the receiver sides have free-running oscillators. Moreover, the normalized MSE under CFO and joint transmit-receive PN are analyzed. The proposed scheme is robust to channel estimation errors.

2) Single-user OFDM systems

We divide the related studies into three categories: 1) pilot-aided estimation and compensation, 2) blind estimation and

compensation, and 3) joint channel and PN estimation and compensation. Note that two first ones assume knowledge of the channel is available in the receiver.

Pilot-aided estimation and compensation: The mitigation of common phase error alone for OFDM systems over frequency-selective channels is studied in [78], [79]. These studies deploy an LS algorithm with pilot subcarriers and null samples to estimate the common phase error term, which is then corrected via constellation derotation. Moreover, [80] compensates for PN with a finite-impulse response equalizer. The filter coefficients are determined by the LS method and by using scattered pilots. However, since the number of pilot tones limits the filter length, ICI from adjacent subcarriers can not be fully compensated. In [81], [82], authors deploy a sinusoidal waveform to parametrize the PN process. And the parameters are estimated by the LS method. However, a sinusoid may not approximate PN very well. To improve the results in [81], Karhunen-Loève representation of the PN process is utilized, and the resulting covariance matrix is deployed as basis elements in [83]. To be specific, the authors improve the data-directed choice of basis elements for LS PN estimation. Finally, the work in [84] shows that any frequency-domain subcarrier signal can be written as a sum of all subcarrier signals weighted by a parameter vector. Moreover, the maximum likelihood (ML) and the linear minimum mean square error (LMMSE) approaches are studied for estimating the weighting vector. However, these techniques require computationally intensive matrix inversion operations.

The shape of the spectrum of PN ($e^{j\phi n}$) contains a low-pass segment near the oscillation frequency, and the bandwidth of this segment is smaller than the subcarrier spacing. Therefore, in most practical cases, low-pass spectral components are sufficient to approximate PN. Authors in [85], [86] use this characteristic and propose an ICI suppression method. The proposed algorithm consists of the following steps: 1) estimate common phase error via an LS estimator and then do a constellation derotation [78], [79], 2) make a decision on the transmitted symbols and deploy the hard-decisions for the MMSE estimation of the low-pass spectral components, 3) suppress PN by convolution of the received discrete symbols and the estimated discrete Fourier transform (DFT) coefficients of $e^{-j\phi n}$. Since this algorithm requires decision-feedback, error propagation is a problem. Thus, increasing the number of reliable symbols for estimating the PN improves estimation and suppression quality. The authors in [44], [87] apply the algorithm mentioned above iteratively to achieve this. They reconstruct the transmitted symbols after PN correction and deploy them again for a consecutive PN estimation and correction. Note that, reference [44] investigates both free-running and PLL oscillators.

However, the authors in [88] show that the PN estimation technique [44] is not acceptable at the symbol boundaries. Thus, they present two linear interpolation-based techniques to improve the estimation of the boundaries. The first interpolates the PN estimate over the adjacent OFDM symbols to improve the pilot-aided common phase error estimation. The second is deployed to improve the iterative ICI estimation technique in [44] by decreasing the error in each OFDM symbol's boundaries. However, these techniques' complexity is high because of matrix inversion operations and correlations between the DFT coefficients of the PN. Therefore, the work in [89] enhances the method in [88] to improve the detection error rate under the conditions of long cyclic prefix duration and large constellation size. Furthermore, the implementation complexity decreases compared to [88].

On the other hand, [90] presents an iterative algorithm. It partitions the received OFDM symbol into sub-blocks in the time domain and estimates the time average of the PN at each sub-block. The system model of [90] is shown in Fig. 11. Since basic building blocks are deployed in the algorithm, the complexity is reduced. Moreover, the authors derive the SINR after PN compensation and show the SINR gains. Furthermore, the work in [91] deploys the codebook representing a set of trajectories to estimate the PN. In this method, the trajectory is chosen that minimizes the Euclidean distance between the constellation of the received symbols at the pilot subcarriers and the known pilot symbols. Although this method reduced PN estimation complexity, its accuracy depends on the number of codebooks and the quantization region's division.

Authors in [92] propose a decision-feedback PN estimation scheme that deploys the geometry structure associated with the spectral components of the complex exponential of the PN process. They express this geometry as a set of non-convex quadratic equations that involves permutation matrices. Moreover, they propose a new PN spectral model to estimate PN more precisely. However, the proposed estimation scheme in [92] has high complexity due to deploying a decision-feedback loop. Thus, in [93], a scattered pilot-based PN estimation scheme without a decision-feedback loop is presented. The authors deploy PN spectral geometry and a dimensionality reduction model proposed in [92]. By using the LS approach and scattered pilot subcarriers, desired PN spectral vector is estimated. They show that the unconstrained optimization problem resulting from the PN estimation problem suffers from amplitude and phase estimation errors. To suppress the amplitude error, the LS estimator is enforced with a PN geometry constraint. This method improves the estimation performance and BER.

Blind estimation and compensation: Blind techniques aim to mitigate the fact that deploying pilot symbols for estimating the PN may reduce the bandwidth efficiency. Reference [94] proposes a blind common phase error estimation by deploying an ML estimator for OFDM systems. However, residual error because of ICI is not negligible and should be suppressed. Thus, based on the probabilistic approach of variational inference, authors in [95] propose an iterative conditional mode algorithm for joint data detection and PN cancellation. Moreover, [96] develops a constrained MMSE algorithm that achieves better performance than [95]. The authors jointly detect the symbol and cancel PN based

This article has been accepted for publication in a future issue of this journal, but has not been fully edited. Content may change prior to final publication. Citation information: DOI 10.1109/ACCESS.2021.3101845, IEEE Access

TABLE 5: Summary of PN estimation and compensation studies for SC systems and single-user OFDM systems with perfect CSI - Oscillator models are free-running (labeled as FR) and PLL

Article	System	Model	TX/ RX	channel	Pilot/ Blind	Est./ Comp.	Ch. Est.	Main approach
[74]	SC	FR	RX	AWGN	pilot	Est.	N/A	MSE minimization between the carrier and recovered phase
[75]	SC	PLL	RX	AWGN	pilot	Both	N/A	Wiener filter for phase error estimation
[76]	SC	FR	RX	AWGN	pilot	Est.	N/A	MAP and modified soft-input extended Kalman smoother
[77]	SC	FR	Both	Freq.Sel.	Blind	Both	No	Estimation algorithm based on low-pass nature of PN process
[79]	OFDM	FR	RX	Freq.Sel.	pilot	Both	No	LS algorithm for common phase error estimation
[80]	OFDM	FR	RX	Freq.Flat.	pilot	Comp.	No	Finite-impulse response equalizer
[81]	OFDM	FR	Rx	AWGN	pilot	Both	N/A	LS algorithm with sinusoidal waveform parameterization
[83]	OFDM	PLL	Rx	Freq.Flat	pilot	Both	No	Karhunen-Loève representation of the PN process
[84]	OFDM	FR	Rx	Freq.Sel.	pilot	Both	No	ML and LMMSE algorithms
[86]	OFDM	FR	Rx	Freq.Sel.	pilot	Both	No	MMSE estimator for approximating low-pass spectral components
[44]	OFDM	Both	Rx	Freq.Sel.	pilot	Both	No	Consecutive estimation with PN correction
[88]	OFDM	Both	Rx	Freq.Sel	pilot	Both	No	Linear interpolation-based estimators
[89]	OFDM	FR	Rx	Freq.Sel.	pilot	Both	No	Improvement the implementation complexity of [88]
[90]	OFDM	FR	Rx	Freq.Sel.	pilot	Both	No	Iterative algorithm with portioning OFDM symbol into sub-blocks
[91]	OFDM	Both	Rx	Freq.Sel.	pilot	Both	No	Estimator based on codebook with a set of trajectories
[92]	OFDM	FR	Rx	Freq.Sel.	pilot	Both	No	Decision-feedback estimator using geometry structure
[93]	OFDM	FR	Rx	Freq.Sel.	pilot	Both	No	Scattered pilot-based estimator without decision-feedback loop
[94]	OFDM	PLL	Rx	Freq.Sel.	Blind	Both	No	ML estimator for common phase error estimation
[95]	OFDM	Both	Rx	Freq.Sel	Blind	Both	No	Iterative conditional mode blind algorithm
[96]	OFDM	FR	Rx	Freq.Flat	Blind	Both	No	Constrained minimum mean squared prediction error algorithm
[97]	OFDM	FR	Rx	Freq.Sel.	Blind	Both	No	Decision-directed estimation algorithm

on the MMSE cost function subject to the symbol's constant modulus constraint. However, the proposed algorithm in [96] requires high computational complexity and suffers from high decision errors. Hence, the investigation in [97] presents a blind estimation method for PN compensation in OFDM systems with constant modulus. In this method, after partitioning a single received OFDM symbol into sub-blocks, each sub-block's PN is approximated as its time average. Then, reducing the variation of PN mitigates the ICI caused by PN. Next, the common phase error is estimated and compensated by a decision-directed approach. However, this method is limited for signalling alphabets of constant modulus. Although blind estimators increase the bandwidth efficiency and are statistically optimal, they are computationally intensive and may not be suitable for delay-sensitive applications.

Table 5 summarizes PN estimation and compensation studies for SC systems and single-user OFDM systems (with perfect channel state information (CSI)).

Joint channel and PN estimation and compensation: All of the compensation schemes mentioned earlier assumes that perfect CSI is available at the receiver. However, this assumption is unrealistic because the receiver must estimate the channel with PN. The channel estimate needs a PN estimate and vice versa. This conundrum sounds like the familiar chicken or the egg causality dilemma.

With cyclic prefix symbols, [98] proposes a channel estimation method, and so does [99] for joint channel estimation deploying soft-decision decoding. Reference [100] addresses joint channel estimation and PN suppression via the expectation-maximization (EM) algorithm, which exploits pilot subcarriers. However, the authors model the ICI as the additive white noise. Thus, in [101], an optimal joint channel, CFO, and PN estimator through the maximization of the likelihood function is proposed. They derive a MAP estimator utilizing prior knowledge of the PN statistics and the training sequence. However, their estimator requires knowledge of channel length, which is not available before channel estimation at the receiver. Therefore, [102] solves this problem and estimates the frequency-domain channel transfer function. In contrast with time-domain channel impulse response estimation in [101], this frequency-domain method eliminates the requirement of a priori knowledge of channel length. However, both [101], [102] are computationally complex and suffer from performance degradation with higher-order modulations.

On the other hand, [103] proposes a method for jointly estimating the channel and common phase error by modeling the PN process over the OFDM symbol with a power series. Moreover, [104] proposes offline and online Monte-Carlo estimators with no prior knowledge of PN and the Gaussian noise power. This work jointly estimates unknown PN, CFO, channel, and Gaussian noise power and proposes a stochastic EM algorithm for offline estimation. Although in [104], the channel is estimated as a Gaussian random vector in a state-space representation, [105] treats the channel as a constant parameter. They present a joint channel, CFO, PN bandwidth, and channel noise variance estimation algorithm based on the sequential Monte-Carlo and ML algorithm. However, the proposed methods incur a higher estimation complexity and inherent error because of the Monte-Carlo approximation. Moreover, reference [106] proposes a scheme for joint channel and PN estimation, which contains two stages. The first stage deploys block-type pilot symbols to jointly estimate channel coefficients and PN in the time-domain by utilizing interpolation techniques. In the second one, a combination of data symbols and pilot symbols is used to estimate PN

components and data symbols.

Additionally, the authors [107] jointly consider PN's effect and the channel distortion in an OFDM system over fast-fading multipath channels. They propose a joint channel equalization and PN compensation technique, which uses a decision-feedback approach. They combine the PN and the fading channel into an equivalent channel matrix. However, this technique requires intensive matrix inversion operations. In fact, non-iterative interpolation can estimate the PN in packet-based OFDM systems by tracking random phase variations [108]. This paper shows that PN can be estimated by maximizing a constrained quadratic form without requiring channel information. The LS estimator exploits the estimated PN to find the channel. However, for tracking the PN [108], pilots throughout an OFDM symbol are required, which penalizes the spectral efficiency. Moreover, the EM method works for the joint channel, CFO, and PN estimation [109]. This method has two steps, 1) PN tracking over the training OFDM symbol with the aid of an extended Kalman filter-based estimator, and 2)channel and CFO estimation by minimizing a likelihood function. Moreover, hybrid Cramér-Rao lower bound (CRLB) for the joint estimation problem is derived. The proposed algorithm not only outperforms the approach in [108] but also is computationally efficient and improves the uncoded and the coded BER performance.

3) Multiuser OFDMA systems

A multiuser OFDMA system divides subcarriers into groups, called subchannels, and allocates them to multiple users for simultaneous transmission. Although different users' signals can overlap in the frequency domain, the orthogonality among subcarriers eliminates multiuser interference (MUI). However, just like OFDM, OFDMA systems are sensitive to PN, which destroys the subcarrier orthogonality and causes ICI between subcarriers and MUI between users. Hence, we need PN estimation and compensation in the uplink and downlink. Each user deals with a single PN in the downlink that can be estimated and compensated for by existing single-user OFDM algorithms. However, the OFDMA uplink is a different story, where each user has its PN, and the received signal in the base station includes multiple PN values. Thus, PN estimation and cancellation in the OFDMA uplink is a challenging problem.

OFDMA systems use three subcarrier assignment schemes: 1) subband-based: bandwidth is divided into small continuous subbands, and one or several of them are assigned to each user, 2) interleaved: allocated subcarriers to each user are interleaved over the whole bandwidth, and 3) generalized: each user can select the subcarriers based on the user's quality of service and channel conditions. Unlike the subband case, the interleaved one provides full channel diversity and increases the capacity in frequency-selective fading channels. Furthermore, the generalized assignment provides more flexibility and allows dynamic resource allocation compared with the other ones. The subcarrier assignment schemes affect the PN mitigation process because of their effects on MUI.

Reference [110] proposes two pilot-aided PN estimation algorithms for OFDM uplink under both subband and interleaved subcarriers assignment schemes. It presents an ML estimation algorithm by exploiting the ICI terms' second-order statistics. Moreover, it also develops an LS estimator with lower computational complexity, albeit with performance degradation. Both estimators compensate for common phase error by exploiting a few pilots per user and for the free-running oscillator model. Moreover, [111] investigates the pilot-aided estimation and mitigation of the spectral spread induced by PN in OFDMA uplinks for the free-running oscillator model. Each OFDMA user suffers from the transmitter PN effect and causes interference. This interference is the spectral spread of each user's subcarriers on other users' subcarriers. The proposed algorithm estimates the common phase error and the channel effect and then detects data symbols. The spectral spread is estimated by using the detected symbols.

Table 6 summarizes PN estimation and compensation studies for single-user OFDM systems (without perfect CSI) and multiuser OFDMA systems.

In sum, pilot-aided PN compensators in all the considered systems are based on biased, e.g., MMSE, and unbiased approaches, e.g., LS. The former ones require no prior knowledge about the statistics of unknown parameters, e.g., channel and phase noise. However, the latter ones require second-order statistics and noise variance. Moreover, the pilot-aided estimators typically require many iterations for convergence, which increases the computational complexity. Furthermore, some ML and MMSE techniques require computationally intensive matrix inversion operations. On the other hand, blind estimators enhance the bandwidth efficiency since they perform estimation without requiring pilot symbols. However, they often require averaging over numerous data symbols for satisfactory performance. Also, they suffer from ill convergence problems, high complexity, and relatively poor performance compared to the pilot-aided ones.

D. PN IN EMERGING/FUTURE TECHNOLOGIES

1) MIMO systems

These, to achieve diversity and capacity gains, deploy multiple antennas in the transmitter and receiver. Suppose the transmit side has N_t antennas and receive side has N_r. Thus, each receive antenna receives a linear combination of the transmit antennas' signals. Before proceeding, it is worthwhile to mention several special cases. If $N_t = N_1$, the system is called single input and single output (SISO), if $N_t = 1$ and $N_r > 1$, the system is called single input and multiple output (SIMO), and if $N_t > 1$ and $N_r = 1$, the system is called multiple input and single output (MISO).

Two distinct oscillator setups exist for transmission and reception branches in MIMO, 1) a single common oscillator, where all branches experience the same PN, 2) independent oscillators, where each branch experiences a PN independent from the other ones (Fig. 12). PN estimation and compensation in the latter are more complex than the former because

TABLE 6: Summary of PN estimation and compensation studies for single-user OFDM systems (without perfect CSI) and multiuser OFDMA systems - Oscillator models are free-running (labeled as FR) and PLL

Article	System	Model	TX/ RX	channel	Pilot/ Blind	Est./ Comp.	Ch. Est.	Main approach
[100]	OFDM	FR	Rx	Freq.Sel.	pilot	Both	Yes	EM algorithm
[101]	OFDM	Both	Rx	Freq.Sel.	pilot	Est.	Yes	Joint channel, CFO and PN estimation via ML algorithm
[102]	OFDM	PLL	Rx	Freq.Sel.	pilot	Est.	Yes	Improving [101] using frequency-domain channel transfer function
[103]	OFDM	FR	Rx	Freq.Sel.	pilot	Both	Yes	Joint channel and common phase error estimation via power series
[104]	OFDM	FR	Rx	Freq.Sel.	pilot	Est.	Yes	Offline and online estimators with Monte-Carlo method
[105]	OFDM	FR	Rx	Freq.Sel.	pilot	Est.	Yes	Sequential Monte-Carlo and EM estimators
[106]	OFDM	Both	Rx	Freq.Sel.	pilot	Both	Yes	Estimation with Interpolation technique
[107]	OFDM	FR	Rx	Freq.Sel.	pilot	Both	Yes	Expressing channel and PN in an equivalent channel matrix
[108]	OFDM	FR	Rx	Freq.Sel.	pilot	Both	Yes	Non-iterative interpolation-based estimator
[109]	OFDM	FR	Rx	Freq.Sel.	pilot	Both	Yes	EM algorithm for joint channel, CFO and PN estimation
[110]	OFDMA	FR	Rx	Freq.Sel.	pilot	Both	No	ML estimators using second-order static of the ICI terms
[111]	OFDMA	FR	Tx	Freq.Sel.	pilot	Both	Yes	Spectral spread estimation

of multiple PN parameters. In the following, we review SC MIMO and MIMO OFDM systems in the presence of PN. We discuss pilot-aided estimation algorithms only.

SC MIMO systems: Before discussing the MIMO literature, we review some papers on MISO and SIMO systems under PN impairment. In [112], capacity for MISO and SIMO PN channels under separate and common oscillators is studied. The authors approximate upper and lower bounds on the high-SNR capacity of both the uplink and the downlink channels of a system. A base station equipped with multiple antennas communicates with a single-antenna user. Moreover, the work in [113] studies ML detection in training-assisted SIMO systems by considering both identical and independent PN processes. This paper considers two channel scenarios, including deterministic and known channels and stochastic and unknown channels. For both scenarios, it derives an optimal detector and performs a high-SNR analysis. For an identical PN process, the symbol error rate (SER) floors are independent of the number of antennas for both channel scenarios. However, with independent PN processes, the SER floors can be made arbitrarily small by increasing antennas.

High-SNR capacity expansion together with finite-SNR capacity upper and lower bounds of an SC MIMO microwave backhaul links affected by Wiener PN are presented in [114]. This paper considers a single common oscillator at the transceiver. Moreover, PN's effects on the capacity of space division multiplexing MIMO systems are studied in [115]. Imperfect knowledge of PN and channel significantly affects the capacity of MIMO systems. Moreover, the upper bound for the ergodic channel capacity is derived. This bound depends on the distribution of the largest eigenvalue of the noise covariance matrix.

Authors in [116] analyze the interference caused by PN and CFO on a MIMO SC-FDMA system with SC space-frequency block coding. They propose a suppression algorithm that directly calculates the interference matrix from the received pilot block and then suppresses ICI terms using the inverse matrix method. The impairments degrade the BER performance of the system, while the proposed algorithm yields a three dB reduction.

On the other hand, [117] studies joint estimation of multiple PN parameters and channel gains in an SC space division multiplexing MIMO system. This system model is shown in Fig. 12. The contribution of [117] can be summarized as 1) a data-aided LS algorithm to estimate channel gains and PN is addressed, 2) a decision-directed weighted LS estimator to track the time-varying PN parameters over a frame is proposed, 3) a decision-directed extended Kalman filter to reduce overhead and delay associated with the estimation process is presented, and 4) finally, CRLBs for the multi-parameter estimation problem are derived. This work shows that a MIMO system's BER performance improves with the proposed channel and time-varying PN estimators. However, the proposed hard-decision-feedback algorithm in [117] requires frequent transmission of pilot symbols. Thus, a soft-symbol-aided estimator using an extended Kalman Smoother is proposed in [118] to track the time-varying PN over a frame. This work also derives the relevant estimation bounds, including data-aided Bayesian CRLBs and non-data-aided Bayesian CRLBs. Furthermore, soft-input MAP estimators for online and offline estimation of PN over the length of a frame are developed. They show that the proposed soft-input estimator outperforms the MAP estimator and the algorithm in [117], and also it improves the BER performance. However, both [117], [118] do not address the problem of joint PN estimation and data detection.

Hence, authors in [119] present algorithms for joint PN

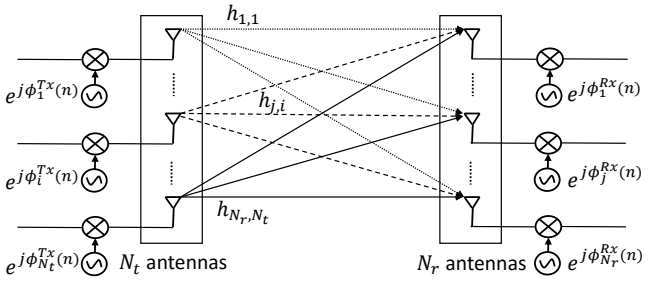

FIGURE 12: MIMO system model with independent PN in all transmission and reception branches.

This article has been accepted for publication in a future issue of this journal, but has not been fully edited. Content may change prior to final publication. Citation information: DOI 10.1109/ACCESS.2021.3101845, IEEE Access

estimation and data detection for MIMO systems affected by Wiener PN and quasi-static fading channels. A MAP symbol detector is proposed that includes the joint estimation of the posteriori PDF of the PN and data detection. Since the optimum receiver has high complexity, they address three low-complexity algorithms based on the sum-product algorithm, the smoother-detector framework, and the variational Bayesian framework.

MIMO OFDM systems: The combination of MIMO with OFDM has the potential for additional interference. Thus, the impact of RF impairments for MIMO OFDM has been widely investigated. The impact of transmit and receive independent PNs on the performance of MIMO OFDM systems is analyzed in [120]. This work shows that PN causes a common phase error and an ICI term in MIMO OFDM systems. The common phase error can be ML estimated and compensated. The ML criterion amounts to a determinant optimization problem. Moreover, simulations show that PN degrades the BER and packet error rate performance, while the proposed common phase error compensation mitigates the problem.

Moreover, PN's influence on MIMO OFDM systems is also investigated. Since the ML estimator for the phase error [120] has high computational complexity, [121] proposes an LS estimation algorithm with lower complexity, which has sub-optimal performance. This work shows that for uncorrelated MIMO channels, LS and ML estimations perform more or less the same. Similarly, in terms of MSE of the common phase error estimation, both have similar performance at low SNR, and the BER of the system is almost identical.

Reference [122] assumes the common phase error is ideally removed by the method in [121]. This work thus investigates the performance degradation caused by the ICI term. To this end, the ICI term's power is derived by a first-order approximation of the PN term for the zero-forcing (ZF) receiver with ideal channel estimation. With frequency-flat-fading and per subcarrier independent Rayleigh fading channels, the influences of transmitter and receiver PNs are different. For frequency-flat Rayleigh fading, receiver and transmitter PNs have the same influence. However, for independent Rayleigh fading, the ratio between the number of transmit and receive branches indicates the influence of received PN. Finally, [123] studies a decision-directed approach for joint compensation of PN and fixed but unknown residual frequency offset in MIMO OFDM systems.

However, the papers mentioned above assumed perfect channel estimation. Thus, the authors in [124] analyze the degradation of receiving common PN and channel estimation in the MIMO OFDM system over doubly-selective Rayleigh fading channels. They derive the Carrier-to-interference power ratio and SINRs. Moreover, an MMSE-based scheme is proposed to mitigate PN's effect and the time-selective fading channel. By increasing the three dB PN bandwidth, the data symbol period, or the number of OFDM subcarriers, the achievable carrier-to-interference power ratio decreases. Furthermore, the work in [125] derives SINR degradation

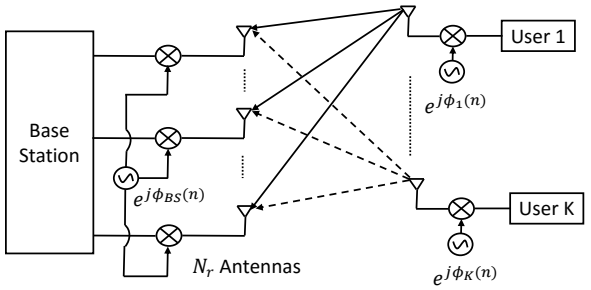

FIGURE 13: System model for massive MIMO systems where a base station with common oscillator communicates with single-antenna users with independent PN processes.

of a MIMO OFDM system considering combined effects of channel estimation error and the receive common PN, with partial common phase error compensation. ZF and MMSE receivers are also investigated.

The proposed algorithms in [124], [125] deploy a common oscillator for the receiver, so they consider one PN process at the transmitter and receiver sides. However, in many MIMO systems, radio frequency chains in transmitter and receiver are equipped with independent oscillators. Thus, channel and PN estimation and data detection for such MIMO OFDM systems have been investigated [126]. This work develops a MAP channel estimator and derives optimal training sequences for channel estimation. Moreover, MAP estimators are deployed for joint transmitter and receiver PN estimation and data symbol detection, and the CRLB is derived.

2) Massive MIMO systems

This technology for future wireless networks provides unprecedented multiplexing gains and energy efficiency [127]. However, PN is a significant challenge that can neutralize the gains of practical massive MIMO. In [128], PN's impact on SC massive MIMO uplink systems with imperfect CSI is investigated. In this work, a massive MIMO base station communicates with multiple single-antenna users. Two operation modes, namely, synchronous and nonsynchronous, are evaluated. These modes lead to identical and independent PN processes for base station antennas, respectively. A linear time-reversal maximum-ratio combining (MRC) strategy is proposed, and achievable sum rates are derived for both modes. This work shows that at low SNR, PN has little impact on the sum-rate performance.

Moreover, PN causes partial coherency loss; e.g., the actual channel during the data transmission and training period can significantly differ. Besides, [129] analyzes the performance of ZF, regularized ZF, and matched-filter (MF) precodings given the PN effect in the SC massive MIMO downlink. Both the number of the base station antennas and the number of users approach infinity. This work also considers two oscillator setups, 1) all base station antennas are connected to a single oscillator, and 2) each base station antenna has its oscillator. This work shows that PN's impact on SINR can be expressed as an effective reduction in the

CSI quality available in the base station, compared with the ideal system without PN. Moreover, the SINR degrades with the increasing number of oscillators in the base station. Furthermore, regularized ZF outperforms two other precodings, and ZF outperforms MF when the CSI is available at the base station.

On the other hand, to suppress PN's adverse effect, compensation schemes are proposed in [130] and [131] for SC massive MIMO uplink and downlink systems, respectively. A low-complexity PN suppression technique based on the ZF detector for massive MIMO uplink systems is proposed in [130]. In this work, independent PN processes are assumed for users, and the common PN caused by a single shared oscillator is assumed for the base station. Fig. 13 shows the system model. The proposed scheme provides the PN increment estimation based on available CSI and the ZF-based detector by a simple iterative process. Moreover, the CRLB of PN estimates is derived. This work shows that the uplink PN suppression scheme can achieve the PN-free performance when the required SNR is satisfied.

On the other hand, authors in [131] propose a low-complexity ZF-based precoding PN suppression scheme for massive MIMO downlink systems. Similar to [130], it is shown that when the required SNR is satisfied, the output SNR of the proposed scheme can approach the upper bound. However, both [130] and [131] consider the flat-fading channel assumption that there is only one path in the channel between each user and each base station antenna. This assumption may limit the application of the schemes in practice. Thus, the work in [132] investigates the symbol detection of an SC massive MIMO uplink system under PN impairments. The system model contains a base station and a user with multiple antennas and independent PN processes. An iterative algorithm using approximate Bayesian inference based on the generalized expectation is proposed to recover the symbol vector from noisy non-linear measurements. The proposed algorithm has superior performance in the high-SNR regime. Furthermore, the investigation in [133] studies joint channel and location estimation in massive MIMO uplink systems in the presence of PN. A sparse representation model for the channel with dynamic-grid parameters is proposed to degrade the location quantization error in this work. Moreover, the joint channel and location estimation problem is modeled as a MAP estimation problem, and a majorization minimization technique is proposed to solve it.

The influence of PN on massive MIMO OFDM downlink systems with linear precoding schemes, ZF, and maximum-ratio transmission (MRT) is investigated in [134]. The SINR and achievable rate are analytically derived. MRT has greater robustness in comparison with ZF but achieves a lower rate per user. When the number of base station antennas is large enough, SINR degradation becomes independent of the number of antennas. Moreover, authors in [135] study the effects of receiving independent PNs in massive MIMO OFDM uplink systems. MRC detector and perfect CSI are considered, and closed-form achievable rates are derived for

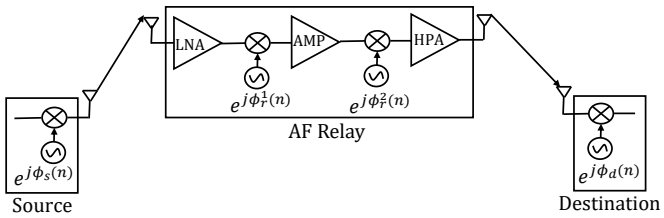

FIGURE 14: OFDM-based dual-hop AF relay network with PN in all nodes.

two different operations: synchronous and nonsynchronous as [128]. Nonsynchronous operation is found superior because of the averaging of the interference. In addition, the work in [136] presents a variational EM-based probabilistic PN compensation scheme for massive MIMO OFDM uplink systems over frequency-selective channels. PN's impacts are considered for both the users and the base station. The proposed scheme includes two stages; channel estimation and data detection. In the first stage, multipath channels of users and the transmitter and receiver PN sequences are estimated by exploiting the transmitted training symbols and the structural sparsity inherent in MIMO channels. In the second stage, by deploying the estimated channels, data symbols are detected in the presence of PN. Finally, in [137], the impacts of PN at both base station and user sides on downlink compressive channel estimation in massive MIMO downlink systems are investigated. In this work, the downlink channel estimation is formulated as a sparse signal recovery problem given an additive correlated perturbation on the pilot matrix.

3) Relaying cooperative systems

Relay systems increase the reliability of data transmission from the source to the destination. This approach can combat long-distance channel distortion and small-scale fading. Relaying protocols can be categorized as 1) amplify-and-forward (AF) and decode-and-forward (DF). The relay transmits an amplified version of the received signal in the previous time slot in AF relay systems. The relay decodes the source message in DF relay systems and transmits the re-encoded message in the next block. However, PN will significantly limit the overall system performance.

Reference [138] studies the impacts of PN on an OFDM-based dual-hop AF relay network. As per Fig. 14, the source and destination nodes suffer from independent PN processes. Moreover, the AF relay experiences the PN in the first time slot, with signal reception from the source, and the second time slot, with signal transmission to the destination. PN induces ICI terms at the relay node, which degrades the system's performance compared to direct transmission. By analytical means, the authors show that the outage probability is larger than the direct transmission. Moreover, a joint frequency-domain channel and PN estimation scheme is proposed by using full pilot OFDM symbols. Furthermore, by modifying the MRC metric, a joint data detection and PN estimation scheme is derived.

This article has been accepted for publication in a future issue of this journal, but has not been fully edited. Content may change prior to final publication. Citation information: DOI 10.1109/ACCESS.2021.3101845, IEEE Access

However, [138] assumes perfect CFO estimation and does not derive the hybrid CRLB for joint impairments estimation. This gap is addressed in [139], which considers the joint estimation of multipath channels, Wiener PN, and CFO in OFDM-based AF relay systems. This work proposes an iterative pilot-aided EM algorithm. The proposed estimator achieves MSE performance close to the derived hybrid CRLB. However, [139] does not study a detector for signal reception at the destination node. Therefore, authors in [140] analyze joint channel, PN, CFO estimation, and data detection in OFDM-based AF relay systems. They propose an iterative joint estimator based on the MAP criterion using the correlation between PN parameters. The estimator's MSE performance is close to the derived hybrid CRLB at medium-SNRs for a small PN variance. Moreover, algorithms for tracking the PN parameters in both the training and data transmission intervals are proposed because of the time-varying nature of PN. The work in [141] proposes an iterative data detection algorithm based on the extended Kalman filter for tracking the unknown time-varying PN throughout the OFDM data packet. This work considers a single source node, multiple DF relay nodes, and a single destination node in the presence of PN. The proposed data detection algorithm outperforms data detection with pilots [140] in terms of BER and PN estimation performance. The authors propose an iterative pilot-aided EM-based algorithm for joint estimation of channels, PN, and CFO in OFDM-based DF relaying systems. They derive the hybrid CRLB for the joint estimation of multiple parameters. Note that this subsection discusses pilot-aided estimation only.

4) Cognitive radio systems

Empirically, we know that pre-assigned spectrum slots often go unused at different times and different spatial locations. The problem is that primary (licensed) users of the spectrum may not be using it temporarily. Secondary users are other users who need to access the same spectrum. Cognitive radio enables secondary users to access the primary users' spectrum provided no degradation to the quality of service of the primary users. Of course, to enable cognitive radios, we need several techniques, such as energy detection [142]–[145]. Thus, cognitive radio improves spectral efficiency. The main challenges for realizing these systems are spectrum sensing and interference management to avoid interference on primary users. However, by introducing interference terms, PN will degrade the spectrum sensing accuracy and cause interference on primary users.

Therefore, the study in [146] investigates the impacts of PN and CFO impairments on spectrum sensing performance in cognitive radios. This work considers conventional energy and MF detectors. The impairments degrade the performance of both conventional detectors. Thus, three spectrum sensing techniques robust to the impairments are proposed, namely, block-coherent detector, second-order MF, and modified second-order MF. The work illustrates that the last one has the best detection performance. Moreover, authors in [147] study the interaction between the PN of the secondary user's receiver and the adjacent channel signals. They illustrate that this interaction results in in-band interference, which degrades the performance of spectrum sensing.

5) Millimeter-wave systems

With the increasing carrier frequency, the variance of the PN increases quadratically. Thus, PN's influence on millimeter-wave wireless systems such as 60 GHz WLAN standards, IEEE 802.11 ad, will be more significant than the low-frequency band under 10 GHz. IEEE 802.11 ad task group recommends the one-pole/one-zero PN model for Millimeter-wave system with PSD given as [148], [149]

$$S(f) = K_0 \frac{1 + (f/f_z)^2}{1 + (f/f_p)^2}, \tag{10}$$

where K_0 is a PN level that is determined by the loop filter in the low frequency, and f_p and f_z are pole and zero frequencies, respectively. The default value of parameters are: $K_0 = -90$ dBc/Hz, $f_p = 1$ MHz, $f_z = 100$ MHz, and $S(\infty)$= -130dBc/Hz. Furthermore, reference [150] derives the auto-correlation function of PN as

$$\rho(\tau) = \frac{K_0 f_p^2}{f_z^2}\delta(\tau) + K_0 \pi f_p \left(1 - \frac{f_p^2}{f_z^2}\right) e^{-2\pi f_p |\tau|}. \tag{11}$$

In the 60 GHz millimeter-wave systems, because of OFDM's high sensitivity to PN, oscillators' design and fabrication are challenging [151]. Authors in [150] propose a low-complexity iterative receiver employing decision-directed receive PN compensation for the 60 GHz millimeter-wave OFDM systems. The proposed receiver iterates low-complexity decision-directed PN compensation and decision-directed channel estimation by utilizing channel decoder output. Decision-directed PN compensation estimates the PN in each sampling time by a one-tap LS algorithm and compensates the received signal. A decision-directed channel estimator then estimates the channel impulse response using the compensated received signal. This proposed receiver can ease the degradation of the channel estimates caused by PN. By utilizing the ISI-free part of the cyclic prefix, reference [148] presents a low-complexity ICI suppression method for millimeter-wave OFDM systems with receive PN. In the proposed method, ISI-free samples are linearly combined with the OFDM symbol's corresponding samples to suppress ICI. By minimizing the ICI power, the optimum combining coefficients are derived, and to reduce the complexity, a set of near-optimum coefficients is proposed. This proposed method improves the BER of the system by 0.5-1.5 dB.

However, the gain of the method in [148] is significant when the difference of cyclic prefix length and channel delay spread is a significant fraction of OFDM symbol length. Compared with OFDM, SC-FDE has a lower peak-to-average power ratio and is more robust to amplifier nonlinearity, which may interest millimeter-wave systems. Thus, authors in [152] propose an iterative decision-aided receive

PN compensation scheme for 60 GHz millimeter-wave SC-FDE systems following the IEEE 802.11ad standard. Each received data block is divided into several sub-blocks of equal length during each iteration in the proposed method. Then, by deploying the data demodulation obtained from the last iteration, PN is estimated in each sub-block. Finally, frequency-domain equalization and data detection for each received data block is conducted. The proposed algorithm has low complexity and also improves performance. However, this work assumes that PN is stationary over each sub-block, which may not apply to practical cases. Note that this subsection discusses pilot-aided estimation and compensation schemes only.

6) Beamforming techniques

These use phase shifting and magnitude weighting with an array of antennas to enhance or attenuate signals in desired directions. Beamforming can help the transmitter and/or receiver achieve spatial selectivity, higher transmission range, and throughput, and for security improvements [153]. However, the distorting effects of PN may affect the performance of beamforming techniques. The authors in [154] analyze beamforming OFDM systems' performance with PN and IQ imbalance. For a MISO system, they derive the exact normalized MSE by considering the free-running oscillator model and the correlation between the channel coefficients at different OFDM subcarriers. Asymptotically, when the antenna array size and the SNR become large, PN's effects decouple from IQ imbalance. Thus, the asymptotic expressions are approximately accurate for a moderate beamforming array size and moderate SNR level.

7) Full-duplex communications

According to the ITU-T definition, full-duplex (aka duplex) is a type of communication where data can flow in both directions simultaneously. Full-duplex devices, therefore, can communicate back and forth simultaneously. We also refer to this as bidirectional communication. Telephones are typical examples of full-duplex devices. They allow both people to hear each other at the same time.

The problem is that all conventional radios cannot transmit and receive simultaneously over the same frequency band. Thus, to create a full-duplex link, such a radio can simultaneously transmit and receive over two frequency bands. Thus, this operation consumes twice as much bandwidth as a full-duplex radio because a full-duplex radio can simultaneously transmit and receive data on the same frequency band. Therefore, full-duplex radios might double the spectral efficiency compared to conventional radios [155], [156] and improve security [157]. However, there is no free lunch. The cost of increased spectral efficiency is the strong self-interference (SI) signal imposed by the transmitter on the same node's receive path. This SI can be 100 dB more than the noise level. Thus, it limits the full-duplex transceiver from realizing its potential gains. Therefore, three classes of SI cancellation schemes exist: 1) the propagation-domain, 2) analog-circuit-domain, and 3) digital-domain approaches [10]. However, PN by inducing interference terms may dwindle the cancellation schemes' capability and cause the residual SI.

The authors in [158] study the impact of PN on general full-duplex transceivers. The PN of transmitter and receiver oscillators significantly limits the SI cancellation capability and is a significant bottleneck in full-duplex systems. Note that the results of [158] limit to narrow-band signal scenarios and separate PN processes in the up-converting and down-converting circuits. Therefore, the study in [159] addresses PN's impacts on full-duplex direct conversion OFDM transceivers. This work considers the isolation between transmitting and receiving antennas, analog SI cancellation, and digital SI cancellation. Moreover, subcarrier-wise residual SI power at the receiver path is derived by considering two oscillator setups for up-conversion and down-conversion, 1) two independent oscillators and 2) a single common oscillator. The latter outperforms the two independent oscillator setup, and full-duplex radios will benefit from that. Moreover, the results show PN has a powerful effect on the digital SI cancellation performance, even when the PN level is relatively low.

However, [159] treats a free-running oscillator model. Thus, authors in [160] extend the analysis of [159] to a generic oscillator case with arbitrary PN spectral shape. In this work, a closed-form expression for the SI's power after the cancellation techniques is derived. Moreover, the impacts of PLL-type oscillator PN on SI cancellation is studied, and this work concludes that even with a very high-quality PLL oscillator, PN degrades the performance in terms of average SI cancellation. Furthermore, the work in [161] studies the digital SI cancellation capability in an OFDM-based full-duplex transceiver under PN and channel estimation errors. The digital cancellation capability is derived from the power of the common phase error, interference-to-noise ratio, desired SNR, channel estimation error, and transmission delay. Moreover, the achievable rate region of this system given PN is derived. PN degrades digital SI cancellation capability and also decreases the rate region. Besides, reference [162] proposes a transceiver design to mitigate the PNs in multipath SI components by deploying one common oscillator. The proposed transceiver utilized two receive chains whose oscillator signals are generated by the transmitter's oscillator but with different delays. In this design, the PN is compensated by dividing the two received signals. Moreover, the investigation in [163] explores the effects of PN and IQ imbalance on OFDM-based full-duplex transceivers' performance. A closed-form expression of the average residual SI power is derived, a function of PN and IQ imbalance levels. Their effects can be decoupled for small PN and IQ imbalance levels, and the average residual SI power is linearly proportional to the parameters.

On the other hand, in [164], pilot-aided PN estimation and compensation in OFDM-based full-duplex systems under transmitter and receiver oscillator PN are investigated. Both free-running and PLL-based oscillators are considered. Two

This article has been accepted for publication in a future issue of this journal, but has not been fully edited. Content may change prior to final publication. Citation information: DOI 10.1109/ACCESS.2021.3101845, IEEE Access

techniques are proposed: 1) frequency-domain technique based on LS estimator, and 2) low-complexity time-domain ICI suppression technique based on the MMSE estimator. Moreover, at low SNR scenarios, the latter achieves a maximum of 6 dB more SI cancellation than the former. However, the PN is estimated in [164] by considering the intended signal as an additive noise which considerably reduces the transmission throughput. Thus, authors in [165] incorporate the intended signal in the estimation process and jointly estimate the transmitter nonlinearities, PN, and both the SI and intended channels at the baseband. To handle the time-varying PN estimation problem, the basis expansion model is adopted to transform the problem to estimate a set of time-invariant coefficients. Then, an ML estimator is developed to estimate the basis expansion model coefficients by using the known SI signal, known pilot symbols, and unknown data symbols received from the other transmitter. Moreover, for time-multiplexed pilot transmission, basis expansion model coefficients are estimated based on the combination of the LS and ML criteria. The proposed methods achieve a superior SI cancellation performance in OFDM-based full-duplex systems. Besides, the investigation in [166] studies digital SI cancellation in a single RF chain massive MIMO-OFDM full-duplex system under PN impairment. In this work, to minimize the power of residual SI, a weighted linear SI channel estimator is proposed. The proposed estimator outperforms the conventional LS, specifically in a high interference-to-noise ratio.

III. CFO

Herein, we first describe the signal model that incorporates the CFO and then discuss its impacts. Second, we review the existing works that evaluate SC and OFDM systems' performance with the CFO impairment. Third, we present a comprehensive survey of CFO estimation and compensation techniques for SC, single-user OFDM, and multiuser OFDMA systems. Moreover, we review joint channel and CFO estimation and compensation. Finally, we discuss CFO's impacts on emerging wireless technologies.

A. SIGNAL MODEL AND IMPACTS

The received continuous-time signal $r(t)$ after shifting by a frequency offset can be modeled as

$$s(t) = r(t)e^{j2\pi\Delta f t}, \tag{12}$$

where Δf indicates the frequency offset between the carrier frequency of the received signal and receiver local oscillator. In literature, the normalized CFO is defined as $\epsilon = \Delta f / f_s$, where f_s indicates subcarrier spacing. The normalized CFO has two parts $\epsilon = \epsilon_I + \epsilon_f$: 1) integer part ϵ_I, which represents the CFO part with an integer multiple of the subcarrier spacing, and 2) fractional part ϵ_f, whose value is less than one subcarrier spacing ($|\epsilon_f| \leq 0.5$). The former one causes the cyclic shift in the received signal, while the latter one leads to phase and amplitude distortion.

To gain insight into the effect of CFO, an OFDM system

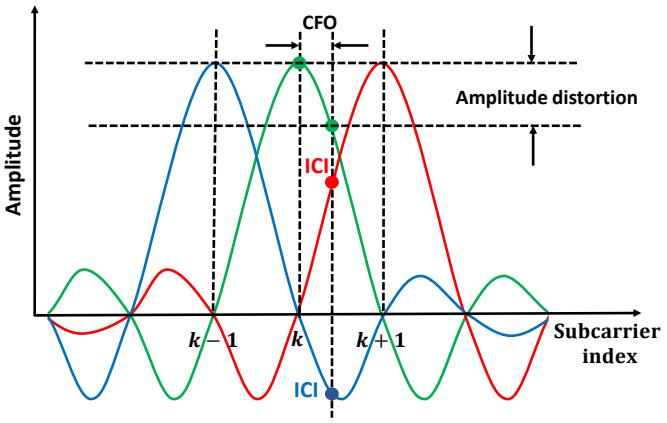

FIGURE 15: Amplitude distortion and phase rotation on the k-th OFDM subcarrier due to CFO.

with N subcarriers over the AWGN channel is considered. The received signal in the k-th subcarrier with CFO impairment can be expressed as [167]

$$r[k] = x[k]I[0] + \sum_{m=0, m\neq k}^{N-1} x[m]I[m-k] + w[k], \tag{13}$$

where $x[k]$ and $w[k]$ are the transmitted symbol and the complex Gaussian noise sample on the k-th subcarrier, $k = 0, ..., N-1$, respectively. The first term in (13) shows the amplitude distortion and phase rotation on the k-th subcarrier due to CFO. The impact of frequency shift has been shown in Fig. 15. Moreover, the second term in (13) indicates the ICI from other subcarriers on k-th subcarrier. Moreover, the term $I[m-k]$ is referred as ICI of the m-th subcarrier on k-th subcarrier, which is given by

$$I[n] = \frac{\sin(\pi(n+\epsilon))}{N\sin(\pi(n+\epsilon)/N)} e^{\frac{j\pi(n+\epsilon)(N-1)}{N}}. \tag{14}$$

Furthermore, Fig. 15 illustrates the ICI from adjacent subcarriers due to CFO in OFDM. This figure also shows the impacts of integer and fractional parts of CFO. The former results in a cyclic shift and a phase distortion of subcarriers, leading to detection errors and the BER degradation. However, the latter causes ICI and destroys orthogonality among subcarriers, which reduces the SNR. Moreover, Fig. 16 illustrate the effect of CFO on the BER performance of an OFDM system with 128 subcarriers. Similar to Fig. 10, we consider ITU outdoor multipath channel model A. We observe that the BER increases because of the increasing power of the interference terms when the normalized CFO increases.

B. PERFORMANCE ANALYSIS

Herein, we first review performance analyses of SC and OFDM systems under CFO.

The impacts of CFO on the performance of a direct-sequence code division multiple access (DS-CDMA) are investigated in [168], [169]. Different users deploy the same

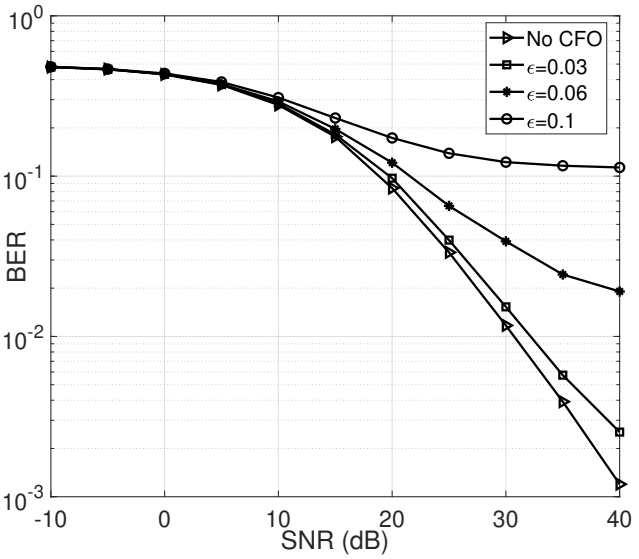

FIGURE 16: BER versus SNR for an OFDM system with different values of normalized CFO.

frequency band in DS-CDMA systems, and each of them is subject to an independent CFO. Therefore, the receiver has to demodulate the desired signal given multiple access interference with different carrier frequencies from that of the desired signal. Moreover, [168] studies the presence of CFO in the multiple access interference for asynchronous transmission. A slight variation of the noise variance could be achieved when the spreading code and CFOs are greater than the symbol rate. Additionally, reference [169] studies the impacts of CFO on quasi-synchronous multicarrier DS-CDMA system. This work analyses multiple access interferences and shows that the time-frequency cross-correlation function can characterize multiple access interference. Furthermore, the BER is derived under the Gaussian assumption on the distribution of the multiple access interference, and also error bounds are derived to check the accuracy of the resultant BER expressions. Finally, multiple access interference can be minimized when the chip period's product and maximum frequency deviation are less than around 0.01. Besides, authors in [170], [171] evaluate CFO's influence on the reception of M-ary spread-spectrum signals; the carrier is modulated with a set of orthogonal code sequences. They analyze the performance of the system and show that the CFO degrades the SER performance remarkably.

Moreover, the BER degradation of SC systems due to CFO in AWGN channels and flat Rayleigh fading channels is investigated in [172], [173]. CFO introduces ISI for a SC system and causes a loss in the useful signal power. Furthermore, [174] investigates CFO impacts on the performance of SC block transmission with frequency-domain MMSE equalization over ultra-wideband channels. This work derives the SINR of the system and shows that CFO degrades the system's performance in terms of BER and SINR.

The literature extensively investigates the effects of CFO on OFDM systems. CFO destroys orthogonality between OFDM subcarriers and introduces ICI [175]. Furthermore, the investigation in [172], [173] shows that an OFDM system is more sensitive to CFO than an SC system due to ICI terms. Moreover, in [64], SNR degradation of an OFDM system in an AWGN channel due to CFO is approximately derived by deploying simple algebraic manipulations. CFO rotates and attenuates the useful signal and also causes interference between subcarriers. Furthermore, the SNR degradation for time-invariant multipath channel and a shadowed multipath channel fading channel are investigated in [176] and [177], respectively. Authors in [177] show that when CFO is small, the SNR degradation is proportional to the square of the CFO and the square of the number of subcarriers. Moreover, reference [178] approximates the average SNR for general multipath fading channels. It is shown that the approximated expression is an upper bound for the average SNR in flat-fading channels and is an exact expression for the AWGN channel. Besides, in [179], the performance of the conventional M-QAM OFDM systems, which uses square pulses is compared with M-Offset QAM, which deploys pulses of finite duration with minimizes excess bandwidth power. The authors show that the latter tolerates a larger carrier frequency deviation than the former. We can conclude that CFO's effects on the OFDM system depend on the number of subcarriers, pulse shaping, and SNR range.

The BER performance of OFDM system in the presence of CFO over AWGN channels is derived in [180]. Three common modulation formats, including BPSK, QPSK, and 16-QAM is considered. The BPSK case is solved by deploying the Beaulieu series, and for the QPSK and 16-QAM cases, an infinite series expression is utilized for the error function. The average probability of error is expressed from the ICI's two-dimensional characteristic function in the latter cases. Moreover, authors in [167] analyze the symbol error probability of M-PSK OFDM systems ($M > 4$) under CFO impairment over AWGN channels. To this end, a signal space decomposition is first proposed to deal with the M-PSK non-rectangular decision region. Then, symbol error probability is derived as the sum of an infinite series with the Beaulieu series. However, studies in [180] and [167] consider the AWGN channels and do not study the effects of CFO in multipath channels.

Hence, [181] approximately derives low-complexity expressions for SERs by assuming Gaussian distribution for the interchannel interference over the multipath channel. Moreover, in [182], BER of M-QAM OFDM systems in the presence of CFO in frequency-selective Rician (or Rayleigh) fading channels is derived. The derived BER is expressed by the sum of a few integrals, whose number depends on the constellation size. In the case of Rayleigh fading, each integral is replaced by a series expansion that involves generalized hypergeometric functions, but in the case of Rician fading, they are computed by numerical techniques. Additionally, [183], [184] derive closed-form BER expressions for BPSK OFDM systems over flat and frequency-selective

This article has been accepted for publication in a future issue of this journal, but has not been fully edited. Content may change prior to final publication. Citation information: DOI 10.1109/ACCESS.2021.3101845, IEEE Access

Rayleigh fading channels. Note that instead of considering Gaussian approximation for ICI [182], the ICI PDF is a mixture of Gaussian densities with properly selected parameters. However, all the papers mentioned above assume that the channel remains static over one OFDM symbol. Thus, authors in [185] study the BER expression for an OFDM system with $\pi/4$-shifted differentially encoded quadrature PSK over frequency-selective fast Rayleigh fading channels. A closed-form BER is derived for a few subcarriers, and the Monte-Carlo method is exploited for numerous subcarriers. The performance degrades because of the Doppler spread and delay spread.

Reference [186] investigates the impacts of both direct current offset and CFO on the BER of BPSK OFDM systems in multipath Rayleigh fading channels. Since CFO compensation spreads the direct current offset overall subcarriers, larger CFO causes more direct current offset energy leaking to other subcarriers. When the direct current offset magnitude and CFO increase, the BER degrades, resulting in an error floor. Furthermore, [187] studies the impacts of random CFO on BER of BPSK OFDM over AWGN, frequency-flat, and frequency-selective Rayleigh fading channels. By using an approximation of CFO-induced ICI coefficients, closed-form BER expressions are derived. For practical OFDM systems, the derived BER based on random CFO is more accurate than considering CFO as a constant.

Furthermore, [188] analyzes SINR of the OFDM system in the presence of CFO over frequency-selective fading channels. When the normalized CFO exceeds 0.05, the average SINR decreases logarithmically with the CFO. Moreover, the OFDM system's capacity in the presence of CFO over frequency-selective Rician fading channel is investigated in [189]. Average capacity expression is derived with and without CSI at the transmitter. Moreover, it is illustrated that the correlations among subcarriers have little effect on the average capacity.

C. ESTIMATION AND COMPENSATION

Because of the CFO's harmful impacts on the performance of the systems, developing estimation and compensation algorithms for mitigating its effects is crucial. We could classify the existing estimators as pilot-aided and blind techniques. All CFO estimators define a general cost function of $f(\widetilde{\epsilon}, P, r)$, and the CFO is estimated by $\hat{\epsilon} = \arg\min_{\widetilde{\epsilon}} f(\widetilde{\epsilon}, P, r)$, where $\widetilde{\epsilon}$, P and r indicate trail value of CFO, training (pilot) sequence and received signal, respectively. Moreover, different approaches allow for finding the cost function in each type of estimators. In the pilot-aided estimators, the CFO is estimated by utilizing known well-designed training symbols or pilot and data symbols at the expense of bandwidth efficiency. Indeed, this approach deploys prior knowledge in the receiver to estimate the CFO. In contrast, in the blind methods, prior knowledge is not available in the receiver, and the cost function is defined based on the CFO trial value and the received signal, which relies on structural and statistical properties of signals and exhaustive search. These techniques improve spectral efficiency since many pilots' transmission is not required, while for satisfactory performance, they often require many data symbols.

This subsection reviews the works in estimation and compensation of CFO in SC, single-user OFDM, and mutiuser OFDMA systems. Moreover, we highlight the studies in joint estimation and compensation of channel and CFO.

1) SC systems

These studies are divided into two categories: 1) pilot-aided and blind estimation and compensation, 2) joint channel and CFO estimation and compensation. Note that the first one needs CSI at the receiver.

Pilot-aided and blind estimation and compensation: A digital CFO estimator for burst mode QPSK is developed [190]. This estimator removes the modulation from QPSK-modulated symbols by a fourth-power non-linearity and averages I and Q components over an estimation interval. Finally, these averages are used to estimate the carrier phase. Similary, CFO estimation is needed for a digital coherent burst demodulator for QPSK [191]. This paper thus estimates timing offset and CFO from the error signal resulting from differential demodulation. However, this CFO estimator works well the normalized CFO is below 2%. Thus, authors in [192] propose a low-overhead coherent burst demodulation technique that performs well with normalized CFOs up to 12.5%. Thus, differential detectors are exploited, and the differential phase between adjacent symbols yields the CFO estimate. In [193], joint timing offset and CFO estimation for a feedforward demodulator is considered for burst-mode minimum shift keying (MSK). This blind method creates periodic components related to carrier and clock frequency by passing the sampled baseband signal through a fourth-order non-linearity and then smoothed by a digital filter. The CFO can be estimated by the phase of the smoothed signal. However, these works consider time division multiple access (TDMA) burst transmission. In addition, authors in [194] design an ML-based CFO estimator for (1) a TDMA radio system with QPSK and (2) a GSM mobile cellular radio system with Gaussian MSK modulation. This method is channel-dependent and also has excessive computational complexity.

The study in [195] explores joint timing offset and CFO blind estimation for non-coherent orthogonal continuous-phase M-ary frequency-shift keying (CPFSK). In this method, a CPFSK signal's complex envelope is sampled at the symbol rate to obtain a single tone whose frequency depends on the CFO. This work estimates timing offset and CFO by finding the largest spectral peak of several versions of the received signal sampled with different epochs. The proposed algorithm can cope with large CFO. Moreover, in [196], [197], authors propose a blind feedforward non-linear LS CFO estimator for QAM. This estimator uses a generalization of a low-SNR approximation of the ML estimator

This article has been accepted for publication in a future issue of this journal, but has not been fully edited. Content may change prior to final publication. Citation information: DOI 10.1109/ACCESS.2021.3101845, IEEE Access

in [198]. In addition to CFO estimation, [199] investigates data detection in burst transmissions under a quasi-static flat-fading channel. Pilot placement is researched to minimize the BER. Optimally, half of the pilot symbols should be at the beginning of the burst and the rest at the end of the burst. Furthermore, joint CFO and code timing estimation are considered for DS-CDMA systems in [200]. An estimator is developed based on the observed signal's subspace structure and analytical tools of polynomial matrices.

In [201], [202], timing offset and CFO are estimated for a linearly modulated signal transmitted through a frequency-flat-fading channel. This method uses second-order cyclostationary statistics by oversampling the receive filter's output. The work [203] analyzes this estimator's asymptotic performance and shows that if the symbol constellation is non-circular, choosing a lower oversampling rate than three not only reduces computational complexity but also improves the estimation performance. However, in [201], the CFO estimate is used for timing offset estimation, which propagates errors because of CFO estimation error. Thus, [202] revises this estimator and proposes a cyclostationary estimator so that timing offset and CFO estimators are independent.

On the other hand, authors in [204], [205] exploit the unconjugated cyclostationary statistics in the oversampled received signal to design a blind CFO estimator for non-circular modulations under frequency-selective channels. Asymptotic performance is analyzed, and an oversampling factor not larger than two achieves the optimum performance. Furthermore, authors in [206] address the CFO estimation for two linearly precoded non-circular transmission systems, including DS-CDMA downlink and OFDM, over frequency-selective channels. The proposed estimator is relied on maximizing a weighted sum of conjugate cyclocorrelations at cyclic frequency. Furthermore, the estimator's asymptotic behavior is analyzed, and a closed-form expression for the asymptotic covariance is derived.

Additionally, [207] studies CFO estimation in mobile digital communications with pilot symbol-assisted modulation over flat-fading channels. The proposed estimator relies on the received signal correlation function. However, this method requires the covariance matrix of the phase estimation errors. Thus, the author in [208] modifies the estimator by exploiting the difference between the phases of the correlation function. Moreover, the covariance matrix is estimated before weighted linear regression. However, this method depends on the assumed form for the correlation of the fading process. Hence, the study in [209] represents an estimator independent of the correlation form. This estimator uses the non-linear LS approach, which assumes an unstructured correlation of the fading process.

Furthermore, a pilot-aided CFO estimator is proposed for PSK transmissions over frequency-selective channels [210]. Near-independent identically distributed (i.i.d.) sequences are considered for pilots. The proposed estimator is an extension of the ML estimator in [194] and performs without requiring CSI.

Joint channel and CFO estimation and compensation: Reference [211] uses known training sequences for joint ML estimation of the channel response and CFO for burst-mode transmissions over frequency-selective fading channels. There are two types of training sequences: arbitrary sequences and periodic sequences. The former has higher complexity, and the latter suffers from a narrower estimation range. Authors in [212] cope with the joint estimation problem of CFO, Doppler spread, and delay-power profile of the multipath channel. They model the channel with a complex band-pass autoregressive model and develop the estimation algorithm. Note that unlike estimator in [211], the proposed estimator has no restrictions on the training signal structure. However, it suffers from MSE performance degradation at high-SNR values. Finally, authors in [213] represent an algorithm for joint pilot-aided estimation of Doppler spread, SNR and CFO in SC block transmission systems over doubly-selective channels. This algorithm deploys the Fourier transform for deriving the PSD of the time-varying channel, and by exploiting the energy distribution property of the PSD, a joint periodogram-based estimator is proposed.

In [214], authors present a blind subspace-based algorithm for joint channel and CFO estimation in multiuser CDMA systems. To this end, the authors first convert the multiuser estimation problem to multiple single-user problems, and the resulting non-linear multivariate optimization problems are solved by exploiting the polynomial matrix projection property. CFO for each user is estimated by a polynomial rooting or one-dimensional spectrum searching, and then the channel is estimated by the LS method. However, this method suffers from computational complexity because of the inverse polynomial matrix manipulation. Thus, authors in [215] propose a simpler joint channel and CFO estimator in terms of complexity for a multicarrier CDMA system. In this method, the non-linear multidimensional parameter estimation problem is transferred into a linear standard eigenvalue problem with a small size matrix, which is very sparse.

Moreover, CFO estimation in the uplink of SC-FDMA systems is investigated in [216], [217]. Authors in [216] propose a blind multiple CFOs estimation algorithm that uses the phase difference between even and odd samples of the received oversampled signal. Moreover, it is shown that the MSE of estimated CFO approaches derived CRLB at high SNR. Besides, reference [217] presents an iterative subspace nulling-based algorithm for joint estimation of CFO, IQ imbalance, and doubly-selective channels in SC-FDMA systems by using pilot symbols. Furthermore, the complexity of the proposed algorithm is reduced by using the first-order Neumann series expansion.

Table 7 shows summary of CFO estimation and compensation studies for SC systems.

2) Single-user OFDM systems

We divide the related studies into four categories: 1) pilot-aided estimation and compensation, 2) blind estimation and

This article has been accepted for publication in a future issue of this journal, but has not been fully edited. Content may change prior to final publication. Citation information: DOI 10.1109/ACCESS.2021.3101845, IEEE Access

TABLE 7: Summary of CFO estimation and compensation studies for SC systems

Article	channel	Pilot/Blind	Est./Comp.	Ch. Est.	Main approach
[190]	AWGN	Blind	Est.	N/A	CFO estimator for burst mode QPSK transmission
[191]	Freq.Flat	Blind	Both	No	Digital coherent burst demodulator for QPSK transmission
[192]	AWGN	Blind	Both	N/A	Estimation by using differential phase between adjacent symbols
[193]	Freq.Sel.	Blind	Both	No	Feedforward demodulator for burst mode MSK with timing offset and CFO
[194]	Freq.Flat	pilot	Both	No	ML estimator
[195]	AWGN	Blind	Both	N/A	Joint timing offset and CFO estimator for a non-coherent CPFSK system
[197]	Freq.Flat	Blind	Est.	No	Feedforward non-linear LS estimator for QAM transmissions
[200]	Freq.Sel.	Blind	Est.	No	Estimation based on the subspace structure of the observed signal in DS-CDMA
[202]	Freq.Flat	Blind	Both	No	Estimation algorithm with second-order cyclostationarity statistics
[204], [205]	Freq.Sel.	Blind	Est.	No	Estimator based on unconjugated cyclostationary statistics
[207]	Freq.Flat	pilot	Both	No	Estimation algorithm using received signal correlation function
[208]	Freq.Flat	pilot	Est.	No	Feedforward algorithm for M-ary PSK transmissions
[209]	Freq.Flat	pilot	Est.	No	Non-linear LS approach
[210]	Freq.Sel.	pilot	Est.	No	ML estimator for PSK transmission
[211]	Freq.Sel.	pilot	Est.	Yes	Estimator based on ML approach
[212]	Freq.Sel.	pilot	Est.	Yes	EM algorithm for joint estimation
[213]	Freq.Sel.	pilot	Est.	Yes	Joint periodogram-based estimator using the energy distribution property
[214]	Freq.Sel.	Blind	Est.	Yes	Subspace-based joint estimator for multiuser CDMA systems
[215]	Freq.Sel.	Blind	Est.	Yes	Estimator using linear standard eigenvalue approach
[216]	Freq.Sel.	Blind	Both	No	Estimation algorithm using phase difference in SC-FDMA
[217]	Freq.Sel.	pilot	Both	Yes	Iterative subspace nulling-based algorithm for joint estimation of CFO, IQ imbalance and doubly-selective channels in SC-FDMA

compensation, 3) ICI self-cancellation, and 4) joint channel and CFO estimation and compensation. Note that first two categories assume knowledge of the channel is available in the receiver. Moreover, the third one reduces the the sensitivity of the OFDM system to the CFO by exploiting signal processing and/or coding approaches without requiring any estimation processing.

Pilot-aided estimation and compensation: Many existing OFDM CFO estimators use periodically transmitted pilots. Pilots reduce bandwidth efficiency, especially for continuous transmissions (e.g., digital video broadcasting — terrestrial (DVB-T)). However, these estimators could be suitable for packet-oriented applications.

Reference [218] proposes an ML CFO estimator in the frequency-domain by deploying two repetitive OFDM blocks. When CFO and the channel impulse response are constant for a period of two symbols, the estimation error depends only on total symbol energy. However, the acquisition range for CFO is limited to ± 0.5 of the subcarrier spacing. Moreover, this estimator has significant overhead due to deploying two repetitive OFDM blocks, which is inappropriate for tracking. The authors in [219] propose a two-step ML CFO acquisition and tracking algorithm. For the acquisition step, known symbol sequences periodically are inserted in the OFDM frame. The decisions on data symbols are used for the tracking step (decision-directed tracking).

Moreover, in [220], pilot-assisted algorithms for CFO acquisition and tracking are proposed by deploying a unique frame format, where elements of a differentially encoded pseudo-noise sequence are carried with adjacent subchannels. On the other hand, the work in [221] modifies the proposed methods in [220] to reduce computation complexity for synchronization and increase the range of CFO acquisition. The proposed estimator also utilizes two training OFDM symbols, which are placed at the frame's start. The first symbol has a repetition within half a symbol period and is used to measure the frequency offset with an ambiguity equal to the subcarrier spacing. The second one, which has a pseudo-noise sequence, is deployed to resolve the ambiguity. The frequency acquisition range of this method is ± 1 of the subcarrier spacing.

Moreover, reference [222] develops an ML-based estimator by using a training symbol's repetitive structure. On the other hand, in [223], two training symbols comprising an equal number of null subcarriers and pilots are deployed for estimating the fractional and integer parts of CFO. The fractional part is less than one subcarrier spacing, and the integer part is an integer multiple of the subcarrier spacing. The estimator for the fractional part uses the LS criterion and is iterative. Moreover, the estimator for the integer part is the likelihood function based on energy difference. This estimator uses a pseudo-noise binary random sequence for subcarrier allocation of null subcarriers and pilots. Moreover, [224] proposes an ML estimator based on time-domain channel estimates with successive pilot symbols. The motivation is that after singular value decomposition-based OFDM channel estimation in [225], CFO information is retained in the form of phase rotation in the estimated channel used for estimation. This method has less restrictions on the pilot patterns.

Besides, a CFO estimator for OFDM-based WLANs is proposed in [226]. This CFO estimator minimizes a proposed non-linear LS cost function. It uses the packet preamble structure of the IEEE 802.11 standard. This preamble packet includes ten identical short OFDM symbols (each containing 16 data samples) and two identical long symbols (each containing 64 data samples). Although it performs well in the high-SNR range, this estimator does not consider the

energy relationship between different data samples in the OFDM symbol. Since signal energies are different, SNRs can be significantly different. Thus, because the non-linear squares CFO estimator in [226] is based on a sum of all data samples, these different SNRs can degrade the estimation performance. Therefore, authors in [227] modify the non-linear squares estimator by weighting elements of the OFDM symbol in terms of their energies. As a result, samples with higher energies contribute more to the CFO estimator. However, this method increases the computational complexity.

On the other hand, a less complex ML CFO estimator exploits the IEEE 802.11a preamble [228]. This estimator first finds the received preamble with an LS method and then maximizes a likelihood function. The computational load of exhaustive search over the entire uncertainty range is reduced by transforming the log-likelihood function into a spectrum polynomial. However, this estimator requires finding the roots of the derivative of the likelihood function, introducing computational complexity. Thus, authors in [229] propose an ML method to solve the likelihood function directly for the CFO estimation by exploiting periodic preambles. The proposed estimator assumes the Gaussian distribution for the time-domain preamble signal based on the central limit theorem. However, the performance of the proposed algorithms degrades when normalized CFO is close to ± 0.5.

All the methods mentioned above require repetitive training symbols or preambles, which is inefficient and causes significant overhead. Therefore, [230] modifies the method in [221], where one training symbol with L identical parts is exploited for the CFO estimation. The proposed algorithm uses a correlation rule applied to the training symbol divided into more than two identical parts. These parts are created by transmitting a pseudo-noise sequence on the frequencies multiple of L/T and keeping zero the remaining ones (T is the OFDM symbol's duration). The frequency acquisition range of this method is $\pm L/2$ of the subcarrier spacing. Moreover, authors in [231] propose a design for a training symbol in which transmitted complex data in frequency-domain are related with an exponential term. Based on the correlation property, a CFO estimator is developed for the flat-fading channel. The proposed estimator outperforms the estimator in [230] in the low-SNR.

Additionally, [232] presents a CFO estimator similar to [221] with one training symbol without degrading performance and increasing the computational complexity. Instead of using a second training symbol for resolving the CFO's ambiguity, authors in [232] exploit a differential coding in the frequency-domain. Furthermore, the study in [233] deploys one training symbol for CFO estimation and designs it to have a sharp timing metric trajectory. The symbol is designed to have repeated identical parts with possible sign inversions. The authors show that the timing offset estimation can be improved by designing the signs of the identical parts to give the sharpest timing metric trajectory. This method uses the ML principle, and it suppresses the interference in the CFO estimation.

However, the training signal in [233] is designed for timing synchronization. Thus, for frequency synchronization, the authors in [234] design an optimal training signal for AWGN channels based on minimizing the CRLB under constraints on the peak and the total training signal energies. Moreover, [235] investigates the optimal training signal design in frequency-selective channels by exploiting a min-max approach based on an asymptotic CRLB. Since this paper assumed that the channel gains remain constant within the training block, the training signal design omits the channel fading effect. Additionally, the authors of [235] extend their approach for designing a training signal for joint CFO and channel impulse response in [236]. However, they assume that both CFO and channel impulse response estimation errors are equally weighted, which may not be equal. Thus, [237] develops an optimal periodic training signal design by finding the optimal weighting between CFO and channel impulse response estimation errors.

However, in all the proposed training sequence designs, the channel is deterministic. Hence, [238] considers a random channel impulse response and statistically averaging the CRLB of the CFO over the channel realizations to obtain channel-independent design criterion. Nevertheless, the design in [238] assumes that components of the channel impulse response are i.i.d., which could be restrictive in practice. Therefore, [239] proposes a training design for the joint CFO and channel estimation under the correlated taps. The designed criteria minimize the MSE on data estimation at the Wiener-type equalizer output averaged over the channel statistics.

The work in [240] explores CFO estimation based on ML criterion with one training symbol with null subcarriers and pilot tones within the range of two subcarriers spacing. All odd subcarriers in the training symbol are null, and all even subcarriers are pilot tones. The correlation operation relied on the loss of orthogonality among subcarriers to estimate the fractional part of the CFO. Then, subcarriers at even positions are deployed for estimating the integer part of the CFO, which causes a shift of the subcarrier indexes. Specific sequences, e.g., almost-perfect autocorrelation sequences [241] and extended m-sequences, are allocated to even null subcarriers.

Moreover, [242] tries to use channel side information to improve the ML-based CFO estimator's performance utilizing pilot tones and null subcarriers. Using the second-order channel statistics, better CFO estimation is achieved for both Rayleigh and Rician fading channels. However, CSI is not always available in the receiver.

Furthermore, authors in [243] presents a frequency-assignment scheme where null subcarriers are inserted among modulated data subcarriers. Based on this assignment, the window function is used to broaden the received signal spectrum, and the effect of residual frequency offset in the received OFDM signal is reduced. Moreover, a frequency-domain estimation algorithm is proposed by deploying the frequency-assignment schemes together with a Hanning win-

dow. However, in this method, the additive noise's influence is enhanced, and the efficiency of spectrum utilization is reduced by using the window. On the other hand, [244] deploys a mixture of limited scattered pilots, null subcarriers, and data for tracking the CFO. The channel remains constant during two consecutive OFDM blocks. The algorithm's performance accuracy increases by deploying pilots, while the null subcarriers reduce the chance of CFO outlier (when residual CFO is greater than a specific threshold is called an outlier).

Based on a preamble comprising distinctively spaced pilot tones, an ML CFO estimator is proposed in [245]. Moreover, a sub-optimal CFO estimator is proposed, which has two phases: 1) the coarse estimation based on the correlation between the received spectrum and the original pattern of the pilot tone, and 2) fine estimation based on the magnitude attenuation of the frequency bins around those CFO-shifted pilot tones. According to the pilot tones' distinctive spacing, this method is channel independent and robust against frequency-selective fading channel. However, since zero-padded fast Fourier transform (FFT) is deployed, the sub-optimal estimator's estimation performance depends on the oversize ratio of zero-padding. Moreover, authors in [246] address a pilot design that ensures consistency of the estimator in [245]. Based on the conventional sequences, the ML estimator pilots are represented in which the estimator has a unique solution for a noiseless channel. However, this criterion for pilot design is not robust to outliers in practical noisy channels. Hence, [247] investigates sequence designs for robust, consistent CFO estimation by using the average error probability of the ML estimator. The proposed pilot designs reduce outliers compared with conventional sequences in [246].

Furthermore, based on pilot subcarriers, a weighted LS algorithm for joint CFO and timing offset estimation is proposed in [248]. Pilot data are differentially encoded with a pseudo-noise sequence, which is known at the receiver. The averaged phase difference in the received pilot subcarrier signals between two consecutive symbols are deployed for developing the estimator. Moreover, for both AWGN and multipath fading channels, the optimal weights are derived. Furthermore, investigation in [249] presents a carrier synchronization algorithm based on the MMSE criterion by exploiting pilot subcarriers. The proposed algorithm has a dual-loop structure. One loop deals with the phase offset in the time-domain caused by CFO, and the other one copes with the phase distortions induced by carrier frequency error and the channel phase variation on each subcarrier in the frequency-domain. Moreover, a different approach is followed in [250], where eigenvalues of the ICI coefficient matrix are exploited for designing a pilot-aided estimator. The eigenvalues are the elements of a geometric series distributed on the unit circle of the complex plane, and by finding the eigenvalues of a two-dimensional ICI coefficient matrix, CFO can be estimated. The authors prove that the proposed estimator is an ML estimator.

References [251], [252] investigate the joint pilot-assisted estimation of the CFO and sampling frequency offset (SFO) in OFDM systems. The mismatch between frequencies of the sampling clocks of the digital-to-analog converter at the transmitter and the analog-to-digital converter at the receiver introduces SFO, which causes ICI in OFDM systems. The authors in [251] propose an ML decoupled estimator for joint residual CFO and SFO estimation. They assume that a coarse synchronization is completed at the beginning of the data frame and residual CFO remains. SFO is first estimated by a simple mono-dimensional grid search in the proposed method, and then residual CFO is obtained by exploiting the estimated SFO. Furthermore, by deploying scattered pilot symbols in time and frequency-domain, the authors in [252], [253] propose a joint CFO and SFO estimator based on the ML approach in [218]. Moreover, for large SFO, the residual CFO increases, which results in an error floor in BER performance. However, the proposed method requires an exhaustive two-dimensional search. Thus, authors in [254] represent a closed-form solution for the ML estimation of CFO in [253] by taking advantage of the second-order Taylor series expansion. Hence, the dimensional of search deployed for SFO estimation is reduced to one. Finally, reference [255] proposes a low-complexity sequential pilot-assisted estimator for SFO and CFO estimation in OFDM systems by deploying specific subcarriers over two subsequent symbols. This work assumes that the channel remains approximately the same over them.

Table 8 shows summary of pilot-aided CFO estimation and compensation studies for single-user OFDM (with perfect CSI).

Blind estimation and compensation: In blind estimators, the principal idea is to exploit the structural and statistical properties of transmitted OFDM signals. However, for satisfactory performance, these estimators often require many OFDM symbols.

In [256], a blind ML-based feedback CFO and timing offset estimator is proposed. However, this estimator suffers from the fractional subcarrier spacing limitation. In [257], by exploiting the redundant cyclic prefix in the OFDM system, ML estimator for CFO blind estimation in AWGN channel is proposed. The proposed method's detection range is limited to half of the symbol rate, which is not sufficient for multicarrier systems (where frequency offset is greater than the symbol rate). Note that knowledge of the distributions of data symbol and noise is required in this method. Thus, reference [258] modifies the proposed method in [257] to cover the entire range of the timing offset. Moreover, reference [259] studies extension of the method in [257] to multipath Rayleigh fading channels and also reference [260] follows the approach in [257] to design a CFO estimator for OFDM systems exploiting non-circular transmissions.

Moreover, authors in [261] propose a blind ML timing and frequency offset estimation algorithm over a fast Rayleigh fading channel. In this method, frame timing instant is estimated without prior knowledge of CFO, and then a method

This article has been accepted for publication in a future issue of this journal, but has not been fully edited. Content may change prior to final publication. Citation information: DOI 10.1109/ACCESS.2021.3101845, IEEE Access

TABLE 8: Summary of pilot-aided CFO estimation and compensation studies for single-user OFDM (with perfect CSI).

Article	channel	Est./Comp.	Ch. Est.	Main approach
[218]	Freq.Sel.	Both	No	ML algorithm by deploying two repetitive OFDM blocks
[219]	Freq.Sel.	Both	No	Two-step CFO acquisition and tracking algorithm based on an ML approach
[220]	Freq.Sel.	Both	No	Special frame format design for CFO acquisition and tracking
[221]	Freq.Sel.	Both	No	Training symbols development for measure the CFO with an ambiguity and resolve the ambiguity
[222]	Freq.Sel.	Both	No	ML algorithm using repetitive structure of a training symbol
[223]	Freq.Sel.	Both	No	Null subcarriers and pilots deployment for estimation the fractional and integer parts of CFO
[224]	Freq.Sel.	Both	No	ML estimator with successive pilot symbols
[226], [227]	Freq.Sel.	Est.	No	Algorithm for OFDM-based WLANs
[228]	Freq.Sel.	Est.	No	LS algorithm using packet preamble (IEEE 802.11a preamble)
[230]	Freq.Sel.	Est.	No	Estimation algorithm based on a correlation rule
[231]	Freq.Flat	Both	No	Estimation algorithm deploying correlation property of a designed training symbol
[233]	Freq.Sel.	Both	No	ML algorithm using one training symbol with a sharp timing metric trajectory
[234]	AWGN	Est.	N/A	Optimal training signals by minimizing the CRLB
[235]	Freq.Sel.	Est.	No	Optimal training signal design using asymptotic CRLB
[237]	Freq.Sel.	Est.	No	Optimal periodic training signal design using CFO and channel estimation errors
[238]	Freq.Sel.	Est.	No	Channel-independent training signal design by averaging the CRLB over channel realizations
[239]	Freq.Sel.	Est.	Yes	Training signal design with minimizing the MSE of data estimation
[240]	Freq.Sel.	Est.	No	ML estimator using null subcarriers and pilot tones
[243]	Freq.Sel.	Both	No	Frequency-domain estimation algorithm using a Hanning window
[245]	Freq.Sel.	Est.	No	ML estimator based on a preamble comprising distinctively-spaced pilot tones
[246]	Freq.Sel.	Est.	No	Pilot design by ensuring consistency of the estimator in [245]
[247]	Freq.Sel.	Est.	No	Training sequence design using the average error probability of ML estimator
[248]	Freq.Sel.	Both	No	Weighted LS algorithm for joint CFO and timing offset estimation
[249]	Freq.Sel.	Both	No	MMSE Carrier synchronization algorithm
[250]	Freq.Sel.	Est.	No	Estimator design using eigenvalues of the ICI coefficient matrix
[251]	Freq.Sel.	Both	No	ML decoupled estimator for joint residual CFO and SFO estimation
[252], [253]	Freq.Sel.	Both	No	ML algorithm for joint CFO and SFO estimation
[254]	Freq.Sel.	Est.	No	ML estimator using second-order Taylor series expansion
[255]	Freq.Sel.	Est.	No	Low-complexity algorithm for SFO and CFO estimation

similar to [257] is used for CFO estimation. The difference is that a fast Rayleigh fading channel is taken into consideration. However, the proposed method can not be used over a fast time-varying multipath channel. Thus, the work in [262] investigates joint CFO and timing offset over fast time-varying multipath channels. The proposed estimator has two stages: 1) coarse synchronization based on the LS method for obtaining a rough estimation of CFO and timing offset, 2) fine synchronization based on ML method for deriving accurate final results by using previous coarse synchronization. Note that timing offset estimation is independent of CFO estimation. However, the blind estimators in [257]–[262] are based on the redundancy of cyclic prefix depends on the length of the cyclic prefix and need this length to be larger than the channel response.

Besides, authors in [263] and [264] propose blind CFO estimation algorithms by utilizing the known structure of the subspace of OFDM signaling because of the placement of null subcarriers. The multiple signal classification searching algorithm in [263] estimates the CFO by minimizing a cost function derived based on inherent orthogonality among OFDM subchannels. The motivation is that the null carriers' outputs are zero when adjacent channel interference does not exist. Moreover, the work [265] examines the proposed blind CFO estimator in [263] in terms of sensitivity against key system parameters in practical implementation, and also the study in [266] proposes a low-cost implementation of [263] without sacrificing the performance. The investigation in [264] proposes an estimator in closed-form based on the standard estimation of signal parameters via rotational invariance technique. This algorithm deploys the shift-invariant structure available in the signal subspace and estimates the CFO by subspace decomposition and eigenvalue calculation. Furthermore, by exploiting receiver diversity and known OFDM signal subspace structure, a weighted non-linear LS CFO estimator is represented in [267]. The authors claim that the derived estimator is a generalization of subspace methods in [263] and [264].

On the other hand, reference [268] shows that the effect of frequency selectivity on the identifiability and performance is not addressed by [263] and [264]. The previous methods are channel-dependent, and the channel zeros on the FFT grid caused a lack of identifiability of the CFO. To cope with this problem, reference [268] proposes the other approach for CFO estimation in which the null subcarriers are placed with distinct spacings. Moreover, it is proved that the proposed cost function has the unique minimum (independent from the channel), and the least-mean-squares (LMS) adaptive gradient descent method is deployed for finding the minimum. Furthermore, the authors in [269] propose a blind CFO ML estimator by taking advantage of both the null subcarriers and the redundancy of the cyclic prefix. In this method, the OFDM signal vector is modeled as a circular complex Gaussian random vector. Additionally, the authors in [270] investigate the null subcarrier placement optimality for blind CFO estimation. They illustrate that the SNR of the CFO es-

timation is a function of the null subcarrier placement. Then, by solving the SNR optimization problem, they find the optimal placement when the number of subcarriers is a multiple of the number of null subcarriers. Note that the derivations are for small CFO values. Finally, reference [271] presents a fast CFO estimation algorithm with low complexity by utilizing null subcarriers. The proposed estimator approximates the cost function as a cosine function by introducing concept of gap subcarriers, which are the fraction of the null subcarriers immediately adjacent to the data subcarrier. Note that all the proposed algorithms in [263], [264], [267]–[271] are designed to work with frequency-selective channels where OFDM systems are not fully loaded. The number of subcarriers that carry the information is smaller than the size of the FFT block. Indeed, they require the insertion of null subcarriers. The other drawback is a requirement of multiple OFDM symbols for achieving desirable performance that introduces extra delay at the receiver.

Furthermore, a blind CFO estimator is proposed in [272] for pulse shaping OFDM/QAM and OFDM/OQAM systems. OFDM/OQAM systems exploit efficient pulse shaping filters to obtain sharper time-frequency localization. Note that these systems do not require the insertion of a guard interval. The proposed algorithm exploits the cyclostationarity of the OFDM signal, which is induced by the cyclic prefix. The acquisition range for CFO in this method is over the entire bandwidth of the OFDM signal. Moreover, a blind CFO estimator for an OFDM/OQAM system is investigated in [273] by exploiting the non-circularity of the received signal. The estimator maximizes a cost function derived by exploiting the conjugate second-order cyclostationary statistics of the received signal. Additionally, the investigation in [274] proposes an unconditional ML algorithm for CFO estimation in an OFDM/OQAM system given a non-dispersive channel. Given numerous subcarriers, the received signal converges to a complex Gaussian random vector. Next, since the OFDM/OQAM signal resulted in a non-circular process, the generalized PDF of non-circular complex Gaussian random vectors is exploited to develop the estimator. In addition, authors in [275] propose a blind CFO estimator for OFDM/OQAM systems by utilizing the header structure of the transmitted signal and the orthogonality among subcarriers.

Moreover, authors in [276] propose an estimator by deploying the time–frequency-domain exchange inherent of the OFDM modulation scheme. The method exploits the similarity of CFO's impact on the OFDM signal with the impact of clock timing offset on the pulse amplitude modulation signal. Hence, the CFO is estimated from the oversampled OFDM signal by adopting the time recovery algorithms. A different approach is followed in [277], where a blind feedforward CFO estimation algorithm is proposed based on the ML criteria using null subcarriers. The proposed method requires approximate statistical knowledge of the communication channel. The authors show that the proposed estimator outperforms the estimator algorithm in [276] at the price of a narrower estimation range and more complexity.

The blind CFO estimator in [278] uses the oversampled signal model. It exploits the intrinsic phase shift between neighboring samples due to the CFO. A single OFDM symbol is used for estimation, which is suitable for systems with stringent delay requirements. However, this method suffers from high computational complexity caused by solving high order polynomial equations. Hence, authors in [279] present a blind CFO estimator by exploiting the cyclic prefix and oversampling. In this estimator, the received OFDM symbol is first separated into two OFDM symbols with a time difference by using cyclic prefix and two-fold oversampling. Then, a cost function is defined as a function of the distance between these two OFDM symbols to estimate the CFO. The proposed estimator outperforms the estimator in [278] in terms of MSE performance.

Moreover, authors in [280] utilize minimum output variance for CFO estimation. In this method, the cost function is defined by minimizing the output variance after the FFT demodulation. The motivation is that the mean magnitude of the output is maximum when the CFO is correctly compensated. However, this method works for only the AWGN channel. Furthermore, authors in [281] design a blind CFO estimator via a diagonality criterion. The motivation is that when CFO is perfectly synchronized, the covariance matrix for the received signal in the frequency-domain is diagonal. Hence, the authors define a cost function based on this property which minimizes the total off-diagonal power induced by ICI in the frequency-domain. However, this method requires a large number of OFDM blocks. On the other hand, the investigation in [282] presents a blind iterative carrier tracking algorithm by taking advantage of OFDM PSD's in-band ripple. Note that the ripple peaks corresponded to the center frequency of the individual data subcarriers. In this algorithm, an estimate of CFO is obtained by tacking the ripple peaks' location with a comb filter. However, the algorithm suffers from a convergence penalty.

Besides, in [283], a blind ML CFO estimator for OFDM systems transmitting constant modulus symbols is proposed. The cost function is derived based on the constant modulus property of the symbol constellations. Note that this method is consistent for fully loaded OFDM systems. Besides, based on the frequency analysis of the received signal, the CFO estimator is proposed for OFDM systems with constant modulus signaling in [284]. When CFO is fully compensated, some specific frequencies of the received signal disappeared. Thus, based on this fact, the cost function for blind CFO estimation is defined. Moreover, authors in [285] propose an estimator for OFDM systems with constant modulus signaling over a slowly time-varying channel. In this type of channel, subcarriers with the same indexes in two consecutive symbols experienced the same channel effect. Thus, they estimate the CFO by maximizing a cost function defined based on products of the signal amplitudes of two subcarriers with the same index in two successive symbols.

References [286], [287] follow a different approach, where

This article has been accepted for publication in a future issue of this journal, but has not been fully edited. Content may change prior to final publication. Citation information: DOI 10.1109/ACCESS.2021.3101845, IEEE Access

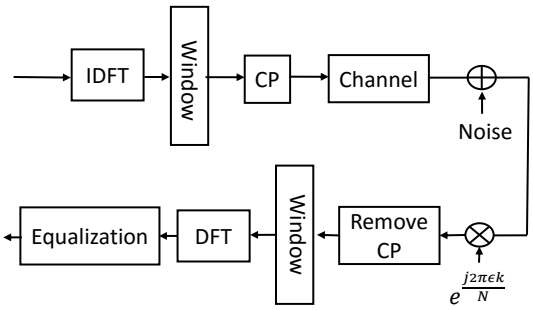

FIGURE 17: Block diagram of an OFDM system with ICI self-cancellation technique (windowing).

spectrum-smoothing schemes for CFO estimation in an OFDM system with constant modulus signaling are developed. The mentioned scheme assumes that the channel frequency response changes slowly in the frequency-domain. Following this assumption, a cost function is defined to minimize the signal power difference between two neighboring subcarriers. However, this assumption is violated when the channel frequency selectivity increased. Hence, authors in [288] present an estimator for the OFDM systems with constant modulus signaling based on the covariance matrix calculated by the circular shifts of the OFDM received signal. The derived covariance matrix has a banded structure with perfect CFO compensation. Therefore, the CFO estimation's cost function forces the out-of-band elements of the matrix to be zero. Nevertheless, this method suffers from channels with large delay spreads, which reduces the number of out-of-band elements of the covariance matrix. Thus, a study in [289] develops an estimator for OFDM systems using constant modulus constellations over highly frequency-selective channels with high delay spread. Similar to [285], the authors deploy the assumption that the channel variation is slow within two adjacent symbols and estimate CFO by minimizing the cost function, which uses a covariance fitting criterion between two nearby symbols.

However, the cited blind estimators assume that the symbol timing is known at the receiver. Hence, the study in [290] explores a blind technique for joint timing offset and CFO estimation based on the LS approach. The proposed estimator considers a fully loaded OFDM system and does not require the channel impulse response knowledge. Moreover, by exploiting cyclic prefix redundancy, a joint ML algorithm for joint timing offset and CFO estimation is proposed in [291]. The authors formulate the likelihood function based on the cyclic prefix's distinctive correlation characteristics at each sampling time over dispersive channels. Note that the proposed estimator's performance depends on the channel length, and it suffers from high computational complexity.

Table 9 shows summary of pilot-aided CFO estimation and compensation studies for single-user OFDM (with perfect CSI).

ICI self-cancellation: CFO is first estimated in previous pilot-aided and blind estimators for OFDM systems and then is accurately removed. However, another approach called ICI self-cancellation technique reduces the OFDM system's sensitivity to the CFO by exploiting signal processing and/or coding approaches. Following this, we review the techniques designed for OFDM systems.

The authors in [292], [293] describe the ICI caused by CFO in complex weighting coefficients. Using the derivations, they propose an ICI cancellation method in which each complex value is modulated on L adjacent subcarriers, using optimized weights, rather than on to a single subcarrier. After maximal ratio combining of the repeated symbols at the receiver, ICI depends on the difference between the adjacent weighting coefficients, and since the difference between them is small, ICI reduces. However, this method is complex and also degrades the transmission rate by factor L. Thus, authors in [294] propose an ICI self-cancellation technique by applying windowing procedure in both transmitter and receiver. Fig. 17 shows the system model of this work. By designing the windows, they reduce side lobes of the spectrum and so suppress the ICI. Furthermore, they prove that the method in [292], [293] is equivalent to a particular case of the proposed windowing method. Besides, in [295], a diversity-based cancellation method is proposed using two processors in transmitter and receiver. The transmitter's processor extended the time-domain signal to add diversity to the frequency-domain symbols, and the processor in the receiver used the diversity to mitigate the ICI.

On the other hand, authors in [296], [297] propose cancellation methods using conjugate transmission. In [296], two-path conjugate transmission is addressed in which the first path is formed by the regular OFDM signal and the second one is represented by a conjugate of the first path. The combination of the two paths forms the conjugate ICI scheme. Moreover, authors in [297] present a phase-rotation-based scheme for ICI cancellation, which is the general form of the scheme in [296]. Furthermore, they derive the transmitter's optimal rotation phase by maximizing the carrier-to-interference ratio based on the CFO estimate in the training mode. Although authors in [297] improve the cancellation performance for high-frequency offset situations compared with [296], the proposed method requires the information of the CFO. A different approach is followed in [298], where transmit and receive processing are deployed for ICI cancellation design. These processes result in an equivalent OFDM system with fewer subcarriers than the original one. Additionally, the transmit and receive processing matrices are designed to achieve common average signal to interference power ratio overall equivalent subchannels in the transformed OFDM system.

Joint channel and CFO estimation and compensation: All the above mentioned schemes assume the availability of perfect CSI in the receiver. However, this assumption is not practical because the receiver must estimate the channel and CFO together. Thus, a non-linear joint ML algorithm for joint channel impulse response and CFO estimation over a

This article has been accepted for publication in a future issue of this journal, but has not been fully edited. Content may change prior to final publication. Citation information: DOI 10.1109/ACCESS.2021.3101845, IEEE Access

TABLE 9: Summary of blind CFO estimation and compensation studies for single-user OFDM (with perfect CSI).

Article	channel	Est./Comp.	Ch. Est.	Main approach
[256]	AWGN	Both	N/A	ML-based feedback CFO and timing offset estimator
[257], [258]	AWGN	Est.	N/A	ML estimator using the redundant cyclic prefix
[259]	Freq.Sel.	Both	No	Extension of the method in [257] to multipath Rayleigh fading channels
[260]	Freq.Sel.	Est.	No	Estimator for OFDM with non-circular transmissions
[261]	Freq.Sel.	Est.	No	ML timing and CFO estimator
[262]	Freq.Sel.	Est.	No	LS and ML algorithms for joint estimation over fast time-varying multipath channels
[263], [264]	Freq.Sel.	Est.	No	Estimators using subspace structure and null subcarriers.
[267]	Freq.Sel.	Est.	No	Weighted non-linear LS estimator using subspace structure
[268]	Freq.Sel.	Est.	No	Estimation algorithm deploying null subcarriers with distinct spacings
[269]	Freq.Sel.	Both	No	ML estimator using null subcarriers and the redundancy of the cyclic prefix
[270]	Freq.Sel.	Est.	No	Investigating the optimality of the null subcarrier placement for blind estimation
[271]	Freq.Sel.	Both	No	Estimation algorithm with with cosine function approximation
[272]	Freq.Sel.	Both	No	Estimator designs for OFDM/QAM and OFDM/OQAM by using cyclostationarity of the signal
[273]	Freq.Flat	Est.	No	Estimator for OFDM/OQAM based on non-circularity of the received signal
[274]	Freq.Flat	Est.	No	ML algorithm for OFDM/OQAM
[275]	Freq.Sel.	Both	No	Estimator for OFDM/OQAM utilizing header structure and the orthogonality among subcarriers
[276]	Freq.Sel.	Both	No	Estimation algorithm deploying the time–frequency-domain exchange inherent of OFDM
[278]	Freq.Sel.	Est.	No	Estimator development using intrinsic phase shift between neighboring samples
[279]	Freq.Sel.	Est.	No	Estimator using the cyclic prefix and oversampling
[280]	AWGN	Est.	N/A	Estimation by minimizing the variance of the output after the FFT demodulation
[281]	Freq.Sel.	Both	No	Estimator via diagonality criterion
[282]	Freq.Sel.	Both	No	Iterative carrier tracking algorithm by taking advantage of the in-band ripple of OFDM PSD
[283]	Freq.Sel.	Est.	No	ML algorithm for OFDM with constant modulus symbols
[285]	Freq.Sel.	Est.	No	Estimator for OFDM with constant modulus signaling using two successive symbols
[286], [287]	Freq.Sel.	Est.	No	Spectrum-smoothing schemes for OFDM with constant modulus signaling
[288]	Freq.Sel.	Est.	No	Estimator for OFDM with constant modulus signaling using covariance matrix
[289]	Freq.Sel.	Est.	No	CFO estimation in OFDM with constant modulus signaling using covariance fitting criterion
[290]	Freq.Sel.	Both	No	LS algorithm for joint timing offset and CFO estimation
[291]	Freq.Sel.	Both	No	ML algorithm using the redundancy of cyclic prefix for joint timing offset and CFO estimation

multipath fading channel is presented [299]. In this proposed iterative method, pilot tones enable initial estimates and a decision-directed technique provides an effective estimate. Moreover, to reduce the complexity of joint ML estimation, an adaptive approach, e.g., the steepest descent algorithm, is utilized. Sensitivity of channel estimation to the unknown CFO is less than sensitivity of the CFO estimation to unknown channel. However, [300] illustrates that the proposed estimator [299] can suffer from quick temporal variations in channel impulse response and CFO. Hence, they develop an iterative ML pilot-aided estimator for an OFDM system over a multipath fading channel and a simplified model of the received signal. If the received signal model is linearized with respect to the CFO, a closed-form estimator could be derived. Although this method improves the estimation performance with rapid channel and CFO changes, it incurs higher computational complexity. Additionally, authors in [301] represent an ML algorithm for joint estimation of channel impulse response and integer part of CFO by deploying one or more pilot blocks placed at the beginning of the data frame. They assume that the fractional part of CFO is already estimated and compensated for.

Using a preamble symbol, the work in [302] proposes joint estimator via an iterative EM algorithm, which has the expectation and the maximization steps. The expectation step estimates the channel under the assumption of a known CFO; then, the resulting channel estimation is deployed to update the CFO estimate in the maximization step. However, the estimator in [302] is developed for quasi-static channels. Hence, [303] introduces an iterative pilot-aided scheme for joint channel and CFO estimation based on the EM algorithm in OFDM systems with very high mobility. This work approximates the time variation of channel complex gains by a basis expansion model, and first-order autoregressive processes are exploited to characterize the variations of the basis expansion model coefficients statistically. The proposed estimator is robust to uncertainties on the delays and the Doppler frequency. Moreover, the study in [304] alternatively exploits Newton's and EM methods to obtain the ML estimates of channel and CFO. The search range for the CFO is partitioned into several subranges, and the mentioned methods are used within each subrange. If the OFDM signal is modeled as Gaussian random variables, a closed-form expression for EM can be derived. Nevertheless, the performance of the estimator depends on the number of subranges. Indeed, a higher number of them results in lower MSE at the cost of computational complexity.

On the other hand, [305] investigates the joint estimation of channel impulse response and CFO by taking advantage of pilot symbols and null subcarriers. The CFO is first estimated through an approximate ML estimator by exploiting the receive-signal correlation structure in the proposed algorithm. The resulted likelihood function is a function of the pilot and null subcarriers locations, noise variance, and channel correlation. An LS estimator then finds the channel impulse response using the estimated CFO. Furthermore, a

decision-directed joint ML estimator is developed to improve the estimates of channel impulse response, CFO and data symbols iteratively. Furthermore, reference [306] investigates the joint estimation problem of CFO, sparse channel and the variance of noise in OFDM systems by deploying sparse Bayesian learning. An iterative algorithm is proposed, which requires one OFDM block of training symbols and simultaneously estimates the unknown parameters.

However, all the cited joint channel and CFO estimators assume perfect time synchronization, a restrictive assumption in practice. Thus, [307] addresses the joint estimation of frequency-selective channel and CFO in the presence of timing offset based on the ML criterion. In this pilot-aided algorithm, optimal estimates are obtained by a two-dimensional search since the timing offset and CFO are mutually coupled. However, the channel length is considered a known parameter in this algorithm. Hence, [308] explores CFO estimation when the timing offset and channel length are not precisely known. The authors model the channel as a mixture of possible models and develop a Bayesian multi-model-based CFO estimator by utilizing one OFDM training symbol. Furthermore, [309] studies the joint estimation of time-varying frequency-selective channel, timing offset and CFO based on ML criteria. The authors assume that the correlation-based method in [221] already achieves a rough estimate of the timing offset.

Besides, authors in [310] study joint estimation of channel impulse response, CFO and SFO based on a recursive LS algorithm using the received signal samples and pilot tones in the frequency-domain. Moreover, a compensation scheme is proposed for eliminating the ICI induced by CFO and SFO in the frequency-domain. An ML scheme is derived from providing a coarse estimation of initial CFO and SFO values utilized in the recursive LS algorithm to reduce the convergence time and enhance stability.

3) Multiuser OFDMA systems

The subcarriers are divided into non-overlapping sets to serve multiple users, each assigned to an individual user. Thus, multiple users can transmit their data simultaneously. This operation is possible because the subcarriers are orthogonal, and hence ICI does not exist, which avoids MUI among users. However, CFO's destroy this orthogonality, which induces the ICI between a user's own set of subcarriers, as well as MUI from other users' subcarriers. Hence, CFO estimation and cancellation techniques in downlink and uplink should be deployed to prevent performance degradation.

Each user estimates a single CFO between its receiver and the base station transmitter in the downlink and cancels accordingly. Since only a single CFO should be handled, we can consider the OFDMA downlink a group of point-to-point OFDM links, and the existing algorithms for single-user OFDM can perform CFO compensation. On the contrary, in the uplink, each user has its CFO, and the base station receiver should perform frequency synchronization by multi-CFOs estimation and compensation. Thus, synchronization in the OFDMA uplink is a multi-variable problem, and adjusting the receiver oscillator to one CFO can not return the orthogonality among subcarriers.

We divide the studies for multiuser OFDMA systems into 1) pilot-aided and blind estimation and compensation, 2) joint channel and CFO estimation and compensation. Note that the first type assumes knowledge of the channel is available in the receiver.

Pilot-aided and blind estimation and compensation: CFO estimation in OFDMA uplink is related to the type of subcarrier assignments. As discussed in the PN section, OFDMA subcarrier assignment schemes are subband-based, interleaved, and generalized. For the subband-based OFDMA uplink, signals from different users can be separated with a bank of digital band-pass filters, each selecting one subband [311], [312]. Then, the CFO of each subband can be estimated by applying the same method deployed in the single-user OFDM. Following this filtering procedure, authors in [311] propose a blind CFO estimation algorithm based on data correlation by the use of the cyclic prefix (extended method in [257]). The authors show that the estimator's performance decreases when the number of subcarriers in one subband decreases. In [312], a blind CFO estimator is proposed by exploiting null subcarriers inserted in each subband. The CFO estimation approach minimizes the energy of the corresponding null subcarriers.

For the interleaved OFDMA uplink, the authors in [313] propose a pilot-aided ML CFO estimator by optimizing a multidimensional cost function. Each user includes a pilot OFDM symbol in its preamble to enable CFO estimation. The key idea is to design a pilot symbol to approximate the multidimensional optimization problem with independent one-dimensional optimization problems. However, the resulting estimator is complex and also vulnerable to being stuck in local minima/maxima. Thus, [314] develops a pilot-aided CFO estimator based on measuring the phase shift between pilot tones transmitted over adjacent OFDMA blocks. Besides, repetitive training sequences are deployed to minimize the MUI power under a constraint on the overall pilot energy. Although this estimator outperforms that of [313] in terms of MSE performance and complexity, it requires several OFDMA symbols. Besides, the study in [315] designs a pilot structure that provides frequency separation between the subcarriers assigned to any two users. Then, a CFO estimator is presented based on the companion matrix derived from the proposed pilot structure. This estimator achieves acceptable performance when the CFO range increases.

Furthermore, studies in [316]–[318] exploit the sparse distribution of CFOs in frequency-domain and develop recovery techniques to estimate CFOs based on sparse prior information inherent in the received signal. In [316], the potential frequency offset ranges are discretized into discrete grid points, and the estimation problem becomes a sparse signal recovery problem. This problem lends itself to a matrix Bayesian compressive sensing-based CFO estimator, which has two stages: 1) coarse estimations of CFOs, which are

generated by reconstructing a hyperparameter vector via a relatively large grid interval, 2) the refined CFOs, which are obtained one by one via searching the frequency-domain with a smaller grid interval. However, the estimation performance degrades due to interfering with the hyperparameters of the estimated CFOs with noise power. Hence, to weaken the effect of noise, the study in [317] mitigates the noise by taking advantage of the noise covariances matrix in the transformed observation data and proposes a sparse recovery-assisted CFO estimator. However, it achieves acceptable performance only for normalized CFO's less than 0.4. The reason is that in a larger amount, the derived regularization parameter used for the proposed sparse estimator is inaccurate. Therefore, in [318], a blind CFO estimator is designed based on a sparse Bayesian learning framework to achieve better estimations for large CFOs. This paper formulates the estimation problem as a sparse non-negative LS problem, wherein the noise is efficiently suppressed. Then, the problem is solved by the sparse Bayesian learning framework with a non-negative Laplace prior algorithm.

On the other hand, authors in [319] address a blind subspace-based CFO estimator based on the principle of multiple signal classification by deploying the deterministic structure of the signals. This estimator takes advantage of the periodic structure of the signals transmitted by each user. Moreover, the absolute values of all the CFOs are less than half of subcarrier spacing. However, the computational complexity of the proposed estimator is high due to grid search over the uncertainty frequency range. Hence, the study in [320] presents a blind CFO estimator that relies on the estimation of signal parameters via the rotational invariance technique. Although the proposed estimator is closed-form without a peak searching procedure, which reduces the computational complexity, the solutions are not optimal, and they do not reach the CRLB. Thus, in [321], a low-complexity blind estimator based on ML criteria is proposed, and an optimum solution is derived by solving a polynomial function. In the ML method, the CFOs in the likelihood function becomes intractable after the correlation matrix. Therefore, to find the closed-form solution, the authors express the correlation matrix with series expansion and then truncate to derive the expression with a root-finding method. Moreover, the proposed estimator can approach the CRLB.

In the case of a generalized OFDMA uplink, authors in [322] investigate the pilot-aided CFO estimation based on correlation function by exploiting the repetition of a fixed pilot symbol. However, this method only considers the CFO of a new user entering the system and assumes all the other users are perfectly synchronized. Moreover, the study in [323] presents a pilot-aided iterative CFO estimator based on the ML principle. Each iteration of the proposed estimator contains two steps, 1) primitive estimation resulting in the exact residual CFO estimate for all the users and 2) local-search-based CFO adjustment. Nevertheless, this iterative estimator suffers from the computation complexity of the second step. Thus, investigation in [324] proposes an estimation algorithm based on two consecutive received OFDMA symbols motivated by the line search method. In this approach, the second symbol is regenerated as a non-linear function of the CFOs and the first symbol. Then, first-order Taylor series expansion is deployed for deriving the linear approximation. Finally, by minimizing the mean square distance between the received second symbol and its regenerated signal, CFOs and data are jointly estimated.

Furthermore, authors in [325] address a solution for pilot-aided residual CFO tracking in the IEEE 802.16e uplink. The coarse estimation is derived by using one of the exciting methods, but residual CFOs are remained due to estimation errors and/or time-varying Doppler shifts. The proposed solution relies on the LMS principle and updates the frequency estimates at each newly received subframe. In [326], an iterative CFO estimator is designed based on the tile structure of IEEE 802.16e. This proposed estimator exploits the pilot symbols in more than two non-consecutive blocks and is relied on the best linear unbiased estimation principle properly. Note that the estimation range of this method is more extensive than other methods, almost half of the subcarrier spacing. On the other hand, in [327], a subspace-based blind CFO estimator is addressed in which the base station is equipped with a uniform linear array of antennas. This estimator separates the CFOs of different users with their spatial information by taking advantage of the uniform array and narrowband signal assumption. Then, CFOs associated with different are estimated individually. However, in this method, by increasing the number of users, the estimation performance decreases due to increasing the dimensions of signal subspace and decreasing dimensions of noise subspace. Moreover, the authors in [328] develop a blind CFO estimator for generalized OFDMA uplink with constant modulus constellation. Finally, reference [329] proposes a blind algorithm for CFO estimation for generalized OFDMA uplink systems based on null subcarriers.

Joint channel and CFO estimation and compensation:

For the interleaved OFDMA uplink, authors in [330] propose an iterative algorithm for channel estimation, frequency synchronization, and data detection. The algorithm uses a pilot training preamble in each frame. The idea is based on space-alternating generalized expectation-maximization (SAGE) for separating the received signal in the base station. In other words, SAGE decomposes the maximization of the multiuser ML cost function into multiple single-user maximization problems. The EM algorithm is then applied to each subproblem to update the CFO estimate and get channel estimation and data detection.

Furthermore, to improve the estimation performance and reduce the computational complexity, a modified SAGE method is proposed in [331] by incorporating MUI cancellation in both time and frequency-domain. In this work, disjoint sets of cyclically equal-spaced, equal energy pilot tones are assigned to the users. Moreover, the study in [332] extends the proposed approach [330] by considering the impact of channel coding. The authors solve the joint problems of chan-

nel estimation, CFO compensation, and channel decoding via iterative executions of SAGE and EM algorithms.

Joint estimation of channel responses, timing offsets, and CFOs based on the ML principle has also been developed [333]. Arbitrary (random) subcarrier allocation shows the capability of the proposed estimator to work with all three subcarrier assignment schemes. However, this estimator requires each user to transmit a training block at the beginning of the uplink frame. Moreover, since the exact ML solution is complex due to search over a multidimensional space, alternating projection frequency estimation method [334] is proposed to convert the search problem into a sequence of one-dimensional searches. Although this algorithm converges fast and reaches the CRLB, it has high computational complexity. Thus, [335] presents an approximate ML algorithm for joint channel and CFOs estimation by exploiting distinct correlation properties of the training sequences. They convert the grid search ML problem into a polynomial root-finding procedure and derive closed-form estimators for moderate CFOs. The computational complexity is reduced in cost of estimation performance compared with [333]. Hence, the work in [336] proposes an ML-based joint channel and CFO estimator and develops an importance sampling-based technique to handle the multidimensional exhaustive search problem. This technique derives the closed-form solution for CFO estimation using an optimization theorem. The importance sampling method removes the difficulty of the multidimensional integral in the solution. Then, the channel responses are estimated by using the CFOs estimates. The proposed method provides globally optimal solutions, and its computational complexity is lower than the schemes based on alternative projection in [333].

On the other hand, authors in [337] address pilot-aided joint estimation of channels and CFO based on the iterative line search algorithm by applying a linearized approximate signal model. The cost function is defined to minimize the mean square distance between the received signal and the reconstructed received signal. The MMSE criterion is exploited for updating estimates in each iteration. Note that all the unknown parameters are considered together as a whole in this work. Additionally, [338] proposes a pilot-aided joint channel and CFO estimator relied on LS criterion. This estimator has two steps: 1) the variable projection method is exploited for solving a separable non-linear LS problem to estimate the CFO, 2) the channel is estimated by using the MMSE approach. The proposed estimator has a faster convergence rate and achieves better estimation performance compared with [337].

However, all the previous papers do not address the estimation of time-varying channel coefficients. Thus, authors in [339] investigate the pilot-aided joint estimation of the doubly-selective channel and CFO in OFDMA uplink system with high mobility users. An iterative scheme is proposed based on the SAGE-MAP probability algorithm [340]. Moreover, to reduce the computational load, Bernstein basis polynomials are exploited to characterize rapid time variations of the channel. However, the proposed estimator requires the knowledge of channel statistics, which is not practical. Thus, in [341], the authors propose an ML-based estimator that does not require channel knowledge. They deployed Chebyshev polynomials of the first kind as the basis set for tracking the time variation of the channels. Then, the SAGE algorithm is used for developing ML estimator for joint estimation of the basis coefficients and CFOs.

Table 10 shows summary of CFO estimation and compensation studies for multiuser OFDMA systems.

In conclusion, pilot-aided CFO compensators in all the considered systems deploy different approaches for defining their cost function, including LS, EM, ML, MMSE, etc. Although blind estimators enhance the bandwidth efficiency, they have relatively poor performance compared to the pilot-aided ones. Moreover, the proposed estimators typically require many iterations for convergence, which results in higher computational complexity. On the other hand, blind estimators rely on structural and statistical properties of signals and exhaustive searches. Moreover, they suffer from high computational complexity since they often require averaging over numerous data symbols for satisfactory performance.

D. CFO IN EMERGING/FUTURE TECHNOLOGIES

1) MIMO systems

These deploy multiple antennas in the transmitter and receiver to achieve multiplexing or capacity gains. A linear combination of the signals transmitted by the transmit antennas is collected at each receive antenna. If independent oscillators are considered for transmitter and/or receiver, the received signal is affected by multiple CFOs. On the other hand, if a single shared oscillator is deployed in each transmitter and receiver side, the received signal is affected by a single CFO. Note that the estimation and compensation of multiple CFOs will be more challenging than the single CFO. Following, we review the papers for SC MIMO and MIMO OFDM systems in the presence of the CFO.

SC MIMO systems: Authors in [342] investigate the pilot-aided CFO estimation problem in an SC MIMO system with BPSK modulation and flat-fading channel. All transmit and receive antenna pairs are affected by the same CFO. The authors propose an ML-based estimator for CFO estimation by deploying training symbols. Moreover, they also provide an iterative code-aided EM-based estimator for the joint channel and CFO estimation. The study in [343] proposes a closed-form solution for pilot-aided ML-based CFO estimation in SC MIMO with QPSK modulation and presents an efficient hardware architecture. Note that similar to [342] a flat-fading channel is considered, and this method loses its performance in the presence of frequency-selective channels.

On the other hand, [344] proposes a pilot-aided phase estimation and compensation method for the MIMO SC-FDE systems to suppress the phase distortion generated by CFOs and reliably detect equalized data. Severely frequency-selective channel fading and multiple unknown CFOs are

This article has been accepted for publication in a future issue of this journal, but has not been fully edited. Content may change prior to final publication. Citation information: DOI 10.1109/ACCESS.2021.3101845, IEEE Access

TABLE 10: Summary of CFO estimation and compensation studies for multiuser OFDMA systems

Article	channel	Pilot/Blind	Est./Comp.	Ch. Est.	Main approach
[311]	Freq.Sel.	Blind	Both	No	Estimation algorithm using cyclic prefix
[312]	Freq.Sel.	Blind	Both	No	Estimator design based on null subcarriers
[313]	Freq.Sel.	pilot	Est.	No	ML algorithm
[314]	Freq.Sel.	pilot	Est.	No	Estimator development using the phase shift between pilot tones
[315]	Freq.Sel.	pilot	Est.	No	Estimation based on a companion matrix
[316]	Freq.Sel.	Blind	Est.	No	Algorithm using sparse prior information in the received signal
[317]	Freq.Sel.	Blind	Est.	No	Estimator design using noise covariance matrix
[318]	Freq.Sel.	Blind	Est.	No	Sparse Bayesian learning frameworks
[319]	Freq.Sel.	Blind	Est.	No	Subspace-based estimator
[320]	Freq.Sel.	Blind	Est.	No	Rotational invariance-based estimator
[321]	Freq.Sel.	Blind	Est.	No	ML algorithm
[322]	Freq.Sel.	pilot	Both	No	Estimator design using the repetition of a fixed pilot symbol
[323]	Freq.Sel.	pilot	Est.	No	ML estimator
[324]	Freq.Sel.	pilot	Est.	No	Line search-based estimator
[326]	Freq.Sel.	pilot	Both	No	Iterative estimator using tile structure of IEEE 802.16e
[327]	Freq.Sel.	Blind	Est.	No	Subspace-based estimator based on narrowband signal assumption
[328]	Freq.Sel.	Blind	Both	No	Estimator for OFDMA uplink with constant modulus constellation
[329]	Freq.Sel.	Blind	Both	No	Estimator design using null subcarriers
[330]	Freq.Flat	pilot	Both	Yes	SAGE estimator
[331]	Freq.Sel.	pilot	Est.	Yes	Modified SAGE algorithm
[332]	Freq.Flat	pilot	Both	Yes	Iterative executions of SAGE and EM algorithms
[333]	Fre.Sel.	pilot	Both	Yes	ML joint channel, timing offsets and CFOs estimator
[335]	Freq.Sel.	pilot	Est.	Yes	ML algorithm using distinct correlation properties of training sequences
[336]	Freq.Sel.	pilot	Est.	Yes	Sampling-based technique to handle the multidimensional exhaustive search problem
[337]	Freq.Sel.	pilot	Est.	Yes	Iterative line search algorithm by applying a linearized approximate signal model
[338]	Freq.Sel.	pilot	Est.	Yes	LS joint estiomator
[339]	Freq.Sel.	pilot	Est.	Yes	SAGE-MAP probability algorithm for joint doubly-selective channel and CFO estimation
[341]	Freq.Sel.	pilot	Both	Yes	ML estimator using Chebyshev polynomials

considered. In this work, the average rotating phase for each data block group is estimated in a decision-directed method. It compensates for the phase distortions based on estimated rotating phases before performing the symbol detection. Additionally, the LS frequency-domain channel estimation algorithm is proposed for tracking time-varying channels. Moreover, references [345], [346] address the training sequence design for joint frequency-selective channel and CFO estimation in the SC MIMO systems. The CRLBs are used as a metric for training sequence design, and the derived sequence facilitates the simple implementation of the ML CFO and channel estimators. Moreover, [346] explores channel gains and multiple CFOs estimation problems over frequency-selective channels by proposing a training sequence with a subspace-based algorithm. The CFOs between transmit and receive antenna pairs are not the same. However, this estimator increases the computational load for improving the estimation performance.

Furthermore, [347] addresses the joint blind channel and single CFO estimation in an SC MIMO system based on orthogonal space-time codes over flat-fading channels. For constant-modulus constellations, an ML estimator is designed, ignoring the finite alphabet constraint for simplicity. CFO can be estimated by maximizing the eigenvalue of a specific data-dependent matrix and whose eigenvector can be exploited for channel estimation.

For an SC uplink asynchronous multiuser MIMO system, [348] proposes a frequency synchronization and equalization algorithm. Each user has a single transmit antenna, and one base station with multiple receive antennas is considered. Based on second-order statistics, a blind method estimates the shaped channels with ambiguity. Using the estimated channels, the MIMO system over frequency-selective channels is converted to an MIMO system with flat-fading channels. Then, pilots are designed to estimate CFOs, based on the ML criterion and resolving the channel ambiguity. Finally, the transmitted symbols are recovered by the equalization method based on the MMSE principle. Moreover, [349] proposes another frequency synchronization scheme for an SC uplink multiuser MIMO system based on space-time beamforming. This work performs subspace analysis on the received space-time snapshots, and the beamforming vector is constrained to lie in the corresponding signal subspace. Then, under this constraint, joint CFO estimation and space-time beamforming are performed by minimizing a cost function defined as the difference between the CFO distorted training block and the beamformed space-time signal.

Table 11 shows summary of CFO estimation and compensation studies for SC MIMO systems.

MIMO OFDM systems: Before we present studies for CFO estimation in MIMO OFDM systems, some investigations for CFO estimation in SIMO OFDM system are addressed. Studies in [350], [351] investigate CFO estimation in SIMO OFDM system by exploiting the multi-antenna redundancy at the receiver. In [350], an ML-based CFO estimator is designed based on the fact that different receive branches contain uncorrelated observations about the same information bits. Moreover, the study in [351] develops a

This article has been accepted for publication in a future issue of this journal, but has not been fully edited. Content may change prior to final publication. Citation information: DOI 10.1109/ACCESS.2021.3101845, IEEE Access

TABLE 11: Summary of CFO estimation and compensation studies for SC MIMO systems

Article	channel	Pilot/Blind	Est./ Comp.	MCFOs/ SCFO	Ch. Est.	Main approach
[342]	Freq.Flat	Pilot-aided	Est.	SCFO	Yes	ML estimator and an iterative code-aided EM-based joint estimator
[343]	Freq.Flat	Pilot-aided	Est.	SCFO	No	Closed-form ML estimator
[344]	Freq.Sel.	Pilot-aided	Both	MCFOs	Yes	Estimator design for SC-FDE MIMO system
[345]	Freq.Sel.	Pilot-aided	Est.	SCFO	Yes	Training sequence design under different energy-distribution constraints
[347]	Freq.Flat	Blind	Est.	SCFO	Yes	Estimator design by maximizing the eigenvalue of a certain data-dependent matrix
[348]	Freq.Sel.	Pilot-aided	Both	MCFOs	Yes	Estimator based on ML approach and second-order statistics for multiuser uplink systems
[349]	Freq.Sel.	Pilot-aided	Both	MCFOs	Yes	Space-time beam forming-based frequency synchronizer for multiuser MIMO uplink

blind CFO estimator based on trilinear decomposition and LS principle. However, this method requires a large number of OFDM blocks to achieve satisfactory performance. Based on the ML principle, blind CFO estimation for OFDM with multi-antenna receiver is studied in [352], which is expanded to the MIMO case. In this method, channels stay constant over more than one successive OFDM block, and the number of the receive antennas is greater than the number of the transmit antennas. The cost function is defined by restoring the rank one property of matrices constructed by the received signal after the CFO cancellation at each subcarrier from each receive antenna. Although this method's performance is acceptable, according to an exhaustive search for finding the optimal value of the CFO, this method requires high order of computations. Thus, the closed-form method for blind CFO estimation for OFDM with a multi-antenna receiver is proposed in [353]. The key idea for defining a cost function is that the received signal at each subcarrier from different receive antennas in different OFDM blocks is spanned by a single common vector of channel frequency response at the given subcarrier, which is caused by assuming the channel to be constant during some OFDM blocks. Moreover, by proving that the defined cost function is precisely a cosine function, a closed-form expression for the CFO estimate is proposed. Although this method supports fully loaded transmissions and can reduce the computational complexity compared with [352], it is not an optimal solution and suffers from performance degradation.

On the other hand, in [354], joint CFO and channel for OFDM with the multi-antenna receiver are blindly estimated by exploiting one received OFDM block. By assuming the channel between the transceivers to be constant within one OFDM block and computing each subcarrier signal in each receive antenna after compensating CFO with trial value, the cost function is derived. To be specific, the cost function is defined by considering the linear relation between the received signal and the channel in the frequency-domain at each subcarrier.

We next review the estimation and compensation studies for MIMO OFDM systems.

Pilot-aided estimation and compensation: an EM-based iterative receiver is designed for the MIMO OFDM system in [355]. The performance of the proposed algorithm depends on the initial estimation of the transmitted symbol. Indeed, since iterative receiver requires a pilot slot to obtain a good initialization, authors utilize this slot for CFO estimation and provide more accurate initialization for the EM-based receiver. In this method, CFO is estimated with ML detection and after CFO cancellation, an LS estimator is deployed to estimate the fading coefficients during the pilot slot. In the following data slots, by knowing the estimated fading coefficients and utilizing the ML algorithm, an initial estimate of the transmitted symbols is derived. Using this initial point, the EM algorithm updates the fading coefficients and detects the transmitted symbols iteratively.

On the other hand, a study in [356] explores a training sequence assisted CFO estimator based on the ML criteria for MIMO OFDM systems over frequency-selective fading channels. Sub-optimal training sequences relied on the Chu sequence are proposed. This estimator finds the integer part of CFO by deploying the orthogonality of the training sequences in the frequency-domain. The fractional part of CFO is estimated by exploiting the uniformly spaced non-zero pilots in the training sequences. Additionally, geometric mapping is exploited to simplify the complex polynomial into a real polynomial for estimation of fractional part by finding the roots. However, implementing the polynomial rooting operation in this estimator is not straightforward in practical systems. Thus, authors in [357] address a CFO estimator for MIMO OFDM systems by exploiting the training sequences generated from the Chu sequence [358]. The CFO is estimated by factor decomposition for the derivative of the ML cost function based on the periodicity property of these sequences. Although this trick reduces the implementation complexity, the critical assumption is that channel taps remain constant during the training period, which may not be realistic.

Blind estimation and compensation: The authors in [359] present an estimator for MIMO OFDM systems based on a kurtosis type of criterion that measures the Gaussianity of a random sequence. They assume that the CFOs for different transmit-receive antenna pairs are approximately the same. The key idea for defining the cost function is that the distribution of the received signal after CFO cancellation with trial value will be more non-Gaussian if CFO is perfectly estimated. Moreover, a closed-form expression for the MSE

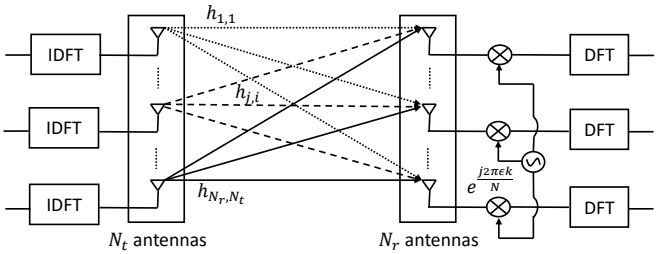

FIGURE 18: MIMO OFDM system with single shared oscillator. A single common CFO appears between the transceivers.

of the estimated CFO is obtained for a frequency-flat channel. However, this estimator suffers from performance degradation in frequency-selective fading channels and requires many OFDM symbols. Thus, authors in [360] propose a blind estimator for MIMO OFDM by exploiting the multi-antenna redundancy at the receiver. The system model of this work is shown in Fig. 18. The cost function is defined based on the correlation matrix constructed by received signal at different antennas in frequency-domain after CFO compensation with a trial value. The proposed cost function can be expressed as the superposition of cosine waves, making it computationally efficient. Note that the difference between the number of receiving and transmitting antennas should be at least one in this estimator.

On the other hand, authors in [361] present a blind CFO estimation approach for orthogonal-space-time-block-coded MIMO OFDM with constant modulus signaling under the assumption of equal channel responses for adjacent subcarriers. The cost function is defined by minimizing the difference between the signal power of two neighboring subcarriers. Nevertheless, the considered assumption is accurate when the channel frequency response changes slowly in the frequency-domain. Thus, the performance of this estimator degrades in the presence of severe fading conditions. Thus, investigation in [362] develops a blind CFO estimator for MIMO OFDM with constant modulus constellations over the frequency-selective fading channels. The cost function is defined by minimizing the components of the signal power spectrum, and computational complexity is reduced by finding a closed-form CFO estimate. However, this scheme requires a large number of OFDM symbols to obtain reliable CFO estimates. Furthermore, this estimator suffers from performance error floor under the moderate and high-SNR regions, which is caused by interference among the signals from multiple transmit antennas. Thus, the study in [363] explores blind CFO estimation for MIMO OFDM with constant modulus constellations by utilizing rank reduction criterion. The key idea is based on the rank of the matrix, which are constructed by signals at each subcarrier in each receive antennas. Since the rank of the mentioned matrix increases under non-perfect CFO compensation, by minimizing the rank of the matrix under the presence of CFO, the cost function is defined. This method avoids the performance error floor by increasing SNR, which outperforms the estimator method in [362] at the cost of a higher order of complexity. Furthermore, authors in [364] propose a blind estimator for MIMO OFDM based on the banded structure of covariance matrices for constant modulus signals. In the absence of the CFO, the covariance matrices formulated by circular shifts of received signals have the banded structure. Hence, the cost function is designed to minimize the out-of-band of the matrices, resulting in a closed-form CFO estimation algorithm. Since the presented estimator suffers from channels with high delay spreads, the authors improve it by deploying both the in-band and out-of-band information of covariance matrices under the assumption of a constant channel over two consecutive symbols.

Besides, authors in [365] investigate the blind CFO estimation problem in multiuser MIMO OFDM uplink systems. They assume that the base station is equipped with multiple antennas (with a single shared oscillator), and each user has a single antenna. Different transmitter and receiver pairs have different CFO that means multiple CFOs are required to be estimated. A subspace-based estimator is proposed, which estimates multiple CFOs from a rank reduction approach. Besides, the estimates improve with an ML-based estimator. However, the later estimator suffers from computational complexity, which is reduced by the alternating projection method.

Joint channel and CFO estimation and compensation: Authors in [366] propose algorithms for sequential estimation in an MIMO OFDM system by using null subcarrier and non-zero pilot symbols inserted and hopped from block to block. In this estimator, CFO is first estimated by measuring the CFO-induced shift in the null space through line search. Then, after removing the CFO terms, the channel is estimated by exploiting LS criteria. However, since residual CFO estimation could destroy the channel estimation performance, phase estimation is performed to find it per block by exploiting non-zero training symbols. This method requires high computational complexity. Furthermore, the study in [367] develops a pilot-aided algorithm to jointly estimate the multipath Rayleigh channel complex amplitude and CFO based on extended Kalman filtering and the equivalent discrete-time channel model. Within one OFDM symbol, the basis expansion model is exploited for approximating time-varying the complex amplitudes. Then the dynamics of basis expansion model coefficients and CFO parameters are modeled through first-order autoregressive processes. Finally, extended Kalman filtering as a recursive algorithm is addressed for the estimations of the parameters. However, this method requires that the system noises be Gaussian with available statistics. Thus, investigation in [368] proposes a pilot-aided joint estimator over time-varying channels based on the extended H_∞ filter. This estimator does not require knowledge of the noise distributions and less sensitive to the noise variance error than the estimator in [367]. Moreover, similar to [367], the basis expansion model is exploited to reduce the number of channel parameters in [369]. Then,

CFO and basis expansion model coefficients are treated as random variables under pilot-aided Bayesian estimation and are estimated by the MAP technique. Additionally, to improve the estimation performance, extrinsic information from the output of the SISO decoder is deployed to derive additional pilot symbols by generating soft estimates of data symbols. Since this estimator is iterative, the computational load may be high.

Moreover, authors in [370] address joint channels and multiple CFO estimation problems in multiuser MIMO OFDM uplink systems. In this paper, CFOs are incorporated into the transmitted symbols and channels. Then, a blind method for channel estimation in [371] (based on second-order statistics of the received signal) is exploited to obtain an estimation for the CFO incorporated channels with an ambiguity matrix. The CFOs and the ambiguity matrix are resolved by using a pilot OFDM block for each user.

Besides, authors in [372] propose a pilot-aided ML-based estimator for joint channel and CFO estimation in multiuser MIMO OFDM uplink. The optimal training sequences are designed by minimizing the asymptotic Cramér–Rao bounds for channel and CFO estimation, given the bounds being channel independent. The multidimensional ML estimator is then solved by the proposed Monte-Carlo importance sampling-based estimator in [373]. Although this estimator reduces the computational complexity related to ML estimation, it can not yield the optimal solution. Furthermore, in [374], a pilot-aided joint channel and CFO estimator is developed for an uplink MIMO OFDM system based on the Schmidt Rao-Blackwellized particle filters. Authors deploy the parallel Schmidt Kalman filter to break down the multiuser estimation problem into subproblems by exploiting a few training blocks (each subproblem deals with one user). They then use the Schmidt Rao-Blackwellized particle filter to solve each subproblem, where the CFO is estimated by sampling importance-resampling technique, and the channel is updated through a bank of Kalman filters conditioned on the generated CFO samples.

However, all the previous papers in multiuser MIMO OFDM assume that the channel is constant within an OFDMA symbol. Thus, studies in [375], [376] address the joint channel and CFO estimation in the presence of doubly-selective channels by using pilot symbols. Authors in [375] propose an joint ML-based estimator. They exploit Bernstein's basis polynomial to capture the time variations of the channel. Also, they address an iterative scheme that relied on the oblique projection that decomposes multidimensional search into many one-dimensional searches for reducing the computational complexity. However, they assume that CFO is constant for all OFDMA symbols, which is not applicable when we have time-varying Doppler shifts. Thus, the study in [376] explores the problem of joint time-varying CFO and doubly-selective channel estimation. Basis expansion modeling is considered for tracking the doubly-selective channel, and Schmidt Kalman filtering is deployed for decomposing the multiuser estimation problem into several more straightforward problems corresponding to each user. Then, two approaches are proposed for solving the channel and time-varying CFO estimation problem of each user. The first one is based on the Schmidt extended Kalman filtering, which suffers from a convergence problem. The second one is based on Gaussian particle filters and Schmidt Kalman filtering by adopting a marginalized Kalman filtering approach.

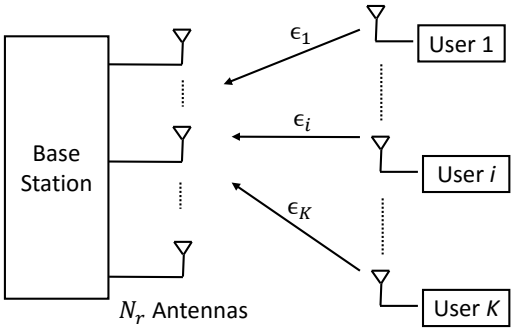

FIGURE 19: Multiuser OFDM uplink transmission with a massive MIMO base station and multiple single-antenna users. ϵ_i is the normalized CFO between the i-th user and the base station.

Table 12 shows summary of CFO estimation and compensation studies for SIMO OFDM and MIMO OFDM systems.

2) Massive MIMO systems

In the multiuser massive MIMO systems, the base station is equipped with hundreds of antennas to simultaneously communicate with multiple users in the same time–frequency resource. These systems increase spectral efficiency by serving more users under perfect frequency synchronization. CFOs from different users could destroy the performance of these systems by introducing ICI and MUI terms. Thus, CFOs estimation and cancellation techniques are developed to suppress these effects.

Authors in [377] investigate the impact of residual CFO (after inadequate CFO estimation/compensation) on the information rate of ZF and MRC receivers in the SC massive MIMO uplink systems over a frequency-flat-fading channel. Both receivers experience the same performance degradation in the presence of residual CFO. Moreover, when the number of base station antennas M is sufficiently large, $\mathcal{O}(\sqrt{M})$ array gain under residual CFO can be achieved, which is the same as the ideal zero CFO. Moreover, the work in [378] further studies the impact of frequency selectivity on the required per-user transmit power in the CFO impaired SC massive MIMO uplink systems. MRC receiver and a fixed per-user information rate are considered. The authors reveal that the gap in the required power between the residual CFO and the zero CFO scenarios decreases by increasing frequency-selectivity. Furthermore, in the residual CFO scenario, $\mathcal{O}(\sqrt{M})$ array gain is achievable in the presence of frequency-selective channels. In contrast to [377] and

TABLE 12: Summary of CFO estimation and compensation studies for SIMO OFDM and MIMO OFDM systems

Article	system	channel	Pilot/ Blind	Est./ Comp.	MCFOs/ SCFO	Ch. Est.	Main approach
[350]	SIMO	Freq.Sel.	Blind	Both	SCFO	No	ML estimator using uncorrelated observations
[351]	SIMO	Freq.Sel.	Blind	Est.	SCFO	No	Developing an estimator based on trilinear decomposition and LS principle
[352]	SIMO	Freq.Sel.	Blind	Est.	SCFO	No	Estimator design using the rank one property of received signal matrices
[353]	SIMO	Freq.Sel.	Blind	Est.	SCFO	No	Closed-form estimator with cosine cost function
[354]	SIMO	Freq.Sel.	Blind	Est.	SCFO	Yes	Joint estimator using linear relation between received signal and channel
[355]	MIMO	Freq.Sel.	pilot	Est.	SCFO	Yes	EM-based iterative receiver
[356]	MIMO	Freq.Sel.	pilot	Est.	SCFO	No	Estimation by orthogonal training sequences and uniformly spaced pilots
[357]	MIMO	Freq.Sel.	pilot	Est.	SCFO	No	Estimation algorithm based on Chu training sequence
[359]	MIMO	Freq.Flat	Blind	Est.	SCFO	No	Kurtosis criterion-based estimator
[360]	MIMO	Freq.Sel.	Blind	Est.	SCFO	No	Estimator design using the multi-antenna redundancy at the receiver
[361]	MIMO	Freq.Sel.	Blind	Est.	SCFO	No	Estimator for MIMO OFDM with constant modulus signaling
[362]	MIMO	Freq.Sel.	Blind	Est.	SCFO	No	Estimation by minimizing the components of the signal power
[363]	MIMO	Freq.Sel.	Blind	Est.	SCFO	No	Rank reduction-based estimation algorithm
[364]	MIMO	Freq.Sel.	Blind	Est.	SCFO	No	Estimator based on the banded structure of covariance matrices
[365]	MIMO uplink	Freq.Sel.	Blind	Est.	MCFOs	No	Subspace-based estimator with rank reduction approach
[366]	MIMO	Freq.Sel.	pilot	Est.	SCFO	Yes	Sequential estimation using null subcarrier and non-zero pilot symbols
[367]	MIMO	Freq.Sel.	pilot	Est.	MCFOs	Yes	Joint estimator based on extended Kalman filtering
[369]	MIMO	Freq.Sel.	pilot	Est.	SCFO	Yes	MAP estimator deploying basis expansion model
[370]	MIMO uplink	Freq.Sel.	Both	Est.	MCFOs	Yes	Exploiting an estimator [371] in for estimating CFO incorporated channels with an ambiguity matrix
[372]	MIMO uplink	Freq.Sel.	pilot	Est.	MCFOs	Yes	Joint ML estimator with optimal training sequence designs
[374]	MIMO uplink	Freq.Sel.	pilot	Est.	MCFOs	Yes	Proposing a joint estimator based on the Schmidt Rao-Blackwellized particle filters
[375]	MIMO uplink	Freq.Sel.	pilot	Est.	MCFOs	Yes	ML algorithm using Bernstein basis polynomial
[376]	MIMO uplink	Freq.Sel.	pilot	Est.	MCFOs	Yes	Estimator designs based on Schmidt extended Kalman filtering, Gaussian particle filters and Schmidt Kalman filtering

[378], the work in [379] investigates the impacts of CFO on frequency-flat massive MIMO downlink. For both MF and ZF precoders, closed-form expressions of achievable rate are derived in the presence of CFO, quasi-static radiofrequency mismatch, and channel estimation error. Moreover, two-oscillator setups are considered for base station antennas, single shared oscillator and independent oscillators. The ZF precoder is asymptotically more desirable for both setups with CFO compensation.

On the other hand, authors in [380] address a pilot-aided frequency synchronization technique based on the angle information of users for multiuser OFDM uplink with a massive uniform linear array at the base station. In this work, CFO for each user is estimated individually by restricting the incident signal at the base station from each user within a specific angular spread. Hence, a joint spatial-frequency alignment procedure, based on an equivalent frequency asynchronous single-user received signal model, is proposed for each user's joint CFO and direction of arrival estimation. Furthermore, investigation in [381] presents a pilot-aided frequency synchronization technique with the aid of scattered pilot symbols. The system model of this work is shown in Fig. 19. The CFO estimation is performed for each user individually by deploying the spatial dimensions offered by many base station antennas. Besides, after CFO estimation, a beamforming matrix is designed for MUI cancellation. Similar to the technique in [380], the computational load of the proposed technique is high, and by increasing the number of antennas, it goes up rapidly. Hence, authors in [382] propose a pilot-based frequency synchronization technique with low computational complexity. They extract the signal of each desired user from the received signal's covariance matrix by exploiting a training sequence that is orthogonal onto space spanned by the desired user's pilot. CFO estimation is performed for each user by using the Golden section search algorithm. Moreover, after channel estimation based on ML criteria, a CFOs compensation scheme is presented, which is performed after combining the received signals at base station antennas. After applying the cancellation scheme, the CFO estimation error generates a constant phase shift, while an algorithm is addressed for canceling it.

Moreover, a study in [383] investigates angle-domain adaptive filtering-based frequency synchronization method for the massive MIMO uplink systems in the presence of overlapping angle-of-arrival regions among users. The authors define an angle-constraining matrix for each user, including a set of selected match-filter beamformers pointing to the angle-of-arrival of the interested user. Then, MUI from non-overlapping users is suppressed through the angle-constraining matrix, and also, the MUI from adjacent overlapping users is mitigated by the angle-domain adaptive filtering. Finally, CFO estimation and data detection are performed independently for each user. However, when angle-of-arrival regions of users are highly overlapping, the proposed frequency synchronization approach can not eliminate the MUI terms perfectly and results in performance degra-

dation. Thus, in [384], a user-coupling angle-domain adaptive filtering-based frequency synchronization method is proposed for CFOs estimation for users with highly overlapping angle-of-arrival regions. To deal with the severe MUI among these users, they are categorized into one or several couples and similar to [383], MUI from non-overlapping users is mitigated by exploiting the angle-constraining matrix. Finally, joint CFO estimation and data detection are performed for the coupled users by the proposed user-coupling angle-domain adaptive filtering-based frequency technique. Moreover, the angle-domain adaptive filtering in [383] is deployed for each of the rest non-overlapping users.

In [385], a blind frequency synchronization method for multiuser uplink transmissions with OFDM modulation and a massive number of receive antennas is presented. Blind CFO estimation for each individual user is performed relied on different null subcarriers assigned to different users. The cost function is defined based on the covariance matrix constructed by corresponding null subcarriers of each user. Bu using estimated CFOs, the MUI cancellation technique is proposed, which reduces the multiuser OFDM uplink system to the OFDM system with a single transmit antenna and multiple receive antennas. Finally, the blind channel estimation and data detection are performed for each user. However, the proposed algorithm relies on an exhaustive grid search, which is not computationally efficient. Thus, the study in [386] proposes a computationally efficient blind CFO estimator for multiuser uplink massive MIMO OFDM system by exploiting orthogonality between channel matrices of different users. In this work, null subcarriers are assigned to each user. MUI cancellation is performed based on subspace analysis of the space-domain snapshots at those null subcarriers of one user. Following the cancellation, the multiuser system reduces to a set of parallel single-user transmission models, and the CFO of each of them is estimated by a single-user conventional estimator in [360].

3) Relaying cooperative systems

In relay systems, transmit signals from the source and relays have different CFOs, which degrade the system's performance, e.g., spatial diversity, by introducing interference terms. For example, consider the standard configuration of one source node, one destination node, and multiple relay nodes. The source to destination protocol can be decomposed into two time-slots. In the first one, a frame of data is transmitted from source to relay nodes. The frame comprises a synchronization preamble and pilot blocks for channels and CFOs estimations. Note that each relay nodes experience a single CFO from the source, which can be removed by single CFO estimation and cancellation techniques in each relay. In the second time slot, the relay nodes forward the source signal to the destination. Hence, the destination experiences multiple CFOs from the relay nodes, which should be estimated and canceled.

Authors in [387] investigate the timing offset and CFO estimations in cooperative space-time block coded OFDM systems with DF-based relays over frequency-selective channels. By exploiting a single OFDM training block with a tile structure in the frequency-domain, timing offsets are estimated based on correlation-type algorithms. A subspace decomposition-based algorithm estimates the CFO by inserting null subcarriers in the proposed tile structure. Besides, optimal tile length is derived in terms of synchronization errors and BER. Moreover, in [388], CRLBs of CFOs estimation are derived for both DF and AF-based space-time block coded OFDM systems over flat-fading channels. One source node, one destination node, and multiple relay nodes are considered. Additionally, this paper proposes two iterative algorithms for CFOs estimations based on multiple signal characterization.

On the other hand, with block-rotated preamble design, the authors in [389] calculate the CRLBs of CFOs estimation for two-way AF relay systems over frequency-selective fading channels. The considered system consists of two sources, two destinations, and one relay that digitally amplifies the baseband's received signal. Note that the block rotation angle property of the designed preamble introduces an artificial block-level frequency offset that separates the preambles from the two sources in the frequency-domain and distinguishes the CFOs of the two sources. However, the derived CRLBs are based on the specific preamble design and do not apply to general cases. Besides, the study in [390] investigates the CRLBs of CFOs estimation for OFDM-based cooperative networks with single AF-based relay over multipath channels. The CFOs of the source-relay and the relay-destination links are evaluated separately. Moreover, the first-order Taylor series expansion is exploited to simplify the inverse of the color noise covariance matrix in the Fisher information matrix. The source-relay link CFO estimation bound is higher than the relay-destination link, and the gap increases when the relay SNR is much smaller than the destination SNR.

Although all the papers mentioned above assume channel information is available, some papers investigate the joint channel and CFO estimation problem. In [391], joint ML-bases channel and CFO estimator is proposed for time-asynchronous SC cooperative systems with DF relays over Rayleigh fading channels. To reduce the computational complexity, an approximation of the estimator is developed in which the SAGE algorithm is exploited to separate the superimposed signals received at the destination. Then, these separated signals are deployed at each iteration to update the channel and CFO estimates for each relay-destination link. Moreover, authors in [392] address the joint estimation of frequency-flat-fading channel gains, timing offsets, and CFOs in SC space-division multiple-access cooperative networks. Note that both DF and AF multi relays are considered. An LS estimator is proposed for joint parameters estimations, and to reduce the complexity, iterative estimators based on expectation conditional maximization and SAGE are presented. Moreover, an ML decoder is designed for detecting the signal in the presence of timing offsets and

This article has been accepted for publication in a future issue of this journal, but has not been fully edited. Content may change prior to final publication. Citation information: DOI 10.1109/ACCESS.2021.3101845, IEEE Access

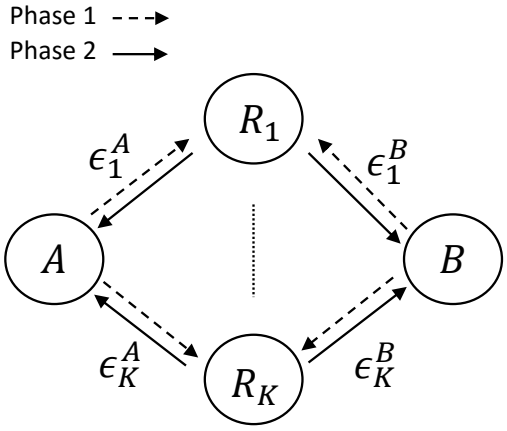

FIGURE 20: Block diagram of a two-way relay network given multiple CFOs with two source nodes, A and B and K number of AF-based relay nodes . In phase 1, two source nodes transmit OFDM signal to relay nodes and in phase 2, relay nodes amplify the superimposed signal and broadcast to the user terminals.

CFOs. However, this estimator is not applicable for distributed space-time block coded cooperative systems. Thus, the same joint estimation of channel gains, timing offsets, and CFOs in distributed space-time block coded-AF relaying cooperative networks is addressed in [393]. Similar to [392], the considered system is SC. LS and differential evolution-based estimators are presented by using training sequences. The latter one is an iterative method that reduces the computational load. Finally, a minimum-square error receiver is developed to decode the received signal by canceling the effect of the timing offsets and CFOs impairments at the destination.

Furthermore, the work in [394] presents the joint estimation of channel and CFOs for an OFDM-based two-way relay network with two source terminals and an AF-based relay over frequency-selective channels. Cyclic prefix-based and zero padding-based OFDM protocols are proposed, and the estimator is designed to rely on nulling-based LS. The authors illustrate that the estimator is unbiased at high-SNR. Also, they derive a closed-form expression of MSEs. Moreover, the zero padding-based OFDM outperforms the Cyclic prefix-based one in terms of the symbol decoding errors. Furthermore, the study in [395] addresses the joint estimation of channel gains and CFOs in a two-way relay network with multiple AF-based relay nodes over the doubly-selective channel. The system model of this work is shown in Fig. 20. Two pilot-based estimators based on the SAGE algorithm and EM approach are proposed. Besides, rapid time variations of the channel are captured by adopting discrete prolate spheroidal and Karhunen–Love basis expansion models. However, both [394], and [395] considers that the two source terminals are perfectly time-synchronized. Thus, the study in [396] investigate joint channel and CFO estimation for AF-based two-way relay networks with timing offsets between the two terminals. Two source nodes and one relaying node are assumed. Also, flat-fading channels are considered, and the timing offset is treated as a known parameter. ML estimator is developed for joint parameters estimations, and to reduce the complexity, an approximate EM-based estimator is presented by exploiting both pilot-carrying and data-carrying samples. Every iteration of the latter estimator has two steps: 1)the expectation step: the expectation of the log-likelihood function for the conditional probability mass function of the hidden data, 2) the maximization step: the result of the first step is maximized for the desired parameters.

Based on the available channel and CFO estimations, CFOs cancellation, ICI reduction, and data detection can be performed. In [397], an Alamouti space-time coded OFDM scheme is designed for cooperative systems with CFOs to achieve spatial diversity. A cooperative system with one source node, one destination node, and two DF-based relay nodes are considered. The channel between relay nodes and destination is quasi-static flat-fading. The source symbols are ideally detected in the relays, and then they are encoded into the Alamouti code. The coded symbols are OFDM modulated and are sent to the destination. The Alamouti code structure on each subcarrier does not hold due to ICI terms introduced by CFOs. To remove these terms, an ICI self-cancellation scheme is proposed by symmetric data-conjugate mapping in relay nodes. However, this scheme relies on real-valued channels, which can be generated by multiplying the normalized complex conjugate of the channel estimation in relay nodes.

A similar system model is considered in [398] with frequency-selective channels. The authors propose a CFOs mitigation scheme by using the redundancy of cyclic prefix. The received signal in the destination is formulated in matrix form based on channels, and OFDM signals with cyclic prefix and CFO mitigation matrix are derived. Although the proposed approach is a prepossessing procedure in the destination and independent from cooperative encoding/decoding details, it requires a long cyclic prefix to achieve proper mitigation performance. Note that both approaches in [397], [398] introduce the redundancies that reduce the data rate critically. Thus, the study in [399] addresses a data detection technique for space-time block coded OFDM systems over frequency-selective channels. In this proposed detector, ICI is first removed by using received two consecutive OFDM blocks, and then iterative symbol detection is performed relied on the ML criterion. Although this detector reduces the computational complexity and enhances the bandwidth efficiency, it is designed for CFOs ranges less than half of subcarrier spacing.

Moreover, authors in [400] present an ICI cancellation scheme for space-frequency coded OFDM systems with multiple CFOs over frequency-selective channels. They assume one source node, one destination node, and many DF-based relay nodes. In this system, ideally detected symbols in relays are encoded to a space-frequency codeword matrix

in a distributed fashion and then are OFDM modulated and sent to the destination. In destination, to mitigate ICI effects, linear filtering is exploited to maximize the SINR of each subcarrier based on the MMSE criterion. Then ML or sphere-decoding methods are deployed for decoding the space-frequency code. Moreover, a study in [401] investigates data-detection for cooperative space-frequency block coded OFDM systems over frequency-selective channels with DF-based relay nodes. The proposed detector is relied on reduced-dimension ML detection and includes coarse detection based on successive interference cancellation and good detection by performing parallel interference reduction. Note that this detector suffers from performance degradation when CFOs are prominent.

On the other hand, authors in [402] study the CFOs induced interference mitigation problem for Alamouti space-time block coded OFDM with AF-based relay nodes over frequency-selective channels. In this work, a partial time-domain compensation scheme is first proposed by decoupling the two blocks of one space-time block coded codeword to reduce the interference, followed by several frequency-domain interference suppression techniques, frequency-domain equalization, and iterative interference cancellation. Moreover, an iterative joint ML decoder is designed for combating the interference in the presence of prominent CFOs.

4) Cognitive radio systems

Cognitive radio systems require spectrum sensing and interference management, e.g., co-channel interference (CCI), to avoid interference on primary users. The CFO will reduce the spectrum sensing accuracy and cause interference on primary users. In the following, we review spectrum sensing techniques robust to CFOs.

Reference [403] proposes a spectrum sensing algorithm robust to the CFO for OFDM-based cognitive radio network. The covariance matrix of the DFT of the detector's input vector is utilized for developing the algorithm. If the input signal contains the primary user's signal, the covariance matrix is not diagonal because of the presence of the CFO. Thus, this property is exploited to detect the primary user's signal by comparing the power of off-diagonal terms with a preset threshold. Note that this algorithm is bandwidth efficient since it requires no training symbols or pilot tones. Moreover, the study in [404] presents a generalized likelihood ratio test-based spectrum sensing technique for MIMO SC-FDMA cognitive radio networks. Several impairments are considered, including timing offset, CFO, and SFO. To evaluate the asymptotic performance of the proposed algorithm, closed-form false alarm probabilities are derived.

On the other hand, the work in [405] studies the impacts of CFO between secondary and primary transceivers in OFDM-based cognitive radio networks. CFO introduces the ICI terms in receivers of both users, which should be eliminated. Thus, the authors propose linear transceivers for the secondary system using the MMSE criterion given interference constraints at the primary receiver. Primary and secondary systems are perfectly synchronized between their transceivers, and just CFO exists between the secondary transmitter and primary receiver. Note that CFO information is assumed available. On the other hand, authors in [406] investigate the CFO estimation problem in OFDM-based cognitive radio systems in the presence of narrowband interference with unknown power. The estimator is derived based on the ML principle assuming the interference is Gaussian distributed across the signal spectrum and deploying two OFDM pilot blocks. The first one is constructed by repeated parts and is used for CFO estimation with residual ambiguity. The second one conveys a known pseudo-noise sequence to resolve the ambiguity. However, this estimator suffers from computational complexity due to the complete search for finding the global maximum of the likelihood function. Thus, the study in [407] considers the same CFO estimation problem and addresses an estimator that relies on the EM algorithm. The proposed scheme reduces the computational load by deriving the CFO estimation in closed-form at the cost of MSE degradation. Moreover, the authors in [408] present an iterative synchronization-assisted OFDM signal detection technique for cognitive radio applications in low-SNR regions. In the cognitive radio network, the secondary user should detect the primary user signals to avoid interference, and also, the signal detection performance depends on synchronization accuracy. Thus, this work proposes a sub-optimal OFDM signal detection and synchronization scheme based on CP redundancy by employing log-likelihood ratio functions. Note that this iterative approach requires high computations to achieve satisfactory performance.

5) Millimeter-wave systems

These offer large bandwidth to enhance the data rate. They also facilitate the implementation of the MIMO architecture with large antenna arrays. In MIMO millimeter-wave systems, the channel has a high dimension and large bandwidth, making its estimation challenging. In [409], channel estimator for millimeter-Wave MIMO systems is proposed by using matrix perturbation theoretic techniques. One of the channel estimation difficulties is CFO, which impairs the received signal. Thus, [410]–[412] investigate channel and CFO estimations in such systems. Reference [410] develops a pilot-aided algorithm for the joint channel and CFO estimation SC-FDE MIMO millimeter-wave systems with one-bit analog-to-digital converters. This algorithm exploits the sparsity of millimeter-wave channels in the angle-delay domain and compressibility of the phase error vector. This work also derives a quantized sparse bilinear formulation of the joint estimation problem and deploys a message-passing-based algorithm for solving it. Moreover, [411] investigates channel and CFO estimation in SC MIMO millimeter-wave systems. Using training frames, an ML estimator is proposed for joint estimation of the channel, CFO, and noise variance. The CFO is time-varying and may change for every training frame. By utilizing estimates of the unknown parameters, an iterative

This article has been accepted for publication in a future issue of this journal, but has not been fully edited. Content may change prior to final publication. Citation information: DOI 10.1109/ACCESS.2021.3101845, IEEE Access

method is proposed to derive the sparse channel coefficients relied on the orthogonal matching pursuit algorithm.

On the other hand, the study in [412] presents a double-sequence frequency synchronization method for a downlink MIMO OFDM millimeter-wave system operating with low-resolution analog-to-digital converters. In this system, a base station with multiple transmission antennas forms an analog domain beam to send two training sequences towards the downlink user, equipped with low-resolution analog-to-digital converters to detect the signal and perform frequency synchronization. Furthermore, the variance of the CFO estimate is derived, and it highly depends on the double-sequence design parameters, which are optimized to minimize the estimation error variance.

6) Beam forming techniques

Beamforming techniques can be exploited for suppressing the interference terms, e.g., canceling CCI. However, CFO affects of these techniques. For example, the CFO affects the beamforming weight vector and results in performance deterioration. In [413], a blind beamforming algorithm for multiuser SC-FDMA systems is proposed in the presence of a CFO. The beamforming weight vectors are designed without assistance from reference signals. This algorithm can cancel the interference caused by insufficient cyclic extension and the wideband CCI with CFOs. Moreover, authors in [414] develop an ML-based algorithm for CFO estimation in distributed SC MIMO-relay beamforming systems. In this work, pilot symbols are deployed, and flat Rayleigh fading channels are considered. The proposed estimator is built upon an approximation of the channel covariance matrix by a two-ray propagation model. Since the estimator needs no matrix inversion, its computational complexity is low.

On the other hand, investigation in [415] proposes a frequency synchronization scheme for OFDMA uplink systems with a massive uniform linear array at the base station. The beamforming network is optimized by minimizing the MSE to cancel MUI terms from the adjacent user in the angle domain. In other words, the weighted steering vectors of the beamforming network are designed to point to the directions of arrival of the target user. Based on the optimized network, the multiuser model is decomposed into a set of parallel single-user models, and then CFO estimation is performed for each user individually.

7) Full-duplex communications

As mentioned before, these are limited by the SI from a local transmitter on the local receiver. Nevertheless, CFO can introduce interference terms and affect SI cancellation techniques. Moreover, CFO compensation based on the desired signal introduces a CFO to the SI signal. Thus, the receiver should perform CFO estimation and compensation, SI cancellation, and desired signal detection.

Thus, in [416], authors proposed an iterative method for CFO estimation, SI cancellation, and signal detection scheme in OFDM full-duplex systems. The pilots for the desired signal and SI signal are designed to enable simultaneous transmission. A subspace-based blind channel estimator is deployed to estimate the desired and SI channels with ambiguity. The designed pilots are used for extracting the ambiguities and CFO through the parametric channel estimation methods. Moreover, investigation in [417] proposes an algorithm for joint estimation of the doubly-selective SI channels and CFOs in a full-duplex OFDM-based two-way relay network. The block diagram is shown in Fig. 21. The discrete prolate spheroidal basis expansion is exploited to capture the time variations of the channel, which results in a SAGE-based estimator. It uses received data symbols and received pilot symbols in the presence of residual SI. The CRLB is derived, and the MSE of the estimation can follow the bound. Besides, the accuracy of the estimator improves at the cost of computational complexity.

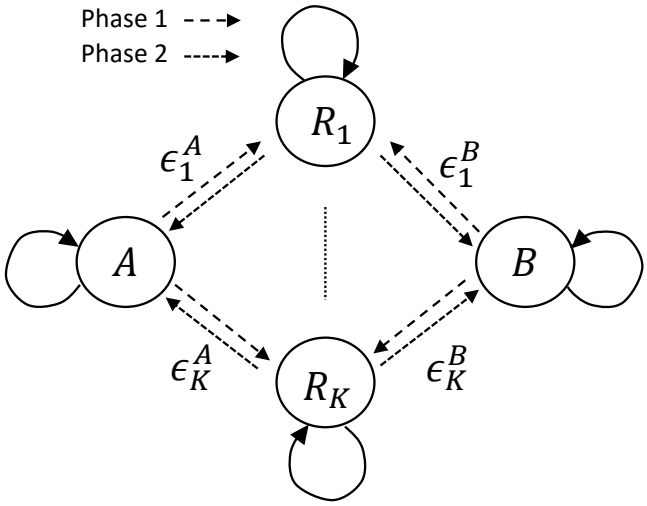

FIGURE 21: A full-duplex OFDM-based two-way relay network under multiple CFOs. Two source nodes A and B, and also K number of relay nodes are equipped with two half-duplex antennas.

IV. IQ IMBALANCE

This section first describes the signal models for IQ imbalance and then discusses its impact on the system. Second, we review the existing works that evaluate the performance of SC and OFDM systems with the IQ imbalance impairment. Third, we present a comprehensive survey of IQ imbalance estimation and compensation in SC, single-user OFDM, and multiuser OFDMA systems. We also review joint channel and IQ imbalance estimation and compensation. Finally, we discuss the impacts of IQ imbalance in emerging technologies and review existing works.

A. SIGNAL MODEL AND IMPACTS

Fig. 22 shows the mathematical models of the IQ modulator and demodulator in the direct-conversion transmitter and receiver without other impairments. In the IQ modulator, the baseband complex signal, $x(t) = x_I(t) + jx_Q(t)$, is passed through the low-pass filters and local oscillators in I and Q

branches, and the corrupted output signal can be represented as

$$y(t) = \left[h_T^I(t) * x_I(t)\right](1-\alpha_T)\cos(2\pi f_c t - \theta_T) - \left[h_T^Q(t) * x_Q(t)\right](1+\alpha_T)\sin(2\pi f_c t + \theta_T), \quad (15)$$

where $*$ denotes convolution, and f_c is the carrier frequency. Also, α_T and θ_T indicate the amplitude mismatch and phase mismatch, respectively. These are constant for different frequency components and are referred to as transmit frequency-flat IQ imbalance. Moreover, $h_T^I(t)$ and $h_T^Q(t)$ are the time-domain response of equivalent RF model of transmit frequency-selective IQ imbalance impairments, e.g., unbalanced low-pass filters, that is different for different frequency components. Furthermore, the output signal in (15) can be written as $y(t) = \mathrm{Re}\{x_{IQ}(t)e^{j2\pi f_c}\}$, where complex baseband signal x_{IQ} is given by

$$x_{IQ}(t) = \mu_I(t) * x(t) + \mu_Q(t) * x^*(t), \quad (16)$$

where

$$\mu_I(t) = \frac{(1-\alpha_T)\,e^{-j\theta_T}h_T^I(t) + (1+\alpha_T)\,e^{j\theta_T}h_T^Q(t)}{2}$$
$$\mu_Q(t) = \frac{(1-\alpha_T)\,e^{-j\theta_T}h_T^I(t) - (1+\alpha_T)\,e^{j\theta_T}h_T^Q(t)}{2}. \quad (17)$$

when $h_T^I(t) = h_T^Q(t) = h_T(t)$, the frequency-selective IQ imbalance does not exist and we have $\mu_I(t) = (\cos(\theta_T) + j\alpha_T\sin(\theta_T))h_T(t)$ and $\mu_Q(t) = -(\alpha_T\cos(\theta_T) + j\sin(\theta_T))h_T(t)$. On the other hand, in receiver side, the received RF signal is $\hat{r}(t) = \mathrm{Re}\{r(t)e^{j2\pi f_c t}\}$ passed through the IQ demodulator, where $r(t) = r_I(t) + jr_Q(t)$ is the equivalent baseband signal. Accordingly, after analog to digital convertering, the corrupted baseband output signal at I and Q branches are given by

$$s_I(t) = (1-\alpha_R)\Big[\big(r_I(t) * h_I^R(t)\big)\cos(\theta_R) - \big(r_Q(t) * h_I^R(t)\big)\sin(\theta_R)\Big] \quad (18)$$

$$s_Q(t) = (1+\alpha_R)\Big[-\big(r_I(t) * h_Q^R(t)\big)\sin(\theta_R) + \big(r_Q(t) * h_Q^R(t)\big)\cos(\theta_R)\Big], \quad (19)$$

where α_R and θ_R indicate the amplitude mismatch and phase mismatch, respectively, which are constant. Moreover, $h_R^I(t)$ and $h_R^Q(t)$ are the time-domain response of equivalent RF model of receive frequency-selective IQ imbalance impairments. According to $s(t) = s_I(t) + js_Q(t)$ in (18), the baseband IQ signal $s(t) = s_I(t) + js_Q(t)$ can be written as

$$s(t) = \kappa_I(t) * r(t) + \kappa_Q(t) * r^*(t), \quad (20)$$

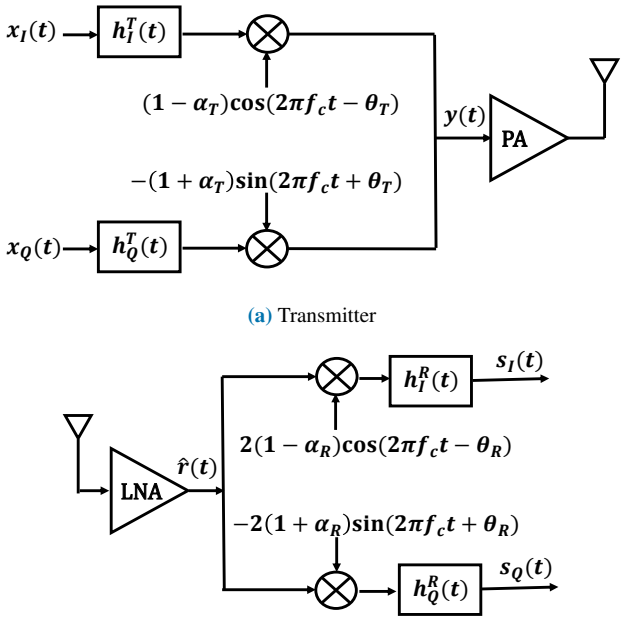

(a) Transmitter

(b) Receiver

FIGURE 22: The mathematical models of IQ modulator and demodulator in the direct-conversion transmitter and receiver without other impairments

where

$$\kappa_I(t) = \frac{(1-\alpha_R)\,e^{j\theta_R}h_R^I(t) + (1+\alpha_R)\,e^{-j\theta_R}h_R^Q(t)}{2}$$
$$\kappa_Q(t) = \frac{(1-\alpha_R)\,e^{-j\theta_R}h_R^I(t) - (1+\alpha_R)\,e^{j\theta_R}h_R^Q(t)}{2}. \quad (21)$$

when $h_R^I(t) = h_R^Q(t) = h_R(t)$, the frequency-selective IQ imbalance does not exist and we have $\kappa_I(t) = (\cos(\theta_R) - j\alpha_R\sin(\theta_R))h_R(t)$ and $\kappa_Q(t) = -(\alpha_R\cos(\theta_R) + j\sin(\theta_R))h_R(t)$.

The Image Rejection Ratio (IRR) is the most crucial figure of merit that characterizes the IQ imbalance behavior, which is the power ratio between the desired and the image signals. For example, according to (20), the IRR for receive IQ imbalance is defined as

$$\mathrm{IRR}(f) = \frac{|\kappa_I(f)|^2}{|\kappa_Q(f)|^2}, \quad (22)$$

where $\kappa_I(f)$ and $\kappa_Q(f)$ are frequency response of $\kappa_I(t)$ and $\kappa_Q(t)$, respectively. Note that the IRR of transmit IQ imbalance can be similarly derived by using (16), and as a practical case, the typical IRR of direct-conversion transmitter without compensation is around 25 to 40 dB [418].

To gain insight into the effect of IQ imbalance, we consider a free noise SC QAM system over the AWGN channel, $\hat{r}(t) = a_1\cos(2\pi f_c t) + a_2\sin(2\pi f_c t), a_1, a_2 = \pm 1$, with only receive frequency-flat IQ imbalance and perfect low-pass filter. For this system, the corrupted baseband signals

This article has been accepted for publication in a future issue of this journal, but has not been fully edited. Content may change prior to final publication. Citation information: DOI 10.1109/ACCESS.2021.3101845, IEEE Access

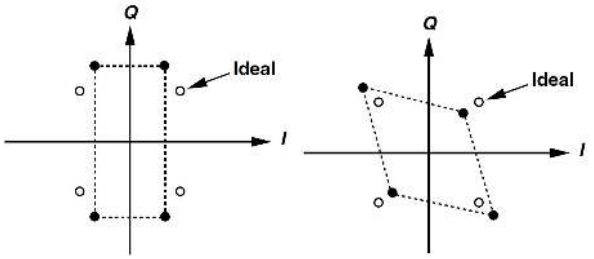

(a) $\theta_R = 0$ **(b)** $\alpha_R = 0$

FIGURE 23: the resulted constellation of the QAM system due to IQ imbalance for two cases, $\alpha_R = 0$ and $\theta_R = 0$. Fig. 23a shows that IQ imbalance scales differently the quadrature baseband symbols in amplitude and Fig. 23b demonstrates that each baseband output is affected by data symbols in the other output which causes constellation displacement [19].

in (18) and (19) can be written as

$$\begin{aligned} s_I(t) &= (1-\alpha_R)\Big[a_1\cos(\theta_R) - a_2\sin(\theta_R)\Big] \\ s_Q(t) &= (1+\alpha_R)\Big[-a_1\sin(\theta_R) + a_2\cos(\theta_R)\Big]. \end{aligned} \tag{23}$$

In Fig. 23, the resulted QAM constellation because of the IQ imbalance is illustrated for $\theta_R = 0$ and $\alpha_R = 0$ [19]. The former shows that IQ imbalance scales the quadrature baseband symbols differently in amplitude. Moreover, the latter demonstrates that each baseband output is affected by data symbols in the other output, which causes constellation displacement. To recap, IQ imbalance scales the signal and introduces ISI terms.

Furthermore, (16) and (20) illustrate that the IQ imbalance causes the spectral content of the upper sideband to mix with the lower sideband and vice versa, which is referred to as mirror interference. Especially, IQ imbalance in multicarrier systems introduces ICI terms on the mirror subcarriers. For example, consider a free noise OFDM system over the AWGN channel, $r(t) = \text{IFFT}_N\{X[k]\}$, with only receive IQ imbalance. $X[k]$ indicates the transmitted complex symbol on the k-th subcarrier, $k = 0, 1, .., N-1$. By taking the FFT from the baseband IQ signal in (20), the complex symbol in the k-th subcarrier corrupted by IQ imbalance can be derived as

$$\tilde{X}[k] = \kappa_I[k]X[k] + \kappa_Q[k]X^*[-k], \tag{24}$$

where $\kappa_I[k]$ and $\kappa_I[k]$ are frequency response of $\kappa_I(t)$ and $\kappa_I(t)$, respectively. Obviously, the IQ imbalance not only imposes complex gain on the subcarrier data $X[k]$ but also introduces ICI from the mirror subcarrier $X[-k]$.

Moreover, BER performance of an OFDM system with 128 subcarriers in the presence of transmit and receive IQ imbalances is demonstrated in Fig. 24. Similar to Fig. 10, ITU outdoor multi-path channel model A is considered. It is illustrated by in higher amount of IRR, impacts of IQ imbalance increase which results in lower BER.

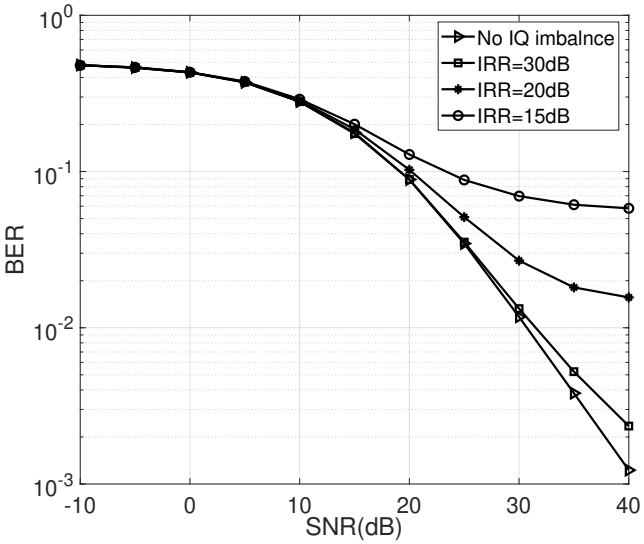

FIGURE 24: BER versus SNR for an OFDM system with different values of IRR.

B. PERFORMANCE ANALYSIS

In this subsection, we first review existing works on performance analysis of SC systems under IQ imbalance, and then we discuss OFDM systems.

The study [419] investigates impacts of IQ imbalance in transmitter and receiver on the SER performance of different coherent and noncoherent modulation schemes under fading channels. The performance degradation depends on the system's parameters, specifically the modulation scheme. Moreover, increasing the modulation order increases the impacts of IQ imbalance. Moreover, the BER performance of the SC-FDE under transmit and receive frequency-flat IQ imbalances is studied [420]. The IQ imbalance causes ISI on neighboring symbols in the time dispersive channel and degrades the BER performance. Moreover, an SC-FDE system is more robust to the IQ imbalance than an OFDM system. Moreover, [421] derives lower bounds on the ergodic capacity and outage capacity of SC-FDMA systems. Furthermore, in [422], the achievable rate of the SC-FDE system under the receive frequency-flat IQ imbalance over Rayleigh fading channels is analyzed. MMSE, ZF and MF are considered. Under IQ imbalance, the achievable rate approaches a saturation level at the high-SNR regime.

The IQ imbalance introduces ICI on mirror carrier [423], which destroys orthogonality between OFDM subcarriers. Moreover, combined effects of receive frequency-flat IQ imbalance and timing jitter are investigated. The interaction between these impairments introduces additional ICI terms. Furthermore, the impacts of non-linear power amplifier, transmit frequency-flat IQ imbalance, and sampling jitter on second-order cyclic statistics of OFDM systems is studied [424]. Analytical expressions for the cyclic statistics are derived. These impairments distort the cyclic statistics and destruct the cyclostationary properties of the signal.

This article has been accepted for publication in a future issue of this journal, but has not been fully edited. Content may change prior to final publication. Citation information: DOI 10.1109/ACCESS.2021.3101845, IEEE Access

The impact of IQ imbalance on the BER performance of OFDM systems has been studied [425], [426]. In [425], BER performance is evaluated for an OFDM system with QPSK modulation, receive frequency-flat IQ imbalance over AWGN channel. Simulation results show that with the amplitude imbalance less than one dB and phase imbalance less than 5 degrees, the BER degradation due to the IQ imbalance is less than 0.5 dB for BER $> 10^{-6}$. Moreover, in [426], a closed-form expression for BER of OFDM systems with M-QAM modulation over Rayleigh fading channels with transmit and receive frequency-flat IQ imbalances and imperfect CSI is derived. Higher order M-QAM constellations suffer from a more BER performance degradation. Moreover, the detrimental effects of transmit IQ imbalance is less than the received one. Unlike the transmit IQ imbalance, the received one causes an irreducible floor in the BER. Finally, the correlation between the channel response at the desired frequency index and the mirror index has a significant harmful effect on the BER.

The studies in [427], [428] explore the impacts of IQ imbalance on EVM of OFDM systems with QPSK and 16-QAM modulations, respectively. In [427], EVM is considered as a random variable, and its statistical distribution is investigated in the presence of PN, non-linear amplifier, and transmit frequency-flat IQ imbalance. The EVM increases due to mirror interference generated by IQ imbalance. On the other hand, the impacts of transmit frequency-selective IQ imbalance plus the other impairments on EVM are studied in [428]. A closed-form expression for EVM is derived, and similar to [427], the sensitivity of EVM to IQ imbalance is shown.

Authors in [429] derive a closed-form expression for SINR of OFDM systems over multipath channels considering joint transmit and receive frequency-flat IQ imbalances with equal levels at the transmitter and the receiver. Both IQ imbalances reduce the average subcarrier SINR, while at high input SNR, transmit IQ imbalance is more harmful than receive IQ imbalance. Moreover, [430] investigates the ergodic capacity of the OFDM systems over Rayleigh fading channels under transmit and receive frequency-flat IQ imbalances. IQ imbalances limit the ergodic capacity and the system capacity with outage upper bounds. This limitation depends on the interference raised at each subcarrier due to IQ imbalance. Finally, [431] studies the outage probability of SC and multicarrier systems, e.g., OFDM, over cascaded Nakagami-m channels given transmit and receive frequency-flat IQ imbalances. IQ imbalances cause significant effects that lead to non-negligible outage probability degradation in both cases.

C. ESTIMATION AND COMPENSATION

Because of the harmful impacts of the IQ imbalance, estimation and compensation algorithms for mitigating its effects are crucial. We could classify existing estimators as pilot-aided and blind techniques. In the IQ imbalance estimators, cost function is defined in general form of $f(\widetilde{\mu}, P, r)$ and the IQ imbalance is estimated by $\hat{\mu} = \arg\min_{\widetilde{\mu}} f(\widetilde{\mu}, P, r)$, where $\widetilde{\mu}$, P and r indicate trail value of IQ imbalance, training (pilot) sequence and received signal, respectively. Moreover, different approaches are proposed for finding the cost function in each type of estimators. In the pilot-aided estimators, the IQ imbalance is estimated by utilizing known well-designed training symbols or a combination of pilot and data symbols at the expense of bandwidth efficiency. Indeed, in this approach, prior knowledge in the receiver is deployed to estimate the IQ imbalance. In contrast, in the blind methods, prior knowledge is not available in the receiver. The receiver defines the cost function based on the IQ imbalance trial value and the received signal, which relies on structural and statistical properties of signals and exhaustive search. These techniques improve spectral efficiency since many pilots' transmission is avoided, while for satisfactory performance, they often require many symbols.

This subsection reviews IQ imbalance estimation and compensation for SC, single-user OFDM, and multiuser OFDMA systems. Moreover, the studies in joint estimation and compensation of channel and IQ imbalance are highlighted.

1) SC systems

We divide the studies for SC systems into 1) Pilot-aided and blind estimation and compensation, 2) Joint channel and IQ imbalance estimation and compensation. Note that the first one assumes knowledge of the channel is available in the receiver.

pilot-aided and blind estimation and compensation: By using pilots, the transmitter can estimate and track transmit frequency-selective IQ imbalance and DC offset in transmitter side using a feedback path from the transmitted RF signal before PA to the baseband unit [432], [433]. The same feedback path is considered, including a down converter, low-pass filter, digital IQ demodulator, and parameters estimation and compensation block in Fig. 25. The proposed algorithms have two phases: 1) initial parameters estimations by exploiting the dedicated pilot signals signal and the corresponding feedback signal, 2) blind parameter tracking during normal data signal transmission iteratively. Instead of using the IQ demodulator in the feedback path, narrow-band and wide-band diodes are deployed in [434] for initial estimation and compensation of frequency-selective IQ imbalance along with DC offset in the transmitter side. The proposed algorithm takes advantage of the energy detector and training signals. Due to using the diodes, the computational complexity of this algorithm is lower than [432], [433].

However, the works in [432]–[434] do not consider the non-linear PA distortions in designing the compensation algorithms. They use the RF signal before PA as the input of the feedback path, while the PA distortions can affect the compensated signal. Hence, in [435], [436], transmit frequency-selective IQ imbalance compensation with non-linear distortions of PA is investigated. The method [435] has a super-heterodyne receiver in the feedback path, which

This article has been accepted for publication in a future issue of this journal, but has not been fully edited. Content may change prior to final publication. Citation information: DOI 10.1109/ACCESS.2021.3101845, IEEE Access

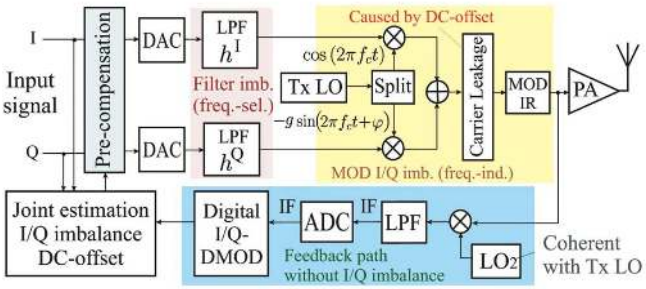

FIGURE 25: Transmitter system model in [432] which has a feedback path from the transmitted RF signal before PA to the baseband unit.

down converts the transmitted signal to baseband. This algorithm estimates IQ imbalance parameters in the frequency-domain using training sequences. Then, based on the estimation results, a digital FIR compensation filter is derived in the time-domain. Moreover, the authors propose a method to separate and subtract PA non-linear distortions. Moreover, the work in [436] proposes a three-input non-linear model for joint compensation of frequency-selective IQ imbalance and PA non-linear distortion based on the real value Volterra series theory. The IQ imbalance cross terms and the input signal's magnitude are considered the model input, and IQ imbalance and PA parameters are modeled individually. Since the presented model is linear in parameters, an LS-based algorithm is exploited for parameter estimations.

Studies in [437], [438] investigate the blind estimation and compensation of transmit IQ imbalance in transmitter side by using a feedback path. Different types of this feedback circuit exist. In [437], a blind adaptive LMS compensation scheme is proposed for frequency-flat transmit IQ imbalance using the squared envelope of the transmitted signal. The feedback circuit of this work is constructed by an envelope detector, an estimation block, and a precompensation block. Similarly, authors in [438] use an envelope detector-based feedback path. They develop a blind recursive algorithm for estimating the frequency-selective IQ imbalance based on the instantaneous power measurement of the transmitted RF signal. However, the proposed algorithms that rely on the envelope detector require a substantial bandwidth for the feedback path, which is not suitable for broadband signals.

Besides, the work in [439] investigates blind compensation of frequency-selective IQ imbalance and DC offset in transmitter side using a one-stage down-converter and digital demodulator in the feedback path. In this study, channel models are proposed for describing the effects of the impairments on the transmitted data streams and the baseband feedback data samples. Then, an LS-based algorithm is developed to estimate the channel models' parameters and construct the IQ imbalance compensation scheme. However, the proposed algorithm suffers from an ill-conditioned matrix problem and has a large estimation error. Thus, authors in [440] present a blind estimation algorithm for frequency-flat IQ imbalance and DC offset based on the instantaneous power measurement of the transmitted signal before PA by a diode detector in the feedback path. The cost function is defined by exploiting the second and fourth moments of the RF transmitted signal. Note that this blind method has an advantage that estimates the parameters without knowing the input signal and its statistic. On the contrary, the investigation in [441] uses RF measurements after the PA stage for developing a compensation scheme for transmit frequency-selective IQ imbalance. The feedback circuit of this work includes an IQ-free RF down-converter, a low-pass filter, an ADC, and an IQ estimator and compensator. The authors model the IQ imbalance problem by a single complex filter. Then, they estimate its coefficients by applying a specific test signal, e.g., sine wave-like test signals, to the uncompensated up-converter.

On the other hand, in [442], a blind algorithm for compensating the receive frequency-flat IQ imbalance in time-domain is proposed to rely on LMS adaptive interference cancellation. The observation signal is subtracted from the interference estimate formed by an adaptive filter and a reference signal in this method. Moreover, authors in [418] investigate blind adaptive compensation of frequency-selective IQ imbalance in the receiver side. The compensation algorithm is proposed based on the LMS principle using the second-order statistical characteristic of the observed signal, namely, the circular or properness property. The proposed algorithm is independent of carrier synchronization and the type of communication channel. However, [442] and [418] may have slow convergence due to filter adaptation, which is not suitable for high-speed applications. A different approach is considered in [443] for blind estimation of transmitter and receiver frequency-flat IQ imbalances by exploiting a Cholesky decomposition of the received signal's covariance matrix. In this work, an intended frequency offset between the oscillator of transmitter and receiver is used to separate their imbalances in the received signal. However, the exact value of the frequency offset may not be known in the receiver, and also, it can be sensitive to CFO between transmitter and receiver.

Channel and IQ imbalance estimation and compensation: Investigations in [444]–[446] deal with Joint estimation and compensation of channel and IQ imbalance for SC-FDE systems. In [444], the joint pilot-aided estimation of frequency-selective channel and frequency-flat IQ imbalances in both transmitter and receiver is investigated. This work first constructs linear models for the channel impulse response and IQ parameters and then develops a pilot-based alternating LS-based algorithm to estimate both groups of parameters iteratively. Moreover, [445] presents a three-stage scheme to compensate channel and IQ imbalance under CFO. Frequency-selective IQ imbalance is considered in both transmitter and receiver sides. Three stages of the proposed algorithm can be summarized as 1) Receiver IQ imbalance is estimated and compensated by using a repetitive preamble, 2) transmitter IQ imbalance and channel are jointly estimated

via time-domain correlation using another preamble, which is designed based on complementary Golay code, 3) joint compensation of transmitter IQ imbalance and the time-varying channel is performed via a minimal MSE algorithm. The study in [446] designs an iterative decision-feedback receiver to compensate Rayleigh fading multipath channel and frequency-selective IQ imbalances in transmitter and receiver sides using training sequences. This study proposes feedforward and feedback filters for mirror carrier interference mitigation because of IQ imbalances in the frequency-domain. Moreover, hard detection and soft detection-based feedback schemes compensate for channel and IQ imbalances. Finally, authors in [447] develop a joint EM algorithm the multipath channel and frequency-flat IQ imbalance in both transmitter and receiver.

2) Single-user OFDM systems

We divide these studies into three categories: 1) Pilot-aided estimation and compensation, 2) Blind estimation and compensation, 3) Joint channel and IQ imbalance estimation and compensation. Note that the first two assume that the receiver knows the channel.

Pilot-aided estimation and compensation: Authors in [23] propose two pilot-aided compensation algorithms for OFDM systems with both frequency-flat and frequency-selective IQ imbalance models in the receiver. The first one relies on the LMS equalization technique, applied after the FFT operation at the receiver. However, the second one is performed before the FFT operation based on the LS principle by using adaptive channel/distortion estimation and unique pilot tones. The authors show that while the first algorithm is suitable for the frequency-flat IQ imbalance model, the second one can be exploited for both frequency-flat and frequency-selective IQ imbalance models. Besides, in [448], authors extend the approach in [23] to the case of IQ imbalances in both transmitter and receiver and present two pilot-aided compensation schemes. The first one operates in the receiver after the FFT operation in order to compensate both the transmitter and receiver distortions based on the LS principle and adaptive equalization. In the second one, a pre-distorter is designed using the pilot pattern in [23] to compensate transmitter imbalance at the transmitter. In contrast, the receiver imbalance is compensated at the receiver. Note that in [448], only the frequency-flat IQ imbalance model is considered.

Moreover, a study in [449] addresses the joint estimation of transmitter and receiver frequency-selective IQ imbalances by using the properties of Golay complementary sequences as frequency-domain training sequences. The IQ imbalance problem is modeled by a widely linear system structure. The estimator is developed by exploiting Hadamard products between the received signal and corresponding components of the sequence. The proposed estimator has a low computational load and is robust to power amplifier non-linearity due to Golay's complementary sequence properties. Furthermore, authors in [450] propose adaptive algorithms for frequency-flat IQ imbalance compensation on the receiver side. They deploy frequency-domain observations to update the filter weights by using a mini-batch gradient descent algorithm.

On the other hand, several studies investigate receiver IQ imbalance compensation with CFO in OFDM systems [451]–[454]. Authors in [451] propose a pilot-aided algorithm for both CFO and frequency-selective IQ imbalance compensation. This work presents a non-linear LS CFO estimator robust to the IQ imbalance by modeling the effects of IQ imbalance on CFO estimation. A finite impulse response filter implemented in the in-phase branch, followed by an asymmetric phase compensator, is deployed for frequency-selective IQ imbalance compensation. This study uses a specific pilot structure that includes multiple identical OFDM symbols in which all the even symbols are rotated with a common phase. Since [451] suffers from computational complexity, authors in [452] propose an algorithm for simultaneously estimating CFO and IQ imbalance in closed-form using a generalized periodic pilot. Based on the periodicity of the pilot structure, the algorithm is developed based on the linear LS approach, which is robust to timing errors. The proposed algorithm has low complexity and outperforms the algorithm in [451] in terms of MSE.

Moreover, work in [453] presents an iterative scheme for joint estimation of CFO and receiver frequency-flat IQ imbalance without channel knowledge requirement. The authors derive the ML-based estimator, and to reduce the computational complexity, they calculate the second-order approximation of the likelihood function. They propose a scheme to solve the approximated function based on the EM algorithm by using a standard-compliant repetitive preamble composed of two long identical sequences. They show that the CFO estimation result converges to that of the ML estimator after a few iterations. At the same time, the accuracy of the IQ imbalance estimate is reduced at low and high-SNR due to the incorrect approximation. Besides, authors in [454] address a frequency-flat IQ imbalance compensation scheme in receiver given CFO and inter-block interference due to larger channel delay spread than cyclic prefix over time-invariant channels. They derive a per-tone equalizer by transferring a time-domain equalizer to the frequency-domain to channel and IQ imbalance compensation. However, this equalizer needs knowledge of all parameters. Thus, a training-based recursive LS direct initialization scheme is developed to skip the estimation of channel and IQ imbalance under the assumption that the CFO is known at the receiver.

Furthermore, works in [455], [456] consider the IQ imbalance in both transmitter and receiver and propose joint CFO and IQ imbalance compensation schemes. In [455], an adaptive compensation scheme for the transmitter and receiver IQ imbalance under CFO impairment is proposed. This scheme eliminates the distortions and designs a four-tap adaptive equalizer for each subcarrier. The equalizer coefficients are updated by a training-based LMS adaptive filtering algorithm. Although this equalizer has low computational complexity, it suffers from slow convergence, especially for

OFDM systems with short training sequences. Hence, authors in [456] propose a pilot-aided algorithm for the joint estimation of CFO and frequency-selective IQ imbalance by using a generalized periodic pilot scheme. In this work, two cosine-based and sine-based CFO estimators are developed by exploiting the null space of a matrix associated with the received samples, independent of IQ imbalance parameters. A linear LS algorithm is then presented for IQ imbalance estimation and compensation based on simple matrix formulation and deploying the periodicity of the generalized periodic pilot sequence. Note that this algorithm does not require CSI and the exact values of the training sequence. It achieves low computational complexity and acceptable estimation performance.

In [457]–[460], IQ imbalance compensation in the presence of CFO and/or DC offset and/or timing offset and/or PN is studied. Authors in [457] propose an estimator for receiver frequency-flat IQ imbalance in OFDM systems with CFO and DC offset. This work develops a differential filter for removing the DC offset. By using the preamble symbols of the IEEE 802.11a/g standards, CFO and IQ imbalance are estimated from the output of the differential filter by exploiting autocorrelation function and first-order approximation of the Taylor expansion. However, the proposed algorithm suffers from significant performance degradation with large DC offset, CFO, and IQ imbalance.

Moreover, the study in [458] presents a calibration scheme for joint compensation of DC offset and frequency-selective IQ imbalance in transmitter and receiver. This scheme exploits a pre-distortion filter and a DC correction term in the transmitter to calibrate IQ imbalance and dc offset. A time-domain calibration filter and a dc correction term are deployed in the receiver for removing the receiver mirror-frequency interference and DC offset. The four calibration parameters are estimated relied on the non-linear LS technique, and also, the optimal training sequence is derived. Besides, authors in [459] investigate the estimation and compensation of CFO and receiver frequency-selective IQ imbalance under timing offset. In this study, CFO estimation is performed based on the LS principle robust against timing offset and IQ imbalance. Using the estimated CFO, IQ imbalance compensation is proposed by minimizing the difference between the compensated signal and a target signal. The former one is derived after the compensation scheme in [451] with a filter and an amplification coefficient, and the latter one is related to the received signal but without IQ imbalance. Finally, in [460], a joint compensation scheme for frequency-flat IQ imbalance and PN in the receiver is proposed by exploiting one OFDM training symbol. In this work, IQ imbalance is estimated and compensated based on channel smoothness criterion, which minimizes the MSE between consecutive sub carriers. Also, the PN is estimated by a decision-directed approach where the mean phase rotation between the received equalized symbol, and the transmitted symbol is calculated.

Blind estimation and compensation: Authors in [461] propose two blind compensation algorithms for receiver frequency-selective IQ imbalance in the OFDM system. The transmitted signal is assumed to be a white noise process. The first algorithm filters the discrete-time down-converted baseband signal to obtain a scaled and delayed version of the baseband received signal. The algorithm then uses a gradient-descent technique to find the compensating filter. On the other hand, the second algorithm relies on the second-order statistics of the received signal for frequency-selective IQ imbalance estimation. Once obtained, a single-tap matrix filter inversion is exploited for compensation. However, the proposed algorithms have no closed-form solution and high computational complexity. Thus, the study in [462] presents a time-domain blind real-valued filter-based compensation scheme with low-complexity for frequency-selective IQ imbalance in the receiver. In this work, this imbalance is modeled as a finite impulse response filter referred to as a difference filter. The IQ imbalance estimation is equivalent to the blind identification of a minimum phase response of the difference filter. Hence, the magnitude response of the difference filter is first obtained from the autocorrelations of the branch signals, and then it is deployed for determining the corresponding minimum phase response. Subsequently, cross-correlation of the branch signals is exploited for estimating the frequency-selective phase imbalance. Authors in [463] address the blind compensation of receiver frequency-selective IQ imbalance based on the kurtosis criterion. They estimated the IQ compensation coefficient for each subcarrier using the kurtosis of the received signal on that subcarrier. Then the derived coefficient is to a one-tap compensation filter. The authors illustrate that the proposed algorithm outperforms the method in [461] in terms of SER.

On the other hand, [464], [465] investigate the blind joint estimation of CFO and receiver IQ imbalance in OFDM systems. Reference [464] proposes a blind joint compensation scheme for CFO and frequency-flat IQ imbalance in the receiver with an asymmetric subcarrier allocation approach. This study develops an ML CFO estimator by exploiting the proposed subcarrier allocation scheme. Then, blind IQ imbalance compensation is presented with asymmetric subcarrier allocation relied on the compensation structure in [451]. Note that the CFO estimation is independent of the IQ imbalance compensation. Moreover, [465] presents a blind algorithm for joint CFO and frequency-flat IQ imbalance estimation in OFDM systems exploiting constant modulus subcarriers. The cost function exploits the fact that the constant modulus of the input constellation is restored when CFO and IQ imbalance are entirely compensated. Moreover, the proposed cost function can be expressed as a superposition of harmonics, reducing the computational complexity by avoiding an exhaustive grid search procedure.

Joint channel and IQ imbalance estimation and compensation:

The above mentioned papers focus on IQ imbalance estimation and compensation only and assume perfect CSI is available. However, since this assumption may not always

This article has been accepted for publication in a future issue of this journal, but has not been fully edited. Content may change prior to final publication. Citation information: DOI 10.1109/ACCESS.2021.3101845, IEEE Access

hold in practice, it is necessary to consider joint channel estimation and IQ imbalance compensation.

Therefore, an iterative, decision-directed algorithm for joint channel estimation and frequency-flat IQ imbalance compensation in a decision-directed fashion using two long training symbols has been proposed [466]. This work estimates IQ imbalance using hard-decisions on the received data symbols coarsely equalized by the estimated channel. Then, the IQ imbalance on data symbols is compensated for by deploying the estimated IQ imbalance. But the long training symbols decrease the spectral efficiency. Thus, [467] investigates the estimation of channel and frequency-flat IQ imbalances in transmitter and receiver using one OFDM training block. The authors derive the channel estimation based on IQ imbalances and prove that when the IQ imbalances are not compensated, the total energy of some last entries of the channel estimated vector is much larger. Thus, they estimate the IQ imbalances without knowing the channel information by minimizing the cost function called channel residual energy quantity, which is defined as the total energy of the entries. Channel estimation is derived by substituting the estimated IQ imbalances in the derived estimation expression.

Furthermore, [468] presents joint channel and IQ imbalance estimation algorithm for OFDM systems over doubly-selective channels. Frequency-flat IQ imbalances for both transmitter and receiver are considered, and scattered subcarriers are allocated for pilot transmission. The proposed algorithm is based on the LS criterion and the system model, which relies on a generalized, exponential expansion model. Moreover, An EM algorithm performs an iterative IQ imbalance compensation. The proposed compensation algorithm improves the BER performance reaching the ideal case with perfect CSI and IQ imbalance information. Besides, authors in [470] investigate joint channel estimation and frequency-selective IQ imbalances occurring at both the transmitter and receiver. In this work, the IQ imbalance effects are combined with the channel impulse response into one parameter, which is estimated. A pilot-aided ML estimation scheme is developed by using the EM algorithm. This algorithm iteratively deploys the soft information from the detector for improving the estimation performance. Finally, in [469], joint estimation of channel and IQ imbalance OQAM-OFDM is addressed. frequency-flat IQ imbalances in both transmitter and receiver sides are considered. The proposed algorithm uses the LS criterion to estimate the mixed-effects channel and IQ imbalances in frequency-domain using a preamble, including one loaded pilot symbol and several successive zero symbols.

Table 13 shows a summary of IQ imbalance estimation and compensation studies for single-user OFDM systems.

3) Multi user OFDMA systems

An OFDMA downlink system is essentially a group of point-to-point OFDM systems, each of which experiences IQ imbalances in the base station's transmitter and its own user's receiver. Thus, existing IQ imbalance estimation and compensation techniques for single-user OFDM can be exploited for suppressing IQ imbalance effects in OFDMA downlink. On the other hand, in the OFDMA uplink, the signal received in the base station includes all users' IQ imbalances, which introduces ICI for each user through its signal image and causes MUI through the image signal of other users. Thus, multi IQ imbalances estimation and compensation algorithms should be developed.

Therefore, authors in [471] propose a widely linear equalization scheme and multi-user detection method based on ZF and MMSE principles for the interleaved OFDMA uplink system. Frequency-flat IQ imbalance is considered for each user, while no IQ imbalance is assumed for the base station receiver. Moreover, a subcarrier mapping scheme is proposed to deal with the MUI caused by the IQ imbalances. Perfect knowledge of the channel and IQ imbalances is assumed. Thus, authors in [472] present a pilot-aided algorithm for estimating channel and IQ imbalances by taking advantage of the two-dimensional LS estimation criterion. For the transmitter of each user, frequency-flat IQ imbalance is considered. Moreover, they propose a ZF equalizer to recover the data symbols.

However, both [471] and [472] assume no IQ imbalance for the base station's receiver, while in practical systems, both the transmit and receive IQ imbalances should be addressed. Hence, a study in [473] investigates joint channel impulse response and transmitters and receiver frequency-selective IQ imbalance for asynchronous OFDMA uplink systems. Distributed subcarrier assignments are assumed, and mirror subcarriers are allocated to the same user. In this study, IQ imbalance effects between each user and the base station are combined with channel impulse response into one parameter. Based on the ML criterion, this parameter, along with propagation delays, is estimated via the SAGE approach.

In sum, in all the discussed systems, pilot-aided IQ imbalance estimators are developed based on biased, e.g., MMSE, and unbiased approaches, e.g., LS. The pilot-aided estimators require prior knowledge in the receiver to estimate the IQ imbalance. Most of the proposed estimators are iterative and require many iterations for convergence. Furthermore, some developed estimators are biased estimators, like MMSE, requiring computationally intensive matrix inversion operations, resulting in higher computational complexity. On the other hand, blind estimators enhance the bandwidth efficiency since many pilots' transmission is avoided, while for satisfactory performance, they often require averaging over numerous data symbols. In addition, they may suffer from ill convergence problems.

D. IQ IMBALANCE IN EMERGING/FUTURE TECHNOLOGIES

1) MIMO systems

In the following, we review the papers for SC MIMO and MIMO OFDM systems in the presence of IQ imbalance impairment.

TABLE 13: Summary of IQ imbalance estimation and compensation studies for single-user OFDM systems

Article	Model	TX/ RX	channel	Pilot/ Blind	Est./ Comp.	Ch. Est.	Main approach
[23]	Both	Rx	Freq.Sel.	pilot	Both	No	LMS equalization compensation algorithm
[448]	Freq.Flat	Both	Freq.Sel	pilot	Both	No	LS compensator and adaptive equalization
[449]	Freq.Sel.	Both	Freq.Sel.	pilot	Est.	No	Estimation using frequency-domain golay complementary sequences
[450]	Freq.Flat	Rx	Freq.Sel.	pilot	Comp.	No	Compensator development using a mini-batch gradient descent algorithm
[451]	Freq.Sel.	Rx	Freq.Sel.	pilot	Both	No	Non-linear LS-based joint CFO and IQ imbalance compensation
[452]	Freq.Flat	Rx	Freq.Sel.	pilot	Both	No	Closed-form estimation of CFO and IQ imbalance with periodic pilot
[453]	Freq.Flat	Rx	Freq.Sel.	pilot	Both	No	Iterative EM estimator for joint estimation of CFO and IQ imbalance
[454]	Freq.Flat	Rx	Freq.Sel.	pilot	Both	No	Compensator design given CFO and inter-block interference
[455]	Freq.Flat	Both	Freq.Sel.	pilot	Both	No	Adaptive compensation scheme given CFO
[456]	Freq.Sel.	Both	Freq.Sel.	pilot	Both	No	Joint estimator design using a generalized periodic pilot scheme
[457]	Freq.Flat	Rx	Freq.Sel.	pilot	Both	No	Joint estimator utilizing autocorrelation function and first-order Taylor expansion
[458]	Freq.Sel.	Both	Freq.Sel.	pilot	Both	No	Calibration schemes for joint compensation of DC offset and IQ imbalance
[459]	Freq.Sel.	Rx	Freq.Sel.	pilot	Both	No	LS algorithm for compensation of CFO and IQ imbalance under timing offset
[460]	Freq.Flat	Rx	Freq.Sel.	pilot	Both	No	Joint compensation scheme for IQ imbalance and PN using one training symbol
[461]	Freq.Sel.	Rx	Freq.Sel.	Blind	Both	No	Compensation by assuming the transmitted signal is a white process
[462]	Freq.Sel.	Rx	Freq.Sel.	Blind	Both	No	Filter-based compensation scheme with low-complexity
[463]	Freq.Sel.	Rx	Freq.Sel.	Blind	Both	No	Estimator based on the kurtosis criterion
[464]	Freq.Flat	Rx	Freq.Sel.	Blind	Both	No	Joint compensation scheme with asymmetric subcarrier allocation approach
[465]	Freq.Flat	Rx	Freq.Sel.	Blind	Both	No	Joint estimator using constant modulus subcarriers
[466]	Freq.Flat	Rx	Freq.Sel.	pilot	Both	Yes	Iterative decision-directed algorithm using two long training symbols
[467]	Freq.Flat	Both	Freq.Sel.	pilot	Est.	Yes	Estimation of channel and IQ imbalances with one training block
[468]	Freq.Flat	Both	Freq.Sel.	pilot	Est.	Yes	LS algorithm relied on generalized complex exponential basis expansion model
[469]	Freq.Flat	Both	Freq.Flat	pilot	Est.	Yes	LS algorithm for OQAM-OFDM systems

SC MIMO: reference [474] designs an optimal ML detector for spatial modulation MIMO systems with receive frequency-flat IQ imbalances. Moreover, an upper bound for average BEP expression is derived, and the IQ imbalances degrade the system performance. Moreover, authors in [475] propose an accurate asymmetric statistical signal model to the aggregate effect of frequency-flat IQ imbalance, PN, and distortion noises at both the transmitter and the receiver (Fig. 26). Using the proposed model, information-theoretic achievable rates for MIMO, SIMO with a linear combiner, and SIMO with selection combiner systems are derived. Also, an optimization framework is developed to derive optimal design for the transmit variance and pseudo-variance to maximize the end-to-end achievable rate of different systems. Finally, in [476], the impacts of imperfect CSI and transmit and receive frequency-flat IQ imbalances in Spatial modulation MIMO systems are studied. An optimum ML detection is presented, which suppresses the SI and signal distortion generated by IQ imbalances. For the proposed detector, upper bounds of the closed-form pairwise error probability and the average BER are presented in the presence of generalized Beckmann fading channels. However, references [474]–[476] assume the knowledge of the IQ imbalance is available, and the estimation and compensation approaches are not considered.

Authors in [477] analyze the impacts of transmit and receive frequency-flat IQ imbalances in space-time coded transmit diversity systems with two transmit antennas and multiple receiver antennas. Closed-form analytical results for SIR are derived, and the IQ imbalances degrade the performance. Moreover, two IQ imbalance compensation schemes are proposed based on the algebraic properties of the derived signal models. The first one is a pilot-aided algorithm, while the second one relies on blind signal separation principles and IQ decomposition of the received signal. On the other hand, the work in [478] investigates the impact of receive frequency-flat IQ imbalance on MIMO maximal ratio combining systems. PDF and cumulative distribution function (CDF) of the output SNR are derived in closed-form over uncorrelated Rayleigh fading channels. Furthermore, the upper bound on the symbol error probability, a closed-form expression for the outage probability, and a lower bound on the ergodic capacity are presented. Additionally, a pilot-aided LS-based algorithm is developed for joint estimation of the coefficients of the channel gain matrix, beamforming and combining weight vectors, and IQ imbalance parameters.

The joint estimation of channel and IQ imbalance in MIMO systems has been explored [479], [480]. Reference [479] proposes a joint estimator of the channels, CFO, receive frequency-selective IQ imbalances, and DC offset in MIMO systems using a training sequence. This work uses FIR filters to cancel self mirror interference caused by IQ imbalances, the normalized CFO, and DC offset. The LS algorithm estimates the filter parameters by exploiting trial values and grid search. However, the complexity of the proposed algorithm is high. Reference [480] studies the joint estimation of channels and receive frequency-flat IQ imbalance in a multiuser uplink system. A base station equipped with multiple receive antennas communicates with multiple single-antenna users. The pilot-aided LMMSE algorithm estimates the channels independent of the IQ imbalance coefficients. An LS algorithm is developed for estimating the IQ imbalances. Finally, based on the derived estimations, the IQ imbalance compensation scheme is presented based only on the estimation of the IQ imbalance coefficients.

MIMO OFDM systems: Authors in [481] investigate the

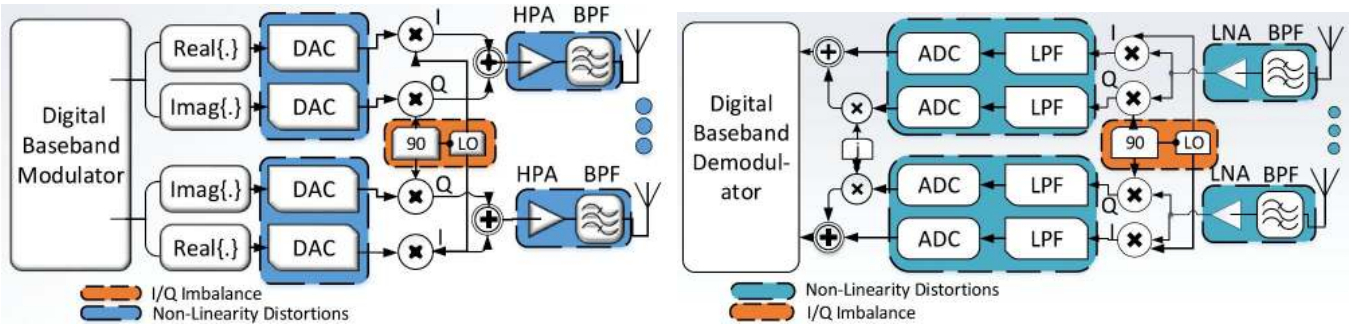

(a) Transmitter **(b)** Receiver

FIGURE 26: RF front-end of an MIMO transceiver in [475] given IQ imbalances and non-linearity distortions

impacts of IQ imbalance on MIMO OFDM systems. The input-output relation of the system is formulated as a function of MIMO channels and separate frequency-flat IQ imbalance for each receive antenna. The IQ imbalance increases the system's complexity at the receiver by four fold and degrades the system's performance, e.g., the achievable BER. Moreover, this work also develops a receiver structure for an Alamout-space-time block coded OFDM system with an IQ imbalance compensation scheme. However, the availability of knowledge of channels and IQ imbalance parameters at the receiver is assumed. Moreover, the ergodic capacity of a MIMO OFDM system in the presence of transmit and receive frequency-selective IQ imbalances along with residual CFO is studied [482]. Note that a separate IQ imbalance is considered for each transmit or receive antenna. The authors derive the capacity expression for the case of the transmit IQ imbalance without CFO. They also extract a lower bound on the capacity for both transmit and receive IQ imbalances with CFO and imperfect channel estimation. The pilot-data power allocation problem is considered to maximize the capacity bound, and the optimal power allocation at a high-SNR regime is derived. IQ imbalance and CFO degrade the capacity performance, while it is more sensitive to CFO than IQ imbalance. Besides, in [483], transmit antenna selection in the presence of frequency-flat transmit and receive IQ imbalances is studied, and closed-form solutions are derived. This work assumes that all of the antennas in both transmitter and receiver are supported by a single local oscillator, resulting in the same IQ imbalance for all of them. The MIMO system with only transmit IQ imbalances has the same capacity maximizing antenna selection as a system with no IQ imbalances. While, in the case of receive IQ imbalances, capacity maximizing antenna selection depends on the channels of the subcarriers and their mirror ones. Note that the works in [481]–[483] are based on perfect knowledge of IQ imbalance parameters, and they leave the question of the estimation of the parameters open.

Thus, authors in [484] propose a pilot-aided scheme for joint compensating frequency-flat transmit and receive IQ imbalances in differential space-time block coding MISO OFDM. Their scheme uses the differential encoding property and a widely-linear adaptive decision-directed algorithm. A parameter-based generalized algorithm is developed for IQ imbalance parameters extraction in the system with high mobility. Also, the authors analytically investigate the impacts of IQ imbalances on the system's performance and illustrate that they cause BER floor.

In [485], a blind algorithm for joint estimation of CFO and receive frequency-flat IQ imbalances in SIMO OFDM systems is proposed by utilizing the multi-antenna redundancy at the receiver. All receive antennas have the same IQ imbalance parameter. Auxiliary matrices are derived for designing the cost function, expressed as a superposition of few harmonically related cosine waves. This method has low computational complexity because it avoids a grid search procedure. On the other hand, a study in [486] proposes a scheme for transmit and receive frequency-selective IQ imbalances compensation in MIMO OFDM systems with independent component analysis. Different IQ imbalance parameters are assumed for different transmit and receive antenna pairs. This study deploys a higher-order statistics-based blind source separation technique for joint IQ imbalance compensation and received signal equalization by exploiting the statistical characteristics and the algebraic structure of the received signal. However, this method requires a known reference signal embedded in the transmitted signal to enable ambiguity elimination. Moreover, authors in [487] develop a pilot-aided algorithm for joint estimation of transmit and receive frequency-selective IQ imbalance in MIMO OFDM systems with CFO. The algorithm has low sensitivity to CFO.

Studies in [488]–[490] deal with joint channel and transmit and receive IQ imbalance estimation problem with the aid of pilot sequences. The study in [490] presents a method for joint estimating the channel and frequency-flat IQ imbalance in Alamouti space-time block coded MISO OFDM systems. In this study, the IQ imbalance effects are combined with the channel into one parameter: the overall channel. An ML-based method is then developed for the overall channel estimation, and an iterative EM algorithm is exploited to the estimation process by using the resulting soft information from the detector. On the other hand, the authors in [488] investigate pilot design for joint estimation of MIMO

frequency-selective channels and frequency-selective IQ imbalances. The effects of channel and IQ imbalances are considered equivalent channels, and pilots are designed to minimize the MSE of the LS-type channel estimators. The pilot design criterion satisfies the estimation identifiability, zero data interference condition, zero cross channel interference, and white noise optimality. Moreover, the work in [489] investigates joint channel and IQ imbalance estimation in mobile space-frequency block coded MIMO OFDM systems. The frequency-selective IQ imbalances are considered, and generalized linear models are derived for them. Furthermore, orthogonal pilots are designed so that joint channel and IQ imbalance parameters estimation is performed for each pair of transmit and receive antennas separately.

Additionally, in [491], joint estimation of channel response, receive frequency-flat IQ imbalance, and CFO in a MIMO OFDM system is studied using training sequences. In this work, IQ imbalances and CFO are jointly estimated without knowing the channel response by minimizing channel residual energy, which is defined based on MIMO channel estimation in the presence of known IQ imbalances and CFO. The channel is estimated by exploiting the estimated parameters. Furthermore, the investigation in [492] proposes an ML-based algorithm for joint estimation of the channel, IQ imbalance, and PN in MIMO OFDM systems. Receive frequency-flat IQ imbalances and independent oscillator for each receive branch are considered. Besides, the transmitted pilots from different transmit antennas are orthogonal to each other. The proposed algorithm first estimates the PN parameters independent of other parameters. Then, IQ imbalance parameters are estimated by using the estimated PN without knowing the channel. Finally, estimation of the channel is derived based on the IQ imbalance and PN parameters estimations.

Finally, studies in [493], [494] explore the IQ imbalance impacts in multiuser OFDM systems where the base station and users are equipped with multiple antennas. In [493], the distribution of uncompensated IQ interference and SINR in a precoded downlink MIMO OFDMA system is studied. All transmission chains have a similar frequency-flat IQ imbalance, and also perfect CSI is available in the base station's transmitter and users' receivers. Moreover, the ergodic and outage capacities are derived in the presence of IQ interference. Also, link-adaptation is analyzed where the transmission rate is optimized based on IQ imbalance awareness, e.g., the statistics of the IQ imbalance interference. On the other hand, authors in [494] investigate the impacts of IQ imbalance on MIMO OFDMA systems where base station's receiver and the users' transmitters experience frequency-selective IQ imbalances. It is illustrated that IQ imbalances destroy the signal properties and introduce ICI and inter-user interference caused by the image subcarrier. Moreover, to mitigate the IQ imbalance effects, augmented subcarrier processing is performed, which jointly processes each subcarrier with its image subcarrier and across all receive antennas. Furthermore, an optimal augmented linear receiver is derived in terms of minimizing the mean-squared error.

2) Massive MIMO systems

IQ imbalances in base stations and users cause the image signals which degrade the performance by introducing ICI and MUI terms. Thus, these impairment should be taken into account in channel estimation, precoding and receivers designs.

Downlink transmissions: The work in [495] investigates widely linear precoding techniques to mitigate transmit frequency-flat IQ imbalances in narrowband SC massive MIMO systems. Single base station with massive transmit antennas and multiple users with multiple receive antennas are considered. In this work, different precoding schemes, including widely linear ZF, widely linear MF, widely linear minimum mean-squared error, and widely linear block-diagonalization type precoding algorithms, are developed based on an equivalent real-valued signal model. The derivations show that widely linear ZF and widely linear block-diagonalization achieve the same sum data rates as ZF and block-diagonalization receivers when IQ imbalances do not exist. Moreover, they have the same multiplexing gain when there are IQ imbalances at the transmitter. Moreover, authors in [496] consider both transmit and receive frequency-flat IQ imbalances and present a regularized ZF precoder scheme in SC massive MIMO downlink systems. In contrast with [495], users are equipped with a single antenna. The proposed scheme is derived based on the optimization problem with the MMSE criterion with multiple regularization parameters for channel qualities and channel correlations. The presented precoder is robust to the severe IQ imbalances and their estimation errors.

On the other hand, the work in [497] investigates joint channels and transmit frequency-flat IQ imbalances in narrowband SC massive MIMO downlink systems. The joint estimation problem is modeled as two-timescale non-convex optimization that relies on the MAP estimate. The IQ imbalance parameter and the sparse channel vector are treated as the long-term and short-term variables. The presented two-timescale sparse problem is solved by a batch algorithm that finds a stationary point of the problem based on all the previously received signals. Moreover, to reduce the computational complexity, a two-timescale online joint sparse estimation algorithm is developed, which solves the current system's short-term problem and updates the long-term variable in each iteration recursive convex approximation.

In uplink transmissions, a widely-LMMSE receiver under transmit and receive frequency-flat IQ imbalances is designed for a narrowband SC massive MIMO systems in [498]. Multi cells are considered in which each cell includes one base station equipped with massive antennas communicating with multiple single-antenna users. Moreover, training sequences are deployed, which are transmitted by users to their serving base station. Since there are not enough orthogonal training sequences for all cells in all cells, pilot contamination is considered. Users with the same index in

different cells use the same training sequence. In this work, a system model contains effects of multi-cell interference, CSI imperfection due to pilot contamination, channel estimation errors and IQ imbalances. The proposed receiver jointly suppresses MUI and IQ imbalances by processing the real and the imaginary parts of the received signal separately. Finally, analytical results for the asymptotic sum-rate performance of the proposed receiver are presented. The authors illustrate that the IQ imbalance in users is more harmful than the IQ imbalance in base stations with massive antennas. The performance of the addressed receiver reaches the LMMSE receiver in an ideal system without IQ imbalances. However, all of these achievements are based on known IQ imbalances in the receiver, which is impossible in practical systems.

Thus, authors in [499], [500] propose an LMMSE algorithm for practical channel estimation under transmit and receive frequency-flat IQ imbalances in a narrowband SC massive MIMO uplink systems. In contrast with [498], single-cell is only considered with a massive MIMO base station and multiple single-antenna users. In these studies, the IQ imbalances are considered random variables, and their effects are combined with channel information states into effective channels. Moreover, an analysis of the asymptotic achievable sum rate for the proposed method is presented. Besides, the study in [501] investigates channel estimation with pilot reuse for the same massive MIMO uplink systems. In this work, the real and imaginary parts of the received signal are processed individually with relative compensation. An augmented real-valued representation for the received signal is obtained. An MMSE algorithm with pilot reuse is developed for estimating the effective channels (similar to [499], [500]). Furthermore, a lower bound of the effective channel estimation MSE is derived. Furthermore, authors in [502] study channel estimation and robust detection in massive MIMO uplink systems with frequency-flat IQ imbalance. A combination of the IQ imbalance and the channel is considered the effective channel, and the MMSE algorithm is deployed for estimating the effective channel.

Studies in [503], [504] address the joint estimation of channels and frequency-flat IQ imbalances in SC single-cell massive MIMO uplink systems with low-resolution ADCs. The system model includes a base station equipped with a massive number of antennas and multiple single-antenna users. In [503], The receive IQ imbalance parameters are estimated in two stages with the aid of a specific transceiver near the base station, which shares flat-fading channels. In the first stage, phase-shifted versions of IQ imbalances are estimated by the gradient descend method and a predefined training sequence emitted by the transceiver. Then, in the second stage, the phase shifts from the first stage are estimated by exploiting a typical sequence transmitted by the base stain antennas to the transceiver. Moreover, two channel estimators and multiuser detectors are developed based on the spectral projected gradient method and vectorized message passing de-quantization algorithm. However, the proposed algorithm requires additional time overhead for IQ imbalances estimations in which training sequences are transmitted between the specific transceiver and the base station. Besides, authors in [504] study the channel estimation and transmit and receive IQ imbalances compensation problems. They present an independent automatic gain control scheme for each receive antenna to calibrate the dynamic range of I and Q branches. Furthermore, channel estimation and IQ imbalance compensation under the impacts of both quantization and IQ imbalance are addressed using a bilinear generalized approximate message passing algorithm.

3) Relaying cooperative systems

IQ imbalance impairments in relay systems can affect the performance. Therefore, these effects have been investigated, and IQ imbalance cancellation techniques have been developed. We next provide a brief overview of such results.

Thus, studies in [505]–[507] explore the impacts of IQ imbalance on AF dual-hop relaying systems where three nodes, a source, a relay, and a destination, are considered. In [505], the outage performance of the system with MRC detection over Rayleigh fading channels is analyzed. The source node has no IQ imbalance, the relay node suffers from both receive and transmit IQ imbalances, and the destination node has receive IQ imbalance. All of the considered IQ imbalances are frequency-flat, and all nodes have a single antenna. Outage performance of the direct transmission (no relay) outperforms AF relay transmission when the IQ imbalance level exceeds a certain threshold, which is inversely proportional to the cube of the signal constellation size. Moreover, a pilot-aided joint channel and IQ imbalance compensation scheme based on the ZF approach is presented, and its EVM is analyzed at high-SNR. In [506], analytical expressions for outage probability and ergodic capacity of the relay system over independent, non-identically distributed Nakagami-m fading channels are derived. In this study, transmit and receive frequency-flat IQ imbalances in only relay nodes are considered. The derived asymptotic outage probability and ergodic capacity in the high-SNR regime illustrate that the relay IQ imbalance results in a ceiling effect on the SINR that depends on the level of IQ imbalances. Moreover, authors in [507] study IQ imbalance compensation in a CSI-assisted AF dual-hop system. The relay uses instantaneous CSI of the first hop to fix the power of the re-transmitted signal. Frequency-flat IQ imbalances are assumed for source and destination nodes, while the relay transmission is perfect. This work presents an ML detection algorithm and two algorithms for IQ imbalance compensation based on weighting the received signal and the ZF approach.

Furthermore, in [508], the outage probability of dual-hop opportunistic AF relaying is derived with frequency-flat IQ imbalances in all nodes. The system model includes one source, multiple relays, and one destination node. In this system, the source node transmits data to the relay nodes in the first slot, while one relay with the highest SINR is selected to retransmit the signal in the second slot. Moreover, authors in [509] derive the outage probability of dual-hop two-way

AF relaying systems with a frequency-flat IQ imbalance at the relay node. This study proposes two schemes, namely, fixed power allocation and instantaneous power allocation, to mitigate the IQ imbalance effects and improve the system reliability under a total transmitpower constraint. The former is effective for asymmetric channel cases, and the latter works better for the symmetric channel case.

On the other hand, studies in [510]–[512] investigate the performance of DF-based rallying systems. In [510], approximate outage probabilities expressions of AF, DF, and Controlled DF dual-hop relaying systems are derived by considering frequency-flat IQ imbalances for the relay and destination nodes. It is shown that the IQ imbalances have no effects on outage probabilities when their levels are lower than $1/\sqrt{\text{SNR}}$. In this case, the system achieves a diversity order of two for AF and Controlled DF relays and one for DF relay. Moreover, direct link transmission outperforms all the relays for reasonable SNR ranges and IQ imbalance levels. Additionally, in [511], the outage probabilities of fixed-gain AF, variable-gain AF, and DF dual-hop relaying systems are derived in the presence of frequency-flat IQ imbalance and additive hardware impairment at all nodes. Fixed-gain AF outperforms the other relay schemes in terms of outage probability and SER. Finally, authors in [512] develop an ML estimator to estimate channel impulse responses in alternate-relaying cooperative systems. One source, two DF relays, and one destination node are deployed, and frequency-flat IQ imbalances are assumed for all nodes. In this system, the two relays transmit and receive alternately, which allows the source to transmit data in every time-slot. Moreover, to reduce the complexity, the EM algorithm is developed to approximate the optimal estimate.

In addition, reference [513] studies impacts of frequency-flat receive IQ imbalance on full-duplex AF-based relay network. Even a low IQ imbalance significantly increases the residual SI power, degrading the performance. Authors in [514] investigate pilot optimization and power allocation for the frequency-domain LS channel estimator in a full-duplex DF-based OFDM relay network with IQ imbalances. The DF relay of the network receives the current data frame from the source, and at the same time, sends the previous data frame to the destination over the same frequency band. The optimum pilot product matrix is derived by minimizing the sum of MSEs and utilizing the Karush-Kuhn-Tucker (KKT) conditions. They present an optimal power allocation strategy under the total transmit power of source and relay nodes. Also, the proposed power allocation outperforms the equal power allocation in terms of the sum of MSEs performance.

4) Cognitive radio networks

These use spectrum sensing to identify temporarily vacant portions of spectrum (i.e., spectrum holes). However, the IQ imbalances in both primary and secondary transceivers can affect the performance of spectrum sensing by introducing image channel crosstalk, which degrade the performance, e.g., BER. We next discuss the literature on impacts of IQ imbalances and spectrum sensing schemes.

Therefore, [515] investigates the combined effect of transmit and receive frequency-flat IQ imbalances and imperfect CSI in cognitive radio secondary systems. Consequently, the performance degrades, and the noise behavior changes from a proper to improper Gaussian distribution. Moreover, to mitigate the effects of IQ imbalances, this work designs an ML receiver and derives the average pairwise error probability and a tight upper bound of the average BER. Furthermore, a widely-linear equalization receiver is proposed to reduce the complexity at the cost of performance degradation.

On the other hand, authors in [516] propose an asynchronous cyclostationary detection method for the spectrum sensing problem in OFDM-based cognitive radio networks by exploiting embedded pilots. Different RF impairments for the secondary user are considered, including IQ imbalance, CFO, PN, and sampling clock frequency offset. The proposed detector is developed based on the pilot's correlation matrix and second-order cyclostationarity of OFDM signals. Moreover, it is shown that the IQ imbalance has little impact on the presented detector. Simultaneously, CFO and PN ruin the gains obtained via cyclostationary feature, and sampling clock frequency offset can strongly degrade the performance when long sensing periods are required. Additionally, the study in [517] presents an optimal blind Neyman-Pearson detector for OFDM signals when there is both transmitter and receiver frequency-flat IQ imbalance. The proposed detector is derived by utilizing the correlation between each subcarrier and its image by assuming known received signal covariance at the subcarrier level. Besides, expressions for the probabilities of detection and false alarm are extracted. It is shown that transmit a secondary user can blindly deploy IQ imbalance to enhance the detection probability. Although the works in [516] and [517] illustrate that the receive IQ imbalance does not affect spectrum sensing performance, they only consider narrowband single-channel sensing.

Therefore, studies in [518]–[520] investigate the energy detection-based wideband multichannel spectrum sensing in the presence of IQ imbalance impairment. The wideband sensing allows simultaneous sensing of multiple RF channels where several primary users are active. In [518], an energy detector is presented by considering frequency-flat IQ imbalance for the secondary receiver, and detection and false alarm probabilities are derived in closed-form. The authors show that despite narrowband sensing, the IQ imbalance has detrimental impacts under multichannel sensing due to introducing the image channel crosstalk terms. In other words, the network's performance depends on the power level of the image channel and IQ imbalance values. For example, in Fig. 27, due to IQ imbalance, the image of primary user2 (PU2) introduces interference term for PU1 at channel -1, and vice versa. Hence, to mitigate the effects of the image channel, an algorithm is developed by subtracting the image channel signal from the primary channel signal with proper scaling. Furthermore, the work in [519] proposes a four-level energy detector for secondary user spectrum sensing

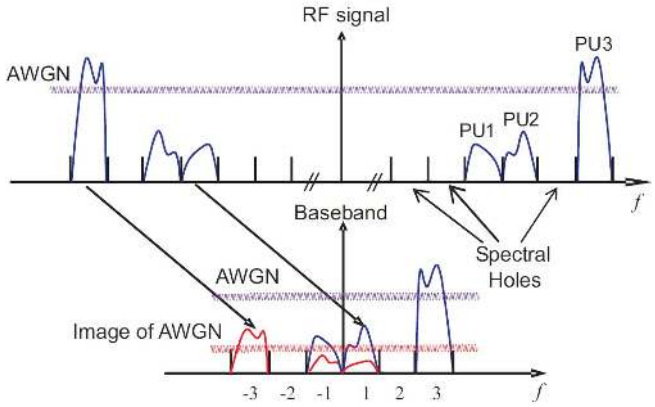

FIGURE 27: Down-conversion of multiple RF channels to baseband in the presence of IQ imbalance. Three channels are occupied with PUs and three others are vacant [518]. PU1 at channel -1 is interfered by the image of PU2, and vice versa. Also, the spectral hole at channel -3 is interfered by the image of PU3.

in OFDMA uplink primary networks where a dedicated number of subcarriers are assigned to multiple primary users with frequency-flat IQ imbalance. The proposed detector can sense a specific subcarrier and decides among four possible cases: 1) there is only noise, 2) there is the interference due to the IQ imbalance, 3) the primary is present with noise, 4) the primary user is present with noise and IQ imbalance interference. Note that the addressed detector is developed based on known a priori information about potential primary systems in the secondary receiver, such as the DFT size and the transmission parameters. Finally, authors in [520] explore the joint effects of RF impairments in secondary receiver, including IQ imbalance, non-linear low-noise amplifier, and PN on energy detection-based wideband multichannel spectrum sensing. In this work, the joint effects of the aforementioned RF impairments are modeled as a complex Gaussian process, and analytical closed-form expressions for the false alarm and detection probabilities are derived.

The authors in [521], [522] study blind spectrum sensing problem in single-channel SIMO cognitive radio systems under transmit and receive frequency-flat IQ imbalances. The system model includes one single-antenna primary user and one secondary user equipped with an array of antennas. In [521], a composite binary hypothesis testing is formulated, and an eigenvalue-based detector is developed by exploiting the likelihood ratio test principle. In this work, a preprocessing stage in the secondary receiver is proposed to mitigate the effect of receive IQ imbalances. Also, the false alarm probability of the proposed detector is derived. Unlike [521], the study in [522] considers joint transmitter and receiver IQ imbalance uncertainties and deal with a non-calibrated receiver. The effects of IQ imbalances on the improperness of the transmitted and received signals are addressed. The spectrum sensing problem is modeled as a composite binary hypothesis testing that is solved by the likelihood ratio test approach. Three spectrum sensing algorithms are presented relied on different assumptions about the impropriety or propriety of the desired and noise signals. Finally, this work derives a closed-form analytical expression for the received SNR in secondary users under IQ imbalances.

In [523], the combined effects of IQ imbalance and partial SI suppression on the energy detection-based single- and multichannel spectrum sensing in full-duplex cognitive radio are studied. The considered cognitive radio system includes several primary users, and two secondary devices operate in full-duplex mode. Also, both frequency-flat transmit and receive IQ imbalances are considered for secondary users. IQ imbalances and partial SI suppression degrade the system performance with single-channel, while the energy detection capability can be entirely restricted for multichannel cases in terms of the false alarm and detection probabilities.

5) Millimeter-wave systems

These have massive bandwidths to support multi-gigabit per-second data rate transmissions. However, IQ imbalance in milliliter-wave transceivers induces the mirror interference terms on top of the desired signal, which have harmful effects on the system performance, .e.g., BER and EVM. Moreover, IQ imbalances can destroy the channel estimation performance and increase the MSE. Because of these reasons, the following works discuss the impacts of IQ imbalance on the millimeter-wave systems and propose estimation and compensation schemes.

Authors in [524], [525] investigate the estimation and compensation of the IQ imbalance impairment in millimeter-wave SC-FDE systems. Reference [524] presents a training-based approach to obtain separate estimates of IQ imbalance and channel information. This work considers both frequency-flat and frequency-selective IQ imbalances in the receiver side. This approach maximizes a likelihood function that captures the IQ imbalance and multipath channel iteratively. Finally, exploiting the estimation results, this work implements IQ compensation and channel equalization in the frequency domain.

On the other hand, [525] addresses the compensation of frequency-selective and frequency-flat IQ imbalances in the transmitter side. Similar to [524], a training-based compensation scheme is presented, which iteratively maximizes the likelihood function to obtain a separate estimation of channel and IQ imbalance. Note that [524] and [525] evaluate the BER performance based on IEEE802.11ad standard and illustrate that both transmit and receive IQ imbalances degrade the BER performance.

The study in [526] develops a model for millimeter-wave MIMO OFDM systems in the presence of RF impairments, including CFO, PN, frequency-selective IQ imbalances, sampling time offset, SFO, and in-phase and quadrature timing mismatch. Moreover, a pilot design is presented for joint estimation and compensation of transmit and receive in-phase and quadrature timing mismatches under other RF impairments.

This article has been accepted for publication in a future issue of this journal, but has not been fully edited. Content may change prior to final publication. Citation information: DOI 10.1109/ACCESS.2021.3101845, IEEE Access

Finally, [527], [528] study the IQ imbalance estimation and compensation problems in Terahertz Communication Systems. Reference [527] develops a precompensation scheme for the effects of non-linear distortions and IQ imbalance in the transmitter side of low-cost Terahertz QAM systems. Moreover, a pilot-aided ML estimator is proposed to estimate the non-linearity and the IQ imbalance parameters, and also a pilot sequence design is addressed. On the other hand, authors in [528] discuss the channel estimation and signal detection in the Terahertz spatial modulation systems. RF impairments, including PN, IQ imbalance, and non-linear power amplifiers are considered, which are modeled as complex-Gaussian distortions at both the transmitter and the receiver. A pilot-aided ML estimator is proposed, which contains two phases of candidate acquirement and exhaustive search. An LS channel estimator is then addressed to reduce the complexity by considering the impairments in an averaging manner.

6) Beamforming techniques

IQ imbalance will affect the performance of these systems by introducing interference terms. Thus, investigating its impacts and developing compensation techniques are crucial.

Reference [529] derives a closed-form expression for the outage probability of beamforming MISO OFDM systems. Frequency-flat IQ imbalances in both transmitter and receiver and frequency-selective fading channels with independent Rayleigh distributed coefficients are assumed. Receive IQ imbalance leads to the outage floor in high-SNR scenarios. Moreover, the asymptotic behavior and diversity order of the system are discussed. Full spatial diversity is achievable when the image leakage ratio of the transmit IQ imbalance is lower than $(2^{R_k}-1)^{-1}$, where R_k is the transmit rate. Besides, [530] explores the impacts of joint transmit and receive frequency-selective IQ imbalances on multiple beamforming OFDM systems, where transmitter and receiver are equipped with multiple antennas. The approximate average subcarrier SINR is derived. The SINR performance with receive IQ imbalance will not improve by increasing the transmit beamforming array size at high input SNR, unlike the case of no IQ imbalance. Additionally, a pilot-aided scheme for channel and IQ imbalance estimation is proposed using the standard linear LS estimation algorithm.

7) Full-duplex communications

The performance of SI cancellation techniques in analog and digital domain can be affected by the mirror interference introduced by the IQ imbalance. Moreover, these interference terms can impair desired and SI channels estimation. Therefore, the literature has treated SI cancellation and channel estimation with IQ imbalance.

In [24], [531], [532], the impacts of IQ imbalance on digital SI cancellation are addressed. Authors in [531] explore the impacts of the non-linear amplifier and the mirror interference induced transmit frequency-flat IQ imbalance on OFDM full-duplex systems. They show that the mentioned impairments limit the precision of digital SI cancellation and heavily limit the receiver path SINR. Thus, they propose an iterative cancellation scheme based on the power amplifier's output signal, which exploits the detection result of the desired signal for improving the SI cancellation performance. Moreover, the study in [24] presents detailed SI signal modeling for OFDM full-duplex systems in the presence of non-linear amplifiers and both transmit and receive frequency-selective IQ imbalances. The image signal caused by IQ imbalances decreases the maximum achievable SINR. Thus, a widely linear-digital SI cancellation technique is proposed, which utilizes both the original transmit data and its complex conjugate for cancellation. Moreover, The cancellation parameters are estimated in the widely linear LS sense. Finally, in [532], an augmented non-linear LMS- based SI canceller is proposed for wideband OFDM full-duplex transceivers given non-linear power amplifier and frequency-selective IQ imbalances. The proposed technique considers both the non-linear SI component and its associated mirror interference.

Furthermore, authors in [533] investigate impacts of PN and frequency-flat IQ imbalance on full-Duplex spatial modulation Systems. The impairments degrade SI cancellation performance, and the system is more sensitive to IQ imbalance at low SNRs. On the other hand, the work in [534] studies the effects of IQ imbalance on the analog LMS loop for SI mitigation in full-duplex radios. This loop is deployed to generate a cancellation signal and subtract it from the received signal at the receiver. This loop comprises multiple taps, in each of which the delayed transmitted signal is multiplied with the looped-back signal using an IQ demodulator. Then the cancellation signal is derived by combining the outputs of all the taps. IQ imbalance reduces the level of SI cancellation and causes loop gain variation, which is compensated by adjusting the gain at other stages inside the loop.

Authors in [535] discuss the channel estimation and pilot design in the presence of both transmit and receive frequency-flat IQ imbalances at OFDM full-duplex systems. In this work, effects of IQ imbalance and channel impulse response are combined into an equivalent channel. A frequency-domain LS algorithm is proposed, which estimates both desired and SI equivalent channels. Furthermore, the optimal training design for the presented estimator is modeled as a convex optimization problem of minimizing the sum of variances under the power constraint. Finally, an ML detector is developed by applying a whitening filer, eigenvalue decomposition, and singular value decomposition beamforming. References [536], [537] investigate SI cancellation in OFDM full-duplex systems with frequency-flat IQ imbalance and a non-linear power amplifier. In [536], a pilot-aided iterative algorithm for estimating the channel, IQ imbalance, and power amplifier and low-noise amplifier non-linearities is proposed. Moreover, in [537], a non-linear algorithm utilizing an auxiliary transmitter is proposed to cancel SI present in the RF domain. In this work, the local transceiver channel is estimated via an LS estimator. The

canceling signal is generated based on the estimation results.

V. OPEN ISSUES AND FUTURE RESEARCH DIRECTIONS

This section discusses open issues and research directions related to RF impairments in the state-of-the-art technologies.

A. CELL-FREE MASSIVE MIMO

In cell-free massive MIMO systems, many geographically distributed service antennas, namely access points (APs), are deployed to serve user equipment (UE) [538]. All APs cooperate with a fronthaul network and a central processing unit to provide all UEs in the same time-frequency resource [539]. Fig. 28 shows a cell-free massive MIMO network. To be specific, these networks eliminate cells or cell boundaries, and all UEs are served by all APs simultaneously, where APs are equipped with single or multiple antennas. Since the users now are close to the APs, coverage probability increases. Therefore, Cell-Free Massive MIMO can be a potential candidate for future indoor and hot-spot coverage scenarios, e.g., shopping malls and small villages [539]. Moreover, it significantly increases the energy efficiency and guarantees uniformly good service for all UEs [540].

In the uplink of these systems, the APs transmit the received data from the UEs to the central processing unit via a fronthaul link. In the downlink, the central processing unit transmits data and power control coefficients to the APS. All transmissions proceed by time-division multiplexing (TDD) operation. Note that APs estimate all channels via pilot transmissions and by exploiting channel reciprocity. The APs use the estimated channels for downlink data precoding and uplink data detection. Rate analysis and the use in cognitive radios of cell-free massive MIMO are considered in [541], [542]. The works in [543]–[545] investigate channel estimation problem in cell-free massive MIMO systems. Authors in [543] explore the uplink channel estimation problem in a cell-free massive MIMO system over Rician fading channels. In this work, to consider phase shifts because of mobility and PN, the line-of-site path phase is regarded as a uniformly distributed random variable.

Moreover, three-channel estimators are developed, namely, the phase-aware MMSE, non-aware LMMSE, and LS. Furthermore, authors in [546] exploit the channel estimators in [543] and study the total downlink power optimization problem with the antenna power and rate constraints. Reference [544] explores downlink channel estimation of cell-free massive MIMO with the aid of downlink pilots beamformed to the UEs using conjugate beamforming. However, both [543], [544] assume that each UE has a single antenna. Hence, [545] investigates uplink and downlink channel estimation with multi-antenna UEs over Rayleigh fading channels.

On the other hand, cell-free massive MIMO systems require many antennas to achieve good performance, which leads to increasing the power consumption and the hardware cost. To handle this issue, one needs low-cost, low-power hardware components, especially for APs associated with multiple antennas. But hardware defects may introduce RF impairments. Studies in [547] and [548] investigate the performance of cell-free massive MIMO systems with low-resolution analog-to-digital converter architecture for APs. Tight approximate expressions for uplink spectral efficiency and energy efficiency are derived. Deploying low-cost, low resolution analog-to-digital converters have a great potential to achieve a better spectral efficiency-energy efficiency trade-off compared to the perfect ones.

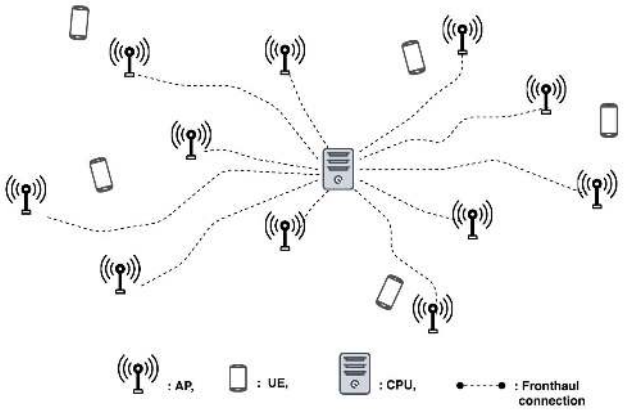

FIGURE 28: Cell-free massive MIMO network [543].

Furthermore, the works in [549], [550] investigate the performance of cell-free massive MIMO systems by leveraging on the Gaussian RF impairment model, which describes the interference terms as Gaussian noises. In [549], closed-form expressions for spectral efficiency and energy efficiency are derived, and by increasing the number of APs, the detrimental effect of hardware impairments at the APS vanishes. Moreover, [550] derives closed-form channel estimation and achievable rate expressions given known RF impairments and low-resolution analog-to-digital converters. The imperfections cause a non-zero floor on the channel estimation error, which is not eliminated by infinitely increasing the SNR. Furthermore, the spectral efficiency of cell-free massive MIMO systems with PN and imperfect CSI is investigated in [551]. The impact of PN on the performance of the system is severe.

The papers mentioned above investigate the impacts of RF impairments, including PN, CFO, and IQ imbalance on the performance of cell-free massive MIMO systems. The works in [549], [550] model all the impairments as Gaussian noise, which may not be accurate. The RF impairments introduce in-band and out-of-band distortions, degrading the system's performance, e.g., spectral efficiency, achievable rate, and BER. They also affect the performance of channel estimation and data detection. For example, [550] shows that RF impairments destroy the channel estimation performance. Therefore, joint channel and RF impairment estimation/compensation techniques are needed.

B. NON-ORTHOGONAL MULTICARRIER SYSTEMS

OFDM is widely used in 4G wireless (Long Term Evolution (LTE) and other standards) because of its robustness against multipath channels and easy implementation based on Fast Fourier Transform algorithms. However, OFDM may not the requirements of certain future networks. For example, machine-to-machine communication and IoT require low power consumption, while the strict synchronization process of OFDM to keep the orthogonality between subcarrier makes it unaffordable [552]. Moreover, OFDM with one CP per symbol may not answer the low latency demand of vehicle-to-vehicle applications [553]. Furthermore, due to the CP insertion, it suffers from low spectral efficiency, which is also a problem for Wireless Regional Area Network (WRAN) applications [554]. Finally, it has a high peak-to-average power ratio [555], [556] and out-of-band emissions, which poses a challenge for opportunistic and dynamic spectrum access.

Therefore, to address these drawbacks, recent research proposes novel non-orthogonal multicarrier systems , which FBMC [552] and generalized frequency division multiplexing (GFDM) [557] are two promising ones. In FBMC, the data symbols are transmitted over different subchannels after pulse shaping with bandlimited filters, which overlap in time. Since subcarriers are narrow bandwidth, the length of the filter impulse response is usually long, typically, four times the length of the symbols. On the other hand, in GFDM, data symbols are divided into subcarriers and subsymbols, using circular pulse shaping for each subcarrier. These non-orthogonal designs can enhance spectral efficiency, reduce latency, reduce peak-to-average power ratio and out-of-band emission. However, due to non-orthogonality between subcarriers, they suffer from ICI and ISI. Moreover, the RF impairments increase these inherent interference levels. Therefore, investigating the impact of them and proposing compensation algorithms are necessary.

The study in [558] investigates impacts of PN impairment in circular FBMC-OQAM systems under imperfect channel estimation. This work proposes a pilot-aided algorithm for PN compensation based on the LS approach. In addition, studies [559]–[563] investigate CFO estimation and compensation in FMBC systems. In [559], a pilot-aided feed-forward ML algorithms for CFO estimation is developed by considering time-frequency-selective channels. In [560], low-complexity joint timing and CFO synchronization algorithms are presented using two uncorrelated consecutive real training symbols. In [561], impacts of CFO on FBMC-QAM with non-orthogonal prototype filters are investigated, and pilot-aided ML estimators are developed. In [562], CFO and channel estimation in MIMO-FBMC/OQAM is investigated by using MMSE approach. Furthermore, the work in [564] investigates joint IQ imbalance, PN, and channel estimation problems in multicarrier systems, including circular FBMC-OQAM, using the LS approach.

On the other hand, reference [565], [566] study impacts of PN, CFO and IQ imbalance on GFDM systems. The impairments significantly degrade the SIR and enhance the symbol error probability of the system. Moreover, authors in [567] proposes filter designs for GFDM systems in the presence of a CFO. Besides, impacts of PN, CFO, and IQ imbalance on the performance of GFDM full-duplex transceivers are investigated in [568], [569]. The impairments increase the power of residual SI after analog and digital SI cancellation. To suppress their effect, the optimal filter is designed, which maximizes the SIR of the system. Furthermore, studies in [570], [571] investigate impacts of RF impairments including PN, CFO, IQ imbalance, and non-linear power amplifier on the performance of cognitive GFDM full-duplex secondary link and solve the power allocation problem to maximize the sum rate of the system.

Compensation of RF impairments in GFDM systems is investigated in [572]–[576]. Pilot-aided algorithms based on non-linear LS approach for joint channel and PN estimation and data detection are developed in [572]. CRLBs for channel and PN estimations are derived, and t MSE of channel estimation meets the CRLB. Furthermore, authors in [573] develop a CP-based ML blind algorithm for CFO synchronization. Moreover, [576] proposes a non-linear LS-based algorithm for joint transmit and receive IQ imbalance and channel estimation. Finally, authors in [575] propose a blind adaptive IQ imbalance compensator for GFDM receivers based on the normalized LMS adaptive self-image cancellation algorithm in [577].

All the works mentioned above show the sensitivity of non-orthogonal multicarrier systems to the RF impairments because they use non-orthogonal subcarriers. However, impacts of RF impairments of such systems in emerging technologies, e.g., MIMO, massive MIMO, relaying cooperative systems, and Millimeter-wave systems, have not been investigated. Since non-orthogonal alternatives to OFDM may be used in future networks, we require a complete investigation of impacts, estimation, and compensation of RF impairments in such systems.

C. NOMA

Multiple access provides communication service for multiple users by deploying multiplexing techniques. These techniques is broadly categorized into two approaches including orthogonal multiple access and NOMA [578]. In former one, users are assigned to orthogonal communication resources within either a specific time-slot, frequency band, or code [579]. The fundamental advantage of this approach is that it allows the receiver of one user to entirely separate unwanted signals from its own signal since signals from different users are orthogonal to each other. Therefore, there is no mutual interference among users. TDMA and OFDMA are examples of orthogonal schemes which multiple users are assigned orthogonal time-slots and subcarriers, respectively. Subcarrier separation ensures that they are orthogonal to each other. However, in orthogonal multiple access, number of supported users is limited by the number of available orthogonal resources [580]. Therefore, to support high number of

users, NOMA is proposed which allows multiple users share the same radio resources in time, frequency and/or code via power domain multiplexing. Due to relaxing orthogonality between users in NOMA, MUI is introduced while successive interference cancellation (SIC) is deployed to eliminate it for accurate detection [578], [579].

Hence, NOMA supports more users and enhances the spectral efficiency at the cost of increased receiver complexity for MUI compensation. On the other hand, RF impairments are able to degrade the performance of NOMA by increasing the degree of non-orthogonality between users and constraint the system's reliability. Reference [581] investigates the impacts of PN on downlink power-domain NOMA networks and illustrates that high PN significantly enhances the outage probability. Furthermore, authors in [582] study the ergodic sum-rates of uplink and downlink OFDM-NOMA systems under residual CFO and perfect SIC. It is shown that the residual CFO results in significant ergodic sum rate loss, e.g., normalized residual CFO of 0.45 causes 30% loss. Besides, in [583], impacts of frequency-flat transmit and receive IQ imbalance on the outage probability of NOMA-based SC and multi-carrier systems are investigated. In both considered systems, the IQ imbalance affects the SIC performance and results in higher outage probability. Finally, outage probability and ergodic sum-rate of full-duplex cooperative NOMA under IQ imbalance and imperfect SIC is studied in [584], which demonstrates deleterious effects of IQ imbalance in the moderate and high SNR regions.

The detrimental impacts of RF impairments on the performance of NOMA is discussed in the above mentioned works. However, compensation of RF impairments for improving the performance including reducing outage probability, enhancing ergodic sum-rates and achieving accurate detection has not been investigated before. As an example, designing robust SIC technique under RF impairments for NOMA is an interesting open problem.

D. AMBIENT BACKSCATTER COMMUNICATIONS

In these systems, backscatter devices exploit surrounding ambient RF sources, e.g., cellular base stations, to communicate with each other – Fig. 29 [585]. To be specific, backscatter transmitters, such as battery-free tags or sensors, modulate and reflect surrounding ambient signals to the backscatter receivers by changing their antenna impedance states. These systems do not require a dedicated frequency spectrum (e.g., legacy spectrum can be used) and since they use already-available RF sources, backscatter nodes do not deploy and maintain dedicated RF sources. For these reasons, these nodes can operate with ultra-low powers and low cost. Thus, ambient backscatter communication is a potential candidate for future low-energy communication systems, e.g., IoT networks [586], [587].

However, ambient backscatter communication faces many challenges. For example, since the RF ambient signal is unknown in the backscatter receivers, signal detection is challenging. Thus, studies in [588]–[592] address some signal

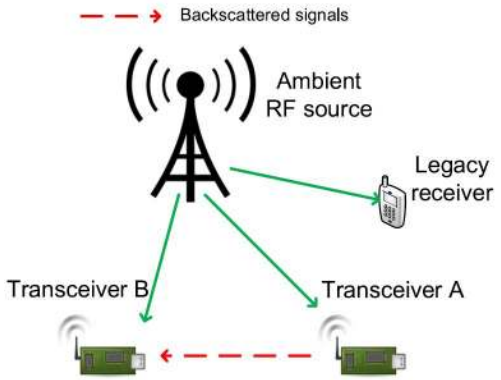

FIGURE 29: Ambient backscatter architecture [585].

detection schemes. In [588], a differential encoding scheme is proposed, which works based on signal power difference. Moreover, authors in [589], [591] investigate signal detection in ambient backscatter communication systems with multiple antennas tags – Fig. 30. The proposed detectors in [591] are based on the chi-squared test, F-test, and Bartlett's test. Finally, the work in [592] presents an energy detector for non-coherent backscatter communications over ambient OFDM signals.

On the other hand, channel estimation in the backscatter receivers is complicated since backscatter transmitters cannot send additional training or pilot signals. Authors in [593], [594] address channel estimation for ambient backscatter communication systems. In [593], a blind channel estimator based on the algorithm is presented, and also the modified Bayesian Cramér–Rao bound is derived. Moreover, the study in [594] proposes a pilot-aided algorithm based on the LS approach for joint estimating channel gains and direction of arrivals in an ambient backscatter communication system with a massive-antenna reader.

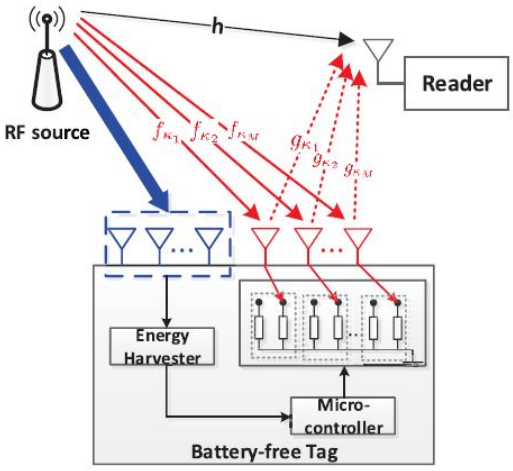

FIGURE 30: Ambient backscatter system with multiple antennas tags [591].

This article has been accepted for publication in a future issue of this journal, but has not been fully edited. Content may change prior to final publication. Citation information: DOI 10.1109/ACCESS.2021.3101845, IEEE Access

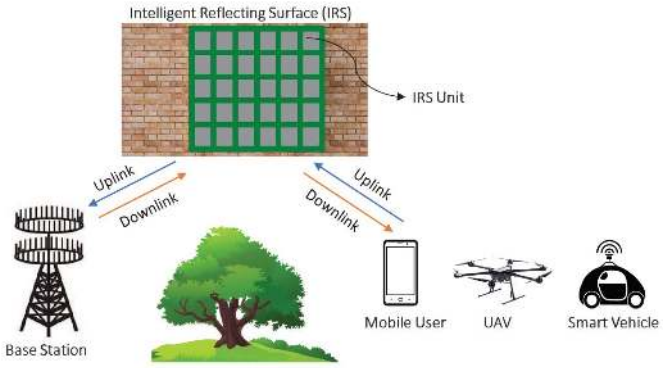

FIGURE 31: IRS-assisted Communications between base stations and mobile users, UAVs, and smart vehicles [598].

However, none of those above papers consider the impacts of RF impairments in the ambient RF source and backscatter receivers. The impairments introduce interference terms and will affect the detection performance and also degrade the channel estimation performance. Therefore, their influence on them should be studied, and estimation and compensation schemes for surprising their effects should be developed.

E. IRS-ASSISTED COMMUNICATIONS

An IRS, made of electromagnetic material, is a two-dimensional surface with numerous nearly passive elements with ultra-low power consummation [595], [596]. This surface can be dynamically reconfigured to electronically control the propagation of the incident electromagnetic waves [597]. As shown in Fig. 31, this surface can help the transmission between base stations and any terminals, e.g., mobile users, unmanned aerial vehicle (UAV)s, and smart vehicles, in order to enhance the channel gain, improve spatial multiplexing capability and energy efficiency [598], [599]. Since the cost, size, weight, and power consumption of this surface are small, it is a potential solution for realizing the emerging concept of intelligent radio environments [600].

However, since additional channels are involved in IRS-assisted communication systems, they face the challenge of a more overhead requirement for channel estimation. Moreover, optimizing the reflection pattern of IRS elements to achieve the best estimation and detection performance is another challenge. Hence, authors in [601] present a transmission protocol to perform channel estimation and reflection optimization for IRS-enhanced OFDM uplink systems. Moreover, in [602], a three-phase framework is proposed to estimate a large number of channel coefficients in the IRS-assisted uplink multiuser communications. Besides, authors in [603] develop an iterative channel estimation method based on alternating LS algorithm for IRS-assisted downlink multiuser communication systems. Furthermore, reference [604] addresses the joint optimal training sequence and reflection pattern to minimize the channel estimation MSE for the IRS-assisted communications. Finally, authors in [605] investigate the achievable uplink rate of IRS-aided millimeter-wave systems in the presence of PN at IRS.

However, these papers do not consider RF impairments in base stations and users. These impairments will destroy the functionality of proposed channel estimation algorithms and reflection patterns. Thus, we need to evaluate the impacts of the impairments on the performance of IRS-assisted communication systems, e.g., sum-rate and BER, and then propose estimation and compensation schemes to mitigate their effects.

F. AI-BASED APPROACHES

AI techniques have received high research attention for signal processing and communication networks [606]. For instance, deep learning and reinforcement learning are two powerful machine learning algorithms, which resemble the perception process in a brain with a deep neural network and trial and error, respectively [607]. The applications include designing signals, estimating channels, detecting data, and developing modulation/demodulation schemes. For example, studies in [608]–[612] develop deep learning-based schemes for channel estimation in OFDM and MIMO systems.

AI-based algorithms may also help estimating and compensating RF impairments. For instance, in [613], a PN compensation method based on neural network optimization for OFDM ranging systems is proposed. Besides, [614] proposes a neural network-based coarse CFO estimator for MIMO systems, and the work in [615] presents a learning method based on a support vector machine for efficient OFDM demodulation in the presence of CFO. Moreover, authors in [616] develop a convolutional neural network algorithm for estimating transmitter-induced and frequency-independent IQ imbalance in SC systems. Reference [617] develops a deep learning-based channel and CFO equalization algorithm for OFDM-based unmanned aerial vehicle communication systems. Finally, in [618], deep learning-based algorithms are proposed for PN compensation in multicarrier systems.

However, these contributions simply scratch the surface of vast possible applications. Such algorithms can thus developed for RF impairments estimation and compensation in many practical systems, e.g., full-duplex and millimeter-wave communications, cell-free massive MIMO systems, and IRS-assisted communications. Additionally, these algorithms can be deployed to improve data detection performance with residual RF impairments.

VI. CONCLUSION

This article presents a literature survey on RF impairments, including PN, CFO, and IQ imbalance in wireless communication transceivers. We discuss signal models for the impairments and their impacts. They cause in-band and out-of-band distortion terms that degrade the systems' performance, e.g., BER, EVM, SINR, and achievable rate. Next, we review the estimation and compensation techniques for suppressing their effects in SC systems, single-user OFDM, multiuser OFDMA, and MIMO systems. Moreover, we explore joint estimation and compensation of channel and the

impairments. These techniques can be pilot-aided or blind, and the former are based on periodically transmitted training symbols or combination of pilot and data symbols, and the latter use structural and statistical properties of signals without using prior knowledge at the receiver. We also review the impact RF impairments in future technologies such as MIMO (SC, MIMO OFDM, and multiuser MIMO OFDMA), massive MIMO, cognitive radio networks, millimeter-wave systems, relaying cooperative communication, beamforming techniques, and full-duplex communications. We review proposed estimation and compensation techniques for these technologies. Finally, we present open research problems and future research directions on RF impairments in state-of-the-art technologies such as cell-free massive MIMO communications, non-orthogonal multicarrier systems, NOMA, ambient backscatter communications, and IRS-assisted communications. Finally, we highlight AI-based approaches for mitigating the impacts of the RF impairments.

Finally, this survey article highlights the body of literature on PN, CFO and IQ imbalance developed over the last three decades. This body of knowledge is continuing to grow with many future research directions.

REFERENCES

[1] "Cisco visual networking index: Global mobile data traffic forecast update, 2017–2022," Cisco white paper, Feb. 2019. Accessed: May 11, 2020.

[2] "IMT vision—framework and overall objectives of the future development of IMT for 2020 and beyond," Int. Telecommun. Union, Geneva, Switzerland, Recommendation ITU-R M.2083, Sep. 2015.

[3] "Study on scenarios and requirements for next generation access technologies," 3GPP, Sophia Antipolis, France, Tech. Rep. 38.913, Jun. 2017.

[4] X. Dai, Z. Zhang, B. Bai, S. Chen, and S. Sun, "Pattern division multiple access: A new multiple access technology for 5G," IEEE Wireless Commun., vol. 25, no. 2, pp. 54–60, 2018.

[5] M. Shafi et al., "5G: A tutorial overview of standards, trials, challenges, deployment, and practice," IEEE J. Sel. Areas Commun., vol. 35, no. 6, pp. 1201–1221, 2017.

[6] "Cisco visual networking index: Global mobile data traffic forecast update, 2017–2022," Cisco white paper, Feb. 2019.

[7] M. A. Albreem, M. Juntti, and S. Shahabuddin, "Massive MIMO detection techniques: A survey," IEEE Commun. Surveys Tuts., vol. 21, no. 4, pp. 3109–3132, 2019.

[8] J. He, V. Tervo, X. Zhou, X. He, S. Qian, M. Cheng, M. Juntti, and T. Matsumoto, "A tutorial on lossy forwarding cooperative relaying," IEEE Commun. Surveys Tuts., vol. 21, no. 1, pp. 66–87, 2019.

[9] M. Amjad, M. H. Rehmani, and S. Mao, "Wireless multimedia cognitive radio networks: A comprehensive survey," IEEE Commun. Surveys Tuts., vol. 20, no. 2, pp. 1056–1103, 2018.

[10] D. Kim, H. Lee, and D. Hong, "A survey of in-band full-duplex transmission: From the perspective of PHY and MAC layers," IEEE Commun. Surveys Tuts., vol. 17, no. 4, pp. 2017–2046, 2015.

[11] A. N. Uwaechia and N. M. Mahyuddin, "A comprehensive survey on millimeter wave communications for fifth-generation wireless networks: Feasibility and challenges," IEEE Access, vol. 8, pp. 62367–62414, 2020.

[12] Khagendra Belbase, Zhang Zhang, Hai Jiang, and Chintha Tellambura, "Coverage analysis of millimeter wave decode-and-forward networks with best relay selection," IEEE Access, vol. 6, pp. 22670–22683, 2018.

[13] Sachitha Kusaladharma, Zhang Zhang, and Chintha Tellambura, "Interference and outage analysis of random d2d networks underlaying millimeter-wave cellular networks," IEEE Transactions on Communications, vol. 67, no. 1, pp. 778–790, 2019.

[14] M.A. Abu-Rgheff, 5G Physical Layer Technologies, John Wiley & Sons, 2019.

[15] L. Chettri and R. Bera, "A comprehensive survey on internet of things (IoT) toward 5G wireless systems," IEEE Internet Things J., vol. 7, no. 1, pp. 16–32, 2020.

[16] "LTE;evolved universal terrestrial radio access (E-UTRA);base station (BS) radio transmission and reception (3GPP TS 36.104 version 14.3.0 release 14)," Apr. 2017.

[17] "3rd generation partnership project; technical specification group radio access network; base station (BS) radio transmission and reception (FDD) (release 16)," Dec. 2018.

[18] "5G; NR; base station (BS) radio transmission and reception (3GPP TS 38.104 version 15.8.0 release 15)," Jan. 2020.

[19] B. Razavi, RF Microelectronics Second Edition, Upper Saddle River, New Jersey, US, Prentice Hall New Jersey, 2012.

[20] T-D. Chiueh and P-Y. Tsai, OFDM baseband receiver design for wireless communications, John Wiley & Sons, 2008.

[21] C. Y. Soo and et al., MIMO-OFDM wireless communications with MATLAB, Wiley, 2010.

[22] L. Weng, E. K. S. Au, P. W. C. Chan, R. D. Murch, R. S. Cheng, W. H. Mow, and V. K. N. Lau, "Effect of carrier frequency offset on channel estimation for SISO/MIMO-OFDM systems," IEEE Trans. Wirele. Commun., vol. 6, no. 5, pp. 1854–1863, 2007.

[23] A. Tarighat, R. Bagheri, and A. H. Sayed, "Compensation schemes and performance analysis of IQ imbalances in OFDM receivers," IEEE Trans. Signal Process., vol. 53, no. 8, pp. 3257–3268, 2005.

[24] D. Korpi, L. Anttila, V. Syrjälä, and M. Valkama, "Widely linear digital self-interference cancellation in direct-conversion full-duplex transceiver," IEEE J. Sel. Areas Commun., vol. 32, no. 9, pp. 1674–1687, 2014.

[25] M. J. M. Pelgrom, A. C. J. Duinmaijer, and A. P. G. Welbers, "Matching properties of MOS transistors," IEEE J. Solid-State Circuits, vol. 24, no. 5, pp. 1433–1439, 1989.

[26] Z. Pengfei et al., "A direct conversion CMOS transceiver for IEEE 802.11a WLANs," in IEEE Int. Solid-State Circuits Conf. Dig. Technical Papers, 2003.

[27] L. Der and B. Razavi, "A 2-GHz CMOS image-reject receiver with LMS calibration," IEEE J. Solid-State Circuits, vol. 38, no. 2, pp. 167–175, 2003.

[28] E. Pankratz and E. Sánchez-Sinencio, "Survey of integrated-circuit-oscillator phase-noise analysis," International Journal of Circuit Theory and Applications, vol. 42, no. 9, pp. 871–938, 2014.

[29] M. D. Mir and A. S. Buttar, "Phase noise mitigation techniques in OFDM system: A survey," in IEEE International Conference on Electrical, Computer and Communication Technologies (ICECCT), 2015, pp. 1–4.

[30] M. Mehra and G. K. Cheema, "Various techniques for frequency offset estimation in OFDM system: A survey," International Journal of Emerging Technologies in Engineering Research (IJETER), vol. 1, no. 2b, 2015.

[31] A.A. Nasir et al., "Timing and carrier synchronization in wireless communication systems: a survey and classification of research in the last 5 years," J. Wireless Com. Network, 2016.

[32] B. Selim, P. C. Sofotasios, S. Muhaidat, and G. K. Karagiannidis, "The effects of I/Q imbalance on wireless communications: A survey," in IEEE International Midwest Symposium on Circuits and Systems (MWSCAS), 2016, pp. 1–4.

[33] G. Fettweis, M. Lohning, D. Petrovic, M. Windisch, P. Zillmann, and W. Rave, "Dirty RF: a new paradigm," in IEEE International Symposium on Personal, Indoor and Mobile Radio Communications (PIMRC), 2005, vol. 4, pp. 2347–2355 Vol. 4.

[34] P. Singh et al., "Semi-blind, training, and data-aided channel estimation schemes for MIMO-FBMC-OQAM systems," IEEE Trans. Signal Process., vol. 67, no. 18, pp. 4668–4682, 2019.

[35] P. Singh et al., "Uplink sum-rate and power scaling laws for multi-user massive MIMO-FBMC systems," IEEE Trans. Commun., vol. 68, no. 1, pp. 161–176, 2020.

[36] S. Srivastava et al., "Bayesian learning-based doubly-selective sparse channel estimation for millimeter wave hybrid MIMO-FBMC-OQAM systems," IEEE Trans. Commun., vol. 69, no. 1, pp. 529–543, 2021.

[37] D. Ham and A. Hajimiri, "Virtual damping and einstein relation in oscillators," IEEE J. Solid-State Circuits, vol. 38, no. 3, pp. 407–418, March 2003.

[38] T. Schenk, "RF impairments in multiple antenna OFDM: influence and mitigation," 2006.

[39] M. Brownlee, P. K. Hanumolu, K. Mayaram, and U. Moon, "A 0.5-GHz to 2.5-GHz PLL with fully differential supply regulated tuning," IEEE J. Solid-State Circuits, vol. 41, no. 12, pp. 2720–2728, Dec 2006.

[40] Alper Demir, "Floquet theory and nonlinear perturbation analysis for oscillators with differential-algebraic equations," International Journal of Circuit Theory and Applications, vol. 28, 03 2000.

[41] A. Demir, A. Mehrotra, and J. Roychowdhury, "Phase noise in oscillators: a unifying theory and numerical methods for characterization," IEEE Trans. Circuits Syst. I, vol. 47, no. 5, pp. 655–674, May 2000.

[42] A. Demir, "Phase noise and timing jitter in oscillators with colored-noise sources," IEEE Trans. Circuits Sys. I. Fundam. Theory Appl., vol. 49, no. 12, pp. 1782–1791, Dec 2002.

[43] A. Demir, "Computing timing jitter from phase noise spectra for oscillators and phase-locked loops with white and$1/f$noise," IEEE Trans. Circuits Sys. I. Reg. Papers, vol. 53, no. 9, pp. 1869–1884, Sep. 2006.

[44] D. Petrovic, W. Rave, and G. Fettweis, "Effects of phase noise on OFDM systems with and without PLL: Characterization and compensation," IEEE Trans. Commun., vol. 55, no. 8, pp. 1607–1616, Aug 2007.

[45] A. Mehrotra, "Noise analysis of phase-locked loops," IEEE Trans. Circuits Sys. I. Fundam. Theory Appl., vol. 49, no. 9, pp. 1309–1316, Sep. 2002.

[46] Jimmin Chang, A. A. Abidi, and C. R. Viswanathan, "Flicker noise in CMOS transistors from subthreshold to strong inversion at various temperatures," IEEE Trans. Electron Devices, vol. 41, no. 11, pp. 1965–1971, Nov 1994.

[47] C. Sanchez-Lopez and E. Tlelo-Cuautle, "Symbolic noise analysis in analog integrated circuits," in IEEE International Symposium on Circuits and Systems (ISCAS), May 2004, vol. 5, pp. V–V.

[48] E. A. M. Klumperink, S. L. J. Gierkink, A. P. van der Wel, and B. Nauta, "Reducing MOSFET 1/f noise and power consumption by switched biasing," IEEE J. Solid-State Circuits, vol. 35, no. 7, pp. 994–1001, July 2000.

[49] N. N. Tchamov et al., "System-and circuit-level optimization of PLL designs for DVB-T/H receivers," Analog Integrated Circuits and Signal Processing, vol. 73, no. 1, pp. 185–200, 2012.

[50] V. Syrjälä, Analysis and Mitigation of Oscillator Impairments in Modern Receiver Architectures, Ph.D. thesis, Tampere University of Technology, 2012.

[51] M. R. Khanzadi, D. Kuylenstierna, A. Panahi, T. Eriksson, and H. Zirath, "Calculation of the performance of communication systems from measured oscillator phase noise," IEEE Trans. Circuits Syst. I, Reg. Papers, vol. 61, no. 5, pp. 1553–1565, 2014.

[52] A. Chorti and M. Brookes, "A spectral model for RF oscillators with power-law phase noise," IEEE Trans. Circuits Syst. I, Reg. Papers, vol. 53, no. 9, pp. 1989–1999, 2006.

[53] J. A. McNeill, "Jitter in ring oscillators," IEEE J. Solid-State Circuits, vol. 32, no. 6, pp. 870–879, 1997.

[54] C.Y. Yoon and W. Lindsey, "Phase-locked loop performance in the presence of CW interference and additive noise," IEEE Trans. Commun, vol. 30, no. 10, pp. 2305–2311, October 1982.

[55] B. C. Sarkar, "Phase error dynamics of a first-order phase locked loop in the presence of cochannel tone interference and additive noise," IEEE Trans. Commun, vol. 38, no. 7, pp. 962–965, July 1990.

[56] A. Blanchard, Phase-locked loops: application to coherent receiver design, New York, Wiley, 1976.

[57] J. R. Alexovich and R. M. Gagliardi, "The effect of phase noise on noncoherent digital communications," IEEE Trans. Commun., vol. 38, no. 9, pp. 1539–1548, Sep. 1990.

[58] H. Jafari, H. Miar-Naimi, and J. Kazemitabar, "Bit error probability of MQAM in the presence of phase noise," IEEE Trans. Veh. Technol., vol. 69, no. 12, pp. 14918–14931, 2020.

[59] L. Tomba and W. A. Krzymien, "Effect of carrier phase noise and frequency offset on the performance of multicarrier CDMA systems," in International Conference on Communications (ICC), June 1996, vol. 3, pp. 1513–1517 vol.3.

[60] L. Tomba and W. A. Krzymien, "Sensitivity of the MC-CDMA access scheme to carrier phase noise and frequency offset," IEEE Trans. Veh. Technol., vol. 48, no. 5, pp. 1657–1665, Sep. 1999.

[61] H. Steendam and M. Moeneclaey, "The effect of carrier phase jitter on MC-CDMA performance," IEEE Trans. Commun., vol. 47, no. 2, pp. 195–198, Feb 1999.

[62] D. W. Matolak, V. Deepak, and F. A. Alder, "Performance of multitone and multicarrier DS-SS in the presence of imperfect phase synchronization," in Military Communications Conference (MILCOM), Oct 2002, vol. 2, pp. 1002–1006 vol.2.

[63] H. Li and D. W. Matolak, "Phase noise and fading effects on system performance in MT-DS-SS," IEEE Trans. Veh. Technol., vol. 54, no. 5, pp. 1759–1767, Sep. 2005.

[64] T. Pollet, M. Van Bladel, and M. Moeneclaey, "BER sensitivity of OFDM systems to carrier frequency offset and wiener phase noise," IEEE Trans. Commun., vol. 43, no. 2/3/4, pp. 191–193, Feb 1995.

[65] L. Tomba, "On the effect of Wiener phase noise in OFDM systems," IEEE Trans. Commun., vol. 46, no. 5, pp. 580–583, May 1998.

[66] A. G. Armada and M. Calvo, "Phase noise and sub-carrier spacing effects on the performance of an OFDM communication system," IEEE Commun. Lett., vol. 2, no. 1, pp. 11–13, Jan 1998.

[67] E. Costa and S. Pupolin, "M-QAM-OFDM system performance in the presence of a nonlinear amplifier and phase noise," IEEE Trans. Commun., vol. 50, no. 3, pp. 462–472, March 2002.

[68] S. Bittner, M. Krondorf, and G. Fettweis, "Numerical performance evaluation of OFDM systems affected by transmitter nonlinearities, phase noise and channel estimation errors," in IEEE Global Telecommunications Conference (GLOBECOM), Nov 2008, pp. 1–6.

[69] P. Mathecken, T. Riihonen, S. Werner, and R. Wichman, "Performance analysis of OFDM with wiener phase noise and frequency selective fading channel," IEEE Trans. Commun., vol. 59, no. 5, pp. 1321–1331, May 2011.

[70] P. Mathecken, T. Riihonen, N. N. Tchamov, S. Werner, M. Valkama, and R. Wichman, "Characterization of OFDM radio link under PLL-based oscillator phase noise and multipath fading channel," IEEE Trans. Commun., vol. 60, no. 6, pp. 1479–1485, June 2012.

[71] A. Gokceoglu, Y. Zou, M. Valkama, P. C. Sofotasios, P. Mathecken, and D. Cabric, "Mutual information analysis of OFDM radio link under phase noise, IQ imbalance and frequency-selective fading channel," IEEE Trans. Wireless Commun., vol. 12, no. 6, pp. 3048–3059, June 2013.

[72] V. Nguyen-Duy-Nhat, H. Nguyen-Le, C. Tang-Tan, and T. Le-Ngoc, "Sir analysis for OFDM transmission in the presence of CFO, phase noise and doubly selective fading," IEEE Commun. Lett., vol. 17, no. 9, pp. 1810–1813, Sep. 2013.

[73] I. Ngebani, Y. Li, X. Xia, S. A. Haider, A. Huang, and M. Zhao, "Analysis and compensation of phase noise in vector OFDM systems," IEEE Trans. Signal Process., vol. 62, no. 23, pp. 6143–6157, Dec 2014.

[74] A. Spalvieri and L. Barletta, "Pilot-aided carrier recovery in the presence of phase noise," IEEE Trans. Commun., vol. 59, no. 7, pp. 1966–1974, 2011.

[75] N. Kamiya and E. Sasaki, "Pilot-symbol assisted and code-aided phase error estimation for high-order QAM transmission," IEEE Trans. Commun., vol. 61, no. 10, pp. 4369–4380, 2013.

[76] M. R. Khanzadi, R. Krishnan, and T. Eriksson, "Estimation of phase noise in oscillators with colored noise sources," IEEE Commun. Lett., vol. 17, no. 11, pp. 2160–2163, 2013.

[77] A. Gomaa and N. Al-Dhahir, "Phase noise in asynchronous SC-FDMA systems: Performance analysis and data-aided compensation," IEEE Trans. Veh. Technol., vol. 63, no. 6, pp. 2642–2652, 2014.

[78] P. Robertson and S. Kaiser, "Analysis of the effects of phase-noise in orthogonal frequency division multiplex (OFDM) systems," in IEEE International Conference on Communications (ICC), June 1995, vol. 3, pp. 1652–1657 vol.3.

[79] S. Wu and Y. Bar-Ness, "A phase noise suppression algorithm for OFDM-based WLANs," IEEE Commun. Lett., vol. 6, no. 12, pp. 535–537, Dec 2002.

[80] M. R. Gholami, S. Nader-Esfahani, and A. A. Eftekhar, "A new method of phase noise compensation in OFDM," in IEEE International Conference on Communications (ICC), May 2003, vol. 5, pp. 3443–3446 vol.5.

[81] R. A. Casas, S. L. Biracree, and A. E. Youtz, "Time domain phase noise correction for OFDM signals," IEEE Trans. Broadcast., vol. 48, no. 3, pp. 230–236, Sep. 2002.

[82] G. Liu and W. Zhu, "Compensation of phase noise in OFDM systems using an ICI reduction scheme," IEEE Trans. Broadcast., vol. 50, no. 4, pp. 399–407, Dec 2004.

[83] A. Leshem and M. Yemini, "Phase noise compensation for OFDM systems," IEEE Trans. Signal Process., vol. 65, no. 21, pp. 5675–5686, Nov 2017.

[84] S. Wu, P. Liu, and Y. Bar-Ness, "Phase noise estimation and mitigation for OFDM systems," IEEE Trans. Wireless Commun., vol. 5, no. 12, pp. 3616–3625, December 2006.

[85] D. Petrovic, W. Rave, and G. Fettweis, "Phase noise suppression in OFDM including intercarrier interference," in Proc. Intl. OFDM Workshop (InOWo). Citeseer, 2003, vol. 3, pp. 219–224.

[86] D. Petrovic, W. Rave, and G. Fettweis, "Intercarrier interference due to phase noise in OFDM - estimation and suppression," in IEEE Vehicular Technology Conference (VTC), Sep. 2004, vol. 3, pp. 2191–2195.

[87] G. Fettweis et al., "Dirty RF: A new paradigm," International Journal of Wireless Information Networks, vol. 14, no. 2, pp. 133–148, 2007.

[88] V. Syrjala, M. Valkama, N. N. Tchamov, and J. Rinne, "Phase noise modelling and mitigation techniques in OFDM communications systems," in Wireless Telecommunications Symposium, April 2009, pp. 1–7.

[89] N. N. Tchamov, J. Rinne, A. Hazmi, M. Valkama, V. Syrjala, and M. Renfors, "Enhanced algorithm for digital mitigation of ICI due to phase noise in OFDM receivers," IEEE Wireless Commun. Lett., vol. 2, no. 1, pp. 6–9, February 2013.

[90] M. Lee, K. Yang, and K. Cheun, "Iterative receivers based on subblock processing for phase noise compensation in OFDM systems," IEEE Trans. Commun., vol. 59, no. 3, pp. 792–802, March 2011.

[91] S. Negusse, P. Zetterberg, and P. Händel, "Phase-noise mitigation in OFDM by best match trajectories," IEEE Trans. Commun., vol. 63, no. 5, pp. 1712–1725, May 2015.

[92] P. Mathecken, T. Riihonen, S. Werner, and R. Wichman, "Phase noise estimation in OFDM: Utilizing its associated spectral geometry," IEEE Trans. Signal Process., vol. 64, no. 8, pp. 1999–2012, April 2016.

[93] P. Mathecken, T. Riihonen, S. Werner, and R. Wichman, "Constrained phase noise estimation in OFDM using scattered pilots without decision feedback," IEEE Trans. Signal Process., vol. 65, no. 9, pp. 2348–2362, May 2017.

[94] K. Nikitopoulos and A. Polydoros, "Phase-impairment effects and compensation algorithms for OFDM systems," IEEE Trans. Commun., vol. 53, no. 4, pp. 698–707, April 2005.

[95] D. D. Lin and T. J. Lim, "The variational inference approach to joint data detection and phase noise estimation in OFDM," IEEE Trans. Signal Process., vol. 55, no. 5, pp. 1862–1874, May 2007.

[96] Y. Gong and X. Hong, "OFDM joint data detection and phase noise cancellation for constant modulus modulations," IEEE Trans. Signal Process., vol. 57, no. 7, pp. 2864–2868, July 2009.

[97] M. Lee, S. Lim, and K. Yang, "Blind compensation for phase noise in OFDM systems over constant modulus modulation," IEEE Trans. Commun., vol. 60, no. 3, pp. 620–625, March 2012.

[98] S. Wu and Y. Bar-Ness, "OFDM channel estimation in the presence of frequency offset and phase noise," in IEEE International Conference on Communications (ICC), May 2003, vol. 5, pp. 3366–3370 vol.5.

[99] Y-H Kim and S-C Kim, "Joint channel estimation with phase noise suppression and soft decision decoding scheme for OFDM-based WLANs," in IEEE Vehicular Technology Conference (VTC), Sep. 2005, vol. 1, pp. 161–165.

[100] J-H. Lee, J-S. Yang, S-C. Kim, and Y-W. Park, "Joint channel estimation and phase noise suppression for OFDM systems," in IEEE Vehicular Technology Conference (VTC), May 2005, vol. 1, pp. 467–470 Vol. 1.

[101] D. D. Lin, R. A. Pacheco, T. J. Lim, and D. Hatzinakos, "Joint estimation of channel response, frequency offset, and phase noise in OFDM," IEEE Trans. Signal Process., vol. 54, no. 9, pp. 3542–3554, Sep. 2006.

[102] J. Tao, J. Wu, and C. Xiao, "Estimation of channel transfer function and carrier frequency offset for OFDM systems with phase noise," IEEE Trans. Veh. Technol., vol. 58, no. 8, pp. 4380–4387, Oct 2009.

[103] F. Munier, T. Eriksson, and A. Svensson, "An ICI reduction scheme for OFDM system with phase noise over fading channels," IEEE Trans. Commun., vol. 56, no. 7, pp. 1119–1126, July 2008.

[104] F. Septier, Y. Delignon, A. Menhaj-Rivenq, and C. Garnier, "Monte Carlo methods for channel, phase noise, and frequency offset estimation with unknown noise variances in OFDM systems," IEEE Trans. Signal Process., vol. 56, no. 8, pp. 3613–3626, Aug 2008.

[105] R. Carvajal, J. C. Aguero, B. I. Godoy, and G. C. Goodwin, "EM-based maximum-likelihood channel estimation in multicarrier systems with phase distortion," IEEE Trans. Veh. Technol., vol. 62, no. 1, pp. 152–160, Jan 2013.

[106] Q. Zou, A. Tarighat, and A. H. Sayed, "Compensation of phase noise in OFDM wireless systems," IEEE Trans. Signal Process., vol. 55, no. 11, pp. 5407–5424, Nov 2007.

[107] R. Corvaja and A. G. Armada, "Joint channel and phase noise compensation for OFDM in fast-fading multipath applications," IEEE Trans. Veh. Technol., vol. 58, no. 2, pp. 636–643, Feb 2009.

[108] P. Rabiei, W. Namgoong, and N. Al-Dhahir, "A non-iterative technique for phase noise ICI mitigation in packet-based OFDM systems," IEEE Trans. Signal Process., vol. 58, no. 11, pp. 5945–5950, Nov 2010.

[109] O. H. Salim, A. A. Nasir, H. Mehrpouyan, W. Xiang, S. Durrani, and R. A. Kennedy, "Channel, phase noise, and frequency offset in OFDM systems: Joint estimation, data detection, and hybrid cramér-rao lower bound," IEEE Trans. Commun., vol. 62, no. 9, pp. 3311–3325, Sep. 2014.

[110] Y. Liao and K. Chen, "Multiuser common phase error estimation for uplink OFDMA communications," in IEEE Wireless Communications and Networking Conference (WCNC), 2007, pp. 1976–1981.

[111] L. Samara et al., "Phase noise mitigation in OFDMA uplink," in International Symposium on Communications, Control and Signal Processing (ISCCSP), 2014, pp. 344–347.

[112] M. R. Khanzadi, G. Durisi, and T. Eriksson, "Capacity of SIMO and MISO phase-noise channels with common/separate oscillators," IEEE Trans. Commun., vol. 63, no. 9, pp. 3218–3231, Sep. 2015.

[113] A. Pitarokoilis, E. Björnson, and E. G. Larsson, "ML detection in phase noise impaired SIMO channels with uplink training," IEEE Trans. Commun., vol. 64, no. 1, pp. 223–235, Jan 2016.

[114] G. Durisi, A. Tarable, C. Camarda, R. Devassy, and G. Montorsi, "Capacity bounds for MIMO microwave backhaul links affected by phase noise," IEEE Trans. Commun., vol. 62, no. 3, pp. 920–929, March 2014.

[115] A. Taparugssanagorn and J. Ylitalo, "Characteristics of short-term phase noise of MIMO channel sounding and its effect on capacity estimation," IEEE Trans. Instrum. Meas., vol. 58, no. 1, pp. 196–201, Jan 2009.

[116] X. Zhang and H. . Ryu, "Joint estimation and suppression of phase noise and carrier frequency offset in multiple-input multiple-output single carrier frequency division multiple access with single-carrier space frequency block coding," IET Communications, vol. 4, no. 16, pp. 1998–2007, November 2010.

[117] H. Mehrpouyan, A. A. Nasir, S. D. Blostein, T. Eriksson, G. K. Karagiannidis, and T. Svensson, "Joint estimation of channel and oscillator phase noise in MIMO systems," IEEE Trans. Signal Process., vol. 60, no. 9, pp. 4790–4807, Sep. 2012.

[118] A. A. Nasir, H. Mehrpouyan, R. Schober, and Y. Hua, "Phase noise in MIMO systems: Bayesian cramér–rao bounds and soft-input estimation," IEEE Trans. Signal Process., vol. 61, no. 10, pp. 2675–2692, May 2013.

[119] R. Krishnan, G. Colavolpe, A. Graell i Amat, and T. Eriksson, "Algorithms for joint phase estimation and decoding for MIMO systems in the presence of phase noise and quasi-static fading channels," IEEE Trans. Signal Process., vol. 63, no. 13, pp. 3360–3375, July 2015.

[120] T.C.W. Schenk and P. Mattheijssen, "Analysis of the influence of phase noise in MIMO OFDM based wlan systems," in Proc. Symp. IEEE Benelux Chapt. on Comm. and Veh. Techn.(SCVT2003), 2003, pp. 1–8.

[121] T. C. W. Schenk, Xiao-Jiao Tao, P. F. M. Smulders, and E. R. Fledderus, "Influence and suppression of phase noise in multi-antenna OFDM," in IEEE Vehicular Technology Conference (VTC), Sep. 2004, vol. 2, pp. 1443–1447 Vol. 2.

[122] T. C. W. Schenk, X. . Tao, P. F. M. Smulders, and E. R. Fledderus, "On the influence of phase noise induced ICI in MIMO OFDM systems," IEEE Commun. Lett., vol. 9, no. 8, pp. 682–684, Aug 2005.

[123] K. Nikitopoulos and A. Polydoros, "Decision-directed compensation of phase noise and residual frequency offset in a space-time OFDM receiver," IEEE Commun. Lett., vol. 8, no. 9, pp. 573–575, Sep. 2004.

[124] Y. Zhang and H. Liu, "MIMO-OFDM systems in the presence of phase noise and doubly selective fading," IEEE Trans. Veh. Technol., vol. 56, no. 4, pp. 2277–2285, July 2007.

[125] R. Corvaja and A. G. Armada, "SINR degradation in MIMO-OFDM systems with channel estimation errors and partial phase noise compensation," IEEE Trans. Commun., vol. 58, no. 8, pp. 2199–2203, August 2010.

[126] T. Lee and Y. Ko, "Channel estimation and data detection in the presence of phase noise in MIMO-OFDM systems with independent oscillators," IEEE Access, vol. 5, pp. 9647–9662, 2017.

[127] M. Ataeeshojai et al., "Energy-efficient resource allocation in single-RF load-modulated massive MIMO HetNets," IEEE Open J. Commun. Soc., vol. 1, pp. 1738–1764, 2020.

[128] A. Pitarokoilis, S. K. Mohammed, and E. G. Larsson, "Uplink performance of time-reversal MRC in massive MIMO systems subject to phase noise," IEEE Trans. Wireless Commun., vol. 14, no. 2, pp. 711–723, Feb 2015.

[129] R. Krishnan, M. R. Khanzadi, N. Krishnan, Y. Wu, A. Graell i Amat, T. Eriksson, and R. Schober, "Linear massive MIMO precoders in the

presence of phase noise—a large-scale analysis," IEEE Trans. Veh. Technol., vol. 65, no. 5, pp. 3057–3071, May 2016.

[130] Y. Wang and J. Lee, "A simple phase noise suppression scheme for massive MIMO uplink systems," IEEE Trans. Veh. Technol., vol. 66, no. 6, pp. 4769–4780, June 2017.

[131] Y. Wang and J. Lee, "A ZF-based precoding scheme with phase noise suppression for massive MIMO downlink systems," IEEE Trans. Veh. Technol., vol. 67, no. 2, pp. 1158–1173, Feb 2018.

[132] X. Yang, S. Jin, and C. Wen, "Symbol detection of phase noise-impaired massive MIMO using approximate bayesian inference," IEEE Signal Process. Lett., vol. 26, no. 4, pp. 607–611, April 2019.

[133] X. Zheng, A. Liu, and V. Lau, "Joint channel and location estimation of massive MIMO system with phase noise," IEEE Trans. Signal Process., vol. 68, pp. 2598–2612, 2020.

[134] R. Corvaja and A. G. Armada, "Phase noise degradation in massive MIMO downlink with zero-forcing and maximum ratio transmission precoding," IEEE Trans. Veh. Technol., vol. 65, no. 10, pp. 8052–8059, Oct 2016.

[135] A. Pitarokoilis, E. Björnson, and E. G. Larsson, "Performance of the massive MIMO uplink with OFDM and phase noise," IEEE Commun. Lett., vol. 20, no. 8, pp. 1595–1598, Aug 2016.

[136] X. Cheng, K. Xu, and S. Li, "Compensation of phase noise in uplink massive MIMO OFDM systems," IEEE Trans. Wireless Commun., vol. 18, no. 3, pp. 1764–1778, March 2019.

[137] R. Zhang, B. Shim, and H. Zhao, "Downlink compressive channel estimation with phase noise in massive MIMO systems," IEEE Trans. Commun., vol. 68, no. 9, pp. 5534–5548, 2020.

[138] P. Rabiei, W. Namgoong, and N. Al-Dhahir, "On the performance of OFDM-based amplify-and-forward relay networks in the presence of phase noise," IEEE Trans. Commun., vol. 59, no. 5, pp. 1458–1466, May 2011.

[139] O. H. Salim, A. A. Nasir, W. Xiang, and R. A. Kennedy, "Joint channel, phase noise, and carrier frequency offset estimation in cooperative OFDM systems," in IEEE International Conference on Communications (ICC), June 2014, pp. 4384–4389.

[140] R. Wang, H. Mehrpouyan, M. Tao, and Y. Hua, "Channel estimation, carrier recovery, and data detection in the presence of phase noise in OFDM relay systems," IEEE Trans. Wireless Commun., vol. 15, no. 2, pp. 1186–1205, Feb 2016.

[141] O. H. Salim, A. A. Nasir, H. Mehrpouyan, and W. Xiang, "Multi-relay communications in the presence of phase noise and carrier frequency offsets," IEEE Trans. Commun., vol. 65, no. 1, pp. 79–94, Jan 2017.

[142] S Atapattu, C Tellambura, and H Jiang, Energy detection for spectrum sensing in cognitive radio, Springer New York, NY, USA, 2014.

[143] Saman Atapattu, Chintha Tellambura, and Hai Jiang, "Energy detection of primary signals over $\eta - \mu$ fading channels," in 2009 International Conference on Industrial and Information Systems (ICIIS), 2009, pp. 118–122.

[144] S. P. Herath, N. Rajatheva, and C. Tellambura, "Unified approach for energy detection of unknown deterministic signal in cognitive radio over fading channels," in 2009 IEEE International Conference on Communications Workshops, 2009, pp. 1–5.

[145] Sachitha Kusaladharma and Chintha Tellambura, "Aggregate interference analysis for underlay cognitive radio networks," IEEE Wireless Communications Letters, vol. 1, no. 6, pp. 641–644, 2012.

[146] Y. F. Sharkasi, D. McLernon, and M. Ghogho, "Robust spectrum sensing in the presence of carrier frequency offset and phase noise for cognitive radio," in Wireless Telecommunications Symposium, 2012, pp. 1–5.

[147] S. Park, L. E. Larson, and L. B. Milstein, "Spectrum broadening due to phase noise interaction in cognitive radio systems," IEEE Commun. Lett., vol. 14, no. 10, pp. 891–893, 2010.

[148] C. Ma, C. Wu, and C. Huang, "A simple ICI suppression method utilizing cyclic prefix for OFDM systems in the presence of phase noise," IEEE Trans. Commun., vol. 61, no. 11, pp. 4539–4550, November 2013.

[149] E. Perahia et al., "TGad evaluation methodology," doc.: IEEE 802.11-09/0296r16, Jan. 2010. Available: http://www.ieee802.org/11/Reports/tgad update.htm.

[150] S. Suyama, H. Suzuki, K. Fukawa, and J. Izumi, "Iterative receiver employing phase noise compensation and channel estimation for millimeter-wave OFDM systems," IEEE J. Sel. Areas in Commun., vol. 27, no. 8, pp. 1358–1366, October 2009.

[151] J. Oh and T. K. Kim, "Phase noise effect on millimeter-wave pre-5G systems," IEEE Access, vol. 8, pp. 187902–187913, 2020.

[152] X. Cheng, N. Lou, and B. Yuan, "Iterative decision-aided compensation of phase noise in millimeter-wave SC-FDE systems," IEEE Commun. Lett., vol. 20, no. 5, pp. 1030–1033, May 2016.

[153] Tiep M. Hoang, Trung Q. Duong, Himal A. Suraweera, Chintha Tellambura, and H. Vincent Poor, "Cooperative beamforming and user selection for improving the security of relay-aided systems," IEEE Transactions on Communications, vol. 63, no. 12, pp. 5039–5051, 2015.

[154] R. Hamila, Ö. Özdemir, and N. Al-Dhahir, "Beamforming OFDM performance under joint phase noise and I/Q imbalance," IEEE Trans. Veh. Technol., vol. 65, no. 5, pp. 2978–2989, May 2016.

[155] M. Mohammadi, H. A. Suraweera, Y. Cao, I. Krikidis, and C. Tellambura, "Full-duplex radio for uplink/downlink wireless access with spatially random nodes," IEEE Trans. Commun., vol. 63, no. 12, pp. 5250–5266, 2015.

[156] M. Mohammadi, H. A. Suraweera, and C. Tellambura, "Uplink/downlink rate analysis and impact of power allocation for full-duplex cloud-RANs," IEEE Trans. Wireless Commun., vol. 17, no. 9, pp. 5774–5788, 2018.

[157] Zahra Mobini, Mohammadali Mohammadi, and Chintha Tellambura, "Wireless-powered full-duplex relay and friendly jamming for secure cooperative communications," IEEE Transactions on Information Forensics and Security, vol. 14, no. 3, pp. 621–634, 2019.

[158] A. Sahai, G. Patel, C. Dick, and A. Sabharwal, "On the impact of phase noise on active cancelation in wireless full-duplex," IEEE Trans. Veh. Technol., vol. 62, no. 9, pp. 4494–4510, Nov 2013.

[159] V. Syrjala, M. Valkama, L. Anttila, T. Riihonen, and D. Korpi, "Analysis of oscillator phase-noise effects on self-interference cancellation in full-duplex OFDM radio transceivers," IEEE Trans. Wireless Commun., vol. 13, no. 6, pp. 2977–2990, June 2014.

[160] V. Syrjälä, K. Yamamoto, and M. Valkama, "Analysis and design specifications for full-duplex radio transceivers under RF oscillator phase noise with arbitrary spectral shape," IEEE Trans. Veh. Technol., vol. 65, no. 8, pp. 6782–6788, Aug 2016.

[161] X. Quan, Y. Liu, S. Shao, C. Huang, and Y. Tang, "Impacts of phase noise on digital self-interference cancellation in full-duplex communications," IEEE Trans. Signal Process., vol. 65, no. 7, pp. 1881–1893, April 2017.

[162] X. Quan, Y. Liu, P. Fan, and Y. Tang, "Full-duplex transceiver design in the presence of phase noise and performance analysis," IEEE Trans. Veh. Technol., vol. 70, no. 1, pp. 558–571, 2021.

[163] L. Samara, M. Mokhtar, Ö. Özdemir, R. Hamila, and T. Khattab, "Residual self-interference analysis for full-duplex OFDM transceivers under phase noise and I/Q imbalance," IEEE Commun. Lett., vol. 21, no. 2, pp. 314–317, Feb 2017.

[164] E. Ahmed and A. M. Eltawil, "On phase noise suppression in full-duplex systems," IEEE Trans. Wireless Commun., vol. 14, no. 3, pp. 1237–1251, March 2015.

[165] R. Li, A. Masmoudi, and T. Le-Ngoc, "Self-interference cancellation with nonlinearity and phase-noise suppression in full-duplex systems," IEEE Trans. Veh. Technol., vol. 67, no. 3, pp. 2118–2129, March 2018.

[166] M. He and C. Huang, "Self-interference cancellation for full-duplex massive MIMO OFDM with single RF chain," IEEE Wireless Commun. Lett., vol. 9, no. 1, pp. 26–29, 2020.

[167] P. Zhou, C. Zhao, Y. Yang, and X. He, "Error probability of MPSK OFDM impaired by carrier frequency offset in AWGN channels," IEEE Commun. Lett., vol. 10, no. 12, pp. 801–803, 2006.

[168] E. S. Sousa, "The effect of clock and carrier frequency offsets on the performance of a direct-sequence spread-spectrum multiple-access system," " IEEE J. Select. Areas Commun., vol. 8, no. 4, pp. 580–587, 1990.

[169] Kun-Wah Yip and Tung-Sang Ng, "Effects of carrier frequency accuracy on quasi-synchronous, multicarrier DS-CDMA communications using optimized sequences," IEEE J. Select. Areas Commun., vol. 17, no. 11, pp. 1915–1923, 1999.

[170] A. L. Kachelmyer and K. W. Forsythe, "M-ary orthogonal signaling in the presence of doppler," IEEE Trans. Commun., vol. 41, no. 8, pp. 1192–1200, 1993.

[171] T. Wada, T. Yamazato, M. Katayama, and A. Ogawa, "A study on non-coherent reception of M-ary spread-spectrum signals in the presence of carrier frequency offset," in IEEE International Conference on Universal Personal Communications (ICUPC), 1995, pp. 412–416.

[172] T. Pollet and M. Moeneclaey, "The effect of carrier frequency offset on the performance of band limited single carrier and OFDM signals," in IEEE Global Telecommunications Conference (GLOBECOM), 1996, vol. 1, pp. 719–723 vol.1.

[173] X. Ma, H. Kobayashi, and S. C. Schwartz, "Effect of frequency offset on BER of OFDM and single carrier systems," in IEEE Proceedings on Personal, Indoor and Mobile Radio Communications (PIMRC), 2003, vol. 3, pp. 2239–2243 vol.3.

[174] Y. Wang and X. Dong, "Comparison of frequency offset and timing offset effects on the performance of SC-FDE and OFDM over UWB channels," IEEE Trans. Veh. Technol., vol. 58, no. 1, pp. 242–250, 2009.

[175] G. Malmgren, "Impact of carrier frequency offset, doppler spread and time synchronisation errors in OFDM based single frequency networks," in IEEE Global Telecommunications Conference, 1996, vol. 1, pp. 729–733 vol.1.

[176] H. Nishookar and R. Prasad, "On the sensitivity of multicarrier transmission over multipath channels to phase noise and frequency offset," in International Symposium on Personal, Indoor, and Mobile Communications (PIMRC), 1996, vol. 1, pp. 68–72 vol.1.

[177] W. Hwang, H. Kang, and K. Kim, "Approximation of SNR degradation due to carrier frequency offset for OFDM in shadowed multipath channels," IEEE Commun. Lett., vol. 7, no. 12, pp. 581–583, 2003.

[178] J. Lee, H. Lou, D. Toumpakaris, and J. M. Cioffi, "SNR analysis of OFDM systems in the presence of carrier frequency offset for fading channels," IEEE Trans. Wireless Commun., vol. 5, no. 12, pp. 3360–3364, 2006.

[179] P. K. Remvik and N. Holte, "Carrier frequency offset robustness for OFDM systems with different pulse shaping filters," in IEEE Global Telecommunications Conference (GLOBECOM), 1997, vol. 1, pp. 11–15 vol.1.

[180] K. Sathananthan and C. Tellambura, "Probability of error calculation of OFDM systems with frequency offset," IEEE Trans. Commun., vol. 49, no. 11, pp. 1884–1888, 2001.

[181] X. Wang, T. T. Tjhung, Y. Wu, and B. Caron, "SER performance evaluation and optimization of OFDM system with residual frequency and timing offsets from imperfect synchronization," IEEE Trans.s Broadcast., vol. 49, no. 2, pp. 170–177, 2003.

[182] L. Rugini and P. Banelli, "BER of OFDM systems impaired by carrier frequency offset in multipath fading channels," IEEE Trans. Wireless Commun., vol. 4, no. 5, pp. 2279–2288, 2005.

[183] P. Dharmawansa, N. Rajatheva, and H. Minn, "An exact error probability analysis of OFDM systems with frequency offset," IEEE Trans. Commun., vol. 57, no. 1, pp. 26–31, 2009.

[184] R. U. Mahesh and A. K. Chaturvedi, "Closed form BER expressions for BPSK OFDM systems with frequency offset," IEEE Commun. Lett., vol. 14, no. 8, pp. 731–733, 2010.

[185] P. Tan and N. C. Beaulieu, "Precise BER analysis of $\pi/4$-DQPSK OFDM with carrier frequency offset over frequency selective fast fading channels," IEEE Trans. Wireless Commun., vol. 6, no. 10, pp. 3770–3780, 2007.

[186] C. Yih, "BER analysis of OFDM systems impaired by DC offset and carrier frequency offset in multipath fading channels," IEEE Commun. Lett., vol. 11, no. 11, pp. 842–844, 2007.

[187] P. C. Weeraddana, N. Rajatheva, and H. Minn, "Probability of error analysis of BPSK OFDM systems with random residual frequency offset," IEEE Trans. Commun., vol. 57, no. 1, pp. 106–116, 2009.

[188] K. A. Hamdi, "Exact SINR analysis of wireless OFDM in the presence of carrier frequency offset," IEEE Trans. Wireless Commun., vol. 9, no. 3, pp. 975–979, 2010.

[189] K. A. Hamdi, "Average capacity analysis of OFDM with frequency offset in Rician fading," in IEEE Global Telecommunications Conference (GLOBECOM), 2007, pp. 1678–1682.

[190] S. Bellini, C. Molinari, and G. Tartara, "Digital frequency estimation in burst mode QPSK transmission," IEEE Trans. Commun., vol. 38, no. 7, pp. 959–961, 1990.

[191] N. R. Sollenberger and J. C. . Chuang, "Low-overhead symbol timing and carrier recovery for TDMA portable radio systems," IEEE Trans. Commun., vol. 38, no. 10, pp. 1886–1892, 1990.

[192] J. C. Chuang and N. R. Sollenberger, "Burst coherent demodulation with combined symbol timing, frequency offset estimation, and diversity selection," IEEE Trans. Commun., vol. 39, no. 7, pp. 1157–1164, 1991.

[193] R. Mehlan, Yong-En Chen, and H. Meyr, "A fully digital feedforward MSK demodulator with joint frequency offset and symbol timing estimation for burst mode mobile radio," IEEE Trans. Veh. Technol., vol. 42, no. 4, pp. 434–443, 1993.

[194] M. Luise and R. Reggiannini, "Carrier frequency recovery in all-digital modems for burst-mode transmissions," IEEE Trans. Commun., vol. 43, no. 2/3/4, pp. 1169–1178, 1995.

[195] G. Caire and C. Elia, "A new symbol timing and carrier frequency offset estimation algorithm for noncoherent orthogonal M-CPFSK," IEEE Trans. Commun., vol. 45, no. 10, pp. 1314–1326, 1997.

[196] Y. Wang, E. Serpedin, and P. Ciblat, "Optimal blind nonlinear least-squares carrier phase and frequency offset estimation for general QAM modulations," IEEE Trans. Wireless Commun., vol. 2, no. 5, pp. 1040–1054, 2003.

[197] P. Ciblat and M. Ghogho, "Blind nlls carrier frequency-offset estimation for QAM, PSK, and PAM modulations: performance at low SNR," IEEE Trans. Commun., vol. 54, no. 10, pp. 1725–1730, 2006.

[198] A. Viterbi, "Nonlinear estimation of PSK-modulated carrier phase with application to burst digital transmission," IEEE Trans. Inf. Theory, vol. 29, no. 4, pp. 543–551, 1983.

[199] Y. Ying and M. Ghogho, "Optimal pilot placement for frequency offset estimation and data detection in burst transmission systems," IEEE Commun. Lett., vol. 9, no. 6, pp. 549–551, 2005.

[200] K. Amleh and Hongbin Li, "An algebraic approach to blind carrier offset and code timing estimation for DS-CDMA systems," IEEE Signal Process. Lett., vol. 10, no. 2, pp. 32–34, 2003.

[201] F. Gini and G. B. Giannakis, "Frequency offset and symbol timing recovery in flat-fading channels: a cyclostationary approach," IEEE Trans. Commun., vol. 46, no. 3, pp. 400–411, 1998.

[202] M. Shi, Y. Bar-Ness, and W. Su, "Revisiting the timing and frequency offset estimation based on cyclostationarity with new improved method," IEEE Commun. Lett., vol. 13, no. 7, pp. 537–539, 2009.

[203] Y. Wang, P. Ciblat, E. Serpedin, and P. Loubaton, "Performance analysis of a class of nondata-aided frequency offset and symbol timing estimators for flat-fading channels," IEEE Trans. Signal Process., vol. 50, no. 9, pp. 2295–2305, 2002.

[204] P. Ciblat, E. Serpedin, and Yan Wang, "On a blind fractionally sampling-based carrier frequency offset estimator for noncircular transmissions," IEEE Signal Process. Lett., vol. 10, no. 4, pp. 89–92, 2003.

[205] P. Ciblat, P. Loubaton, E. Serpedin, and G. B. Giannakis, "Performance analysis of blind carrier frequency offset estimators for noncircular transmissions through frequency-selective channels," IEEE Trans. Signal Process., vol. 50, no. 1, pp. 130–140, 2002.

[206] P. Ciblat and L. Vandendorpe, "Blind carrier frequency offset estimation for noncircular constellation-based transmissions," IEEE Trans. Signal Process., vol. 51, no. 5, pp. 1378–1389, 2003.

[207] W-Y. Kuo and M. P. Fitz, "Frequency offset compensation of pilot symbol assisted modulation in frequency flat fading," IEEE Trans. Commun., vol. 45, no. 11, pp. 1412–1416, 1997.

[208] M. Morelli, U. Mengali, and G. M. Vitetta, "Further results in carrier frequency estimation for transmissions over flat fading channels," IEEE Commun. Lett., vol. 2, no. 12, pp. 327–330, 1998.

[209] O. Besson and P. Stoica, "On frequency offset estimation for flat-fading channels," IEEE Commun. Lett., vol. 5, no. 10, pp. 402–404, 2001.

[210] E-R. Jeong, G. Choi, and Y. H. Lee, "Data-aided frequency estimation for PSK signaling in frequency-selective fading," IEEE J. Sel. Areas Commun., vol. 19, no. 7, pp. 1408–1419, 2001.

[211] M. Morelli and U. Mengali, "Carrier-frequency estimation for transmissions over selective channels," IEEE Trans. Commun., vol. 48, no. 9, pp. 1580–1589, 2000.

[212] M. Nissila and S. Pasupathy, "Joint estimation of carrier frequency offset and statistical parameters of the multipath fading channel," IEEE Trans. Commun., vol. 54, no. 6, pp. 1038–1048, 2006.

[213] J. Hua, L. Meng, X. Xu, D. Wang, and X. You, "Novel scheme for joint estimation of SNR, doppler, and carrier frequency offset in double-selective wireless channels," IEEE Trans. Veh. Technol., vol. 58, no. 3, pp. 1204–1217, 2009.

[214] K. Li and H. Liu, "Joint channel and carrier offset estimation in CDMA communications," IEEE Trans. Signal Process., vol. 47, no. 7, pp. 1811–1822, 1999.

[215] S. Attallah and Hongyi Fu, "Joint channel and carrier offset estimation in a multiuser CDMA system," IEEE Commun. Lett., vol. 6, no. 10, pp. 428–430, 2002.

[216] S. Kumar, M. S. Chaudhari, R. Gupta, and S. Majhi, "Multiple CFOs estimation and implementation of SC-FDMA uplink system using over-sampling and iterative method," IEEE Trans. Veh. Technol., vol. 69, no. 6, pp. 6254–6263, 2020.

[217] P. S. Sanoopkumar, P. Muneer, and S. M. Sameer, "Joint estimation of RF impairments, channel, and low complexity iterative equalization technique for high mobility SC-FDMA/OFDMA uplink systems," IEEE Trans. Wireless Commun., vol. 19, no. 6, pp. 4276–4289, 2020.

[218] P. H. Moose, "A technique for orthogonal frequency division multiplexing frequency offset correction," IEEE Trans. Commun., vol. 42, no. 10, pp. 2908–2914, 1994.

[219] M. Luise and R. Reggiannini, "Carrier frequency acquisition and tracking for OFDM systems," IEEE Trans. Commun., vol. 44, no. 11, pp. 1590–1598, 1996.

[220] F. Classen and H. Meyr, "Frequency synchronization algorithms for OFDM systems suitable for communication over frequency selective fading channels," in IEEE Vehicular Technology Conference (VTC), 1994, pp. 1655–1659 vol.3.

[221] T. M. Schmidl and D. C. Cox, "Robust frequency and timing synchronization for OFDM," IEEE Trans. Commun., vol. 45, no. 12, pp. 1613–1621, 1997.

[222] K. Shi and E. Serpedin, "Coarse frame and carrier synchronization of OFDM systems: a new metric and comparison," IEEE Trans. Wireless Commun., vol. 3, no. 4, pp. 1271–1284, 2004.

[223] J. Zhu and W. Lee, "Carrier frequency offset estimation for OFDM systems with null subcarriers," IEEE Trans. Veh. Technol., vol. 55, no. 5, pp. 1677–1690, 2006.

[224] H. Zhou, A. V. Malipatil, and Y. Huang, "OFDM carrier synchronization based on time-domain channel estimates," IEEE Trans. Wireless Commun., vol. 7, no. 8, pp. 2988–2999, 2008.

[225] O. Edfors et al., "OFDM channel estimation by singular value decomposition," IEEE Trans. Commun., vol. 46, no. 7, pp. 931–939, 1998.

[226] J. Li, G. Liu, and G. B. Giannakis, "Carrier frequency offset estimation for OFDM-based WLANs," IEEE Signal Processing Letters, vol. 8, no. 3, pp. 80–82, 2001.

[227] Y. Ma, "Modified nonlinear least square approaches to carrier frequency offset estimation in OFDM systems," IEEE Commun. Lett., vol. 7, no. 4, pp. 177–179, 2003.

[228] J. H. Yu and Y. T. Su, "Pilot-assisted maximum-likelihood frequency-offset estimation for OFDM systems," IEEE Trans. Commun., vol. 52, no. 11, pp. 1997–2008, 2004.

[229] H. Hsieh and W. Wu, "Maximum likelihood timing and carrier frequency offset estimation for OFDM systems with periodic preambles," IEEE Trans. Veh. Technol., vol. 58, no. 8, pp. 4224–4237, 2009.

[230] M. Morelli and U. Mengali, "An improved frequency offset estimator for OFDM applications," IEEE Commun. Lett., vol. 3, no. 3, pp. 75–77, 1999.

[231] A. Laourine, A. Stephenne, and S. Affes, "A new OFDM synchronization symbol for carrier frequency offset estimation," IEEE Signal Process. Lett., vol. 14, no. 5, pp. 321–324, 2007.

[232] Y. H. Kim, I. Song, S. Yoon, and S. R. Park, "An efficient frequency offset estimator for OFDM systems and its performance characteristics," IEEE Trans. Veh. Technol., vol. 50, no. 5, pp. 1307–1312, 2001.

[233] H. Minn, V. K. Bhargava, and K. B. Letaief, "A robust timing and frequency synchronization for OFDM systems," IEEE Trans. Wireless Commun., vol. 2, no. 4, pp. 822–839, 2003.

[234] H. Minn and S. Xing, "An optimal training signal structure for frequency-offset estimation," IEEE Trans. Commun., vol. 53, no. 2, pp. 343–355, 2005.

[235] O. Besson and P. Stoica, "Data-aided frequency offset estimation in frequency selective channels: Training sequence selection," in IEEE International Conference on Acoustics, Speech, and Signal Processing (ICASSP), 2002, vol. 3, pp. III–2445–III–2448.

[236] P. Stoica and O. Besson, "Training sequence design for frequency offset and frequency-selective channel estimation," IEEE Trans. Commun., vol. 51, no. 11, pp. 1910–1917, 2003.

[237] M. Ghogho, P. Ciblat, A. Swami, and P. Bianchi, "Training design for repetitive-slot-based CFO estimation in OFDM," IEEE Trans. Signal Process., vol. 57, no. 12, pp. 4958–4964, 2009.

[238] H. Minn, X. Fu, and V. K. Bhargava, "Optimal periodic training signal for frequency offset estimation in frequency-selective fading channels," IEEE Trans. Commun., vol. 54, no. 6, pp. 1081–1096, 2006.

[239] P. Ciblat, P. Bianchi, and M. Ghogho, "Training sequence optimization for joint channel and frequency offset estimation," IEEE Trans. Signal Process., vol. 56, no. 8, pp. 3424–3436, 2008.

[240] D. Huang and K. B. Letaief, "Carrier frequency offset estimation for OFDM systems using null subcarriers," IEEE Trans. Commun., vol. 54, no. 5, pp. 813–823, 2006.

[241] J. Wolfmann, "Almost perfect autocorrelation sequences," IEEE Trans. Inf. Theory, vol. 38, no. 4, pp. 1412–1418, 1992.

[242] D. Huang and K. B. Letaief, "Enhanced carrier frequency offset estimation for OFDM using channel side information," IEEE Trans. Wireless Commun., vol. 5, no. 10, pp. 2784–2793, 2006.

[243] R. Zhang, T. T. Tjhung, H. J. Hu, and P. He, "Window function and interpolation algorithm for OFDM frequency-offset correction," IEEE Trans. Veh. Technol., vol. 52, no. 3, pp. 654–670, 2003.

[244] F. Gao, T. Cui, and A. Nallanathan, "Scattered pilots and virtual carriers based frequency offset tracking for OFDM systems: Algorithms, identifiability, and performance analysis," IEEE Trans. Commun., vol. 56, no. 4, pp. 619–629, 2008.

[245] J. Lei and T.-S. Ng, "A consistent OFDM carrier frequency offset estimator based on distinctively spaced pilot tones," IEEE Trans. Wireless Commun., vol. 3, no. 2, pp. 588–599, 2004.

[246] Y. Li, H. Minn, N. Al-Dhahir, and A. R. Calderbank, "Pilot designs for consistent frequency-offset estimation in OFDM systems," IEEE Trans. Commun., vol. 55, no. 5, pp. 864–877, 2007.

[247] K. Lee, S. Moon, S. Kim, and I. Lee, "Sequence designs for robust consistent frequency-offset estimation in OFDM systems," IEEE Trans. Veh. Technol., vol. 62, no. 3, pp. 1389–1394, 2013.

[248] P-Y. Tsai, H-Y. Kang, and T-D. Chiueh, "Joint weighted least-squares estimation of carrier-frequency offset and timing offset for OFDM systems over multipath fading channels," IEEE Trans. Veh. Technol., vol. 54, no. 1, pp. 211–223, 2005.

[249] C. Wu, M. Shiue, and C. Wang, "Joint carrier synchronization and equalization algorithm for packet-based OFDM systems over the multipath fading channel," IEEE Trans. Veh. Technol., vol. 59, no. 1, pp. 248–260, 2010.

[250] A. A. M. Al-Bassiouni, M. Ismail, and W. Zhuang, "An eigenvalue based carrier frequency offset estimator for OFDM systems," IEEE Wireless Commun. Lett., vol. 2, no. 5, pp. 475–478, 2013.

[251] M. Morelli and M. Moretti, "Fine carrier and sampling frequency synchronization in OFDM systems," IEEE Trans. Wireless Commun., vol. 9, no. 4, pp. 1514–1524, 2010.

[252] H. Lee and J. Lee, "Joint clock and frequency synchronization for OFDM-based cellular systems," IEEE Signal Processing Letters, vol. 18, no. 12, pp. 757–760, 2011.

[253] Y. Kim and J. Lee, "Joint maximum likelihood estimation of carrier and sampling frequency offsets for OFDM systems," IEEE Trans. Broadcast., vol. 57, no. 2, pp. 277–283, 2011.

[254] X. Wang and B. Hu, "A low-complexity ML estimator for carrier and sampling frequency offsets in OFDM systems," IEEE Commun. Lett., vol. 18, no. 3, pp. 503–506, 2014.

[255] A. Rotem and R. Dabora, "A novel low-complexity estimation of sampling and carrier frequency offsets in OFDM communications," IEEE Access, vol. 8, pp. 194978–194991, 2020.

[256] M. Morelli, A. N. D'Andrea, and U. Mengali, "Feedback frequency synchronization for OFDM applications," IEEE Commun. Lett., vol. 5, no. 1, pp. 28–30, 2001.

[257] J. J. van de Beek, M. Sandell, and P. O. Borjesson, "ML estimation of time and frequency offset in OFDM systems," IEEE Trans. Signal Process., vol. 45, no. 7, pp. 1800–1805, 1997.

[258] N. Lashkarian and S. Kiaei, "Class of cyclic-based estimators for frequency-offset estimation of OFDM systems," IEEE Trans. Commun., vol. 48, no. 12, pp. 2139–2149, 2000.

[259] E. Chiavaccini and G. M. Vitetta, "Maximum-likelihood frequency recovery for OFDM signals transmitted over multipath fading channels," IEEE Trans. Commun., vol. 52, no. 2, pp. 244–251, 2004.

[260] T. Fusco and M. Tanda, "Ml-based symbol timing and frequency offset estimation for OFDM systems with noncircular transmissions," IEEE Trans. Signal Process., vol. 54, no. 9, pp. 3527–3541, 2006.

[261] Jia-Chin Lin, "Maximum-likelihood frame timing instant and frequency offset estimation for OFDM communication over a fast Rayleigh-fading channel," IEEE Trans. Veh. Technol., vol. 52, no. 4, pp. 1049–1062, 2003.

[262] T. Lv, Hua Li, and Jie Chen, "Joint estimation of symbol timing and carrier frequency offset of OFDM signals over fast time-varying multipath channels," IEEE Trans. Signal Process., vol. 53, no. 12, pp. 4526–4535, 2005.

[263] H. Liu and U. Tureli, "A high-efficiency carrier estimator for OFDM communications," IEEE Commun. Lett., vol. 2, no. 4, pp. 104–106, 1998.

[264] U. Tureli, H. Liu, and M. D. Zoltowski, "OFDM blind carrier offset estimation: ESPRIT," IEEE Trans. Commun., vol. 48, no. 9, pp. 1459–1461, 2000.

[265] U. Tureli, D. Kivanc, and Hui Liu, "Experimental and analytical studies on a high-resolution OFDM carrier frequency offset estimator," IEEE Trans. Veh. Technol., vol. 50, no. 2, pp. 629–643, 2001.
[266] S. Attallah, "Blind estimation of residual carrier offset in OFDM systems," IEEE Signal Process. Letters, vol. 11, no. 2, pp. 216–219, 2004.
[267] U. Tureli, P. J. Honan, and Hui Liu, "Low-complexity nonlinear least squares carrier offset estimator for OFDM: identifiability, diversity and performance," IEEE Trans. Signal Process., vol. 52, no. 9, pp. 2441–2452, 2004.
[268] X. Ma et al., "Non-data-aided carrier offset estimators for OFDM with null subcarriers: identifiability, algorithms, and performance," IEEE J. Sel. Areas Commun., vol. 19, no. 12, pp. 2504–2515, 2001.
[269] Yang-Seok Choi, P. J. Voltz, and F. A. Cassara, "Ml estimation of carrier frequency offset for multicarrier signals in Rayleigh fading channels," IEEE Trans. Veh. Technol., vol. 50, no. 2, pp. 644–655, 2001.
[270] Y. Wu, S. Attallah, and J. W. M. Bergmans, "On the optimality of the null subcarrier placement for blind carrier offset estimation in OFDM systems," IEEE Trans. Veh. Technol., vol. 58, no. 4, pp. 2109–2115, 2009.
[271] Y. Meng, W. Zhang, G. L. Stüber, and W. Wang, "Blind fast CFO estimation and performance analysis for OFDM," IEEE Trans. Veh. Technol., vol. 69, no. 10, pp. 11501–11514, 2020.
[272] H. Bolcskei, "Blind estimation of symbol timing and carrier frequency offset in wireless OFDM systems," IEEE Trans. Commun., vol. 49, no. 6, pp. 988–999, 2001.
[273] P. Ciblat and E. Serpedin, "A fine blind frequency offset estimator for OFDM/OQAM systems," IEEE Trans. Signal Process., vol. 52, no. 1, pp. 291–296, 2004.
[274] T. Fusco and M. Tanda, "Blind frequency-offset estimation for OFDM/OQAM systems," IEEE Trans. Signal Process., vol. 55, no. 5, pp. 1828–1838, 2007.
[275] M. Besseghier and A. B. Djebbar, "Novel blind CFO estimation method for OFDM/OQAM system," IEEE Commun. Lett., vol. 24, no. 7, pp. 1451–1454, 2020.
[276] M. Luise, M. Marselli, and R. Reggiannini, "Low-complexity blind carrier frequency recovery for OFDM signals over frequency-selective radio channels," IEEE Trans. Commun., vol. 50, no. 7, pp. 1182–1188, 2002.
[277] F. Z. Merli and G. M. Vitetta, "Blind feedforward frequency estimation for OFDM signals transmitted over multipath fading channels," IEEE Trans. Wireless Commun., vol. 6, no. 6, pp. 2055–2059, 2007.
[278] B. Chen and H. Wang, "Blind estimation of OFDM carrier frequency offset via oversampling," IEEE Trans Signal Process., vol. 52, no. 7, pp. 2047–2057, 2004.
[279] H. Jeon, K. Kim, and E. Serpedin, "An efficient blind deterministic frequency offset estimator for OFDM systems," IEEE Trans. Commun., vol. 59, no. 4, pp. 1133–1141, 2011.
[280] F. Yang, K. H. Li, and K. C. Teh, "A carrier frequency offset estimator with minimum output variance for OFDM systems," IEEE Commun. Lett., vol. 8, no. 11, pp. 677–679, 2004.
[281] T. Roman, S. Visuri, and V. Koivunen, "Blind frequency synchronization in OFDM via diagonality criterion," IEEE Trans. Signal Process., vol. 54, no. 8, pp. 3125–3135, 2006.
[282] S. L. Talbot and B. Farhang-Boroujeny, "Spectral method of blind carrier tracking for OFDM," IEEE Trans. Signal Process., vol. 56, no. 7, pp. 2706–2717, 2008.
[283] M. Ghogho and A. Swami, "Blind frequency-offset estimator for OFDM systems transmitting constant-modulus symbols," IEEE Commun. Lett., vol. 6, no. 8, pp. 343–345, 2002.
[284] L. Wu, X. Zhang, P. Li, and Y. Su, "A closed-form blind CFO estimator based on frequency analysis for OFDM systems," IEEE Trans. Commun., vol. 57, no. 6, pp. 1634–1637, 2009.
[285] S. Lmai, A. Bourré, C. Laot, and S. Houcke, "An efficient blind estimation of carrier frequency offset in OFDM systems," IEEE Trans. Veh. Technol., vol. 63, no. 4, pp. 1945–1950, 2014.
[286] X. N. Zeng and A. Ghrayeb, "A blind carrier frequency offset estimation scheme for OFDM systems with constant modulus signaling," IEEE Trans. Commun., vol. 56, no. 7, pp. 1032–1037, 2008.
[287] L. Wu, X. Zhang, P. Li, and Y. Su, "A blind CFO estimator based on smoothing power spectrum for OFDM systems," IEEE Trans. Commun., vol. 57, no. 7, pp. 1924–1927, 2009.
[288] J. Oh, J. Kim, and J. Lim, "Blind carrier frequency offset estimation for OFDM systems with constant modulus constellations," IEEE Commun. Lett., vol. 15, no. 9, pp. 971–973, 2011.
[289] A. Jayaprakash and G. R. Reddy, "Covariance-fitting-based blind carrier frequency offset estimation method for OFDM systems," IEEE Trans. Veh. Technol., vol. 65, no. 12, pp. 10101–10105, 2016.
[290] T. Fusco and M. Tanda, "Blind synchronization for OFDM systems in multipath channels," IEEE Trans. Wireless Commun., vol. 8, no. 3, pp. 1340–1348, 2009.
[291] W. Chin, "ML estimation of timing and frequency offsets using distinctive correlation characteristics of OFDM signals over dispersive fading channels," IEEE Trans. Veh. Technol., vol. 60, no. 2, pp. 444–456, 2011.
[292] J. Armstrong, "Analysis of new and existing methods of reducing intercarrier interference due to carrier frequency offset in OFDM," IEEE Trans. Commun., vol. 47, no. 3, pp. 365–369, 1999.
[293] Y. Zhao and S. Haggman, "Intercarrier interference self-cancellation scheme for OFDM mobile communication systems," IEEE Trans. Commun., vol. 49, no. 7, pp. 1185–1191, 2001.
[294] A. Seyedi and G. J. Saulnier, "General ICI self-cancellation scheme for OFDM systems," IEEE Trans. Veh. Technol., vol. 54, no. 1, pp. 198–210, 2005.
[295] M. Chang, "A novel algorithm of inter-subchannel interference self-cancellation for OFDM systems," IEEE Trans. Wireless Commun., vol. 6, no. 8, pp. 2881–2893, 2007.
[296] H. Yeh, Y. Chang, and B. Hassibi, "A scheme for cancelling intercarrier interference using conjugate transmission in multicarrier communication systems," IEEE Trans. Wireless Commun., vol. 6, no. 1, pp. 3–7, 2007.
[297] C. Wang and Y. Huang, "Intercarrier interference cancellation using general phase rotated conjugate transmission for OFDM systems," IEEE Trans. Commun., vol. 58, no. 3, pp. 812–819, 2010.
[298] J. Ma, P. V. Orlik, J. Zhang, and G. Y. Li, "Reduced-rate OFDM transmission for inter-subchannel interference self-cancellation over high-mobility fading channels," IEEE Trans. Wireless Commun., vol. 11, no. 6, pp. 2013–2023, 2012.
[299] X. Ma, H. Kobayashi, and S. C. Schwartz, "Joint frequency offset and channel estimation for OFDM," in IEEE Global Telecommunications Conference (GLOBECOM), 2003, vol. 1, pp. 15–19 Vol.1.
[300] F. Z. Merli and G. M. Vitetta, "Iterative ML-based estimation of carrier frequency offset, channel impulse response and data in OFDM transmissions," IEEE Trans. Commun., vol. 56, no. 3, pp. 497–506, 2008.
[301] M. Morelli and M. Moretti, "Integer frequency offset recovery in OFDM transmissions over selective channels," IEEE Trans. Wireless Commun., vol. 7, no. 12, pp. 5220–5226, 2008.
[302] J-H. Lee, J. C. Han, and S-C.l Kim, "Joint carrier frequency synchronization and channel estimation for OFDM systems via the em algorithm," IEEE Trans. Veh. Technol., vol. 55, no. 1, pp. 167–172, 2006.
[303] E. P. Simon, L. Ros, H. Hijazi, and M. Ghogho, "Joint carrier frequency offset and channel estimation for OFDM systems via the EM algorithm in the presence of very high mobility," IEEE Trans. Signal Process., vol. 60, no. 2, pp. 754–765, 2012.
[304] R. Mo, Y. H. Chew, T. T. Tjhung, and C. C. Ko, "An EM-based semiblind joint channel and frequency offset estimator for OFDM systems over frequency-selective fading channels," IEEE Trans. Veh. Technol., vol. 57, no. 5, pp. 3275–3282, 2008.
[305] T. Cui and C. Tellambura, "Joint frequency offset and channel estimation for OFDM systems using pilot symbols and virtual carriers," IEEE Trans. Wireless Commun., vol. 6, no. 4, pp. 1193–1202, 2007.
[306] S. Salari and F. Chan, "Joint CFO and channel estimation in OFDM systems using sparse bayesian learning," IEEE Commun. Lett., vol. 25, no. 1, pp. 166–170, 2021.
[307] J. Chen, Y. Wu, S. Ma, and T. Ng, "Ml joint CFO and channel estimation in OFDM systems with timing ambiguity," IEEE Trans. Wireless Commun., vol. 7, no. 7, pp. 2436–2440, 2008.
[308] K. Cai, X. Li, J. Du, Y. Wu, and F. Gao, "CFO estimation in OFDM systems under timing and channel length uncertainties with model averaging," IEEE Trans. Wireless Commun., vol. 9, no. 3, pp. 970–974, 2010.
[309] H. Abdzadeh-Ziabari, W. Zhu, and M. N. S. Swamy, "Joint maximum likelihood timing, frequency offset, and doubly selective channel estimation for OFDM systems," IEEE Trans. Veh. Technol., vol. 67, no. 3, pp. 2787–2791, 2018.
[310] H. Nguyen-Le, T. Le-Ngoc, and C. C. Ko, "RLS-based joint estimation and tracking of channel response, sampling, and carrier frequency offsets for OFDM," IEEE Trans. Broadcasy., vol. 55, no. 1, pp. 84–94, 2009.
[311] J. . van de Beek, P. O. Borjesson, M. . Boucheret, D. Landstrom, J. M. Arenas, P. Odling, C. Ostberg, M. Wahlqvist, and S. K. Wilson, "A time

and frequency synchronization scheme for multiuser OFDM," IEEE J. Sel. Areas Commun., vol. 17, no. 11, pp. 1900–1914, 1999.

[312] S. Barbarossa, M. Pompili, and G. B. Giannakis, "Channel-independent synchronization of orthogonal frequency division multiple access systems," IEEE J. Sel. Areas Commun., vol. 20, no. 2, pp. 474–486, 2002.

[313] Y. Zeng and A. R. Leyman, "Pilot-based simplified ML and fast algorithm for frequency offset estimation in OFDMA uplink," IEEE Trans. Veh. Technol., vol. 57, no. 3, pp. 1723–1732, 2008.

[314] L. Sanguinetti and M. Morelli, "A low-complexity scheme for frequency estimation in Uplink ofdma systems," IEEE Trans. Wireless Commun., vol. 9, no. 8, pp. 2430–2437, 2010.

[315] S. Keum, D. Kim, and H. Kim, "An improved frequency offset estimation based on companion matrix in multi-user uplink interleaved OFDMA systems," IEEE Signal Process. Lett., vol. 21, no. 4, pp. 409–413, 2014.

[316] P. Cheng, Z. Chen, F. de Hoog, and C. K. Sung, "Sparse blind carrier-frequency offset estimation for OFDMA uplink," IEEE Trans. Commun., vol. 64, no. 12, pp. 5254–5265, 2016.

[317] M. Huang, L. Huang, C. Guo, P. Zhang, J. Zhang, and L. Yang, "Carrier frequency offset estimation in uplink OFDMA systems: An approach relying on sparse recovery," IEEE Trans. Veh. Technol., vol. 66, no. 10, pp. 9592–9597, 2017.

[318] M. Huang, L. Huang, W. Sun, W. Bao, and J. Zhang, "Sparse bayesian learning assisted CFO estimation using nonnegative laplace priors," IEEE Trans. Veh. Technol., vol. 68, no. 6, pp. 6151–6155, 2019.

[319] Z. Cao, U. Tureli, and Yu-Dong Yao, "Deterministic multiuser carrier-frequency offset estimation for interleaved OFDMA uplink," IEEE Trans. Commun., vol. 52, no. 9, pp. 1585–1594, 2004.

[320] J. Lee, S. Lee, K. Bang, S. Cha, and D. Hong, "Carrier frequency offset estimation using ESPRIT for interleaved ofdma uplink systems," IEEE Trans. Veh. Technol., vol. 56, no. 5, pp. 3227–3231, 2007.

[321] H. Hsieh and W. R. Wu, "Blind maximum-likelihood carrier-frequency-offset estimation for interleaved OFDMA uplink systems," IEEE Trans. Veh. Technol., vol. 60, no. 1, pp. 160–173, 2011.

[322] M. Morelli, "Timing and frequency synchronization for the uplink of an OFDMA system," IEEE Trans. Commun., vol. 52, no. 2, pp. 296–306, 2004.

[323] Z. Wang, Y. Xin, and G. Mathew, "Iterative carrier-frequency offset estimation for generalized OFDMA uplink transmission," IEEE Trans. Wireless Commun., vol. 8, no. 3, pp. 1373–1383, 2009.

[324] K. Lee, S. Moon, S. Lee, and I. Lee, "Low complexity pilot assisted carrier frequency offset estimation for OFDMA uplink systems," IEEE Trans. Wireless Commun., vol. 11, no. 8, pp. 2690–2695, 2012.

[325] P. Sun, M. Morelli, and L. Zhang, "Carrier frequency offset tracking in the ieee 802.16e OFDMA uplink," IEEE Trans. Wireless Commun., vol. 9, no. 12, pp. 3613–3619, 2010.

[326] L. Bai and Q. Yin, "Frequency synchronization for the OFDMA uplink based on the tile structure of IEEE 802.16e," IEEE Trans. Veh. Technol., vol. 61, no. 5, pp. 2348–2353, 2012.

[327] H. Wang and Q. Yin, "Multiuser carrier frequency offsets estimation for OFDMA uplink with generalized carrier assignment scheme," IEEE Trans. Wireless Commun., vol. 8, no. 7, pp. 3347–3353, 2009.

[328] Y. Wang and S. Phoong, "Blind CFO estimation in OFDMA uplink transmission with general carrier assignment scheme," IEEE Commun. Lett., vol. 22, no. 5, pp. 1014–1017, 2018.

[329] S. Li and S. Phoong, "Blind estimation of multiple carrier frequency offsets in OFDMA uplink systems employing virtual carriers," IEEE Access, vol. 8, pp. 2915–2923, 2020.

[330] M. Pun, M. Morelli, and C. . J. Kuo, "Iterative detection and frequency synchronization for OFDMA uplink transmissions," IEEE Trans. Wireless Commun., vol. 6, no. 2, pp. 629–639, 2007.

[331] X. Fu, H. Minn, and C. D. Cantrell, "Two novel iterative joint frequency-offset and channel estimation methods for OFDMA uplink," IEEE Trans. Commun., vol. 56, no. 3, pp. 474–484, 2008.

[332] T. Wang and S. C. Liew, "Frequency-asynchronous multiuser joint channel-parameter estimation, CFO compensation, and channel decoding," IEEE Trans. Veh. Technol., vol. 65, no. 12, pp. 9732–9746, 2016.

[333] M. . Pun, M. Morelli, and C. . J. Kuo, "Maximum-likelihood synchronization and channel estimation for OFDMA uplink transmissions," IEEE Transactions on Communications, vol. 54, no. 4, pp. 726–736, 2006.

[334] I. Ziskind and M. Wax, "Maximum likelihood localization of multiple sources by alternating projection," IEEE Trans. Acoust., Speech, Signal Process., vol. 36, no. 10, pp. 1553–1560, 1988.

[335] L. Haring, S. Bieder, A. Czylwik, and T. Kaiser, "Estimation algorithms of multiple channels and carrier frequency offsets in application to multiuser OFDM systems," IEEE Trans. Wireless Commun., vol. 9, no. 3, pp. 865–870, 2010.

[336] J. Chen, Y. Wu, S. C. Chan, and T. Ng, "Joint maximum-likelihood CFO and channel estimation for OFDMA uplink using importance sampling," IEEE Trans. Veh. Technol., vol. 57, no. 6, pp. 3462–3470, 2008.

[337] Y. Na and H. Minn, "Line search based iterative joint estimation of channels and frequency offsets for uplink OFDMA systems," IEEE Trans. Wireless Commun., vol. 6, no. 12, pp. 4374–4382, 2007.

[338] X. N. Zeng and A. Ghrayeb, "Joint CFO and channel estimation for OFDMA uplink: an application of the variable projection method," IEEE Trans. Wireless Commun., vol. 8, no. 5, pp. 2306–2311, 2009.

[339] P. Muneer and S. M. Sameer, "Pilot-aided joint estimation of doubly selective channel and carrier frequency offsets in OFDMA uplink with high-mobility users," IEEE Trans. Veh. Technol., vol. 64, no. 1, pp. 411–417, 2015.

[340] J. A. Fessler and A. O. Hero, "Space-alternating generalized expectation-maximization algorithm," IEEE Trans. Signal Process., vol. 42, no. 10, pp. 2664–2677, 1994.

[341] P. Muneer and S. M. Sameer, "Joint ML estimation of CFO and channel, and a low complexity turbo equalization technique for high mobility OFDMA uplinks," IEEE Trans. Wireless Commun., vol. 14, no. 7, pp. 3642–3654, 2015.

[342] F. Simoens and M. Moeneclaey, "reduced complexity data-aided and code-aided frequency offset estimation for flat-fading MIMO channels," IEEE Trans. Wireless Commun., vol. 5, no. 6, pp. 1558–1567, 2006.

[343] M. Zhou, Z. Feng, Y. Liu, and X. Huang, "An efficient algorithm and hardware architecture for maximum-likelihood based carrier frequency offset estimation in MIMO systems," IEEE Access, vol. 6, pp. 50105–50116, 2018.

[344] J. Zhang, Y. R. Zheng, C. Xiao, and K. B. Letaief, "Channel equalization and symbol detection for single-carrier MIMO systems in the presence of multiple carrier frequency offsets," IEEE Trans. Veh. Technol., vol. 59, no. 4, pp. 2021–2030, 2010.

[345] M. Ghogho and A. Swami, "Training design for multipath channel and frequency-offset estimation in MIMO systems," IEEE Trans. Signal Process., vol. 54, no. 10, pp. 3957–3965, 2006.

[346] D. Qu, G. Zhu, and T. Jiang, "Training sequence design and parameter estimation of MIMO channels with carrier frequency offsets," IEEE Trans. Wireless Commun., vol. 5, no. 12, pp. 3662–3666, 2006.

[347] S. Shahbazpanahi, A. B. Gershman, and G. B. Giannakis, "Blind and semiblind channel and carrier frequency-offset estimation in orthogonally space-time block coded MIMO systems," IEEE Trans. Signal Process., vol. 56, no. 2, pp. 702–711, 2008.

[348] Y. Zeng and A. R. Leyman, "Time, frequency synchronization, and equalization for asynchronous multiuser MIMO systems," IEEE Trans. Wireless Commun., vol. 6, no. 7, pp. 2593–2601, 2007.

[349] W. Zhang, "Frequency synchronization for multi-user MIMO without cyclic-prefix based on space-time equalization," IEEE Wireless Commun. Lett., vol. 6, no. 4, pp. 426–429, 2017.

[350] J. Zhang and V. K. N. Lau, "Carrier frequency synchronization and tracking for OFDM systems with receive antenna diversity," IEEE Trans. Wireless Commun., vol. 6, no. 9, pp. 3277–3286, 2007.

[351] X. Zhang, X. Gao, and D. Xu, "Novel blind carrier frequency offset estimation for OFDM system with multiple antennas," IEEE Trans. Wireless Commun., vol. 9, no. 3, pp. 881–885, 2010.

[352] W. Zhang and Q. Yin, "Blind maximum likelihood carrier frequency offset estimation for OFDM with multi-antenna receiver," IEEE Trans.Signal Process., vol. 61, no. 9, pp. 2295–2307, 2013.

[353] W. Zhang, Q. Yin, and W. Wang, "Blind closed-form carrier frequency offset estimation for OFDM with multi-antenna receiver," IEEE Trans. Veh. Technol., vol. 64, no. 8, pp. 3850–3856, 2015.

[354] W. Zhang, Q. Yin, W. Wang, and F. Gao, "One-shot blind CFO and channel estimation for OFDM with multi-antenna receiver," IEEE Trans.Signal Process., vol. 62, no. 15, pp. 3799–3808, 2014.

[355] Y. Sun, Z. Xiong, and X. Wang, "EM-based iterative receiver design with carrier-frequency offset estimation for MIMO OFDM systems," IEEE Trans. Commun., vol. 53, no. 4, pp. 581–586, 2005.

[356] Y. Jiang, H. Minn, X. Gao, X. You, and Y. Li, "Frequency offset estimation and training sequence design for MIMO OFDM," IEEE Trans. Wireless Commun., vol. 7, no. 4, pp. 1244–1254, 2008.

[357] Y. Jiang, H. Minn, X. You, and X. Gao, "Simplified frequency offset

estimation for MIMO OFDM systems," IEEE Trans. Veh. Technol., vol. 57, no. 5, pp. 3246–3251, 2008.

[358] D. Chu, "Polyphase codes with good periodic correlation properties (corresp.)," IEEE Trans. Inf. Theory, vol. 18, no. 4, pp. 531–532, 1972.

[359] Y. Yao and G. B. Giannakis, "Blind carrier frequency offset estimation in SISO, MIMO, and multiuser OFDM systems," IEEE Trans. Commun., vol. 53, no. 1, pp. 173–183, 2005.

[360] W. Zhang, Q. Yin, and F. Gao, "Computationally efficient blind estimation of carrier frequency offset for MIMO-OFDM systems," IEEE Trans. Wireless Commun., vol. 15, no. 11, pp. 7644–7656, 2016.

[361] X. N. Zeng and A. Ghrayeb, "A blind carrier frequency offset estimation scheme for OFDM systems with constant modulus signaling," IEEE Trans. Commun., vol. 56, no. 7, pp. 1032–1037, 2008.

[362] L. Wu, X. D. Zhang, and P. S. Li, "A low-complexity blind carrier frequency offset estimator for MIMO-OFDM systems," IEEE Signal Process. Lett., vol. 15, pp. 769–772, 2008.

[363] W. Zhang and Q. Yin, "Blind carrier frequency offset estimation for MIMO-OFDM with constant modulus constellations via rank reduction criterion," IEEE Trans. Veh. Technol., vol. 65, no. 8, pp. 6809–6815, 2016.

[364] L. Yang, H. Zhang, Y. Cai, and H. Yang, "Blind carrier frequency offset estimation for MIMO-OFDM systems based on the banded structure of covariance matrices for constant modulus signals," IEEE Access, vol. 6, pp. 51804–51813, 2018.

[365] W. Zhang, F. Gao, Q. Yin, and A. Nallanathan, "Blind carrier frequency offset estimation for interleaved OFDMA uplink," IEEE Trans. Signal Process., vol. 60, no. 7, pp. 3616–3627, 2012.

[366] X. Ma et al., "Hopping pilots for estimation of frequency-offset and multiantenna channels in MIMO-OFDM," IEEE Trans. Commun., vol. 53, no. 1, pp. 162–172, 2005.

[367] E. P. Simon, L. Ros, H. Hijazi, J. Fang, D. P. Gaillot, and M. Berbineau, "Joint carrier frequency offset and fast time-varying channel estimation for MIMO-OFDM systems," IEEE Trans. Veh. Technol., vol. 60, no. 3, pp. 955–965, 2011.

[368] Y. Yu and Y. Liang, "Joint carrier frequency offset and channel estimation for MIMO-OFDM systems using extended h_∞ filter," IEEE Commun. Lett., vol. 16, no. 4, pp. 476–478, 2012.

[369] H. Nguyen-Le, T. Le-Ngoc, and N. H. Tran, "Iterative receiver design with joint doubly selective channel and CFO estimation for coded MIMO-OFDM transmissions," IEEE Trans. Veh. Technol., vol. 60, no. 8, pp. 4052–4057, 2011.

[370] Y. Zeng, A. R. Leyman, and T. Ng, "Joint semiblind frequency offset and channel estimation for multiuser MIMO-OFDM uplink," IEEE Trans. Commun., vol. 55, no. 12, pp. 2270–2278, 2007.

[371] Y. Zeng and T-S. Ng, "A semi-blind channel estimation method for multiuser multiantenna OFDM systems," IEEE Trans. Signal Process., vol. 52, no. 5, pp. 1419–1429, 2004.

[372] J. Chen, Y. Wu, S. Ma, and T. Ng, "Joint cfo and channel estimation for multiuser MIMO-OFDM systems with optimal training sequences," IEEE Trans. Signal Process., vol. 56, no. 8, pp. 4008–4019, 2008.

[373] S. Kay and S. Saha, "Mean likelihood frequency estimation," IEEE Trans. Signal Process., vol. 48, no. 7, pp. 1937–1946, 2000.

[374] K. J. Kim, M. Pun, and R. A. Iltis, "Joint carrier frequency offset and channel estimation for uplink MIMO-OFDMA systems using parallel Schmidt Rao-Blackwellized Particle filters," IEEE Trans. Commun., vol. 58, no. 9, pp. 2697–2708, 2010.

[375] P. Muneer and S. M. Sameer, "Iterative joint carrier frequency offset and doubly selective channel estimation in high-mobility MIMO-OFDMA uplink using oblique projection," IEEE Trans. Veh. Technol., vol. 65, no. 9, pp. 7110–7121, 2016.

[376] H. Abdzadeh-Ziabari, W. Zhu, and M. N. S. Swamy, "Joint carrier frequency offset and doubly selective channel estimation for MIMO-OFDMA uplink with Kalman and Particle filtering," IEEE Trans. Signal Process., vol. 66, no. 15, pp. 4001–4012, 2018.

[377] S. Mukherjee, S. K. Mohammed, and I. Bhushan, "Impact of CFO estimation on the performance of ZF receiver in massive MU-MIMO systems," IEEE Trans. Veh. Technol., vol. 65, no. 11, pp. 9430–9436, 2016.

[378] S. Mukherjee and S. K. Mohammed, "Impact of frequency selectivity on the information rate performance of CFO impaired single-carrier massive MU-MIMO uplink," IEEE Wireless Commun. Lett., vol. 5, no. 6, pp. 648–651, 2016.

[379] C. Shan, Y. Zhang, L. Chen, X. Chen, and W. Wang, "Performance analysis of large scale antenna system with carrier frequency offset, quasi-static mismatch and channel estimation error," IEEE Access, vol. 5, pp. 26135–26145, 2017.

[380] W. Zhang, F. Gao, S. Jin, and H. Lin, "Frequency synchronization for uplink massive MIMO systems," IEEE Trans. Wireless Commun., vol. 17, no. 1, pp. 235–249, 2018.

[381] W. Zhang, F. Gao, H. Minn, and H. Wang, "Scattered pilots-based frequency synchronization for multiuser OFDM systems with large number of receive antennas," IEEE Trans. Commun., vol. 65, no. 4, pp. 1733–1745, 2017.

[382] P. Sabeti, A. Farhang, N. Marchetti, and L. Doyle, "Frequency synchronization for OFDM-based massive MIMO systems," IEEE Trans. Signal Process., vol. 67, no. 11, pp. 2973–2986, 2019.

[383] Y. Ge, W. Zhang, F. Gao, and G. Y. Li, "Frequency synchronization for uplink massive MIMO with adaptive MUI suppression in angle domain," IEEE Trans. Signal Process., vol. 67, no. 8, pp. 2143–2158, 2019.

[384] Y. Ge and W. Zhang, "User-coupling angle-domain adaptive filtering based frequency synchronization for massive MIMO multiuser uplink," IEEE Access, vol. 7, pp. 98034–98044, 2019.

[385] W. Zhang and F. Gao, "Blind frequency synchronization for multiuser OFDM uplink with large number of receive antennas," IEEE Trans. Signal Process., vol. 64, no. 9, pp. 2255–2268, 2016.

[386] Y. Feng, W. Zhang, F. Gao, and Q. Sun, "Computationally efficient blind CFO estimation for massive MIMO uplink," IEEE Trans. Veh. Technol., vol. 67, no. 8, pp. 7795–7799, 2018.

[387] Q. Huang, M. Ghogho, J. Wei, and P. Ciblat, "Practical timing and frequency synchronization for OFDM-based cooperative systems," IEEE Trans. Signal Process., vol. 58, no. 7, pp. 3706–3716, 2010.

[388] H. Mehrpouyan and S. D. Blostein, "Bounds and algorithms for multiple frequency offset estimation in cooperative networks," IEEE Trans. Wireless Commun., vol. 10, no. 4, pp. 1300–1311, 2011.

[389] C. K. Ho, P. H. W. Fung, and S. Sun, "Carrier frequency offset estimation for two-way relaying: Optimal preamble and estimator design," IEEE Trans. Wireless Commun., vol. 12, no. 4, pp. 1898–1909, 2013.

[390] C. Chen and M. Ku, "Carrier frequency offset estimation bound for OFDM-based single relay networks with multipath receptions," IEEE Access, vol. 7, pp. 63900–63912, 2019.

[391] T. Liu and S. Zhu, "Joint CFO and channel estimation for asynchronous cooperative communication systems," IEEE Signal Process. Lett., vol. 19, no. 10, pp. 643–646, 2012.

[392] A. A. Nasir, H. Mehrpouyan, S. D. Blostein, S. Durrani, and R. A. Kennedy, "Timing and carrier synchronization with channel estimation in multi-relay cooperative networks," IEEE Trans. Signal Process., vol. 60, no. 2, pp. 793–811, 2012.

[393] A. A. Nasir, H. Mehrpouyan, S. Durrani, S. D. Blostein, R. A. Kennedy, and B. Ottersten, "Transceiver design for distributed STBC based AF cooperative networks in the presence of timing and frequency offsets," IEEE Trans. Signal Process., vol. 61, no. 12, pp. 3143–3158, 2013.

[394] G. Wang, F. Gao, Y. Wu, and C. Tellambura, "Joint CFO and channel estimation for OFDM-based two-way relay networks," IEEE Trans. Wireless Commun., vol. 10, no. 2, pp. 456–465, 2011.

[395] S. Chakraborty and D. Sen, "Joint estimation of MCFOs and channel gains for two-way multi-relay systems with high mobility," IEEE Wireless Commun. Lett., vol. 6, no. 5, pp. 610–613, 2017.

[396] S. Abdallah, A. I. Salameh, and M. Saad, "Spectrum efficient joint frequency offset and channel estimation for time-asynchronous amplify-and forward two-way relay networks," IEEE Access, vol. 7, pp. 71972–71985, 2019.

[397] Z. Li and X. Xia, "An Alamouti coded OFDM transmission for cooperative systems robust to both timing errors and frequency offsets," IEEE Trans. Wireless Commun., vol. 7, no. 5, pp. 1839–1844, 2008.

[398] X. Li, F. Ng, and T. Han, "Carrier frequency offset mitigation in asynchronous cooperative OFDM transmissions," IEEE Trans. Signal Process., vol. 56, no. 2, pp. 675–685, 2008.

[399] Q. Huang, M. Ghogho, and J. Wei, "Data detection in cooperative STBC-OFDM systems with multiple frequency offsets," IEEE Signal Process. Lett., vol. 16, no. 7, pp. 600–603, 2009.

[400] F. Tian, X. Xia, P. C. Ching, and W. Ma, "Signal detection in a space–frequency coded cooperative communication system with multiple carrier frequency offsets by exploiting specific properties of the code structure," IEEE Trans. Veh. Technol., vol. 58, no. 7, pp. 3396–3409, 2009.

[401] Q. Huang, M. Ghogho, D. Ma, and J. Wei, "Low-complexity data-detection algorithm in cooperative SFBC-OFDM systems with multiple

frequency offsets," IEEE Trans. Veh. Technol., vol. 59, no. 9, pp. 4614–4620, 2010.

[402] Y. Yao and X. Dong, "Multiple CFO mitigation in amplify-and-forward cooperative OFDM transmission," IEEE Trans. Commun., vol. 60, no. 12, pp. 3844–3854, 2012.

[403] W. Xu, W. Xiang, M. Elkashlan, and H. Mehrpouyan, "Spectrum sensing of OFDM signals in the presence of carrier frequency offset," IEEE Trans. Veh. Technol., vol. 65, no. 8, pp. 6798–6803, 2016.

[404] A. Kumar, S. Dwivedi, and A. K. Jagannatham, "GLRT-based spectrum sensing for MIMO SC-FDMA cognitive radio systems in the presence of synchronization impairments," IEEE Wireless Commun. Lett., vol. 5, no. 3, pp. 280–283, 2016.

[405] Z. Xu and C. Yang, "Secondary transceiver design in the presence of frequency offset between primary and secondary systems," IEEE Trans. Wireless Commun., vol. 9, no. 11, pp. 3461–3471, 2010.

[406] M. Morelli and M. Moretti, "Robust frequency synchronization for OFDM-based cognitive radio systems," IEEE Trans. Wireless Commun., vol. 7, no. 12, pp. 5346–5355, 2008.

[407] L. Sanguinetti, M. Morelli, and G. Imbarlina, "An em-based frequency offset estimator for OFDM systems with unknown interference," IEEE Trans. Wireless Commun., vol. 8, no. 9, pp. 4470–4475, 2009.

[408] W. Chin, C. Kao, H. Chen, and T. Liao, "Iterative synchronization-assisted detection of OFDM signals in cognitive radio systems," IEEE Trans. Veh. Technol., vol. 63, no. 4, pp. 1633–1644, 2014.

[409] P. Singh, S. Srivastava, A. K. Jagannatham, and L. Hanzo, "Second-order statistics-based semi-blind techniques for channel estimation in millimeter-wave MIMO analog and hybrid beamforming," IEEE Trans. Commun., vol. 68, no. 11, pp. 6886–6901, 2020.

[410] N. J. Myers and R. W. Heath, "Message passing-based joint CFO and channel estimation in mmwave systems with one-bit ADCs," IEEE Trans. Wireless Commun., vol. 18, no. 6, pp. 3064–3077, 2019.

[411] J. Rodríguez-Fernández and N. González-Prelcic, "Channel estimation for hybrid mmwave MIMO systems with CFO uncertainties," IEEE Trans. Wireless Commun., vol. 18, no. 10, pp. 4636–4652, 2019.

[412] D. Zhu, R. Bendlin, S. Akoum, A. Ghosh, and R. W. Heath, "Double-sequence frequency synchronization for wideband millimeter-wave systems with few-bit ADCs," IEEE Trans. Wireless Commun., vol. 19, no. 2, pp. 1357–1372, 2020.

[413] C. Liu, Y. Chen, and C. Li, "Blind beamforming schemes in SC-FDMA systems with insufficient cyclic prefix and carrier frequency offset," IEEE Trans. Veh. Technol., vol. 58, no. 9, pp. 4848–4859, 2009.

[414] S. B. Amor, S. Affes, F. Bellili, U. Vilaipornsawai, L. Zhang, and P. Zhu, "Multi-node ML time and frequency synchronization for distributed MIMO-relay beamforming over time-varying flat-fading channels," IEEE Trans. Commun., vol. 67, no. 4, pp. 2702–2715, 2019.

[415] Y. Feng, W. Zhang, and Y. Ge, "Frequency synchronization with beamforming network optimization for uplink massive MIMO systems," IEEE Trans. Veh. Technol., vol. 69, no. 3, pp. 3486–3490, 2020.

[416] Y. Liu, X. Zhu, E. G. Lim, Y. Jiang, and Y. Huang, "Iterative semi-blind CFO estimation, SI cancelation and signal detection for full-duplex systems," in IEEE Global Communications Conference (GLOBECOM), 2018, pp. 1–7.

[417] S. Chakraborty and D. Sen, "Iterative SAGE-based joint MCFOs and channel estimation for full-duplex two-way multi-relay systems in highly mobile environment," IEEE Trans. Wireless Commun., vol. 17, no. 11, pp. 7379–7394, 2018.

[418] L. Anttila, M. Valkama, and M. Renfors, "Circularity-based I/Q imbalance compensation in wideband direct-conversion receivers," IEEE Trans. Veh. Technol., vol. 57, no. 4, pp. 2099–2113, 2008.

[419] B. Selim, S. Muhaidat, P. C. Sofotasios, B. S. Sharif, T. Stouraitis, G. K. Karagiannidis, and N. Aldhahir, "Performance analysis of coherent and noncoherent modulation under I/Q imbalance effects," IEEE Access, vol. 9, pp. 36125–36139, 2021.

[420] F. Horlin and A. Bourdoux, "Comparison of the sensitivity of OFDM and SC-FDE to CFO, SCO and IQ imbalance," in International Symposium on Communications, Control and Signal Processing (ISCCSP), 2008, pp. 111–116.

[421] A. Ishaque, P. Sakulkar, and G. Ascheid, "Capacity analysis of uplink multi-user SC-FDMA system with frequency-dependent I/Q imbalance," in Annual Allerton Conference on Communication, Control, and Computing (Allerton), 2013, pp. 1067–1074.

[422] N. Hajiabdolrahim and M. Sabbaghian, "Analysis of the impact of the receiver I/Q imbalance on the achievable rate of SC-FDE systems," IEEE Trans. Veh. Technol., vol. 67, no. 6, pp. 5530–5534, 2018.

[423] L. Yang, K. Panta, and J. Armstrong, "Impact of timing jitter and I/Q imbalance in OFDM systems," IEEE Commun. Lett., vol. 17, no. 2, pp. 253–256, 2013.

[424] M. Oner and O. A. Dobre, "On the second-order cyclic statistics of signals in the presence of receiver impairments," IEEE Trans. Commun., vol. 59, no. 12, pp. 3278–3284, 2011.

[425] C-L. Liu, "Impacts of I/Q imbalance on QPSK-OFDM-QAM detection," IEEE Trans. Consum. Electron., vol. 44, no. 3, pp. 984–989, 1998.

[426] F. J. Lopez-Martinez, E. Martos-Naya, J. F. Paris, and J. T. Entrambasaguas, "Exact closed-form BER analysis of OFDM systems in the presence of IQ imbalances and ICSI," IEEE Trans. Wireless Commun., vol. 10, no. 6, pp. 1914–1922, 2011.

[427] C. Zhao and R. J. Baxley, "Error vector magnitude analysis for OFDM systems," in Fortieth Asilomar Conference on Signals, Systems and Computers(ACSSC), 2006, pp. 1830–1834.

[428] F. Gregorio, J. Cousseau, S. Werner, T. Riihonen, and R. Wichman, "EVM analysis for broadband OFDM direct-conversion transmitters," IEEE Trans. Veh. Technol., vol. 62, no. 7, pp. 3443–3451, 2013.

[429] Ö. Özdemir, R. Hamila, and N. Al-Dhahir, "Exact average OFDM subcarrier SINR analysis under joint transmit–receive I/Q imbalance," IEEE Trans. Veh. Technol., vol. 63, no. 8, pp. 4125–4130, 2014.

[430] S. Krone and G. Fettweis, "Capacity analysis for OFDM systems with transceiver i/q imbalance," in IEEE Global Telecommunications Conference(GLOBECOM), 2008, pp. 1–6.

[431] A. A. Boulogeorgos, P. C. Sofotasios, B. Selim, S. Muhaidat, G. K. Karagiannidis, and M. Valkama, "Effects of RF impairments in communications over cascaded fading channels," IEEE Trans. Veh. Technol., vol. 65, no. 11, pp. 8878–8894, 2016.

[432] J. Luo, A. Kortke, W. Keusgen, and M. Valkama, "A novel adaptive calibration scheme for frequency-selective I/Q imbalance in broadband direct-conversion transmitters," IEEE Trans. Circuits Syst. II, Exp. Briefs, vol. 60, no. 2, pp. 61–65, 2013.

[433] J. Luo, A. Kortke, W. Keusgen, and M. Valkama, "Efficient estimation and pilot-free online re-calibration of i/q imbalance in broadband direct-conversion transmitters," IEEE Trans. Veh. Technol., vol. 63, no. 6, pp. 2506–2520, 2014.

[434] W. Li, Y. Zhang, L. Huang, J. Cosmas, C. Maple, and J. Xiong, "Self-IQ-demodulation based compensation scheme of frequency-dependent IQ imbalance for wideband direct-conversion transmitters," IEEE Trans. Broadcast, vol. 61, no. 4, pp. 666–673, 2015.

[435] K. S. Lorenz, J. Goodman, G. Stantchev, and N. A. Pendergrass, "Generalized transmitter compensation of frequency dependent I/Q imbalance," IEEE Trans. Signal Process., vol. 64, no. 9, pp. 2220–2231, 2016.

[436] Y. Yao, Y. Jin, M. Li, Z. Dai, and S. He, "An accurate three-input nonlinear model for joint compensation of frequency-dependent I/Q imbalance and power amplifier distortion," IEEE Access, vol. 7, pp. 140651–140664, 2019.

[437] R. Marchesani, "Digital precompensation of imperfections in quadrature modulators," IEEE Trans. Commun., vol. 48, no. 4, pp. 552–556, 2000.

[438] Z. Zhu, X. Huang, and H. Leung, "Joint I/Q mismatch and distortion compensation in direct conversion transmitters," IEEE Trans. Wireless Commun., vol. 12, no. 6, pp. 2941–2951, 2013.

[439] L. Ding, Z. Ma, D. R. Morgan, M. Zierdt, and G. T. Zhou, "Compensation of frequency-dependent gain/phase imbalance in predistortion linearization systems," IEEE Trans. Circuits Syst. I. Reg. Papers, vol. 55, no. 1, pp. 390–397, 2008.

[440] Z. Zhu, X. Huang, M. Caron, and H. Leung, "Blind self-calibration technique for I/Q imbalances and dc-offsets," IEEE Trans. Circuits Syst. I. Reg. Papers, vol. 61, no. 6, pp. 1849–1859, 2014.

[441] V. Rampa, "I/Q compensation of broadband direct-conversion transmitters," IEEE Trans. Wireless Commun., vol. 13, no. 6, pp. 3329–3342, 2014.

[442] M. Valkama, M. Renfors, and V. Koivunen, "Advanced methods for I/Q imbalance compensation in communication receivers," IEEE Trans. Signal Process., vol. 49, no. 10, pp. 2335–2344, 2001.

[443] J. J. de Witt and G. van Rooyen, "A blind i/q imbalance compensation technique for direct-conversion digital radio transceivers," IEEE Trans. Veh. Technol., vol. 58, no. 4, pp. 2077–2082, 2009.

[444] W. Hou and M. Jiang, "Enhanced joint channel and IQ imbalance parameter estimation for mobile communications," IEEE Commun. Lett., vol. 17, no. 7, pp. 1392–1395, 2013.

[445] C. Zhang, Z. Xiao, B. Gao, L. Su, and D. Jin, "Three-stage treatment of TX/RX IQ imbalance and channel with CFO for SC-FDE systems," IEEE Commun. Lett., vol. 18, no. 2, pp. 297–300, 2014.

[446] X. Zhang, H. Li, W. Liu, and J. Qiao, "Iterative IQ imbalance compensation receiver for single carrier transmission," IEEE Trans. Veh. Technol., vol. 66, no. 9, pp. 8238–8248, 2017.

[447] X. Cheng, Y. Yang, and S. Li, "Joint compensation of transmitter and receiver I/Q imbalances for SC-FDE systems," IEEE Trans. Veh. Technol., vol. 69, no. 8, pp. 8483–8498, 2020.

[448] A. Tarighat and A. H. Sayed, "Joint compensation of transmitter and receiver impairments in OFDM systems," IEEE Trans. Wireless Commun., vol. 6, no. 1, pp. 240–247, 2007.

[449] R. Rodriguez-Avila, G. Nunez-Vega, R. Parra-Michel, and A. Mendez-Vazquez, "Frequency-selective joint Tx/Rx I/Q imbalance estimation using Golay complementary sequences," IEEE Trans. Wireless Commun., vol. 12, no. 5, pp. 2171–2179, 2013.

[450] E. Nayebi, P. Dayal, and K. B. Song, "Adaptive IQ mismatch compensation in time-domain using frequency-domain observations," IEEE Trans. Signal Process., vol. 69, pp. 655–668, 2021.

[451] G. Xing, M. Shen, and H. Liu, "Frequency offset and I/Q imbalance compensation for direct-conversion receivers," IEEE Trans. Wireless Commun., vol. 4, no. 2, pp. 673–680, 2005.

[452] H. Lin, X. Zhu, and K. Yamashita, "Low-complexity pilot-aided compensation for carrier frequency offset and I/Q imbalance," IEEE Trans. Commun., vol. 58, no. 2, pp. 448–452, 2010.

[453] F. Horlin, A. Bourdoux, and L. Van Der Perre, "Low-complexity EM-based joint acquisition of the carrier frequency offset and IQ imbalance," IEEE Trans. Wireless Commun., vol. 7, no. 6, pp. 2212–2220, 2008.

[454] I. Barhumi and M. Moonen, "IQ-imbalance compensation for OFDM in the presence of IBI and carrier-frequency offset," IEEE Trans. Signal Process., vol. 55, no. 1, pp. 256–266, 2007.

[455] D. Tandur and M. Moonen, "Joint adaptive compensation of transmitter and receiver IQ imbalance under carrier frequency offset in OFDM-based systems," IEEE Trans. Signal Process., vol. 55, no. 11, pp. 5246–5252, 2007.

[456] Y. Pan and S. Phoong, "A time-domain joint estimation algorithm for CFO and I/Q imbalance in wideband direct-conversion receivers," IEEE Trans. Wireless Commun., vol. 11, no. 7, pp. 2353–2361, 2012.

[457] M. Inamori, A. M. Bostamam, Y. Sanada, and H. Minami, "IQ imbalance compensation scheme in the presence of frequency offset and dynamic DC offset for a direct conversion receiver," IEEE Trans. Wireless Commun., vol. 8, no. 5, pp. 2214–2220, 2009.

[458] C. Hsu and W. Sheen, "Joint calibration of transmitter and receiver impairments in direct-conversion radio architecture," IEEE Trans. Wireless Commun., vol. 11, no. 2, pp. 832–841, 2012.

[459] X. Cai, Y. Wu, H. Lin, and K. Yamashita, "Estimation and compensation of CFO and I/Q imbalance in OFDM systems under timing ambiguity," IEEE Trans. Veh. Technol., vol. 60, no. 3, pp. 1200–1205, 2011.

[460] J. Tubbax, B. Come, L. Van der Perre, S. Donnay, M. Engels, Hugo De Man, and M. Moonen, "Compensation of IQ imbalance and phase noise in OFDM systems," IEEE Trans. Wireless Commun., vol. 4, no. 3, pp. 872–877, 2005.

[461] Y. Tsai, C. Yen, and X. Wang, "Blind frequency-dependent I/Q imbalance compensation for direct-conversion receivers," IEEE Trans. Wireless Commun., vol. 9, no. 6, pp. 1976–1986, 2010.

[462] H. Lin and K. Yamashita, "Time domain blind I/Q imbalance compensation based on real-valued filter," IEEE Trans. Wireless Commun., vol. 11, no. 12, pp. 4342–4350, 2012.

[463] Z. Zhu, X. Huang, and H. Leung, "Blind compensation of frequency-dependent I/Q imbalance in direct conversion OFDM receivers," IEEE Commun. Lett., vol. 17, no. 2, pp. 297–300, 2013.

[464] H. Lin and K. Yamashita, "Subcarrier allocation based compensation for carrier frequency offset and I/Q imbalances in OFDM systems," IEEE Trans. Wireless Commun., vol. 8, no. 1, pp. 18–23, 2009.

[465] Y. Meng, W. Zhang, W. Wang, and H. Lin, "Joint CFO and I/Q imbalance estimation for OFDM systems exploiting constant modulus subcarriers," IEEE Trans. Veh. Technol., vol. 67, no. 10, pp. 10076–10080, 2018.

[466] S. Traverso, M. Ariaudo, I. Fijalkow, J. Gautier, and C. Lereau, "Decision-directed channel estimation and high I/Q imbalance compensation in OFDM receivers," IEEE Trans. Commun., vol. 57, no. 5, pp. 1246–1249, 2009.

[467] Y. Chung and S. Phoong, "Channel estimation in the presence of transmitter and receiver I/Q mismatches for OFDM systems," IEEE Trans. Wireless Commun., vol. 8, no. 9, pp. 4476–4479, 2009.

[468] L. He, S. Ma, Y. Wu, Y. Zhou, T. Ng, and H. V. Poor, "Pilot-aided iq imbalance compensation for OFDM systems operating over doubly selective channels," IEEE Trans. Signal Process., vol. 59, no. 5, pp. 2223–2233, 2011.

[469] M. Sakai, H. Lin, and K. Yamashita, "Joint estimation of channel and I/Q imbalance in OFDM/OQAM systems," IEEE Commun. Lett., vol. 20, no. 2, pp. 284–287, 2016.

[470] M. Marey, M. Samir, and O. A. Dobre, "EM-based joint channel estimation and IQ imbalances for OFDM systems," IEEE Trans. Broadcast., vol. 58, no. 1, pp. 106–113, 2012.

[471] Y. Yoshida, K. Hayashi, H. Sakai, and W. Bocquet, "Analysis and compensation of transmitter iq imbalances in OFDMA and SC-FDMA systems," IEEE Trans. Signal Process., vol. 57, no. 8, pp. 3119–3129, 2009.

[472] H. A. Mahmoud, H. Arslan, M. K. Ozdemir, and F. E. Retnasothie, "IQ imbalance correction for OFDMA uplink systems," in IEEE International Conference on Communications (ICC), 2009, pp. 1–5.

[473] M. Marey and H. Steendam, "Novel data detection and channel estimation algorithms for BICM-OFDMA uplink asynchronous systems in the presence of IQ imbalance," IEEE Trans. Wireless Commun., vol. 13, no. 5, pp. 2706–2716, 2014.

[474] A. E. Canbilen, M. M. Alsmadi, E. Basar, S. S. Ikki, S. S. Gultekin, and I. Develi, "Spatial modulation in the presence of I/Q imbalance: Optimal detector performance analysis," IEEE Commun. Lett., vol. 22, no. 8, pp. 1572–1575, 2018.

[475] S. Javed, O. Amin, S. S. Ikki, and M. Alouini, "Multiple antenna systems with hardware impairments: New performance limits," IEEE Trans. Veh. Technol., vol. 68, no. 2, pp. 1593–1606, 2019.

[476] A. E. Canbilen, S. S. Ikki, E. Basar, S. S. Gultekin, and I. Develi, "Joint impact of I/Q imbalance and imperfect CSI on SM-MIMO systems over generalized Beckmann fading channels: Optimal detection and Cramer-Rao bound," IEEE Trans. Wireless Commun., vol. 19, no. 5, pp. 3034–3046, 2020.

[477] Y. Zou, M. Valkama, and M. Renfors, "Digital compensation of I/Q imbalance effects in space-time coded transmit diversity systems," IEEE Trans. Signal Process., vol. 56, no. 6, pp. 2496–2508, 2008.

[478] J. Qi and S. Aissa, "Analysis and compensation of I/Q imbalance in MIMO transmit-receive diversity systems," IEEE Trans. Commun., vol. 58, no. 5, pp. 1546–1556, 2010.

[479] C. Hsu, R. Cheng, and W. Sheen, "Joint least squares estimation of frequency, DC offset, I-Q imbalance, and channel in MIMO receivers," IEEE Trans. Veh. Technol., vol. 58, no. 5, pp. 2201–2213, 2009.

[480] N. Kolomvakis, M. Matthaiou, and M. Coldrey, "IQ imbalance in multiuser systems: Channel estimation and compensation," IEEE Trans. Commun., vol. 64, no. 7, pp. 3039–3051, 2016.

[481] A. Tarighat and A. H. Sayed, "MIMO OFDM receivers for systems with IQ imbalances," IEEE Trans. Signal Process., vol. 53, no. 9, pp. 3583–3596, 2005.

[482] V. K. V. Gottumukkala and H. Minn, "Capacity analysis and pilot-data power allocation for MIMO-OFDM with transmitter and receiver IQ imbalances and residual carrier frequency offset," IEEE Trans. Veh. Technol., vol. 61, no. 2, pp. 553–565, 2012.

[483] B. Maham and O. Tirkkonen, "Transmit antenna selection OFDM systems with transceiver I/Q imbalance," IEEE Trans. Veh. Technol., vol. 61, no. 2, pp. 865–871, 2012.

[484] L. Chen, A. G. Helmy, G. Yue, S. Li, and N. Al-Dhahir, "Performance analysis and compensation of joint TX/RX I/Q imbalance in differential STBC-OFDM," IEEE Trans. Veh. Technol., vol. 66, no. 7, pp. 6184–6200, 2017.

[485] Y. Meng, W. Zhang, and W. Wang, "Blind frequency synchronization for OFDM systems with I/Q imbalance," IEEE Trans. Veh. Technol., vol. 66, no. 9, pp. 7862–7876, 2017.

[486] J. Gao, X. Zhu, H. Lin, and A. K. Nandi, "Independent component analysis based semi-blind I/Q imbalance compensation for MIMO OFDM systems," IEEE Trans. Wireless Commun., vol. 9, no. 3, pp. 914–920, 2010.

[487] M. Sandell, E. Tsimbalo, S. Jardak, D. Uchida, K. Akita, D. Yoda, T. Kawaguchi, and M. Sano, "Estimation of wideband IQ imbalance in MIMO OFDM systems with CFO," IEEE Trans. Wireless Commun., pp. 1–1, 2021.

[488] H. Minn and D. Munoz, "Pilot designs for channel estimation of MIMO OFDM systems with frequency-dependent I/Q imbalances," IEEE Trans. Commun., vol. 58, no. 8, pp. 2252–2264, 2010.

[489] B. Narasimhan, S. Narayanan, H. Minn, and N. Al-Dhahir, "Reduced-complexity baseband compensation of joint Tx/Rx I/Q imbalance in

mobile MIMO-OFDM," IEEE Trans. Wireless Commun., vol. 9, no. 5, pp. 1720–1728, 2010.

[490] M. Marey, M. Samir, and M. H. Ahmed, "Joint estimation of transmitter and receiver IQ imbalance with ML detection for Alamouti OFDM systems," IEEE Trans. Veh. Technol., vol. 62, no. 6, pp. 2847–2853, 2013.

[491] Y. Chung and S. Phoong, "Joint estimation of I/Q imbalance, CFO and channel response for MIMO OFDM systems," IEEE Trans. Commun., vol. 58, no. 5, pp. 1485–1492, 2010.

[492] P. Rabiei, W. Namgoong, and N. Al-Dhahir, "Reduced-complexity joint baseband compensation of phase noise and I/Q imbalance for MIMO-OFDM systems," IEEE Trans. Wireless Commun., vol. 9, no. 11, pp. 3450–3460, 2010.

[493] U. Oruthota and O. Tirkkonen, "Link adaptation of precoded MIMO-OFDMA system with I/Q interference," IEEE Trans. Commun., vol. 63, no. 3, pp. 780–790, 2015.

[494] A. Hakkarainen, J. Werner, K. R. Dandekar, and M. Valkama, "Analysis and augmented spatial processing for uplink OFDMA MU-MIMO receiver with transceiver I/Q imbalance and external interference," IEEE Trans. Wireless Commun., vol. 15, no. 5, pp. 3422–3439, 2016.

[495] W. Zhang, R. C. de Lamare, C. Pan, M. Chen, J. Dai, B. Wu, and X. Bao, "Widely linear precoding for large-scale MIMO with IQI: Algorithms and performance analysis," IEEE Trans. Wireless Commun., vol. 16, no. 5, pp. 3298–3312, 2017.

[496] J. Jee, G. Kwon, and H. Park, "Regularized zero-forcing precoder for massive MIMO system with transceiver I/Q imbalances," IEEE Wireless Commun. Lett., vol. 8, no. 4, pp. 1028–1031, 2019.

[497] Y. Teng, L. Jia, A. Liu, and V. K. N. Lau, "Joint estimation of channel and I/Q imbalance in massive MIMO: A two-timescale optimization approach," IEEE Trans. Wireless Commun., vol. 18, no. 10, pp. 4723–4737, 2019.

[498] S. Zarei, W. H. Gerstacker, J. Aulin, and R. Schober, "I/Q imbalance aware widely-linear receiver for uplink multi-cell massive MIMO systems: Design and sum rate analysis," IEEE Trans. Wireless Commun., vol. 15, no. 5, pp. 3393–3408, 2016.

[499] N. Kolomvakis, M. Coldrey, T. Eriksson, and M. Viberg, "Massive MIMO systems with IQ imbalance: Channel estimation and sum rate limits," IEEE Trans. Commun., vol. 65, no. 6, pp. 2382–2396, 2017.

[500] Y. Xiong, N. Wei, and Z. Zhang, "An LMMSE-based receiver for uplink massive MIMO systems with randomized IQ imbalance," IEEE Commun. Lett., vol. 22, no. 8, pp. 1624–1627, 2018.

[501] Y. Chen, L. You, X. Gao, and X. Xia, "Channel estimation with pilot reuse in IQ imbalanced massive MIMO," IEEE Access, vol. 8, pp. 1542–1555, 2020.

[502] Y. Chen, L. You, A. A. Lu, X. Gao, and X. G. Xia, "Channel estimation and robust detection for IQ imbalanced uplink massive MIMO-OFDM with adjustable phase shift pilots," IEEE Access, vol. 9, pp. 35864–35878, 2021.

[503] S. Wang and L. Zhang, "Signal processing in massive MIMO with IQ imbalances and low-resolution ADCs," IEEE Trans. Wireless Commun., vol. 15, no. 12, pp. 8298–8312, 2016.

[504] Y. Xiong, N. Wei, Z. Zhang, B. Li, and Y. Chen, "Channel estimation and IQ imbalance compensation for uplink massive MIMO systems with low-resolution ADCs," IEEE Access, vol. 5, pp. 6372–6388, 2017.

[505] M. Mokhtar, A. Gomaa, and N. Al-Dhahir, "OFDM AF relaying under I/Q imbalance: Performance analysis and baseband compensation," IEEE Trans. Commun., vol. 61, no. 4, pp. 1304–1313, 2013.

[506] J. Li, M. Matthaiou, and T. Svensson, "I/Q imbalance in AF dual-hop relaying: Performance analysis in Nakagami-m fading," IEEE Trans. Commun., vol. 62, no. 3, pp. 836–847, 2014.

[507] A. E. Canbilen, S. S. Ikki, E. Basar, S. S. Gultekin, and I. Develi, "Impact of I/Q imbalance on amplify-and-forward relaying: Optimal detector design and error performance," IEEE Trans. Commun., vol. 67, no. 5, pp. 3154–3166, 2019.

[508] M. Mokhtar, A. A. Boulogeorgos, G. K. Karagiannidis, and N. Al-Dhahir, "OFDM opportunistic relaying under joint transmit/receive I/Q imbalance," IEEE Trans. Commun., vol. 62, no. 5, pp. 1458–1468, 2014.

[509] J. Li, M. Matthaiou, and T. Svensson, "I/Q imbalance in two-way AF relaying," IEEE Trans. Commun., vol. 62, no. 7, pp. 2271–2285, 2014.

[510] A. Gouissem, R. Hamila, and M. O. Hasna, "Outage performance of cooperative systems under IQ imbalance," IEEE Trans. Commun., vol. 62, no. 5, pp. 1480–1489, 2014.

[511] Y. Gao, Y. Chen, N. Chen, and J. Zhang, "Performance analysis of dual-hop relaying with I/Q imbalance and additive hardware impairment," IEEE Trans. Veh. Technol., vol. 69, no. 4, pp. 4580–4584, 2020.

[512] M. Marey, "Soft-information aided channel estimation with IQ imbalance for alternate-relaying OFDM cooperative systems," IEEE Wireless Commun. Lett., vol. 7, no. 3, pp. 308–311, 2018.

[513] L. Samara, A. Gouissem, R. Hamila, M. O. Hasna, and N. Al-Dhahir, "Full-duplex amplify-and-forward relaying under I/Q imbalance," IEEE Trans. Veh. Technol., vol. 69, no. 7, pp. 7966–7970, 2020.

[514] J. Wang, H. Yu, Y. Wu, F. Shu, J. Wang, R. Chen, and J. Li, "Pilot optimization and power allocation for OFDM-based full-duplex relay networks with IQ-imbalances," IEEE Access, vol. 5, pp. 24344–24352, 2017.

[515] M. M. Alsmadi, A. E. Canbilen, N. Abu Ali, S. S. Ikki, and E. Basar, "Cognitive networks in the presence of I/Q imbalance and imperfect CSI: Receiver design and performance analysis," IEEE Access, vol. 7, pp. 49765–49777, 2019.

[516] A. Zahedi-Ghasabeh, A. Tarighat, and B. Daneshrad, "Spectrum sensing of OFDM waveforms using embedded pilots in the presence of impairments," IEEE Trans. Veh. Technol., vol. 61, no. 3, pp. 1208–1221, 2012.

[517] A. ElSamadouny, A. Gomaa, and N. Al-Dhahir, "A blind likelihood-based approach for OFDM spectrum sensing in the presence of I/Q imbalance," IEEE Trans. Commun., vol. 62, no. 5, pp. 1418–1430, 2014.

[518] A. Gokceoglu, S. Dikmese, M. Valkama, and M. Renfors, "Energy detection under IQ imbalance with single- and multi-channel direct-conversion receiver: Analysis and mitigation," IEEE J. Sel. Areas Commun., vol. 32, no. 3, pp. 411–424, 2014.

[519] O. Semiari, B. Maham, and C. Yuen, "On the effect of I/Q imbalance on energy detection and a novel four-level hypothesis spectrum sensing," IEEE Trans. Veh. Technol., vol. 63, no. 8, pp. 4136–4141, 2014.

[520] A. A. Boulogeorgos, N. D. Chatzidiamantis, and G. K. Karagiannidis, "Energy detection spectrum sensing under RF imperfections," IEEE Trans. Commun., vol. 64, no. 7, pp. 2754–2766, 2016.

[521] A. Mehrabian and A. Zaimbashi, "Robust and blind eigenvalue-based multiantenna spectrum sensing under IQ imbalance," IEEE Trans. Wireless Commun., vol. 17, no. 8, pp. 5581–5591, 2018.

[522] A. Zaimbashi and M. Valkama, "Impropriety-based multiantenna spectrum sensing with I/Q imbalanced radios," IEEE Trans. Veh. Technol., vol. 68, no. 9, pp. 8693–8706, 2019.

[523] A. A. Boulogeorgos, H. A. B. Salameh, and G. K. Karagiannidis, "Spectrum sensing in full-duplex cognitive radio networks under hardware imperfections," IEEE Trans. Veh. Technol., vol. 66, no. 3, pp. 2072–2084, 2017.

[524] X. Cheng, Z. Luo, and S. Li, "Joint estimation for I/Q imbalance and multipath channel in millimeter-wave SC-FDE systems," IEEE Trans. Veh. Technol., vol. 65, no. 9, pp. 6901–6912, 2016.

[525] X. Cheng and Z. Luo, "Compensation of transmitter I/Q imbalance in millimeter-wave SC-FDE systems," IEEE Trans. Veh. Technol., vol. 66, no. 5, pp. 4472–4476, 2017.

[526] H. Minn, Q. Zhan, N. Al-Dhahir, and H. Huang, "In-phase and quadrature timing mismatch estimation and compensation in millimeter-wave communication systems," IEEE Trans. Wireless Commun., vol. 16, no. 7, pp. 4317–4331, 2017.

[527] Y. R. Ramadan, H. Minn, and M. E. Abdelgelil, "Precompensation and system parameters estimation for low-cost nonlinear Tera-Hertz transmitters in the presence of I/Q imbalance," IEEE Access, vol. 6, pp. 51814–51833, 2018.

[528] T. Mao, Q. Wang, and Z. Wang, "Spatial modulation for terahertz communication systems with hardware impairments," IEEE Trans. Veh. Technol., vol. 69, no. 4, pp. 4553–4557, 2020.

[529] B. Maham, O. Tirkkonen, and A. Hjorungnes, "Impact of transceiver I/Q imbalance on transmit diversity of beamforming OFDM systems," IEEE Trans. Commun., vol. 60, no. 3, pp. 643–648, 2012.

[530] O. Ozdemir, R. Hamila, and N. Al-Dhahir, "I/Q imbalance in multiple beamforming OFDM transceivers: SINR analysis and digital baseband compensation," IEEE Trans. Commun., vol. 61, no. 5, pp. 1914–1925, 2013.

[531] S. Li and R. D. Murch, "An investigation into baseband techniques for single-channel full-duplex wireless communication systems," IEEE Trans. Wireless Commun., vol. 13, no. 9, pp. 4794–4806, 2014.

[532] Z. Li, Y. Xia, W. Pei, K. Wang, and D. P. Mandic, "An augmented nonlinear LMS for digital self-interference cancellation in full-duplex direct-conversion transceivers," IEEE Trans. Signal Process., vol. 66, no. 15, pp. 4065–4078, 2018.

[533] Y. Zhou, F. Hutu, and G. Villemaud, "Impact of receiver non-idealities on a full duplex spatial modulation system performance," IEEE Wireless Commun. Lett., vol. 9, no. 12, pp. 2083–2087, 2020.

[534] A. T. Le, L. C. Tran, X. Huang, and Y. J. Guo, "Analog least mean square loop with I/Q imbalance for self-interference cancellation in full-duplex radios," IEEE Trans. Veh. Technol., vol. 68, no. 10, pp. 9848–9860, 2019.

[535] F. Shu, J. Wang, J. Li, R. Chen, and W. Chen, "Pilot optimization, channel estimation, and optimal detection for full-duplex OFDM systems with IQ imbalances," IEEE Trans. Veh. Technol., vol. 66, no. 8, pp. 6993–7009, 2017.

[536] K. Komatsu, Y. Miyaji, and H. Uehara, "Iterative nonlinear self-interference cancellation for in-band full-duplex wireless communications under mixer imbalance and amplifier nonlinearity," IEEE Trans. Wireless Commun., vol. 19, no. 7, pp. 4424–4438, 2020.

[537] T. Fukui, K. Komatsu, Y. Miyaji, and H. Uehara, "Analog self-interference cancellation using auxiliary transmitter considering IQ imbalance and amplifier nonlinearity," IEEE Trans. Wireless Commun., vol. 19, no. 11, pp. 7439–7452, 2020.

[538] H. Q. Ngo, A. Ashikhmin, H. Yang, E. G. Larsson, and T. L. Marzetta, "Cell-free massive MIMO versus small cells," IEEE Trans. Wireless Commun., vol. 16, no. 3, pp. 1834–1850, 2017.

[539] J. Zhang, S. Chen, Y. Lin, J. Zheng, B. Ai, and L. Hanzo, "Cell-free massive MIMO: A new next-generation paradigm," IEEE Access, vol. 7, pp. 99878–99888, 2019.

[540] H. Q. Ngo, L. Tran, T. Q. Duong, M. Matthaiou, and E. G. Larsson, "On the total energy efficiency of cell-free massive MIMO," IEEE Trans. Green Commun. Netw., vol. 2, no. 1, pp. 25–39, 2018.

[541] Fatemeh Rezaei, Ali Reza Heidarpour, Chintha Tellambura, and Aliakbar Tadaion, "Underlaid spectrum sharing for cell-free massive MIMO-NOMA," IEEE Communications Letters, vol. 24, no. 4, pp. 907–911, 2020.

[542] Fatemeh Rezaei, Chintha Tellambura, Ali Akbar Tadaion, and Ali Reza Heidarpour, "Rate analysis of cell-free massive MIMO-NOMA with three linear precoders," IEEE Transactions on Communications, vol. 68, no. 6, pp. 3480–3494, 2020.

[543] Ö. Özdogan, E. Björnson, and J. Zhang, "Performance of cell-free massive MIMO with Rician fading and phase shifts," IEEE Trans. Wireless Commun., vol. 18, no. 11, pp. 5299–5315, 2019.

[544] G. Interdonato, H. Q. Ngo, P. Frenger, and E. G. Larsson, "Downlink training in cell-free massive MIMO: A blessing in disguise," IEEE Trans. Wireless Commun., vol. 18, no. 11, pp. 5153–5169, 2019.

[545] T. C. Mai, H. Q. Ngo, and T. Q. Duong, "Downlink spectral efficiency of cell-free massive MIMO systems with multi-antenna users," IEEE Trans. Commun., pp. 1–1, 2020.

[546] J. Qiu, K. Xu, X. Xia, Z. Shen, and W. Xie, "Downlink power optimization for cell-free massive MIMO over spatially correlated Rayleigh fading channels," IEEE Access, vol. 8, pp. 56214–56227, 2020.

[547] Y. Zhang, M. Zhou, X. Qiao, H. Cao, and L. Yang, "On the performance of cell-free massive MIMO with low-resolution ADCs," IEEE Access, vol. 7, pp. 117968–117977, 2019.

[548] Y. Zhang, M. Zhou, H. Cao, L. Yang, and H. Zhu, "On the performance of cell-free massive MIMO with mixed-ADC under Rician fading channels," IEEE Commun. Lett., vol. 24, no. 1, pp. 43–47, 2020.

[549] J. Zhang, Y. Wei, E. Björnson, Y. Han, and S. Jin, "Performance analysis and power control of cell-free massive MIMO systems with hardware impairments," IEEE Access, vol. 6, pp. 55302–55314, 2018.

[550] Y. Zhang, M. Zhou, Y. Cheng, L. Yang, and H. Zhu, "Rf impairments and low-resolution ADCs for nonideal uplink cell-free massive MIMO systems," IEEE Syst. J., pp. 1–12, 2020.

[551] S. N. Jin, D. W. Yue, and H. H. Nguyen, "Spectral efficiency of a frequency-selective cell-free massive MIMO system with phase noise," IEEE Wireless Commun. Lett., vol. 10, no. 3, pp. 483–487, 2021.

[552] G. Wunder, P. Jung, M. Kasparick, T. Wild, F. Schaich, Y. Chen, S. T. Brink, I. Gaspar, N. Michailow, A. Festag, L. Mendes, N. Cassiau, D. Ktenas, M. Dryjanski, S. Pietrzyk, B. Eged, P. Vago, and F. Wiedmann, "5GNOW: non-orthogonal, asynchronous waveforms for future mobile applications," IEEE Commun. Mag., vol. 52, no. 2, pp. 97–105, 2014.

[553] M. Nekovee, "Quantifying performance requirements of vehicle-to-vehicle communication protocols for rear-end collision avoidance," in IEEE Vehicular Technology Conference (VTC), 2009, pp. 1–5.

[554] H. Kim, J. Kim, S. Yang, M. Hong, and Y. Shin, "An effective MIMO–OFDM system for IEEE 802.22 WRAN channels," IEEE Trans. Circuits Sys. II. Exp. Briefs, vol. 55, no. 8, pp. 821–825, 2008.

[555] Luqing Wang and Chintha Tellambura, "An overview of peak-to-average power ratio reduction techniques for OFDM systems," in 2006 IEEE International Symposium on Signal Processing and Information Technology, 2006, pp. 840–845.

[556] A.D.S. Jayalath and C. Tellambura, "A blind SLM receiver for PAR-reduced OFDM," in Proceedings IEEE 56th Vehicular Technology Conference, 2002, vol. 1, pp. 219–222 vol.1.

[557] N. Michailow, M. Matthé, I. S. Gaspar, A. N. Caldevilla, L. L. Mendes, A. Festag, and G. Fettweis, "Generalized frequency division multiplexing for 5th generation cellular networks," IEEE Trans. Commun., vol. 62, no. 9, pp. 3045–3061, 2014.

[558] L. D. Le and H. H. Nguyen, "Phase noise compensation for CF-BMC–OQAM systems under imperfect channel estimation," IEEE Access, vol. 8, pp. 47247–47263, 2020.

[559] V. Lottici, R. Reggiannini, and M. Carta, "Pilot-aided carrier frequency estimation for filter-bank multicarrier wireless communications on Doubly-selective channels," IEEE Trans. Signal Process., vol. 58, no. 5, pp. 2783–2794, 2010.

[560] H. Cho and X. Ma, "Generalized synchronization algorithms for FBMC-OQAM systems," IEEE Trans. Veh. Technol., vol. 67, no. 10, pp. 9764–9774, 2018.

[561] H. Han, N. Kim, and H. Park, "Analysis of CFO estimation for QAM-FBMC systems considering non-orthogonal prototype filters," IEEE Trans. Veh. Technol., vol. 68, no. 7, pp. 6761–6774, 2019.

[562] P. Singh, E. Sharma, K. Vasudevan, and R. Budhiraja, "CFO and channel estimation for frequency selective MIMO-FBMC/OQAM systems," IEEE Wireless Commun. Lett., vol. 7, no. 5, pp. 844–847, 2018.

[563] K. Lai, Y. Huang, C. Chen, and C. Lin, "A family of MMSE-based decision feedback equalizers and their properties for FBMC/OQAM systems," IEEE Trans. Veh. Technol., vol. 68, no. 3, pp. 2346–2360, 2019.

[564] L. D. Le and H. H. Nguyen, "Compensation of phase noise and IQ imbalance in multi-carrier systems," IEEE Access, vol. 8, pp. 191263–191277, 2020.

[565] B. Lim and Y. Ko, "SIR analysis of OFDM and GFDM waveforms with timing offset, CFO, and phase noise," IEEE Trans. Wireless Commun., vol. 16, no. 10, pp. 6979–6990, 2017.

[566] M. Lupupa and J. Qi, "I/Q imbalance in generalized frequency division multiplexing under Weibull fading," in IEEE Annual International Symposium on Personal, Indoor, and Mobile Radio Communications (PIMRC), 2015, pp. 471–476.

[567] S. Han, Y. Sung, and Y. H. Lee, "Filter design for generalized frequency-division multiplexing," IEEE Trans. Signal Process., vol. 65, no. 7, pp. 1644–1659, 2017.

[568] A. Mohammadian and C. Tellambura, "Full-duplex GFDM radio transceivers in the presence of phase noise, CFO and IQ imbalance," in IEEE International Conference on Communications (ICC), 2019, pp. 1–6.

[569] A. Mohammadian, C. Tellambura, and M. Valkama, "Analysis of self-interference cancellation under phase noise, CFO, and IQ imbalance in GFDM full-duplex transceivers," IEEE Trans. Veh. Technol., vol. 69, no. 1, pp. 700–713, 2020.

[570] A. Mohammadian and C. Tellambura, "GFDM-modulated full-duplex cognitive radio networks in the presence of RF impairments," in IEEE Annual International Symposium on Personal, Indoor and Mobile Radio Communications (PIMRC), 2019, pp. 1–6.

[571] A. Mohammadian and C. Tellambura, "Cognitive GFDM full-duplex radios with RF impairments and ACI constraints," IEEE Open J. Commun. Soc., vol. 1, pp. 732–749, 2020.

[572] A. Mohammadian and C. Tellambura, "Joint channel and phase noise estimation and data detection for GFDM," IEEE Open J. Commun. Soc., pp. 1–1, 2021.

[573] P. Wang and D. W. Lin, "Maximum-likelihood blind synchronization for GFDM systems," IEEE Signal Process. Lett., vol. 23, no. 6, pp. 790–794, 2016.

[574] H. Shayanfar, H. Saeedi-Sourck, and A. Farhang, "CFO and channel estimation techniques for GFDM," in IEEE International Microwave Workshop Series on 5G Hardware and System Technologies (IMWS-5G), 2018, pp. 1–3.

[575] H. Cheng et al., "A normalized complex LMS based blind I/Q imbalance compensator for GFDM receivers and its full second-order performance analysis," IEEE Trans. Signal Process., vol. 66, no. 17, pp. 4701–4712, 2018.

[576] H. Cheng, Y. Xia, Y. Huang, L. Yang, and D. P. Mandic, "Joint channel estimation and Tx/Rx I/Q imbalance compensation for GFDM systems," IEEE Trans. Wireless Commun., vol. 18, no. 2, pp. 1304–1317, 2019.

[577] G T. Gil, "Normalized LMS adaptive cancellation of self-image in direct-conversion receivers," IEEE Trans. Veh. Technol., vol. 58, no. 2, pp. 535–545, 2009.

[578] B. Makki, K. Chitti, A. Behravan, and M. -S. Alouini, "A survey of NOMA: Current status and open research challenges," IEEE Open J. Commun. Soc., vol. 1, pp. 179–189, 2020.

[579] S. M. R. Islam, N. Avazov, O. A. Dobre, and K. Kwak, "Power-domain non-orthogonal multiple access (NOMA) in 5G systems: Potentials and challenges," IEEE Commun. Surveys Tuts., vol. 19, no. 2, pp. 721–742, 2017.

[580] L. Dai et al., "A survey of non-orthogonal multiple access for 5G," IEEE Commun. Surveys Tuts., vol. 20, no. 3, pp. 2294–2323, 2018.

[581] Alexandros-Apostolos A. Boulogeorgos, Nestor D. Chatzidiamantis, and George K. Karagiannidis, "Non-orthogonal multiple access in the presence of phase noise," IEEE Commun. Lett., vol. 24, no. 5, pp. 1133–1137, 2020.

[582] Y. Mao, H. Zhao, and Y. Tang, "Impacts of residual frequency offset on the sum rate performance of OFDM based NOMA systems," in IEEE International Conference on Communications Workshops (ICC Workshops), 2019, pp. 1–5.

[583] B. Selim et al., "Performance analysis of non-orthogonal multiple access under I/Q imbalance," IEEE Access, vol. 6, pp. 18453–18468, 2018.

[584] X. Li, M. Liu, C. Deng, P. T. Mathiopoulos, Z. Ding, and Y. Liu, "Full-duplex cooperative NOMA relaying systems with I/Q imbalance and imperfect SIC," IEEE Wireless Commun. Lett., vol. 9, no. 1, pp. 17–20, 2020.

[585] N. Van Huynh, D. T. Hoang, X. Lu, D. Niyato, P. Wang, and D. I. Kim, "Ambient backscatter communications: A contemporary survey," IEEE Commun. Surveys Tuts., vol. 20, no. 4, pp. 2889–2922, 2018.

[586] W. Zhang, Y. Qin, W. Zhao, M. Jia, Q. Liu, R. He, and B. Ai, "A green paradigm for internet of things: Ambient backscatter communications," China Commun., vol. 16, no. 7, pp. 109–119, 2019.

[587] Fatemeh Rezaei, Chintha Tellambura, and Sanjeewa Herath, "Large-scale wireless-powered networks with backscatter communications—a comprehensive survey," IEEE Open Journal of the Communications Society, vol. 1, pp. 1100–1130, 2020.

[588] G. Wang, F. Gao, R. Fan, and C. Tellambura, "Ambient backscatter communication systems: Detection and performance analysis," IEEE Trans. Commun., vol. 64, no. 11, pp. 4836–4846, 2016.

[589] C. Kang, W. Lee, Y. You, and H. Song, "Signal detection scheme in ambient backscatter system with multiple antennas," IEEE Access, vol. 5, pp. 14543–14547, 2017.

[590] J. Qian, F. Gao, G. Wang, S. Jin, and H. Zhu, "Noncoherent detections for ambient backscatter system," IEEE Trans. Wireless Commun., vol. 16, no. 3, pp. 1412–1422, 2017.

[591] C. Chen, G. Wang, H. Guan, Y. Liang, and C. Tellambura, "Transceiver design and signal detection in backscatter communication systems with multiple-antenna tags," IEEE Trans. Wireless Commun., vol. 19, no. 5, pp. 3273–3288, 2020.

[592] M. A. ElMossallamy, M. Pan, R. Jäntti, K. G. Seddik, G. Y. Li, and Z. Han, "Noncoherent backscatter communications over ambient OFDM signals," IEEE Trans. Commun., vol. 67, no. 5, pp. 3597–3611, 2019.

[593] S. Ma, G. Wang, R. Fan, and C. Tellambura, "Blind channel estimation for ambient backscatter communication systems," IEEE Commun. Lett., vol. 22, no. 6, pp. 1296–1299, 2018.

[594] W. Zhao, G. Wang, S. Atapattu, R. He, and Y. Liang, "Channel estimation for ambient backscatter communication systems with massive-antenna reader," IEEE Trans. Veh. Technol., vol. 68, no. 8, pp. 8254–8258, 2019.

[595] E. Basar, M. Di Renzo, J. De Rosny, M. Debbah, M. Alouini, and R. Zhang, "Wireless communications through reconfigurable intelligent surfaces," IEEE Access, vol. 7, pp. 116753–116773, 2019.

[596] L. Dai, B. Wang, M. Wang, X. Yang, J. Tan, S. Bi, S. Xu, F. Yang, Z. Chen, M. D. Renzo, C. Chae, and L. Hanzo, "Reconfigurable intelligent surface-based wireless communications: Antenna design, prototyping, and experimental results," IEEE Access, vol. 8, pp. 45913–45923, 2020.

[597] M. A. El Mossallamy, H. Zhang, L. Song, K. G. Seddik, Z. Han, and G. Y. Li, "Reconfigurable intelligent surfaces for wireless communications: Principles, challenges, and opportunities," IEEE Trans. Cog. Commun. Netw., pp. 1–1, 2020.

[598] J. Zhao and Y. Liu, "A survey of intelligent reflecting surfaces (IRSs): Towards 6G wireless communication networks," arXiv:1907.04789, 2019.

[599] C. Huang, A. Zappone, G. C. Alexandropoulos, M. Debbah, and C. Yuen, "Reconfigurable intelligent surfaces for energy efficiency in wireless communication," IEEE Trans. Wireless Commun., vol. 18, no. 8, pp. 4157–4170, 2019.

[600] M. Di Renzo, K. Ntontin, J. Song, F. H. Danufane, X. Qian, F. Lazarakis, J. De Rosny, D. Phan-Huy, O. Simeone, R. Zhang, M. Debbah, G. Lerosey, M. Fink, S. Tretyakov, and S. Shamai, "Reconfigurable intelligent surfaces vs. relaying: Differences, similarities, and performance comparison," IEEE Open J. Commun. Soc., vol. 1, pp. 798–807, 2020.

[601] B. Zheng and R. Zhang, "Intelligent reflecting surface-enhanced OFDM: Channel estimation and reflection optimization," IEEE Wireless Commun. Lett., vol. 9, no. 4, pp. 518–522, 2020.

[602] Z. Wang, L. Liu, and S. Cui, "Channel estimation for intelligent reflecting surface assisted multiuser communications: Framework, algorithms, and analysis," IEEE Trans. Wireless Commun., pp. 1–1, 2020.

[603] L. Wei, C. Huang, G. C. Alexandropoulos, and C. Yuen, "Parallel factor decomposition channel estimation in RIS-assisted multi-user MISO communication," in Sensor Array and Multichannel Signal Processing Workshop (SAM), 2020, pp. 1–5.

[604] J. Kang, "Intelligent reflecting surface: Joint optimal training sequence and refection pattern," IEEE Commun. Lett., pp. 1–1, 2020.

[605] K. Zhi, C. Pan, H. Ren, and K. Wang, "Uplink achievable rate of intelligent reflecting surface-aided millimeter-wave communications with low-resolution ADC and phase noise," IEEE Wireless Commun. Lett., vol. 10, no. 3, pp. 654–658, 2021.

[606] E. Calvanese Strinati, S. Barbarossa, J. L. Gonzalez-Jimenez, D. Ktenas, N. Cassiau, L. Maret, and C. Dehos, "6G: The next frontier: From holographic messaging to artificial intelligence using subterahertz and visible light communication," IEEE Veh. Technol. Mag., vol. 14, no. 3, pp. 42–50, 2019.

[607] L. Zhang, Y. Liang, and D. Niyato, "6G visions: Mobile ultra-broadband, super internet-of-things, and artificial intelligence," China Commun., vol. 16, no. 8, pp. 1–14, 2019.

[608] H. Huang, J. Yang, H. Huang, Y. Song, and G. Gui, "Deep learning for super-resolution channel estimation and DOA estimation based massive MIMO system," IEEE Trans. Veh. Technol., vol. 67, no. 9, pp. 8549–8560, 2018.

[609] H. Ye, G. Y. Li, and B. Juang, "Power of deep learning for channel estimation and signal detection in OFDM systems," IEEE Wireless Commun. Lett., vol. 7, no. 1, pp. 114–117, 2018.

[610] Y. Yang, F. Gao, X. Ma, and S. Zhang, "Deep learning-based channel estimation for doubly selective fading channels," IEEE Access, vol. 7, pp. 36579–36589, 2019.

[611] M. Soltani, V. Pourahmadi, A. Mirzaei, and H. Sheikhzadeh, "Deep learning-based channel estimation," IEEE Commun. Lett., vol. 23, no. 4, pp. 652–655, 2019.

[612] Q. Bai, J. Wang, Y. Zhang, and J. Song, "Deep learning-based channel estimation algorithm over time selective fading channels," IEEE Trans. Cog. Commun. Netw., vol. 6, no. 1, pp. 125–134, 2020.

[613] J. Yuan, X. Li, X. Yang, and W. Pu, "Phase-noise compensation based on artificial neural network optimization for OFDM ranging systems," IEEE Commun. Lett., vol. 22, no. 11, pp. 2294–2297, 2018.

[614] M. Zhou, X. Huang, Z. Feng, and Y. Liu, "Coarse frequency offset estimation in MIMO systems using neural networks: A solution with higher compatibility," IEEE Access, vol. 7, pp. 121565–121573, 2019.

[615] P. Siyari, H. Rahbari, and M. Krunz, "Lightweight machine learning for efficient frequency-offset-aware demodulation," IEEE J. Sel. Areas Commun., vol. 37, no. 11, pp. 2544–2558, 2019.

[616] L. J. Wong, W. C. Headley, and A. J. Michaels, "Specific emitter identification using convolutional neural network-based IQ imbalance estimators," IEEE Access, vol. 7, pp. 33544–33555, 2019.

[617] S. Kumari, K. K. Srinivas, and P. Kumar, "Channel and carrier frequency offset equalization for OFDM based UAV communications using deep learning," IEEE Commun. Lett., vol. 25, no. 3, pp. 850–853, 2021.

[618] A. Mohammadian and C. Tellamburaand G. Y. Li, "Deep learning-based phase noise compensation in multicarrier systems," IEEE Wireless Commun. Lett., pp. 1–1, 2021.

This article has been accepted for publication in a future issue of this journal, but has not been fully edited. Content may change prior to final publication. Citation information: DOI 10.1109/ACCESS.2021.3101845, IEEE Access

AMIRHOSSEIN MOHAMMADIAN (Graduate Student Member, IEEE) received his B.Sc. and M.Sc. degrees in electrical engineering from Amirkabir University of Technology, Tehran, Iran, in 2014 and 2017, respectively. He is currently pursuing the Ph.D. degree in electrical engineering at the University of Alberta, Edmonton, AB, Canada. His current research interests include wireless communication, full-duplex transmission, cognitive radio networks, dirty RF and MIMO structure.

He was a recipient of the Recruitment Doctor of Philosophy Scholarship and the University of Alberta Graduate Fellowships in 2017 and 2019, respectively. He was also a recipient of Alberta Innovates Graduate Student Data-Enabled Innovation Scholarship in 2020.

CHINTHA TELLAMBURA (Fellow Member, IEEE)received the B.Sc. degree in electronics and telecommunications from the University of Moratuwa, Sri Lanka, the M.Sc. degree in electronics from the Kings College, University of London, and the Ph.D. degree in electrical engineering from the University of Victoria, Canada.

He was with Monash University, Australia, from 1997 to 2002. Since 2002, he has been with the Department of Electrical and Computer Engineering, University of Alberta, where he is currently a Full Professor. He has authored or coauthored over 560 journal and conference papers, with an h-index of 77 (Google Scholar). He has supervised or co-supervised 70 M.Sc., Ph.D., and PDF trainees. His current research interests include future wireless networks and machine learning algorithms. He was elected as a fellow of The Canadian Academy of Engineering in 2017. He received the Best Paper Awards from the IEEE International Conference on Communications (ICC) in 2012 and 2017. He is the winner of the prestigious McCalla Professorship and the Killam Annual Professorship from the University of Alberta. He served as an Editor for the IEEE TRANSACTIONS ON COMMUNICATIONS from 1999 to 2012 and IEEE TRANSACTIONS ON WIRELESS COMMUNICATIONS from 2001 to 2007. He was an Area Editor of Wireless Communications Systems and Theory from 2007 to 2012.